DISCRETE ALUMINIUM COMPOUNDS – TOWARDS A SOLUBLE ALUMINIUM TRIFLUORIDE

Evelin Gruden

Doctoral Dissertation
Jožef Stefan International Postgraduate School
Ljubljana, Slovenia

Supervisor: Asst. Prof. Dr. Gašper Tavčar, Jožef Stefan International Postgraduate School and Jožef Stefan Institute, Ljubljana, Slovenia

Evaluation Board:
Prof. Dr. Maja Ponikvar-Svet, Chair, Jožef Stefan International Postgraduate School and Jožef Stefan Institute, Ljubljana, Slovenia
Prof. Dr. Uroš Grošelj, Member, Faculty of Chemistry and Chemical Technology, University of Ljubljana, Ljubljana, Slovenia
Prof. Dr. Jaroslav Kvíčala, Member, University of Chemistry and Technology, Prague, Czech Republic

MEDNARODNA PODIPLOMSKA ŠOLA JOŽEFA STEFANA
JOŽEF STEFAN INTERNATIONAL POSTGRADUATE SCHOOL

Evelin Gruden

DISCRETE ALUMINIUM COMPOUNDS – TOWARDS A SOLUBLE ALUMINIUM TRIFLUORIDE

Doctoral Dissertation

DISKRETNE ALUMINIJEVE SPOJINE – NA POTI K TOPNEMU ALUMINIJEVEMU TRIFLUORIDU

Doktorska disertacija

Supervisor: Asst. Prof. Dr. Gašper Tavčar

Ljubljana, Slovenia, November 2022

Acknowledgments

First of all, I would like to thank my family for supporting me during my years of study and for letting me become the person I am today. A big thank you goes to my partner who stood by me during my doctoral studies. Thank you for supporting me and listening to me when I needed someone to talk to. I would also like to thank my friends who know me very well and have always been there for me. You have shown me what is most important in life.

A special thanks goes to my mentor, Asst. Prof. Dr. Gašper Tavčar. Thank you for believing in me. I would also like to thank the members of the committee, Prof. Dr. Maja Ponikvar-Svet, Prof. Dr. Uroš Grošelj, and Prof. Dr. Jaroslav Kvíčala, for their expert review of the PhD theses.

Next, I would like to thank all my colleagues from the K-1 department (former and new) who have helped me in any way with my work. I would also like to thank Prof. Dr. Maja Ponikvar-Svet and Mira Zupančič for performing CHN elemental analysis, Asst. Prof. Evgeny Goreshnik for the help with crystal structure analysis, Dr. Melita Tramšek for molecular calculations and Robert Moravec for performing the reactions with anhydrous HF. Dear colleagues, thank you for the long conversations about chemistry and beyond. Without you, this work would not be the same.

And finally, I would like to thank the colleagues from the Slovenian NMR Centre at the National Institute of Chemistry for their support and resources, and the Slovenian Research Agency for financially supporting my research.

Abstract

In the past, the search for soluble aluminium trifluoride (AlF_3) led to the discovery of organoaluminium compounds (AlR_3) and organoaluminium fluorides. However, suitable methods for the introduction of fluorine into AlR_3 are still scarce, making the discrete AlF_3 and organoaluminium fluoride compounds rare. Our investigation of the reactivity of cyclic (alkyl)(amino)carbene (CAAC) stabilised $AlMe_3$ has shown that when a suitable neutral fluorinating reagent is used, one, two or three methyl groups on the aluminium centre can be substituted by fluorine, leading to discrete dimethylaluminium fluoride, methylaluminium difluoride and AlF_3 adduct, respectively. Further fluorination led to the formation of salts with discrete fluoroaluminate anions.

AlR_3 compounds have a Lewis acidic aluminium centre that tends to react with fluoride anions to form various organofluoroaluminates. However, discrete anions are still rare as fluorine atoms tend to engage in the formation of oligomeric or polymeric species. Our study on the reactivity of AlR_3 compounds with fluorinating reagents based on imidazolium salts has shown that by using a suitable fluorinating reagent with the appropriate HF content, compounds with discrete $[R_3AlF]^-$, $[R_2AlF_2]^-$ and $[RAlF_3]^-$ anions can be selectively prepared. Compounds with $[AlF_4]^-$ anions were prepared when AlR_3 reacted with an excess of HF-based reagents. The formation of salts was accompanied by the release of RH. We have developed selective synthesis procedures for the synthesis of various organofluoroaluminates.

Aluminium hydrides (AlH_3) are important reagents in materials science and synthetic chemistry. However, relatively little attention has been paid to their partially substituted derivatives. Our study on the reactivity of N-heterocyclic carbene (NHC) stabilised AlH_3 showed that even unusual reagents such as aldiminium-based triflate and chloride salts can be useful reagents for hydride/triflate and hydride/chloride substitution reactions, respectively. We have successfully prepared the first NHC-stabilised aluminium dihydride triflate adduct and a new NHC-stabilised aluminium hydride chloride adduct.

Fluorinating reagents based on imidazolium salts have recently been shown to be useful for the fluorination of organic and inorganic compounds. However, since the number of reliable methods for the introduction of fluorine into aluminium compounds is still limited and reagents based on imidazolium salts resulted in anionic species, we decided to prepare a series of new fluorinating reagents based on aldiminium salts. In our work, we prepared a series of poly(hydrogen fluoride) compounds starting from aldiminium-base chloride salt and anhydrous HF. By gradually removing HF, we also obtained an aldiminium-based fluoride compound.

Finally, we tested the reactivity of the newly prepared aldiminium-based fluorinating reagents on AlR_3 compounds. The poly(hydrogen fluoride) reagents converted the $AlMe_3$ into salts with discrete $[RAlMe_3]^-$ and $[AlF_4]^-$ anions, while the aldiminium-based fluoride compound successfully fluorinated the CAAC-stabilised $AlMe_3$ to form the corresponding diorganoaluminium fluoride. These preliminary results show the potential of the newly prepared fluorinating reagents. In the future, their reactivity still needs to be exploited, not only in aluminium chemistry but also in other research areas.

Povzetek

V preteklosti so raziskovalci precej pozornosti posvečali iskanju topnega aluminijevega trifluorida (AlF_3). Raziskave, ki so bile izvedene na tem področju, so vodile do odkritja organoaluminijevih spojin (AlR_3) in organoaluminijevih fluoridov. Dandanes je število metod, s katerimi lahko vnesemo fluor v AlR_3 spojine, še vedno omejeno. Zaradi tega so redke tudi spojine z diskretnimi enotami AlF_3 ter organoaluminijevih fluoridov. Naša raziskava se je osredotočala na reaktivnost $AlMe_3$ aduktov, stabiliziranih s cikličnimi (alkil)(amino)karbeni (CAAC). Z uporabo primernega nevtralnega fluorirnega reagenta smo pokazali, da lahko eno, dve ali tri metilne skupine na aluminiju uspešno nadomestimo s fluorom in tako pripravimo diskretne spojine z dimetilaluminijevim fluoridom, metilaluminijevim difluoridom ter AlF_3. Nadaljnje fluoriranje je privedlo do nastanka soli z diskretnimi fluoroaluminatnimi anioni.

Spojine tipa AlR_3 so znane kot močne Lewisove kisline s kislim aluminijevim centrom. Običajno reagirajo s fluoridnimi ioni, tako da tvorijo različne organofluoroaluminatne anione. Le-ti so redko določeni v diskretni obliki, saj fluorovi atomi običajno sodelujejo pri tvorbi oligomernih ali polimernih spojin. Pri našem delu smo raziskali reaktivnost AlR_3 spojin s fluorirnimi reagenti na osnovi imidazolijevih soli. Pokazali smo, da lahko z uporabo ustreznega fluorirnega reagenta s primerno vsebnostjo HF selektivno pripravimo spojine z diskretnimi $[R_3AlF]^-$, $[R_2AlF_2]^-$ in $[RAlF_3]^-$ anioni. Spojine z $[AlF_4]^-$ anioni smo dobili pri reakciji AlR_3 s presežkom reagenta na osnovi HF. Pri reakcijah z [IPrH][F(HF)] in $[IPrH][F(HF)_2]$ so se nam kot stranski produkti tvorile RH spojine. Tekom študije smo razvili selektivne sintezne postopke za pripravo različnih diskretnih organofluoroaluminatnih spojin.

Aluminijevi hidridi (AlH_3) so pomembni reagenti v znanosti o materialih in v sintezni kemiji. Njihovim delno substituiranim derivatom pa je bilo do sedaj posvečeno razmeroma malo pozornosti. Pri našem delu smo testirali reaktivnost AlH_3, stabiliziranega z N-heterocikličnim karbenom (NHC). Pokazali smo, da lahko tudi nenavadna reagenta, kot sta triflatna in kloridna sol na osnovi aldiminija, uporabimo za substitucijo hidrida na Al s triflatom oziroma kloridom. Uspešno smo pripravili prvi NHC stabilizirani adukt aluminijevega dihidrid triflata in nov NHC stabilizirani adukt aluminijevega hidrid klorida.

Dandanes je število zanesljivih metod za vnos fluora v aluminijeve spojine še vedno omejeno, zato smo se odločili pripraviti serijo novih fluorirnih reagentov na osnovi aldiminijevih soli. Pri našem delu smo pripravili vrsto reagentov na osnovi polivodikovih fluoridov iz aldiminijevega klorida in brezvodnega HF. S postopnim odstranjevanjem HF smo pripravili tudi aldiminijev fluorid.

Na koncu smo preizkusili reaktivnost novo pripravljenih fluorirnih reagentov pri reakcijah z AlR_3. Reagenti na osnovi polivodikovih fluoridov so selektivno pretvorili $AlMe_3$ v soli z diskretnimi $[RAlMe_3]^-$ in $[AlF_4]^-$ anioni, medtem ko je aldiminijev fluorid uspešno fluoriral $AlMe_3$ adukt, stabiliziran s CAAC-om, in tvoril ustrezen diorganoaluminijev fluorid. Naši rezultati kažejo na potencial pripravljenih fluorirnih reagentov. Z nadaljnjimi raziskavami bo potrebno njihovo reaktivnost še proučiti, ne le v kemiji aluminija, temveč tudi na drugih področjih.

Contents

List of Figures

List of Schemes

List of Tables

Abbreviations

CAAC	...	Cyclic (Alkyl)(Amino)Carbene; also used for the simplest CAAC 1-(2,6-diisopropylphenyl)-3,3,5,5-tetramethylpyrrolidin-2-ylidene
$CAAC^{Et}$	...	1-(2,6-diisopropylphenyl)-3,3-diethyl-5,5-dimethylpyrrolidin-2-ylidene
CSD	...	The Cambridge Structural Database
DCM	...	Dichloromethane
Dipp	...	2,6-diisopropylphenyl
DMSO	...	Dimethyl sulfoxide (IUPAC: (Methanesulfinyl)methane)
DMPU	...	1,3-dimethyl-3,4,5,6-tetrahydro-2(1H)-pyrimidinone
Et	...	Ethyl group
FEP	...	Tetrafluoroethylene-hexafluoropropylene
FLP	...	Frustrated Lewis Pair
HOMO	...	Highest occupied molecular orbital
i-Bu	...	*Iso*butyl (IUPAC: 2-methylpropan-1-yl)
i-Pr	...	*Iso*propyl (IUPAC: propan-2-yl)
IBn	...	1,3-dibenzylimidazol-2-ylidene
IiPr	...	1,3-diisopropylimidazol-2-ylidene
^{Me}IiPr	...	1,3-diisopropyl-4,5-dimethylimidazol-2-ylidene
IMe	...	1,3-trimethylimidazol-2-ylidene
^{Me}IMe	...	1,3,4,5-tetramethylimidazol-2-ylidene
IMes	...	1,3-bis(2,4,6-trimethylphenyl)imidazol-2-ylidene
^{Br}IMes	...	1,3-bis(2,4,6-trimethylphenyl)-4,5-dibromoimidazol-2-ylidene
IPr	...	1,3-bis(2,6-diisopropylphenyl)imidazol-2-ylidene
IR	...	Infrared spectroscopy
ItBu	...	1,3-di-*tert*-butylimidazol-2-ylidene
aItBu	...	1,3-di-*tert*-butylimidazol-4-ylidene
LUMO	...	Lowest unoccupied molecular orbital
MAO	...	Methylaluminoxane ($[MeAl(\mu\text{-}O)]_n$)
Me	...	Methyl group
MeCN	...	Acetonitrile
Mes	...	2,4,6-trimethylphenyl group
n-Bu	...	*N*-butyl group (IUPAC: butyl, butan-1-yl)
NacNac	...	β-diketiminato ligand
NHC	...	N-Heterocyclic Carbene
NMR	...	Nuclear Magnetic Resonance
Ph	...	Phenyl group
PNP	...	Bis(triphenylphosphane)iminium
PP	...	Polypropene
PTFE	...	Polytetrafluoroethylene
py	...	Pyridine
pyNO	...	Pyridine-*N*-oxide (IUPAC: $1\lambda^5$-Pyridin-1-one)
SIMes	...	1,3-bis(2,4,6-trimethylphenyl)-4,5-dihydroimidazol-2-ylidene

t-Bu ... *Tert*-butyl (IUPAC: 2-methylpropan-2-yl)
t-BuOH ... *Tert*-butanol (IUPAC: 2-methylpropan-2-ol)
TBAF ... *Tetra-n*-butylammonium fluoride
THF ... Tetrahydrofuran (IUPAC: 1,4-epoxybutane)
TMS ... Tetramethylsilane

Symbols

Ar . . . Aryl group
L . . . Ligand
M . . . Metal
R . . . Alkyl group
X . . . Halide

Chapter 1

Introduction

1.1 Aluminium Trifluoride

Aluminium trifluoride (AlF_3) has attracted the attention of chemists for many decades. It is an important material that plays a crucial role in industry due to its catalytic properties [1]. Various aluminium fluoride phases are used in heterogeneous catalysis [2]. For example, they are studied as active catalysts for isomerisation, elimination and halogen exchange reactions or as acidic catalysts in cracking or polymerisation reactions [3]. However, the reactivity of AlF_3 strongly depends on the structure of the material. In the gas phase, AlF_3 adopts a trigonal-planar geometry, whereas in the solid state, the fluorine and aluminium atoms arrange themselves into octahedral units. The AlF_6 octahedra interconnect by corner-sharing and form a rich variety of polymeric 3D structures [2]. Fluorine, due to its small size and high charge density, confers the acceptor metal with the ability to form F−M−F bridging units that enable the assembly of clusters and frameworks *via* fluoride bridges [4]. The materials with a more open or distorted structure have been shown to be more catalytically active due to their higher Lewis acidity. The α-AlF_3, the most stable crystalline form of AlF_3, shows no activity, while the more open metastable phases, such as the β-AlF_3, are active catalysts. However, the metastable β-, θ-, κ-, and η-phases tend to transform irreversibly to α-AlF_3 upon heating [3]. The structures of the different phases are shown in Figure 1.1 [5]. In amorphous solids such as high surface AlF_3, even higher Lewis acidity was observed. The amorphous phases tend to form at low temperatures when the AlF_6 octahedra are arranged in non-periodic networks. Such phases exhibit different structural and catalytic properties and are also quite reactive [2].

According to quantum chemical calculations, pure discrete metal fluorides should be excellent Lewis acids. The Lewis acidity of AlF_3 as a single molecule has been estimated to be similar to $SbF_{5(g)}$, which is commonly regarded as the strongest conventional Lewis acid [2]. But as described above, solid crystalline AlF_3 does not exhibit a strong Lewis acidity. The same has been observed for $AlCl_3$. In its solid crystalline state, $AlCl_3$ exhibits almost no Lewis acidity. Coordinatively saturated aluminium with a coordination number of six does not act as an electron pair acceptor [6]. However, when coordinatively unsaturated aluminium species are formed and the inert sphere is broken, $AlCl_3$ becomes a strong Lewis acid, which can act as an electron pair acceptor and forms adducts with Lewis bases [(L)$AlCl_3$]. The tetrahedrally coordinated adducts often act as catalytically active species [2]. Thus, to utilise the high Lewis acidity of AlF_3, the formation of adducts with Lewis bases is required.

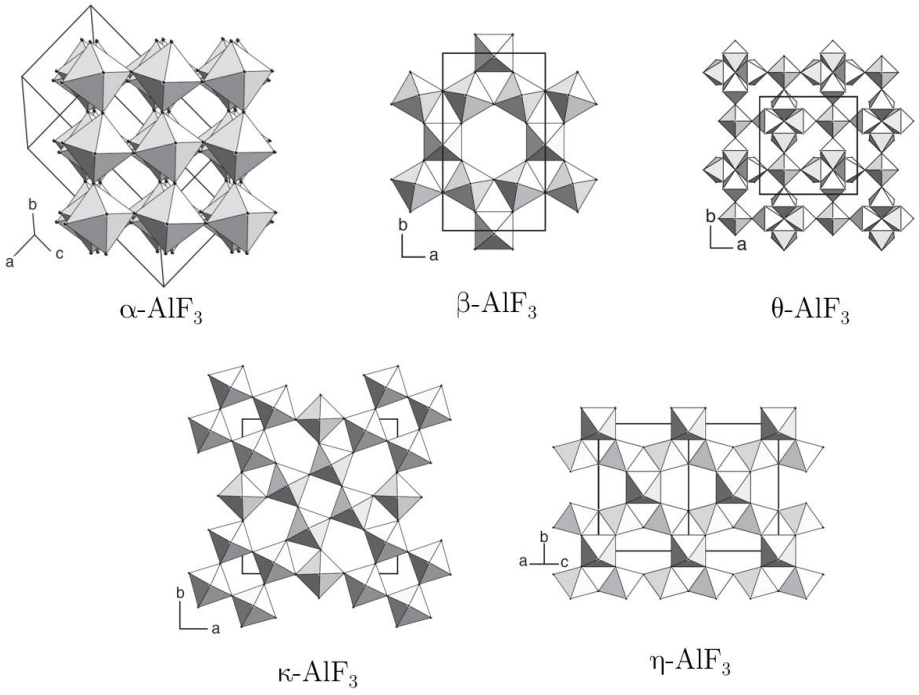

Figure 1.1: Different crystalline AlF_3 phases.

However, the properties of AlF_3 differ drastically from those of its heavier halogen analogues. Unlike $AlCl_3$, which is known for its good solubility in organic solvents and its low melting point (192 °C), solid AlF_3 does not react with coordinating solvents and has a much higher melting point (1291 °C) [7]. Even when exposed to strong Lewis bases, no molecular species of the $[(L)AlF_3]$ type are formed. Nevertheless, the Al−F bond is one of the strongest bonds known in fluorine chemistry. Even if uncoordinated AlF_3 forms, its high association energy will lead to the formation of solid AlF_3 [2], [7].

1.1.1 Neutral AlF_3 compounds

As described above, AlF_3 is not a suitable starting material for the synthesis of monomeric compounds. Therefore, the synthesis of discrete aluminium fluorides turned out to be challenging. To date, there are only a small number of described compounds containing discrete AlF_3 units [8]. Of these, only three have been structurally characterised. All three possess octahedrally coordinated aluminium centres and are stabilised by triaza macrocyclic frameworks [9], [10]. The scarcity of discrete AlF_3 compounds is due to the difficulties in preparing, isolating and growing of single crystals.

Discrete AlF_3 compounds have been prepared either by fluoride exchange reactions from pre-formed chloride complexes or by the use of a hydrate synthone $AlF_3 \cdot 3H_2O$ [8]. Recently, another method involving fluoride/alkyl exchange reactions has been proposed [11]. The pre-formed octahedral $AlCl_3$ complexes stabilised by triaza macrocyclic frameworks were reacted with KF or $[E_4N][F]$ in aqueous solutions to form the corresponding AlF_3 complexes [10], [12]. However, the same reaction between $[AlCl_3(py)_3]$ and Me_3SnF led to the formation of an ionic compound with a monomeric octahedrally coordinated cation $[AlF_2(Py)_4][Cl]$ [13]. Otherwise, the synthon was prepared in aqueous solution by precipitating an aluminium salt with HF. The octahedral $AlF_3 \cdot 3H_2O$ molecules thus prepared were then reacted with various N-donor ligands in hydrothermal vessels to form octahedral complexes [9]. The $AlF_3 \cdot 3H_2O$ synthon also reacted with the O-donor ligands DMSO and pyNO to

form $[AlF_3(H_2O)_2(DMSO)]$ and $[AlF_3(H_2O)_2(pyNO)]$, respectively [14]. Recently, the tetrahedrally coordinated AlF_3 adduct $[(SIMes)AlF_3]$ stabilised by an NHC was prepared from the corresponding $AlMe_3$ adduct by fluoride/alkyl substitution reactions with SF_4 or Me_3SnF [11]. The compound was characterised by NMR but could not be structurally characterised. To the best of our knowledge, the only discrete tetrahedrally coordinated group 13 metal trifluoride adduct that has been structurally characterised is $[(IPr)GaF_3]$. It was prepared by fluoride/halide exchange reaction starting from the $[(IPr)GaCl_3]$ and using $AgBF_4$. However, the direct reaction of IPr and GaF_3 did not give the desired product, but led to the formation of the imidazolium salt $[IPrH][GaF_4]$ [15].

1.1.2 Ionic fluoroaluminate compounds

Most of the fluoride minerals found in nature are fluoroaluminates. For example, there is cryolite (K_2NaAlF_6), weberite ($LiCaAlF_6$), elpasolite (Na_2MgAlF_7), cryolithionite ($Na_3Li_3Al_2F_{12}$), etc. The naturally occurring fluoroaluminates usually consist of octahedral $[AlF_6]^{3-}$ anions or similar polynuclear derivatives. Structurally, the polynuclear fluoroaluminate anions could be described as associated octahedral AlF_6 units connected by a corner or edge [5]. So far, several polynuclear fluoroaluminate anions have been prepared and structurally characterised, including $[Al_2F_9]^{3-}$, $[Al_2F_{10}]^{4-}$, $[Al_2F_{11}]^{5-}$, $[Al_3F_{16}]^{7-}$, $[Al_4F_{18}]^{6-}$, $[Al_4F_{20}]^{8-}$, $[Al_5F_{26}]^{11-}$, $[Al_7F_{30}]^{9-}$ and $[Al_8F_{35}]^{11-}$ [5], [16]. Discrete octahedral $[AlF_6]^{3-}$ are not only observed in natural minerals, but also in combination with organic cations. After the publication of the first discrete hexafluoroaluminate salt with guanidinium cations, which was prepared from aqueous solution by Bukovec in 1983 [17], many others followed. Today, there are 26 crystallographically characterised structures with discrete octahedral $[AlF_6]^{3-}$ anions in the CSD database.

Furthermore, the octahedral coordination of aluminium is also observed in salts that stoichiometrically appear to contain $[AlF_5]^{2-}$ or $[AlF_4]^-$ anions [18], [19]. However, structures with discrete $[AlF_5]^{2-}$ or $[AlF_4]^-$ anions are much less studied. Known geometries of discrete fluoroaluminate anions are shown in Figure 1.2.

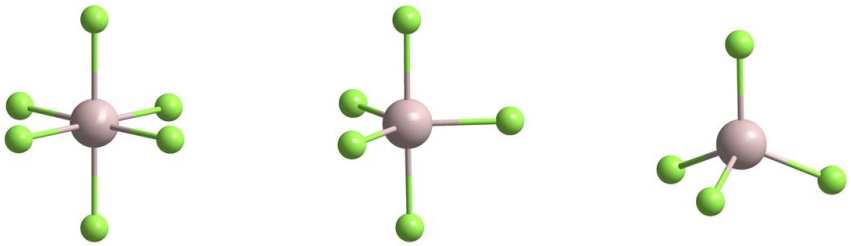

Figure 1.2: Structures of known discrete fluoroaluminate anions.

Discrete pentacoordinated fluoroaluminates are extremely rare. Their existence was suggested by Gilbert in 1990. When NaF/AlF_3 melts were studied by Raman spectroscopy, the Raman bands for $[AlF_6]^{3-}$, $[AlF_5]^{2-}$ and $[AlF_4]^-$ were observed and assigned at 515 cm^{-1}, 555 cm^{-1} and 622 cm^{-1}, respectively [20]. Quantum chemical calculations of $[AlF_5]^{2-}$ also confirmed its existence. Bouyer's group calculated the Raman spectra of $[AlF_6]^{3-}$, $[AlF_5]^{2-}$ and $[AlF_4]^-$ anions in melts and confirmed the experimentally obtained results of Gilbert [21]. They also proved that the $[AlF_6]^{3-}$ anions are the less stable in the series of fluoroaluminate anions and tend to dissociate to $[AlF_5]^{2-}$, which in turn dissociate to $[AlF_4]^-$. The latter proved to be the most stable form in melts [21], [22].

The first compound with discrete $[AlF_5]^{2-}$ anions was only described by Raman and NMR spectroscopy in 2003 by the group of Groß and Kemnitz [23]. Moreover, the structural characterisation of a discrete $[AlF_5]^{2-}$ anion in $[Et_4N]_2[AlF_5]\cdot(H_2O)_2$ salt was published only in 2015 by the group of Matsumoto [18]. The reaction of $[Et_4N][AlF_4]$ with $[Me_4N][F]$ in a 2:1 stoichiometry led to the formation of a mixture of $[Et_4N][Me_4N][AlF_5]$ and unreacted $[Et_4N][AlF_4]$. However, single crystals only formed when the mixture was in the presence of water. It turned out that water molecules are essential for the stabilisation of the lattice [18].

Discrete tetracoordinated fluoroaluminate anions are also rare. The first compound with $[AlF_4]^-$ anions was described by Herron in 1993. They prepared an $[AlF_4]^-$ salt by reacting $AlMe_3$ with 4 equivalents of HF using a pyridine-based poly(hydrogen fluoride) reagent. After cation substitution, single crystals of [1,8-bis(dimethylamino)naphthalene-H]$[AlF_4]$ and [collidine-H]$[AlF_4]$ were obtained [19]. In the CSD database, there are 4 other structurally characterised compounds with discrete $[AlF_4]^-$ anions: $[PPh_4][AlF_4]$ was described in 2001, the $[RePO_3NC_{20}H_{20}][AlF_4]$ in 2004 [24], [PNP]$[AlF_4]$ in 2020 [25] and our [IPrH]$[AlF_4]$ in 2022 [26].

Nevertheless, crystallographic data for discrete fluoroaluminate anions are still limited due to difficulties in growing single crystals.

1.2 Organoaluminium Fluorides

The non-reactive nature of AlF_3 makes it an unsuitable starting material for the synthesis of monomeric units. To further explore the chemistry of aluminium fluorides, it is necessary to prepare compounds with higher solubility in organic solvents. This can be achieved either by replacing one or two fluorine atoms with bulky substituents or by stabilising the monomeric units with electron-donating ligands [9], [10]. Replacing one or two fluorine atoms with carbon changes the physical properties of the molecules, making them more volatile, lowering their melting point and improving their solubility in organic solvents. The increased solubility could consequently enable their use in homogeneous catalysis [27]. In addition, bulky substituents have the potential to form an organic shell around the metal centre, preventing the dimerisation or aggregation of monomeric compounds [27]. The use of neutral ligands to stabilise monomeric units also has a very similar effect. As described in the previous chapters, many discrete aluminium fluoride compounds can be prepared with Lewis bases.

The search for soluble aluminium fluoride compounds led to the development of organoaluminium fluorides. A distinct family of compounds containing both the Al—F and Al—C bonds [7]. On the one hand, the Al—F bond is highly polar and very strong (580–670 kJ/mol), which often contributes to fluorine bridging. On the other hand, the much weaker and more covalent Al—C bond (255–280 kJ/mol) can be easily cleaved by HF or other fluorinating reagents [3], [7]. These opposing properties of the bonds play an important role in the chemistry of organoaluminium fluorides.

Organoaluminium fluorides were discovered by Ziegler and co-workers in the 1950s. In their pioneering work, they prepared sodium salts of anionic organofluoride species to be used in Ziegler-Natta catalytic systems for olefin polymerisation [28]. Many years later, Zielger and Natta received a Nobel Prize for their work [29]. However, it was not until the era of the modern polymer industry that the compounds containing the C–Al–F fragment received much attention. In the 1970s, the development of a new type of catalysts began when scientists discovered that group 4 metallocene complexes $(\eta^5\text{-}C_5H_5)_2MX_2$ (M = Ti, Zr, Hf) catalysed the polymerization of propene in the presence of MAO $[MeAl(\mu\text{-}O)]_n$ [30]. In the 1990s, many research papers were published on the mechanism of homogeneous

catalysis in olefin polymerisation [28]. Several complex structures containing C–Al–F fragments were also published at this time by the Roesky's group, starting with metallocene complexes of titanium-fluorides [31], zirconium-fluorides [32], and hafnium-fluorides [33].

In general, pure organoaluminium fluorides are colourless, air-sensitive compounds that have a trimeric or tetrameric structure in the solid state or in solution. They can act as electron pair acceptors and form adducts with Lewis bases. Some of them are also pyrophoric [34]. They can be prepared from the corresponding heavier halides or organoaluminium compounds and using appropriate fluorinating reagents. Pure R_2AlF with alkyl substituents have been prepared from the corresponding halides using NaF and some other alkali-earth metal fluorides, and from organoaluminium compounds using XeF_2, $[(Et_2O)BF_3]$, SiF_4, SF_6 or other similar fluorides [28], [34]. On the other hand, data for the preparation of $RAlF_2$ are limited. They were prepared from the corresponding halides using NaF, from organoaluminium compounds using BF_3 or HF-based reagents, and by commutation reaction between AlR_3 and freshly prepared AlF_3 according to the following equation [34]:

$$AlR_3 + 2AlF_3 \rightarrow 3RAlF_2$$

Further developments in this field of chemistry soon led to the synthesis and characterisation of discrete mononuclear organoaluminium fluoride species, either in their neutral or ionic form. For the sake of clarity, representatives of both forms are presented separately in the following chapters.

Discrete neutral compounds have been successfully prepared so far by fluoride/halide exchange reactions, fluoride/alkyl exchange reactions, fluoride/hydride exchange reactions and by oxidative additions of Al(I), while the corresponding ionic compounds were formed by the formation of complexes with other metal fluorides or by reactions with HF-based reagents [3]. The reactions are presented in the following chapters.

1.2.1 Neutral organoaluminium fluoride compounds

Discrete organoaluminium fluorides stabilised by electron-donating ligands are rare. This is mainly due to the lack of suitable methods for introducing fluorine into organoaluminium compounds [7]. In the following paragraphs, different types of discrete organoaluminium fluoride compounds are described. Their structures are shown in Figure 1.3.

The first discrete structure of an organoaluminium fluoride compound was reported by Roesky's group in 1999. The stable organoaluminium difluoride adduct with THF $[(THF)Al(C(Me_3Si)_3)F_2]$ was prepared by a fluoride/alkyl exchange reaction from the corresponding dimethyl parent compound and Me_3SnF. However, the complex converted to the THF-free trimeric product $[(RAlF_2)_3]$ upon heating [35]. Later, the same group found that polynuclear organoaluminium fluoride compounds such as $[(Me_2AlF)_4]$ can be used to prepare aluminium fluoride clusters and cage compounds [36].

Me_3SnF has proven to be a versatile reagent in organoaluminium chemistry. Its usefulness can be found in many different reaction systems. Me_3SnF was introduced as a fluoride/chloride exchange reagent to convert main group chlorides to their corresponding fluorides [37]. Later, it was also used in fluoride/alkyl and fluoride/hydride exchange reactions [3]. In aluminium chemistry, its ability to convert organoaluminium compounds into their fluoride counterparts was first tested on aminodimethylaluminium compounds and proved to be very effective. When a methyl group was exchanged with fluorine, Me_4Sn was formed. This volatile molecule was easily removed from the product under low pressure [38].

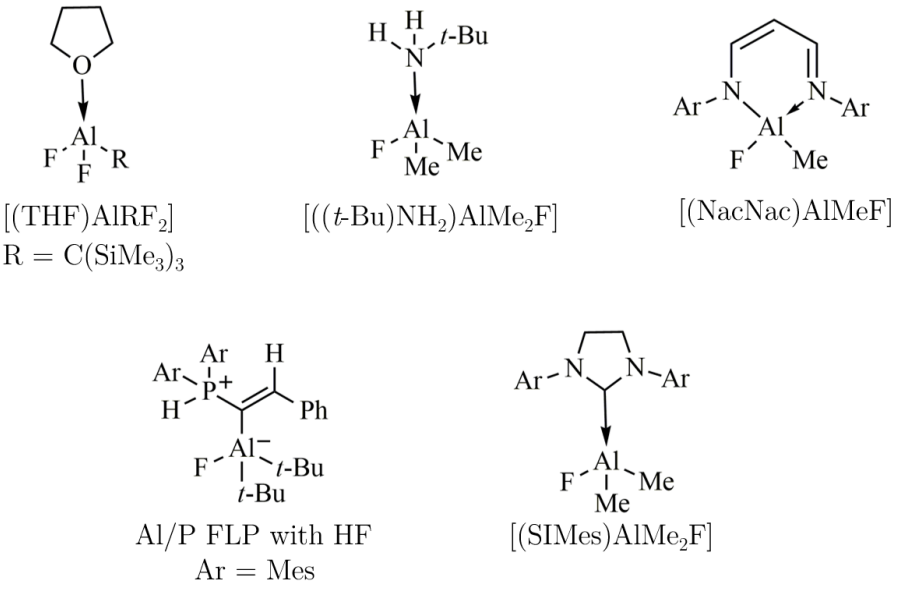

Figure 1.3: Different discrete organoaluminium fluoride compounds.

In 2000, the first discrete diorganoaluminium fluoride was described by Roesky's group. [((*t*-Bu)NH_2)$AlMe_2F$] was prepared by the reaction of (*t*-Bu)NH_2 with Me_2AlF in toluene [39]. Similar reactions between primary amines and organoaluminium compounds were already known at that time. They led to the formation of trimers $[MeAlNR]_3$ *via* a two-step elimination reaction [40]. Similarly, Me_2AlF also reacted with a more acidic primary amine to form a tetrameric ring system $[(Me_2Al)_4(NH(Dipp))_2F_2]$ [39].

An important development in the chemistry of organoaluminium fluorides is due to the introduction of β-diketiminato ligands [41]. These bidentate ligands are able to incorporate metal atoms as part of stable C_3N_2M six-membered rings by bonding with their two nitrogen atoms. They are also able to stabilise species in low oxidation state and low coordination number at the metal centre [27]. In 2006, a series of organoaluminium fluoride compounds stabilised by β-diketiminato ligands was published. The [(NacNac)AlMeF] was prepared by a fluoride/halide exchange reaction from the corresponding chloride counterpart using Me_3SnF, while the aluminium difluoride compound [(NacNac)AlF_2] was obtained by a fluoride/hydride exchange reaction from the corresponding aluminium dihydride using $[(Et_2O)BF_3]$ [42].

Later, β-diketiminato ligands allowed chemists to use other synthetic methods for the preparation of C−Al−F bonds. Oxidative addition of fluorinated organic compounds to the stabilised Al(I) centres by C−F bond activation produces a diverse array of organoaluminium fluoride compounds. Monomeric [(NacNac)Al] reacted with fluoroarenes, fluoroalkanes [43], [44], and fluoroalkenes giving various [(NacNac)AlArF] and [(NacNac)AlRF] compounds [45]. In parallel, the use of [(NacNac)AlH_2] was also employed for the synthesis of [(NacNac)AlRF] compounds through alumination reactions. In the presence of a catalyst [(NacNac)AlH_2] is capable of selectively converting C−F and C−H bonds of fluoroarenes and heteroarenes to C−Al bonds [46]. Catalytic amounts of zirconium, rhodium or palladium complexes were used as catalysts [46]–[48].

Furthermore, Uhl's group showed that the formation of C−Al−F motifs is also possible by using frustrated Lewis pairs. Various molecular ambiphilic compounds were synthesised by the reaction of Al/P FLPs with HF [49], CsF [50], and BF_3 [51].

Recently, the use of NHCs proved to be efficient for the stabilisation of discrete organoaluminium fluoride and aluminium fluoride compounds. Kemnitz's group prepared and spectroscopically characterised the [(SIMes)AlMe$_2$F] and [(SIMes)AlF$_3$]. They were prepared by fluoride/alkyl exchange reactions starting from the corresponding organoaluminium compound and by using Me$_3$SnF and SF$_6$ or Me$_3$SnF and SF$_4$, respectively [11].

1.2.2 Ionic organofluoroaluminate compounds

Orgaoaluminium compounds tend to react with Lewis bases to form tetrahedrally coordinated compounds. In the presence of fluoride anions, they usually form different organofluoroaluminate species $[R_{4-n}AlF_n]^-$ (n = 1–4). Furthermore, the high electronegativity of fluorine stimulates the formation of M−F−M bridging bonds, leading to the formation of polynuclear anions [3]. Depending on the number of bridging fluorides, dimeric [52]–[56], and sometimes even trimeric anions are formed [53]. Organofluoroaluminate fragments are also found in higher complex ionic compounds with electropositive metals such as lithium [57], sodium [58], potassium [59], titanium [31], zirconium [32], and hafnium [33].

However, compounds containing discrete organofluoroaluminate anions are still rare. Prior to our publication [26], there was only one structurally characterised compound with discrete $[R_3AlF]^-$ anions, three with discrete $[R_2AlF_2]^-$ anions and one with discrete $[RAlF_3]^-$ anion, in the CSD database. The structurally characterized organofluoroaluminate anions are shown in Figure 1.4.

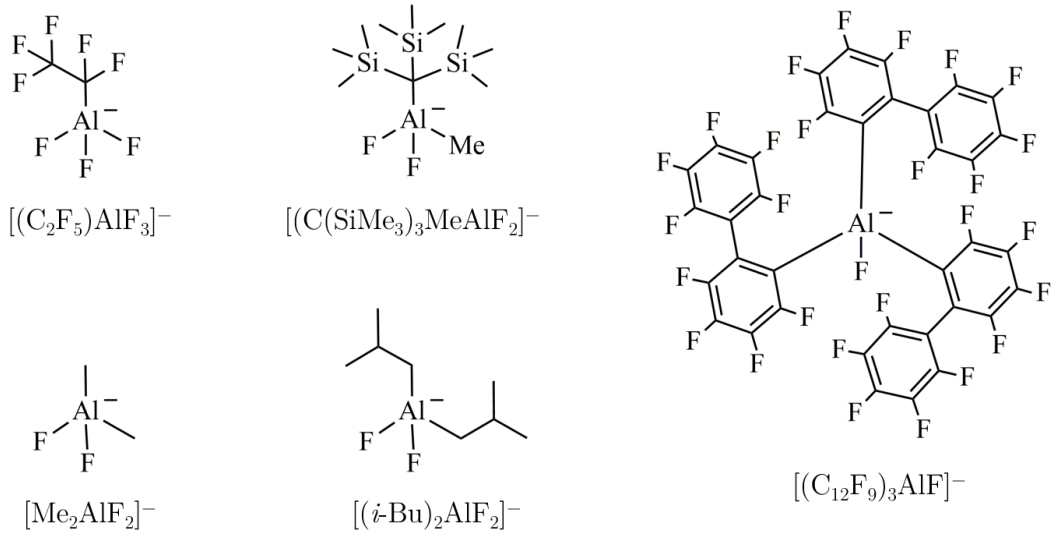

Figure 1.4: Structurally characterised organofluoroaluminate anions, prior to our publication.

Compounds containing $[AlF_4]^-$ anions do not belong to the organofluoroaluminate family, but are related to them. The reactions with excess HF lead to the complete removal of the substituents and the formation of $[AlF_4]^-$ anions. They also tend to form when HF-based reagents react uncontrollably with AlR_3 compounds [19], [60]. Compounds containing such anions have already been described in Chapters 1.1.2.

Prior to our publication [26], there was no suitable synthetic procedure for the preparation of discrete organotrifluoroaluminate anions $[RAlF_3]^-$. The only crystallographically known representative is the $[(C_2F_5)AlF_3]^-$ anion, which was crystallised

in the [PNP][$(C_2F_5)AlF_3]\cdot Et_2O$ structure. It formed during the degradation of the $[Al(C_2F_5)_4]^-$ anion in diethyl ether. The replacement of the C_2F_5 substituent by fluorine was associated with the loss of $CF(CF_3)$ [25].

On the other hand, an effective synthetic procedure for the preparation of discrete diorganodifluoroaluminate anions $[R_2AlF_2]^-$ was reported by Roesky's group in 2000. The syntheses were carried out by protolysis of AlR_3 compounds with reagents based on bifluoride. During the reaction, two fluoride ions are added to the aluminium centre and an alkane (RH) is eliminated [60], [61]. Three discrete $[R_2AlF_2]^-$ anions were prepared by the same group and structurally characterised in the structures of $[(n\text{-}Bu)_4N][Me_2AlF_2]$ [61], $[(n\text{-}Bu)_4N][(C(SiMe_3)_3MeAlF_2]$ [61], and $[Me_4N][(i\text{-}Bu)_2AlF_2]$ [60].

In the past, Ziegler's group synthesised compounds with triorganofluoroaluminate fragments $[R_3AlF]^-$ [62]. They obtained $M[R_3AlF]$ compounds by mixing AlR_3 compounds with alkali metal fluorides. However, careful electronic and spectroscopic study of these species indicated that they are not fully ionic [63]. In fact, fluorine atoms tend to form bridging bonds between the two metals, leading to the formation of dimeric structures, such as the structurally characterised dimer of $Cs[Me_3AlF]$ [3], [64]. To date, there is only one example of structurally characterised discrete triorganofluoroaluminate anion $[(C_{12}F_9)_3AlF]^-$, which could be isolated due to steric stabilisation of large perfluoroaryl groups. The anion was prepared by the reaction of $C_{12}F_9Li$ and $AlCl_3$, forming $[Li][(C_{12}F_9)_3AlF]$. After cation exchange with $[Ph_3C]^+$, the salt $[Ph_3C][(C_{12}F_9)_3AlF]$ was structurally characterised [65], [66].

1.3 N-Heterocyclic Carbenes

Carbenes are defined as neutral compounds with the R_2C: moiety. The divalent carbon atom has only six electrons in its valence shell, making it coordinatively unsaturated due to its incomplete electron octet. For a long time, carbenes were known as highly reactive and unstable intermediates formed only during organic transformations [67]. However, after the isolation of the first carbene species in 1988 [68], and the structural characterisation of the first "bottleable" N-heterocyclic carbene in 1991 [69], carbene chemistry underwent a tremendous expansion. Nowadays, N-heterocyclic carbenes are indispensable in various research areas and applications, e.g. materials science, homogeneous catalysis, organocatalysis and medicine [70].

By definition, N-heterocyclic carbenes are heterocyclic species that contain a divalent carbon and at least one nitrogen atom within the heterocyclic ring. The size of the ring, the number of nitrogen atoms, the structure and the functionalisation of the ring are not defined. Therefore, a large number of different N-heterocyclic carbene classes can be found in the literature, each with different properties [67]. The most common classes are presented in Figure 1.5. The largest class of N-heterocyclic carbenes are still those with five-membered rings and two nitrogen atoms. Therefore, in this work, the abbreviation NHC is used to describe imidazolylidene and imidazolidinylidene compounds. Recently, the pyrrolidinylidenes have been the most researched group of the N-heterocyclic carbene family. They are also known as cyclic alkyl(amino)carbenes or CAACs [71]. The NHCs and CAACs are both important compounds in our work. Therefore, we will explain their properties and bonding to metal centres in more detail.

In general, the properties of an N-heterocyclic carbene are influenced by its steric and electronic parameters. Since N-heterocyclic carbenes can have different substituents and different ring structures, their properties can be fine-tuned. Bulky substituents contribute to the kinetic stabilisation of a carbene centre. Consequently, bulky ligands usually have better stabilising properties, but in some cases their steric bulk may prevent the overlap of

orbitals between the ligand and the metal. The backbone also provides additional stabilisation by forming an aromatic system. In addition, the backbone can also carry other substituents that affect the properties of an N-heterocyclic carbene [67].

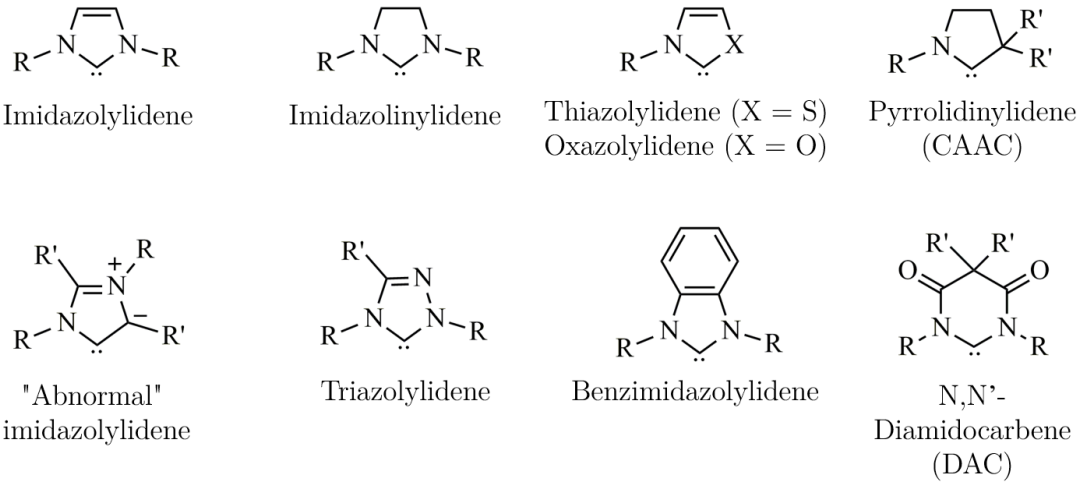

Figure 1.5: Different classes of N-heterocyclic carbenes.

On the other hand, the electronic parameters of N-heterocyclic carbenes are strongly influenced by the nitrogen atoms within the imidazolium ring [72]. To understand the electronic effect of hetero-atoms, one needs to know where the electrons are located in a singlet carbene. The carbene singlet carbon atom is sp^2-hybridized with two non-bonding electrons occupying the σ-orbital while the p_π-orbital remains unoccupied. The nitrogen atoms contribute to the stabilisation of the carbene moiety in two ways. First, due to their high electronegativity, they are able to withdraw electrons from the σ-bonds with carbon, lowering the energy of the occupied σ-orbital through the negative inductive effect. Secondly, they are able to donate their lone electron pairs into the empty p_π-orbital of the carbene, thus further stabilising the carbene moiety by their positive mesomeric effect [73], [74]. The described influences of the heteroatoms in the NHCs and CAACs are presented in Figure 1.6.

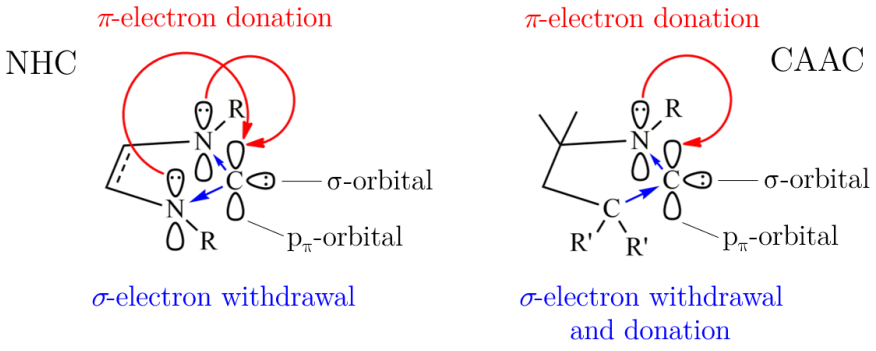

Figure 1.6: Electronic stabilization of NHC and CAAC carbenes.

The donating abilities of a ligand are associated with the energy of the HOMO (σ-orbital), while its accepting properties are characterised by the energy of the LUMO (p_π-orbital). A higher HOMO energy leads to ligands with better electron donating ability, while a lower LUMO energy gives the ligands better electron accepting properties. The

energy gap between HOMO and LUMO represents the energy difference between the singlet and triplet ground states and determines the stability of carbene ligands [75]. The steric and electronic nature of NHCs confers them the ability to be strong σ-donating ligands with strong nucleophilic and basic properties, while they also possess slight π-accepting ability due to the free p_π-orbital [71].

On the other hand, CAACs possess only one nitrogen atom within the heterocyclic ring. Consequently, the σ-donating ability of the quaternary carbon atom next to the carbene carbon atom increases the energy of HOMO, while the lack of π-donating abilities decreases the energy of LUMO. Compared with NHCs, CAACs exhibit stronger σ-donating and better π-accepting properties, which makes them not only more nucleophilic and electrophilic than NHCs, but also more basic. In addition, the quaternary carbon atom at α position provides a steric environment that distinguishes CAACs from other ligands. The peculiar electronic and steric properties enable CAACs to stabilise unusual main group element species [76].

NHCs and CAACs usually form complexes with metals of the $[(NHC)MX_n]$ type, in which they act as σ-donating ligands with little metal-to-ligand π-backdonation. In aluminium chemistry, such complexes are usually described as donor-acceptor adducts. Schematically the dative C−Al bonds are usually drawn as arrows, which suggest that carbenes act as two-electron donor ligands. Alternatively, the adducts can be represented as ylide imidazolium compounds with polarised bonds [70]. Both forms are shown in Figure 1.7.

Donor-acceptor adduct

Ylide imidazolium compound

Figure 1.7: Schematic representation of donor-acceptor aluminium adducts.

Carbenes are usually considered as spectator ligands in metal complexes or as robust organocatalysts [67] that do not react with metals or interfere with the catalytic process. However, it has been shown that N-heterocyclic carbenes are anything but innocent, as they can react with various compounds in a variety of ways. For example, in the presence of Brønsted acids such as hydrogen halides or phenols, the basic character of the carbenes predominates, leading to deprotonation and the formation of the corresponding NHC salt. Singlet carbenes can also activate some element-element bonds and undergo various oxidative addition reactions [77]. NHCs can undergo dehydrocoupling reactions when they act as hydrogen acceptors [78], ring-opening or ring-expansion reactions. Ring-opening reactions usually occur by solvolysis [79]. For example, the formation of ring-opening products has been observed in the activation of B−H and Al−H bonds [77], [80]. But this type of reaction is rarely studied. Ring-expansion reactions occur when a main group element is inserted into the five-membered carbene ring. In recent years, ring-expansion reactions of NHCs with Lewis acidic hydrides such as silanes, boranes or beryllium hydrides have been reported [77].

CAACs, with their smaller HOMO-LUMO gap and higher electrophilicity compared to NHCs, allow the activation of various E−H and E−E bonds (E = B, N, Si, P) and the formation of bond-cleaved products [77]. CAACs are also able to activate small molecules under mild conditions [81]. They can react with CO to form a stable ketene CAAC=C=O

[82], activate molecules such as H_2 and NH_3 to form stable cleaved products $CAACH_2$ and $CAAC(H)NH_2$ [83], undergo intramolecular C−H activation to form a tricycle, and react with a variety of sp-, sp^2-, and sp^3-hybridised C−H groups to form CAAC(H)R compounds [84].

1.4 Aluminium Hydrides

The chemistry of aluminium hydrides has developed enormously, since the first synthesis of AlH_3 by Stecher and Wiberg in 1942 [85]. At that time, it was difficult to work with group 13 metal hydrides. All binary hydrides of group 13 metals are extremely sensitive to air and moisture [30]. They are also not thermally stable as they tend to decompose at ambient temperature. Working with such compounds requires careful handling *in vacuo* and other special procedures [86]. Because of their instability, the synthesis of binary metal hydrides was only studied in laboratories and had no applicable value at the time [87].

Binary aluminium hydrides form various polymeric AlH_3 structures in the solid state [88]. However, only the α-AlH_3 form is stable under normal conditions. Other modifications (α´, β and γ) eventually decompose to α-AlH_3 [89]. The structure of AlH_3 is very similar to that of AlF_3. It consists of octahedrally coordinated AlH_6 units arranged in a polymeric formation by corner or edge shearing [90], [91].

In 1946, $LiAlH_4$ was introduced by Schlesinger and his group as a new reducing agent for various organic and inorganic compounds [92]. More than 70 years later, $LiAlH_4$ is still one of the most effective commercially available reducing agents. It has evolved from a laboratory-scale reagent to mass-produced product used on a large industrial scale. Its widespread use is mainly due to its good solubility in ethereal solvents, which makes it highly reactive towards a wide range of substrates [93].

In order to expand the use of aluminium hydrides, researchers have attempted to prepare aluminium hydride compounds with increased thermal stability that can be easily handled. To achieve this, the reactive AlH_3 fragments can be stabilised either by forming adducts with Lewis bases or by replacing one or two hydride atoms with another substituent [87]. Stabilised and functionalised aluminium hydrides have proven to be useful for many applications, for example as precursors in materials science [94], or as catalysts in organic transformations [95]. Both approaches are described in detail in the following chapters.

In the second half of the 20^{th} century, interest in aluminium hydrides came to a halt. Their use was overshadowed by the growing field of transition metal catalysis. Interest in the chemistry of aluminium hydrides has been revived in the last 15 years as researchers have found that there are many advantages to using aluminium instead of transition metals. Aluminium is not only less toxic compared to other heavier metals, but also inexpensive, which makes it suitable for catalytic applications [96].

Nowadays, aluminium hydrides are no longer used in catalysis as simple salts, but in the form of new, tailor-made catalysts. Aluminium hydrides with well-designed ligands and substituents at the metal centre have the potential to be used as catalysts for selective organic transformations [95].

1.4.1 Neutral AlH_3 adducts with Lewis bases

AlH_3 stabilised by neutral Lewis bases is usually more thermally stable and more soluble in common organic solvents than binary AlH_3, making it easier to handle. Aluminium hydrides can be prepared by the reaction of $LiAlH_4$ with H_2SO_4 [97], poly(hydrogen chloride)-based reagents [98], or from other sources [99]. The reactions are usually

accompanied by the evolution of H_2 and the formation of LiCl salt [98]. The aluminium hydrides obtained readily form adducts with neutral electron-donating ligands, such as ethereal solvents or amines. In THF, relatively stable adducts form, such as $[(THF)_2AlH_3]$ and $[(THF)AlH_3]_2$ [100]. Anime adducts can also be easily obtained by displacing the ethers with amine bases [101]. Adducts with other Lewis bases are usually prepared by ligand exchange reactions, starting from the amine adducts, such as $[(Me_3N)AlH_3]$ [102].

Aluminium hydrides can react with Lewis donors in a 1:1 and 1:2 stoichiometry, resulting in adducts with 4- or 5-coordination at the Al centre. Adducts with 4-coordination generally adopt a pseudo-tetrahedral configuration at the metal centre, while the adducts with 5-coordinated centres usually adopt a trigonal bipyramidal arrangement in the solid state [103]. An overview of different structurally characterised adducts, depending on the coordination at the metal centre, can be found in Figures 1.8 and 1.9.

$AlH_3 : L = 1 : 1$

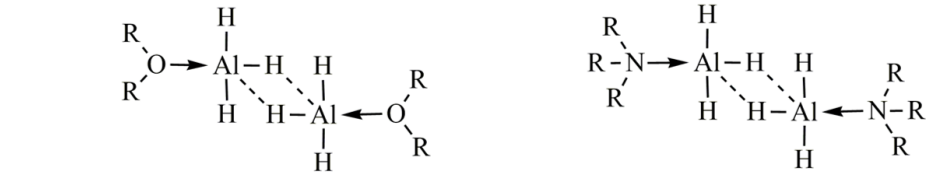

$AlH_3 : L = 1 : 2$

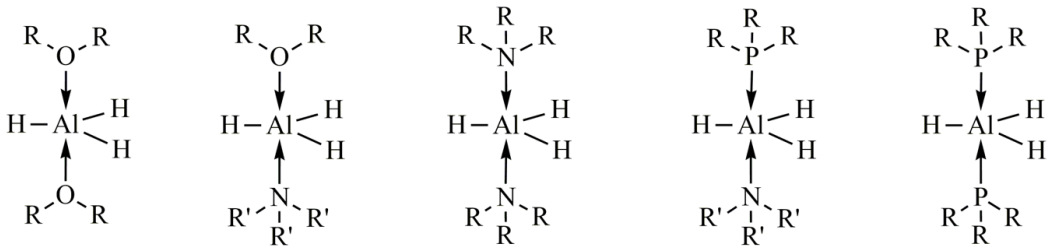

Figure 1.8: Different types of 5-coordinated AlH_3 adducts with trigonal bipyramidal arrangement at the metal centre. AlH_3 and donor ligands are in 1:1 and 1:2 stoichiometry.

In the last 70 years, a large number of aluminium hydride adducts with electron-donating ligands such as ethers, amines, phosphines and carbenes have been synthesised and structurally characterised. Small ligands, such as tertiary amines and ethers, tend to form adducts with AlH_3 in a 1:1 and 1:2 stoichiometry [100], [104]. 1:1 adducts usually have a dimeric structure with five-coordinated Al centres in the solid state, whereas in the gas phase they act as tetrahedrally coordinated monomers [105]. 1:1 adducts with secondary amines can also be prepared, but they are only stable at low temperatures, as secondary amines tend to undergo metalation in the presence of AlH_3 [106]. 1:2 adducts have a monomeric structure with five-coordinated aluminium centres [107]. Bulkier ligands, such as tertiary phosphines and carbenes, tend to form tetrahedrally coordinated adducts with AlH_3. Carbene ligands have a similar binding tendency to phosphines. However, since carbene chemistry is of interest to us, carbene adducts are presented separately in the following chapters. Tertiary phosphines react with AlH_3 to form monomeric adducts such as $[(Ph_3P)AlH_3]$, while the use of bidentate ligands leads to the formation of bridging products, as they do not tend to form chelating bonds [108]. Mixed complexes with phosphine and amine ligands have also been prepared. All of them have a five-coordinate configuration at the aluminium centre [109], [110].

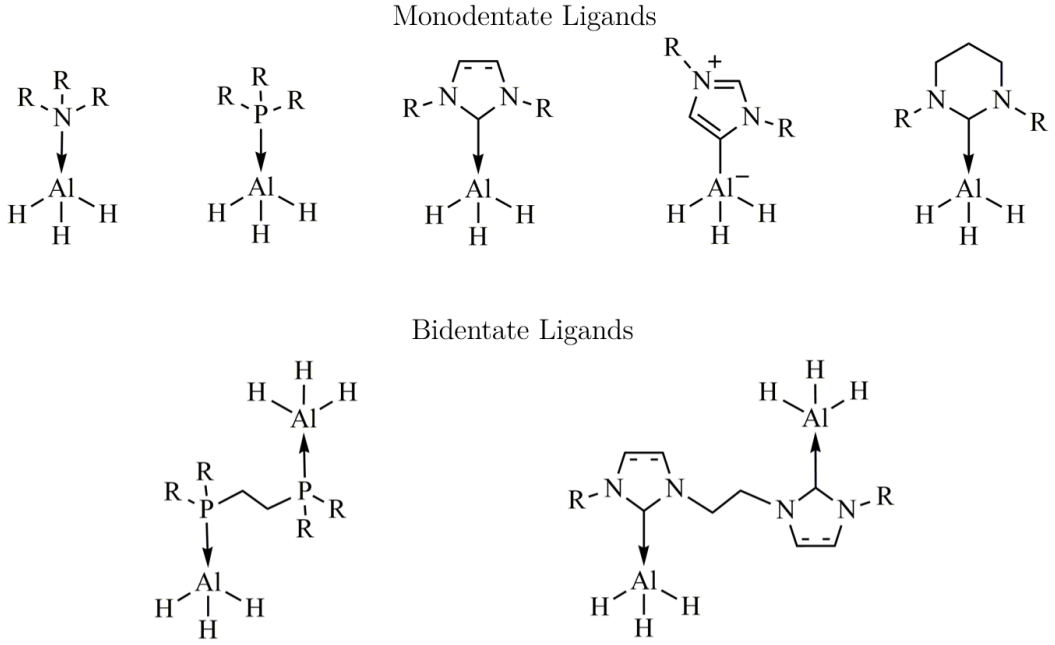

Figure 1.9: Different types of 4-coordinated AlH_3 adducts with pseudo-tetrahedral configuration at the metal centre. AlH_3 and donor ligands are in 1:1 and 2:1 stoichiometry.

In the last 20 years, the chemistry of amine-stabilised aluminium hydrides has developed enormously. Various anionic ligands have been investigated in the search for highly developed ligands. Through their use, numerous aluminium dihydride compounds have been isolated. Such species can be obtained when one hydride atom is replaced by an anionic ligand while the other heteroatom of the ligand binds in a coordinative manner [111]. A wide range of aluminium hydride compounds have been prepared by using different anionic ligands, such as pyrrolyl ligands [112], and their structurally related pincer-type ligands [113], triazenide ligands [114], iminophosphonamide ligands [115], boraamidinate ligands [116], amidinate ligands [117], amido-amine ligands [118], [119], amidophosphine ligands [120], β-diketiminato ligands [121]–[125], their structurally related methanediide ligands [126], [127], phosphinimine-amide ligands [128], and guanidinate ligands [129]–[131], phosphinimine ligands [132], their structurally related imidazolyl-2-iminato ligands [111], and other amine ligands [133]–[135].

1.4.1.1 N-heterocyclic carbene stabilised AlH_3 compounds

The first NHC-aluminium hydride adduct [(IMes)AlH_3] was prepared and structurally characterised by Arduengo in 1992 [136]. This first example was followed by many others, and today a large variety of NHC-stabilised AlH_3 adducts are known [70].

NHCs react with AlH_3 as two electron donors in a similar way to tertiary phosphines and ethers [137]. Reactions in 1:1 stoichiometry lead to monomeric adducts with a tetrahedrally coordinated aluminium centre. Many complexes of this type have been structurally characterised, including [(IMes)AlH_3] [136], [(IiPr)AlH_3] [137], [(IPr)AlH_3][138], [(IBn)AlH_3] [139], [(ItBu)AlH_3] and its abnormal isomer [(aItBu)AlH_3] [140]. The use of a bidentate carbene of the NHC–CH_2–CH_2–NHC type led to the formation of bridging products rather than chelating species [141]. The same behaviour was observed for tertiary phosphines. NHCs form particularly strong Al−C σ-bonds, which are usually stronger than the corresponding M−P bonds in phosphine adducts [70]. Consequently, NHC-aluminium hydride adducts exhibit significantly higher thermal stability than P-donor adducts [142].

The outstanding stabilisation properties of NHC ligands are also evident in the formation of species with aluminium in the low oxidation state. In 2010, the synthesis of an unprecedented NHC-stabilised dialane(4) (Al_2H_2) was reported [143].

The bulkiness of NHCs plays an important role in the kinetic stabilisation of adducts with main group elements [138]. In 2017, a bis-NHC-aluminium hydride adduct bearing a penta-coordinated aluminium centre [$(NHC)_2AlH_3$] was prepared. However, this penta-coordinated product was never structurally characterised [77]. Later, Trose's group demonstrated that the addition of an NHC to a pre-formed [$(NHC)AlH_3$] complex leads to a fluctuation of AlH_3 between two NHC ligands. They proposed the formation of a penta-coordinated intermediate species that exists only in solution [142].

1.4.1.2 Cyclic alkyl(amino)carbene stabilised AlH_3 compounds

In recent years, many attempts have been made to prepare complexes between CAACs and AlH_3. They all failed because of the special electronic properties of CAACs. In the presence of hydrides, these compounds do not react as two electron donors. Instead, they have the ability to activate Al−H bonds and insert themselves between aluminium and hydrogen. The products formed are the result of the oxidative addition of aluminium hydrides to CAACs [77]. An overview of the different CAAC-aluminium hydride species can be found in Figure 1.10.

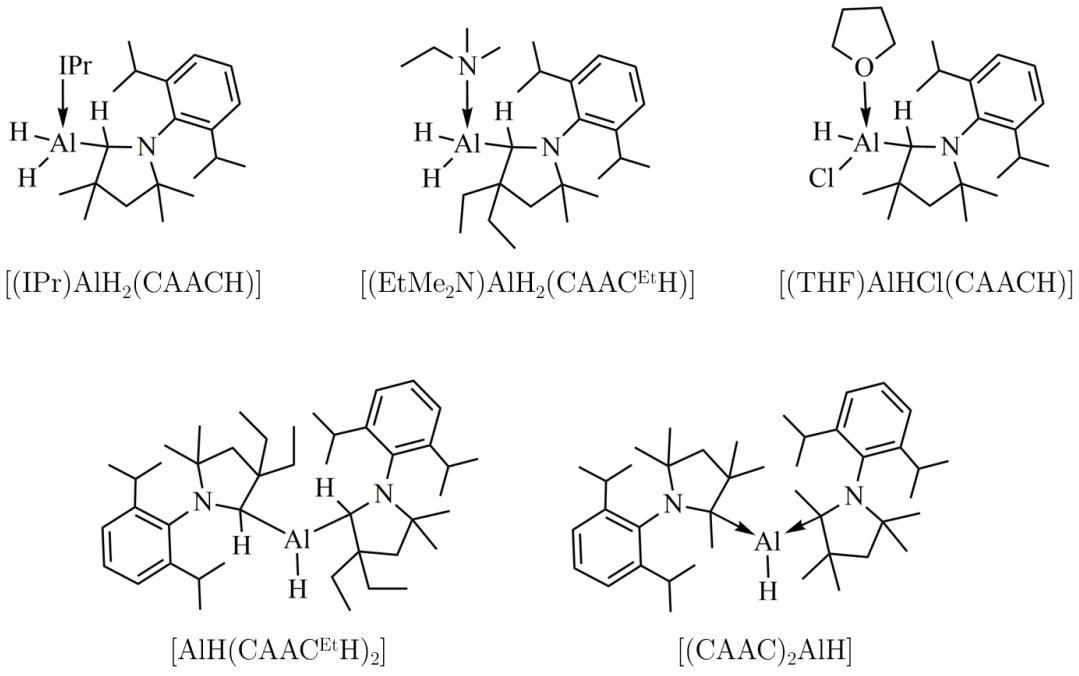

Figure 1.10: Structurally characterised CAAC aluminium hydride compounds.

The insertion of CAACs into Al−H bonds was first observed by Radius's group. They attempted to prepare CAAC-stabilised aluminium hydrides by ligand substitution starting from [$(NHC)AlH_3$] and free CAAC. Regardless of the steric requirements of the NHC, they always obtained oxidative addition products [$(IPr)AlH_2(CAACH)$] [77]. A similar result was published a year later by Stephen's group. They prepared [$(EtMe_2N)AlH_2(CAAC^{Et}H)$] starting from amine-stabilised aluminium hydride and free CAAC [144]. Recently, Roesky and co-workers reported another oxidative addition product using of a mixed aluminium hydride chloride and CAAC in THF [(THF)AlHCl(CAACH)] [145].

Stephen's group also reported the formation of a monomeric aluminium hydride species [AlH(CAAC^{Et}H)$_2$] by the reaction of amine-stabilised AlH_3 with two equivalents of CAAC, which is the first isolated example of a neutral monomeric dialkylaluminium hydride [144]. Careful evaluation of this compound revealed that C_{CAAC}—H and Al—H exchange protons. The migration of a C_{CAAC}—H proton to the aluminium centre presumably produces an intermediate aluminium dihydride stabilised by the CAAC [(CAAC^{Et})AlH$_2$(CAAC^{Et}H)] [144]. A similar reaction was previously observed for the boron analogue [(CAAC)BH$_2$(CAACH)] [146].

CAACs have surprising stabilising properties for low-valent and radical species. While Al(III) acts as a Lewis acid, Al(I) is a rare, nucleophilic variant that is thermodynamically unstable under ambient conditions. Recently, a monomeric CAAC-stabilised Al(I) hydride was prepared. It was described as an Al(I) hydride with non-negligible open-shell Al(III) singlet diradical character [(CAAC)$_2$AlH] [147].

1.4.2 Functionalisation of AlH_3

Partial replacement of the hydride by another substituent is another method that improves the stability of aluminium hydride compounds. The presence of a more electronegative atom instead of hydrogen leads to a hydride species with improved thermal and air stability, higher Lewis acidity and stronger M—H bonds [148]. Functionalised aluminium hydride adducts have excellent catalytic properties in organic transformations comparable to those of parent aluminium hydrides [149]. In addition, they are non-pyrophoric due to their larger Lewis acidity and exhibit improved regioselectivity [150].

The substitution of one or two hydride atoms by bulky organic substituents allows the formation of monomeric derivatives of the $RAlH_2$ and R_2AlH type. The steric effect of the organic substituents prevents the aggregation of the MH_n units and allows the formation of monomeric compounds even without Lewis bases [87]. Many other substituents have been used to functionalise Lewis base-stabilised aluminium hydride adducts, such as halides and triflates [148]. In our research, we were particularly interested in substituted aluminium hydrides stabilised by NHCs. Therefore, the literature review is mainly focused on them.

Recently, Radius's group proved that NHC-stabilised AlH_3 adducts are susceptible to functionalisation with secondary amines and phenols [151]. The resulting functionalised compounds were thermally stable and showed no tendency to undergo ring-expansion or ring-opening reactions, which are readily available to [(NHC)AlH_3] adducts [151]. Increased stability was also observed for aluminium hydride chloride [148], and aluminium hydride triflate compounds [149]. Both types of partially substituted aluminium hydrides are relevant to our work and are described in detail in the following chapters.

1.4.2.1 Aluminium hydride halide compounds

The chemistry of aluminium hydride halide compounds has been explored to some extent. In the second half of the 20th century, many aluminium hydride halides stabilised by ethers or tertiary amines were prepared. Many procedures have been proposed in the literature to obtain mono- and disubstituted products, ranging from reactions of $LiAlH_4$ with AlX_3 or LiH with AlX_3 in ethereal solvents [152], to halogenation of preformed aluminium hydride adducts with anhydrous HX, HgX_2, ammonium or phosphonium salts (X = Cl, Br or I) [148].

Some attention has also been given to NHC-stabilised aluminium hydride halide adducts. An overview of the synthetic methods for the preparation of various NHC-stabilised aluminium hydride halide adducts proposed prior to our publication [153] is given in Schemes 1.1 and 1.2.

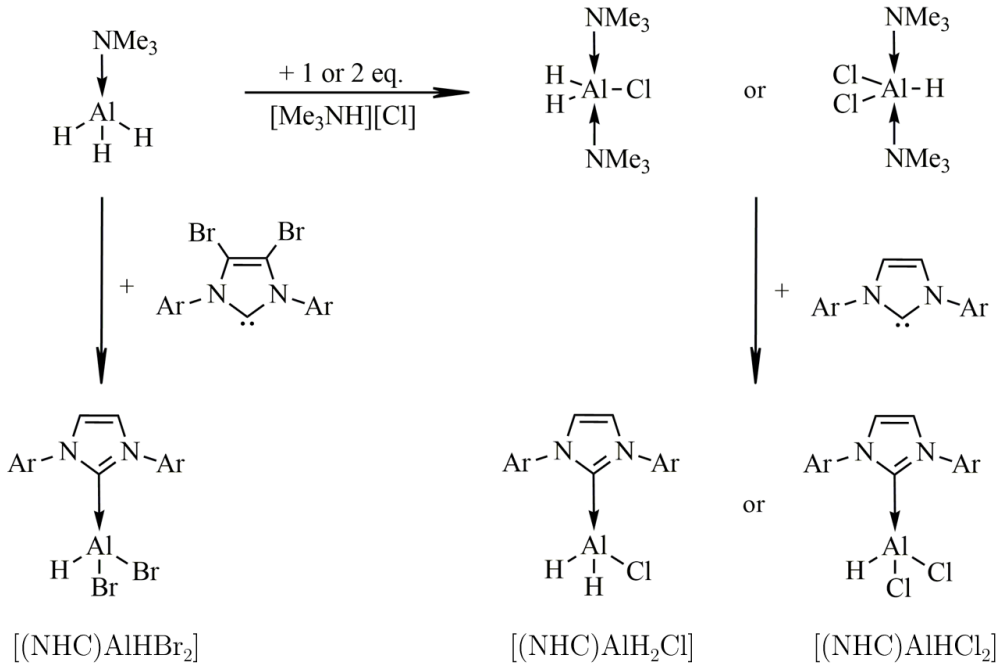

Scheme 1.1: Reported methods for the preparation of NHC-stabilised aluminium hydride chloride and bromide adducts.

Cole's group succeeded in preparing chloro- and bromo-substituted aluminium hydrides by two different methods. NHC-stabilised aluminium hydride chlorides were accessible by ligand exchange reactions from the pre-formed tertiary amine adducts. Mono- and disubstituted adducts [(IMes)AlH_2Cl] and [(IMes)$AlHCl_2$] were prepared in this way [150], [154]. The NHC-stabilised aluminium hydride bromide was obtained by an exchange reaction between hydride atoms on aluminium and bromine atoms on the NHC backbone (^{Br}IMes). Only the disubstituted adduct [(IMes)$AlHBr_2$] was prepared in this way [155].

Recently, many NHC-stabilised aluminium hydride iodide adducts have been prepared. The disubstituted NHC adducts [(IPr)$AlHI_2$] and [(IMes)$AlHI_2$] were prepared by a halide/hydride exchange reaction from the corresponding [(NHC)AlH_3] adduct with MeI [142], while the monosubstituted NHC adducts [(IPr)AlH_2I] and [(IMes)AlH_2I] were obtained by the redistribution reaction between the corresponding AlH_3 and AlI_3 adducts [142]. The monosubstituted adducts [(^{Me}IMe)AlH_2I] and [(^{Me}IiPr)AlH_2I] were also prepared by the reaction of the corresponding AlH_3 adduct with elemental iodine [156].

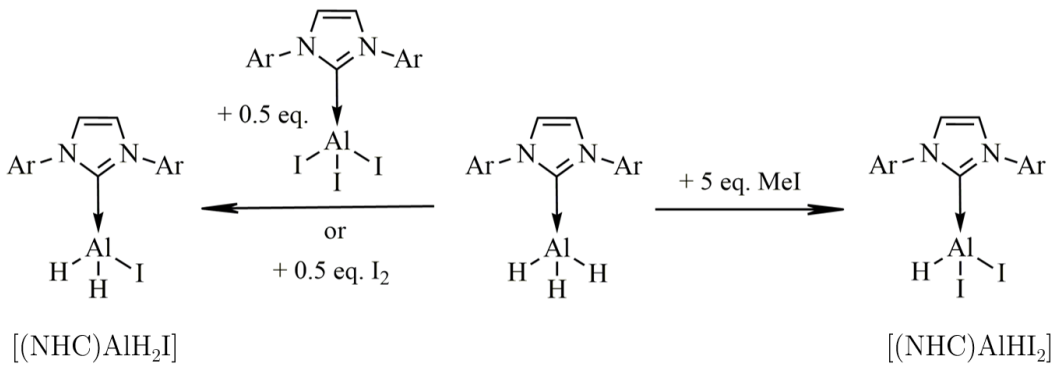

Scheme 1.2: Reported methods for the preparation of NHC-stabilised aluminium hydride iodide adducts.

So far, only one mixed aluminium hydride fluoride compound has been structurally characterised. The [(NacNac)AlHF] stabilised by a β-diketiminato ligand was prepared by a redistribution reaction between [(NacNac)AlH_2] and [(NacNac)AlF_2] [47].

1.4.2.2 Aluminium hydride triflate compounds

The substitution of hydrides by triflates is less studied compared to halides. As far as we know, no NHC-stabilised compounds are known, except the one we reported [153]. Only 4 other examples of Lewis base-stabilised mixed aluminium hydride triflates have been structurally characterised. The 4 compounds are shown in Figure 1.11. Phosphinimine, imidazolin-2-imine, and amidophosphine-stabilised aluminium dihydrides reacted easily with Me_3SiOTf affording the corresponding mixed aluminium hydride triflates [111], [132], while the [(NacNac)AlH_2] was converted to [(NacNac)AlHOTf] with MeOTf [149].

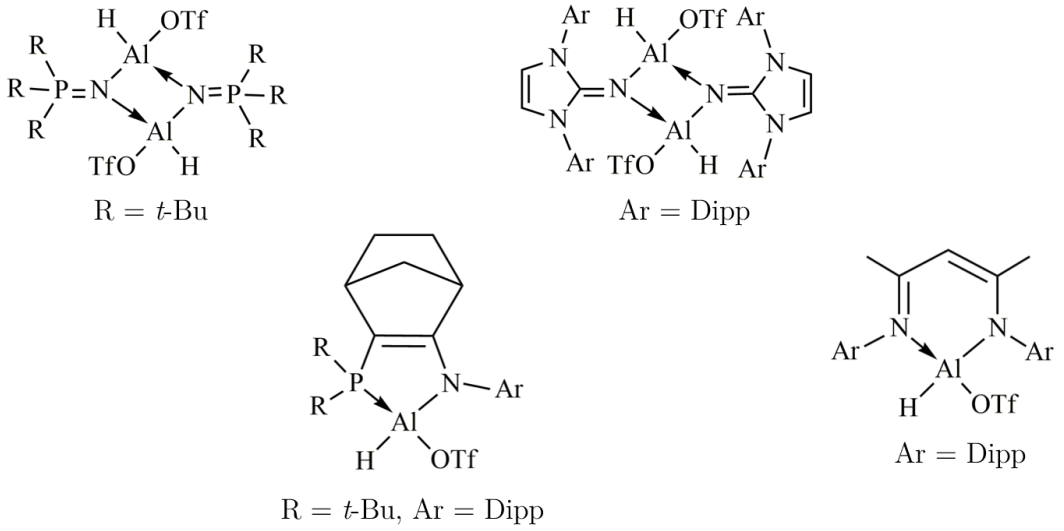

Figure 1.11: Aluminium hydride triflate compounds. They are stabilized by phosphinimine (upper left), imidazolyl-2-imine (upper right), amidophosphine (bottom left) and β-diketiminato ligands (bottom right).

1.5 Fluorinating Reagents

In Chapters 1.1 and 1.2 we described various synthetic approaches to the formation of discrete aluminium fluoride and organoaluminium fluoride compounds, either in their neutral or ionic forms. In both cases, the number of discrete species is very limited. On the one hand, this is due to the fact that there is no conventional synthetic procedure for the introduction of fluorine into aluminium compounds [7]. On the other hand, a bulky stabilising reagent is required to stabilise discrete aluminium fluoride or fluoroaluminate species, as they usually tend to form polymeric and polynuclear formations [7]. In 2017, our group showed that the stabilisation of monomeric anionic species is possible by using a sterically demanding cation [157]. $[GeF_5]^-$ anions, which tend to polymerise and form infinite chains of GeF_6 octahedra [158], could be stabilised in discrete form by the bulky $[IPrH]^+$ cation. Stabilisation was possible not only because of the steric hindrance by the cation, but also because of its electrostatic interactions with the anions [157].

In the last decades, a variety of fluorinating reagents and different fluorination methods have been tested on inorganic and organic compounds and some of them are already used

in industry [159], [160]. Nevertheless, chemists are still searching for innovative, selective and easy-to-use reagents. The formation of C−F bonds significantly alters the physical, chemical and biological properties of organic compounds [161], making them invaluable to the pharmaceutical industry, medicine, agrochemistry and materials science [162].

In general, nucleophilic fluorinating reagents are based on fluoride or poly(hydrogen fluoride) anions. Both types are relevant to our work. Therefore, their development is presented in the following chapters. In a separate chapter, the imidazolium-based fluorination reagents are described.

1.5.1 Fluoride reagents

Fluorinating reagents that serve as sources of $[F]^-$ anions and have considerable solubility in organic solvents are often referred to as "naked fluorides". Although a truly naked fluoride cannot exist in solution or in the solid state, its "nakedness" can be measured by how easily a $[F]^-$ anion is transferred to the acceptor [163]. The use of soluble fluoride sources such as $[R_4N][F]$ or alkali metals has enabled the synthesis of many complexes with high coordination numbers [4]. They are also commonly used as nucleophilic fluorinating reagents in reactions to form C−F bonds [164].

Alkali metal fluorides such as KF and CsF are natural fluoride sources that are not expensive, abundant and readily available. However, their use is limited due to their low solubility in organic solvents. On the other hand, they form strong hydrogen bonds in protic solvents such as water, which reduces their nucleophilicity [164]. To overcome this problem, many phase transfer catalysts and salts with non-coordinating cations have been tested to allow the use of soluble "naked" fluorides. For example, crown ethers form a complex with KF that acts as a "naked" fluoride [165], while TBAF has a bulky cation that allows the salt to be readily soluble in organic solvents [166]. These "naked" fluorides act not only as strong nucleophiles but also as strong bases, which implicates them in many side reactions and reduces their selectivity [167]. In recent years, many methods have been developed to make $[F]^-$ anions from $[R_4N][F]$ or MF sources more "controllable" [164]. Hydrogen bonding with protic solvents lowers the basicity of such compounds while increasing their effective nucleophilicity [167].

Protic solvents such as water and alcohol were long considered unsuitable for nucleophilic fluorination. However, bulky alcohols tend to interact with $[F]^-$ anions to form solvated fluorides. An example can be found in Figure 1.12.

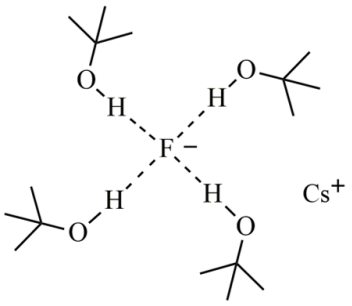

Figure 1.12: Interaction of *t*-BuOH with CsF.

Solvation weakens the strength of the ionic bond of the MF so that the solvated fluoride acts as a strong nucleophile that is much more "controllable". The nonpolar protic *t*-BuOH increased the rate of nucleophilic fluorination reactions with alkali metal fluorides and reduced the formation of by-products [168]. A similar effect was also obtained by using

t-BuOH in combination with TBAF. Furthermore, the formation of the TBAF(*t*-BuOH)$_4$ adduct was also proven by X-ray structural analysis [169]. Alcohols are not the only molecules that can influence the nucleophilicity of $[F]^-$ anions. Recently, the interactions with hydrogen bond-donating molecules such as urea have also been studied [170].

1.5.2 Poly(hydrogen fluoride) reagents

Hydrogen fluoride would be an ideal reagent for the fluorination of organic and inorganic compounds because it is cheap and atomically efficient. It can serve as both a fluoride donor and as a solvent [171]. However, the low boiling point, high toxicity and corrosiveness of gaseous HF make it difficult to handle [167]. A much safer method is to bind HF in a complex with a basic partner such as amine and pyridine. Both commercially available $Et_3N \cdot 3HF$ [172], and pyridine$\cdot n$HF, also known as Olah's reagent [173], [174], are easier to handle and their usefulness has been demonstrated with various substrates [175]. The structures of the poly(hydrogen fluoride) reagents described are shown in Figure 1.13.

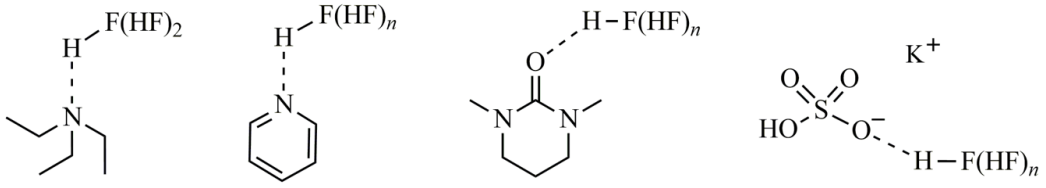

$Et_3N \cdot 3HF$ Pyridine$\cdot n$HF DMPU$\cdot n$HF $KHSO_4 \cdot n$HF

Figure 1.13: Poly(hydrogen fluoride)-based fluorinating reagents.

However, the basicity of the amine or pyridine can interfere with the course of some organic transformations. In addition, their Lewis base character also contributes to the formation of complexes with metals [167].

Later, more specific HF-base reagents were developed to perform selective transformations. They were developed after it was found that HF interacts with Lewis bases *via* hydrogen bonding rather than ionic interactions. Therefore, a strong hydrogen bond acceptor was a better candidate for selective fluorinating reagents because it is not necessarily a strong base. Strong bases also tend to decrease the acidity of HF, making it less active [167]. One such alternative is DMPU. A hydrogen bond acceptor that forms a complex with HF. It is weakly coordinating to metals and less basic compared to Et_3N and pyridine [176]. The DMPU$\cdot n$HF proved to be suitable for reactions requiring more acidic conditions [177]–[179]. Another fluorinating reagent developed is $KHSO_4 \cdot n$HF. It is characterised by high acidity, due to the -OH group on the anion, and high fluoride nucleophilicity, as the $[HSO_4]^-$ anion is a strong hydrogen bond acceptor. It proved to be a suitable reagent for reactions requiring acidic conditions. It can easily engage in the hydrofluorination of alkenes [180].

Imidazolium-based poly(hydrogen fluoride) fluorinating reagents are another class of reagents currently being explored. In the past, they were largely studied as ionic liquids prepared by the reaction of the corresponding chloride salt with anhydrous HF [181]–[186]. Today, as described earlier, they are successfully used in many organic and inorganic transformations.

1.5.3 Imidazolium-based fluorinating reagents

In the last 20 years, many imidazolium-based fluorinating reagents have been prepared. Most of them are in the form of salts, while some also have a neutral form. The different structures of imidazolium-based fluorinating reagents are shown in Figure 1.14.

Imidazolium-based poly(hydrogen fluoride) | Imidazolium-based fluoride | Ar = Dipp AlkylFluor™ | Ar = Dipp PhenoFluor™

Figure 1.14: Different imidazolium-based fluorinating reagents.

Among the various imidazolium-based salts, there are those with poly(hydrogen fluoride) anions [187], [188], with fluoride anions [189]–[192], or salts with a halide atom on C2 position such as AlkylFluor or PhenoFluorMix [193], [194]. On the other hand, PhenoFluor and its structural analogues are neutral fluorinating reagents with the CF_2 fragments within the imidazole rings. These compounds have received much attention recently. Due to their neutral structure, they are soluble in nonpolar solvents and have proved to be indispensable in the deoxyfluorination of organic compounds [195], [196]. Some of the neutral difluoro-reagents have also been used as carbene precursors for the formation of NHC−Ge, NHC−Sn and NHC−P bonds [197], [198].

In 2016, the [IPrH][F] was prepared by our group from the IPr carbene and KHF_2. Similarely, the poly(hydrogen fluoride) congeners [IPrH][(HF)F] and [IPrH][$(HF)_2$F] were also prepared from IPr carbene and the corresponding amount of HF-based reagents [199]. The three salts were also tested as nucleophilic fluorinating reagents on inorganic and organic substrates. The [IPrH][F] proved to be very useful for the synthesis and stabilisation of discrete anionic species. In 2017, our group showed that $[GeF_5]^-$ anions could be stabilised in discrete form by the sterically demanding $[IPrH]^+$ cation [157]. Other discrete fluoride containing anions, including $[VOF_4]^-$, $[NbF_6]^-$ and $[TaF_6]^-$, were also prepared by the use of [IPrH][F] [200], [201]. The high stability of the imidazolium-based fluorinating reagent and its solubility in polar organic solvents are also a major advantage compared to other fluoride reagents, such as alkali metal fluorides or TBAF [157]. On the other hand, [IPrH][$(HF)_2$F] proved to be the most suitable for organic transformations among the imidazolium-based fluorinating reagents. Its stability on air and solubility in polar organic solvents contributed greatly to its wide usability. It proved to be useful for the fluorination of benzyl chlorides, bromides, and iodides, aliphatic halides, mesylates, tosylates, α-haloketones, acyl and sulfuryl chlorides, a silyl chloride and a nitroarene [202].

Chapter 2

Aims and Hypothesis

The aim of this work was to prepare discrete aluminium compounds in their neutral or ionic form. The focus was on aluminium fluoride compounds that are soluble in common organic solvents. Due to the extent of the research, the work was divided into four subsections:

1. Discrete neutral aluminium fluorides.

AlF_3 is an important material with remarkable Lewis acidity that has attracted the attention of chemists for many decades. However, due to its chemical properties, AlF_3 is insoluble. It usually adopts a polymeric 3D structure and is rarely found in discrete compounds. To further explore its chemistry, it is necessary to increase its solubility by either replacing one or two fluorine atoms with organic substituents or stabilising the monomeric AlF_3 units with electron-donating ligands.

The aim of our work was to synthesise a discrete AlF_3 compound. In the past, many such attempts have proved unsuccessful, because aluminium fluorides have a strong tendency to polymerise and form solid AlF_3 with polymeric 3D structures. In our work, we tested the reactivity of CAAC-stabilised $AlMe_3$ with different fluorinating reagents. CAACs are strong electron donating ligands that have the ability to stabilise otherwise unstable main group species. In our opinion, they have the potential to stabilise discrete aluminium fluoride species as well as AlF_3 unit. The sterically demanding nature of CAACs has the potential to prevent the polymerisation of AlF_3 by hindering the contacts between the discrete AlF_3 units. At the same time, their electronic nature could influence the exchange of carbon atoms with fluorine in the coordination sphere of aluminium, thus enabling the stabilisation of rare aluminium fluoride and organoaluminium fluoride species.

2. Discrete organofluoroaluminates

Organoaluminium compounds are strong Lewis acids that tend to form various anionic species in the presence of fluoride anions. However, discrete organofluoroaluminate anions are still rare.

The aim of our work was to prepare compounds containing discrete triorganofluoroaluminate $[R_3AlF]^-$, diorganodifluoroaluminate $[R_2AlF_2]^-$ and organotrifluoroaluminate $[RAlF_3]^-$ anions. So far, compounds containing discrete $[R_3AlF]^-$ and $[RAlF_3]^-$ anions have rarely been characterised due to the lack of suitable synthetic procedures and the tendency of fluorine atoms to form bridging formations leading to polynuclear species. In our work, we have investigated the reactivity of AlR_3 compounds with nucleophilic fluorinating reagents based on imidazolium salts $[IPrH][(HF)_nF]$ ($n = 0$–2). The fluorinating reagents used have sterically demanding cations that have the ability to stabilise otherwise unstable anionic species. In our opinion, the imidazolium

cations in $[IPrH][(HF)_nF]$ ($n = 0$–2) are able to stabilise discrete organofluoroaluminate anions by hindering contacts between aluminium species and consequently preventing the formation of polyanions. Furthermore, reagents containing an appropriate amount of HF (1, 2 or 3 equivalents) have the potential to react selectively with AlR_3 compounds, leading to the formation of the desired discrete $[R_3AlF]^-$, $[R_2AlF_2]^-$ and $[RAlF_3]^-$ anions.

3. Functionalisation of NHC-stabilised aluminium hydride

Aluminium hydrides are important reagents in synthetic chemistry and materials science. However, relatively little is known about their partially substituted adducts.

The aim of our work was to prepare NHC-stabilised aluminium hydride triflate and aluminium hydride chloride adducts and to prove that aldiminium-based triflate and chloride salts can be used as group transfer reagents. To date, partially substituted aluminium hydride compounds have been studied to some extent. However, NHC-stabilised aluminium hydride triflate compounds were not known. Moreover, aldiminium-based salts have never been tested as group transfer reagents in aluminium chemistry. NHC carbenes are strong electron donating ligands capable of stabilising discrete AlH_3 species. We believe that the properties of NHC-stabilised AlH_3 can be fine-tuned by replacing the hydride atoms with more electronegative substituents. The exchange of hydride atoms by triflate or chloride could be achieved by using aldiminium-based reagents.

4. Aldiminium-based fluorinating reagents

In the last decade, many new selective nucleophilic fluorinating reagents have been proposed. Despite that, the search for useful reagents for the fluorination of organic and inorganic compounds is still ongoing.

The aim of our work was to prepare new nucleophilic fluorinating reagents based on aldiminium salts. We have focused on the synthesis of aldiminium-based fluoride and poly(hydrogen fluoride) salts. We believe that poly(hydrogen fluoride) salts can be prepared from the corresponding chloride salt by using anhydrous HF, while aldiminium salts with lower HF content can be obtained by subsequent abstraction of HF.

Chapter 3

Methodology

3.1 General Information

Most compounds used and prepared in this work are not stable in the presence of water or oxygen. To avoid decomposition, the syntheses, storage and other manipulations were carried out under an inert atmosphere of dry argon. Samples were stored and weighed in a glovebox (M. Braun) in which the content of O_2 and H_2O was kept below 0.1 ppm. Samples were stored in glass or PP containers depending on their nature. Most reactions were carried out in Schlenk flasks using the standard Schlenk technique. Reactions with reagents based on HF or other compounds, which tend to react with glass, were carried out in custom-made FEP reaction vessels with PTFE valves. Anhydrous HF was handled in a vacuum line made entirely of perfluorinated polymers. Glassware was oven dried at 150 °C, while plastic vessels and containers were oven dried overnight at 60 °C before use and evacuated hot.

Solvents were obtained from Acros Organics, Carlo Erba, Honeywell, Merck, Sigma-Aldrich, and Deutero. Before their use, all solvents were degassed and dried. Toluene, diethyl ether and THF were dried in a mixture of sodium and benzophenone. When the solution turned deep purple, the solvents were distilled under an argon atmosphere, degassed by freeze-thaw cycles and stored over 3 Å molecular sieves for at least 48 hours before use. Deuterated solvents were stored over 3 Å molecular sieves in a glovebox.

Commercially available reagents were purchased from Acros Organics, Sigma-Aldrich or Linde and used as received unless otherwise stated. CsF and KF were dried overnight in vacuum at 150 °C and stored in a glovebox. Anhydrous HF was dried by mixing with K_2NiF_6 before use.

Caution! *Anhydrous HF is an extremely corrosive and highly dangerous gas. It should be handled with care in a well-ventilated fume hood. Protective clothing should be worn at all times.*

Reagents not commercially available were prepared as described in the literature: [(CAAC)$AlMe_3$] [203], Me_3SnF [204], [IPrH][$(HF)_nF$] (n = 0−2) [199], [(IPr)AlH_3] [136], [CAACH][OTf] [205]; or by methods described previously with slight modifications: Al(*n*-Bu)$_3$ based on [206], $AlPh_3$ based on [207], [CAACH][$H_{0.5}Cl_{1.5}$] based on [208] (see Appendix A.1).

Synthetic procedures and characterisation results for each compound prepared are given in Appendix A.2.

3.2 NMR Spectroscopy

Samples for NMR analysis were prepared in a glovebox under an inert atmosphere in deuterated solvents: CD_3CN, C_6D_6, THF-d_8 and toluene-d_9. Samples that tend to react with glass were measured using FEP inlays for NMR tubes. ^{1}H, ^{13}C, $^{1}H-^{13}C$ HSQC, ^{19}F and ^{27}Al NMR spectra were recorded at the Slovenian NMR Centre (National Institute of Chemistry) using a Bruker AVANCE NEO 400 or 600 MHz NMR spectrometer. Unless otherwise stated, the spectra were recorded at 298 K. The chemical shifts of ^{1}H and ^{13}C were referenced to the residual signals of the deuterated solvent and are given relative to (TMS). The ^{19}F and ^{27}Al references were calculated according to IUPAC guidelines and are given relative to $CFCl_3$ and $Al(NO_3)_3$ in deuterated water, respectively [209].

3.3 Raman Spectroscopy

Samples for Raman analysis were prepared under an inert atmosphere in a glovebox. Solid samples were placed in 0.3 mm quartz capillaries and sealed with grease at the top to prevent contact with air. Raman spectra were recorded at room temperature using a Horiba Jobin Yvon Labram-HR spectrometer coupled with an Olympus BXFM-ILHS microscope. The samples were excited with the 633 nm emission line of the He-Ne laser. The instrument was calibrated to the peak of the silicon wafer.

3.4 Elemental Analysis

The samples for elemental analysis were prepared in a glovebox under an inert atmosphere. Approximately 4 mg of the dry powdered products were transferred in silver foils and pressed into small discs. The contents of carbon, hydrogen and nitrogen were determined with a CHNS elemental analyser vario EL cube (Elementar) operating in the CHN mode.

3.5 Crystal Structure Determination

Single crystals suitable for X-ray analysis were prepared under an inert atmosphere by various methods, e.g. by storing the saturated solution at low temperature or by slowly evaporating the solvent under static vacuum. The crystals formed were immersed in silicon oil and transferred under the microscope. Single crystals suitable for X-ray analysis were handpicked with looped pin and mounted onto the diffractometer.

Crystal data were collected on a Gemini A diffractometer equipped with an Atlas CCD detector using graphite monochromated Cu Kα radiation ($\lambda = 1.54184$ Å). All crystal data were collected at 150 K unless otherwise stated. The data were processed using the CrysAlisPro software package [210]. Analytical absorption correction was applied to all data sets [211]. Structures were solved with the intrinsic phase method using the SHELXT programme [212]. Structure refinement was performed using the SHELXL software implemented in the Olex2 programme package [213], [214]. All non-hydrogen atoms were refined anisotropically. Hydrogen atoms except hydride substituents were assigned ideal positions and refined with a rigid model, while hydride substituents were located and refined isotropically. The figures were created with Diamond 4.6.4 [215]. The crystallographic data for all compounds are given in Appendix A.3.

3.6 Molecular Calculations

Molecular gas-phase calculations were performed with the programme Gaussian 16 [216] using the Perdew–Burke–Ernzerhof (PBE) exchange-correlation functional [217] and an empirical D3 dispersion correction of Grimme [218] with Becke-Johnson damping [219]. The electrons were described with all electron basis sets. We used the triple-ζ basis set with polarisation functions, in particular Def2-TZVP [220], [221]. In addition to the full crystal structures, we also calculated stand-alone $[R_{4-n}AlF_n]$ anions (n = 1−4, R = Me, n-Bu, Ph) as described above. For the anion calculations, we also used the B3LYP potential [222]. The calculated electronic energies and the calculated reaction energies are shown in Appendix A.4.

Chapter 4

Results and Discussion

Results and Discussion section is divided into four subsections to cover the four main topics of our research. They represent different aspects of the chemistry of discrete aluminium compounds. Although they are presented separately, some parts are closely related.

Chapter 4.1: "Discrete neutral aluminium fluorides" is based on previously unpublished results on the synthesis of discrete neutral aluminium fluorides stabilised by CAACs.

Chapter 4.2: "Discrete organofluoroaluminates" is based on the results published in the article "Discrete Organofluoroaluminate Anions: Synthetic, Structural and Spectroscopic Aspects" published in Organometallics in 2022 [26].

Chapter 4.3: "Functionalisation of NHC-stabilised aluminium hydride" is based on the results published in the article "Synthesis and characterization of partially substituted NHC supported alane adducts using triflate or chloride salts" published in Polyhedron in 2021 [153].

Chapter 4.4: "Aldiminium-based fluorinating reagents" is based on previously unpublished results on the synthesis and reactivity of aldiminium-based poly(hydrogen fluoride) salts.

4.1 Discrete Neutral Aluminium Fluorides

This chapter is based on as of yet unpublished results. The data presented are part of an ongoing study on the reactivity of organoaluminium compounds with fluorinating reagents.

In this chapter, the reactivity of CAAC-stabilised $AlMe_3$ adduct [(CAAC)$AlMe_3$] with Me_3SnF is presented. A series of CAAC-stabilised organoaluminium fluorides were prepared and characterised by the stepwise exchange of methyl groups for fluorine. Further fluorination led to the formation of salts with discrete fluoroaluminate anions. Where possible, the products were characterised by X-ray structural analysis and NMR spectroscopy. The structural features of the characterised compounds were compared with DTF calculations of structurally optimised salts.

4.1.1 Synthesis and crystal structure determination

The detailed synthesis procedures of all compounds are listed in Appendix A.2, together with all data obtained by their characterisation.

4.1.1.1 Synthesis of [(CAAC)$AlMe_2F$] (1)

The reaction of [(CAAC)$AlMe_3$] with 1 equivalent of Me_3SnF was carried out in toluene at 55 °C for 7 days. The reaction proceeds slowly and its progress can be monitored by the dissolving of Me_3SnF. During the reaction, a methyl substituent at the aluminium centre is exchanged for a fluorine atom, as shown in Scheme 4.1. Me_4Sn forms as a by-product and is easily removed from the reaction mixture under vacuum. After removal of the volatiles, single crystals of [(CAAC)$AlMe_2F$] (**1**) were obtained. The crystals were collected and analysed without further purification.

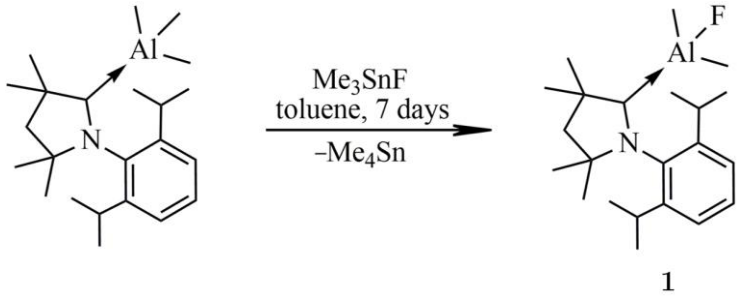

1

Scheme 4.1: Reactivity of [(CAAC)$AlMe_3$] with 1 equivalent of Me_3SnF.

The preparation of organoaluminium fluorides by a fluoride/alkyl exchange reaction using Me_3SnF has already been reported in the literature [35], [38]. Recently, it was also used for the synthesis of a discrete NHC-stabilised dimethylaluminium fluoride [(SIMes)$AlMe_2F$] [11]. However, discrete diorganoaluminium fluorides are rarely structurally characterised. To our knowledge, the crystal structure of [((*t*-Bu)NH_2)$AlMe_2F$] is the only representative so far [39].

Single crystals of [(CAAC)$AlMe_2F$] (**1**) were formed by slow evaporation of toluene during product isolation. It crystallises in the monoclinic space group $I2/a$ and its crystal structure is shown in Figure 4.1.

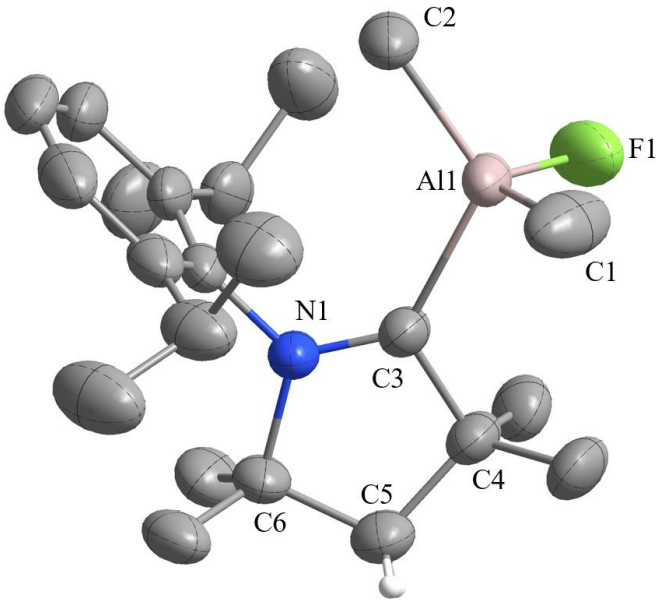

Figure 4.1: Crystal structure of [(CAAC)$AlMe_2F$] (**1**). The ellipsoids are drawn at 50 % probability. For clarity, all hydrogen atoms are omitted, except those on the heterocyclic ring.

The asymmetric unit contained a molecule of [(CAAC)$AlMe_2F$] (**1**) which, as expected, adopts a tetrahedral arrangement around the aluminium centre. The structural features of the adduct are consistent with similar reported structures. The Al−F distance of 1.751(2) Å agrees well with previously reported Al−F distances of discrete organoaluminium fluorides 1.703(1) Å [39], and 1.761(1) Å [223]. Moreover, the Al−C_{CAAC} distance of 2.100(2) Å and the Al−C_{Me} distances of 1.890(4) Å and 1.964(4) Å are comparable to the Al−C_{CAAC} distance of 2.124(1) Å and the average Al−C_{Me} distances of 1.994 Å reported for the parent [(CAAC)$AlMe_3$] [203]. The Al−C_{Me} distances are also consistent with the Al−C_{Me} distance of 1.944(2) Å of the structurally related β-diketiminato complex [42].

In one case we obtained single crystals of [(CAAC)$AlMe_2F$]·LiOTf·THF (**1a**), when a small amount of LiOTf was present in the reaction mixture due to the CAAC preparation method. The compound crystallises in the monoclinic space group $P2_1/c$. The asymmetric unit contains two tetrahedrally coordinated dimethylaluminium fluoride adducts in which the fluorine forms bridging bonds with the Li. Two [(CAAC)$AlMe_2F$]·LiOTf·THF units combine to form a dimer with an eight-membered ring *via* the following atoms: Li(1), O(2), S(1) and O(4). The crystal structure of a monomeric unit and the formation of a dimer are shown in Figure 4.2. The structural features of the compound are consistent with a similar reported fluorine bridging structure. The Al−F distance of 1.717(1) Å and Li−F distance of 1.820(4) Å agree well with the reported Al−F distance of 1.761(1) Å and Li−F distance of 1.762(4) Å of the structurally related fluorine bridging compound [223]. Moreover, the Al−C_{CAAC} distance of 2.087(2) Å and the Al−C_{Me} distances of 1.963(2) Å and 1.886(3) Å are similar to those described for [(CAAC)$AlMe_2F$] (**1**) and the parent compound [(CAAC)$AlMe_3$] [203]. The Al−C_{Me} distances are also consistent with the distances of 2.019(2) Å in 2.012(3) Å reported for the structurally related fluorine bridging compound [223].

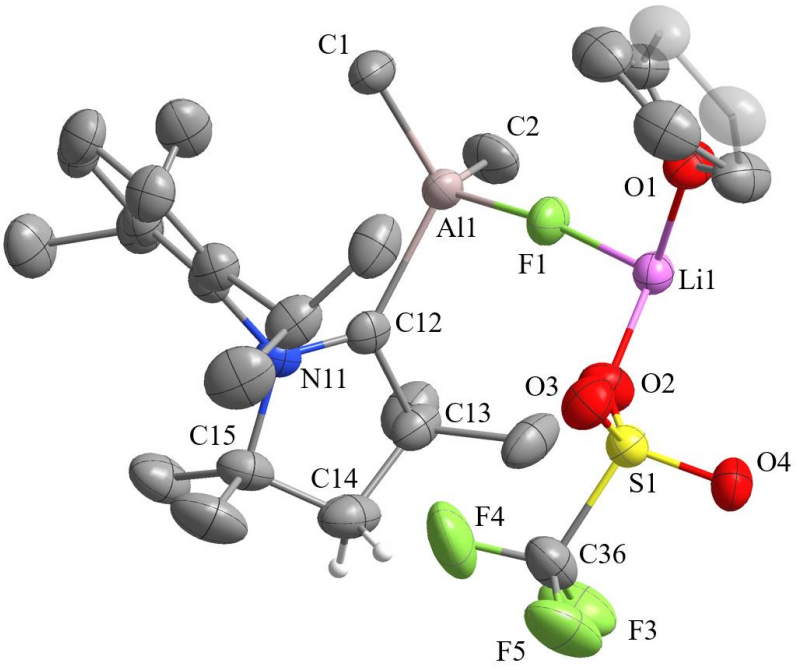

(a)

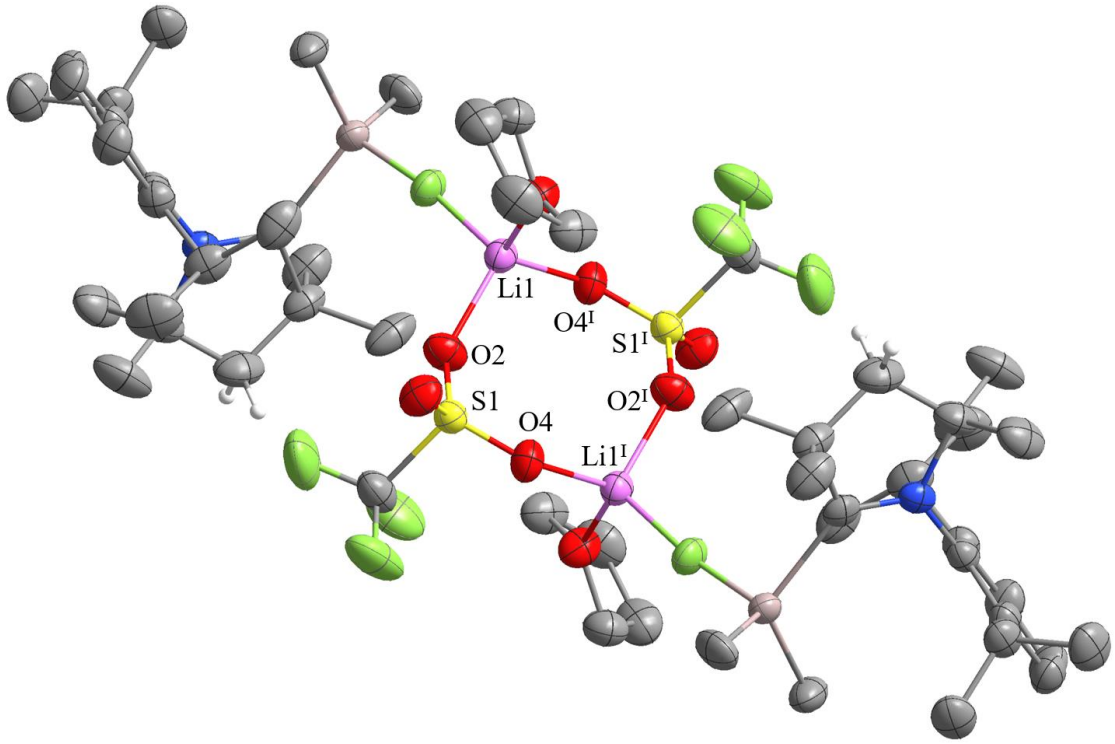

(b)

Figure 4.2: Crystal structure of [(CAAC)AlMe$_2$F]·LiOTf·THF (**1a**). (a) Structure of the monomeric unit. The positions of the disordered atoms are shown in domain A and B (shaded). And (b) packing of two monomeric units in a dimer with an eight-membered ring. The ellipsoids are drawn at 50 % probability. For clarity, all hydrogen atoms are omitted, except those on the heterocyclic ring.

4.1.1.2 Synthesis of [(CAAC)AlMeF$_2$] (2)

The reaction of [(CAAC)AlMe$_3$] with 2 equivalents of Me$_3$SnF was carried out in toluene at 55 °C for 7 days. The reaction proceeds slowly and its progress can be monitored by the dissolving of Me$_3$SnF. During the reaction, two methyl substituents at the aluminium centre are exchanged for fluorine atoms, as shown in Scheme 4.2. Me$_4$Sn forms as a by-product and is easily removed from the reaction mixture under vacuum. Removal of the volatiles gave [(CAAC)AlMeF$_2$] (**2**) as a white solid, which was purified by washing with hexane.

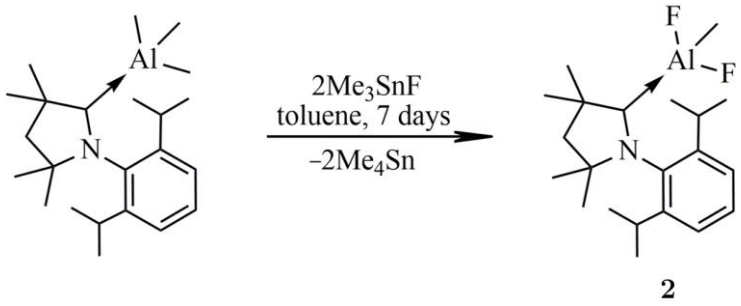

Scheme 4.2: Reactivity of [(CAAC)AlMe$_3$] with 2 equivalents of Me$_3$SnF.

Single crystals of [(CAAC)AlMeF$_2$] (**2**) were formed by slow evaporation of toluene under static vacuum. It crystallises in the monoclinic space group $I2/a$ and its crystal structure is shown in Figure 4.3. Discrete organoaluminium difluorides are rarely structurally characterised. As far as we know, only the structure of [(THF)Al(SiMe$_3$)$_3$F$_2$] has been characterised so far, although the reported structure has extensive disorder that could not be modelled to a satisfactory quality [35].

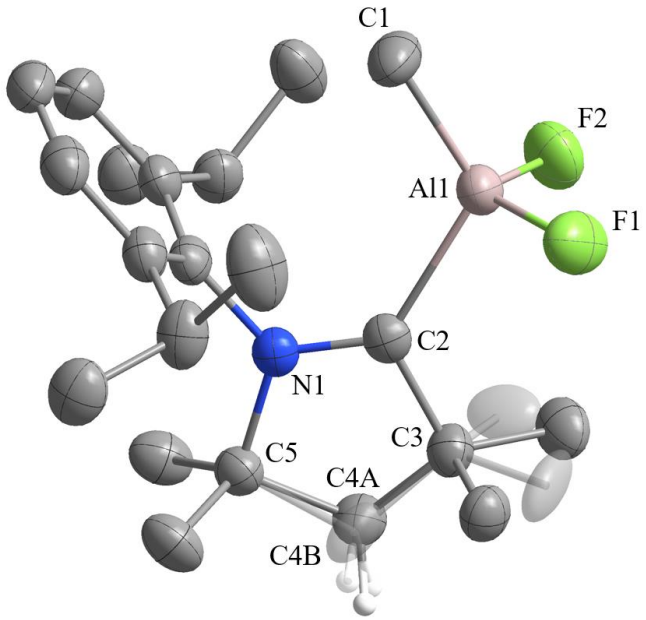

Figure 4.3: Crystal structure of [(CAAC)AlMeF$_2$] (**2**). The ellipsoids are drawn at 50 % probability. For clarity, all hydrogen atoms are omitted, except those on the heterocyclic ring. The positions of the disordered atoms are shown in domain A and B (shaded).

The asymmetric unit of [(CAAC)AlMeF$_2$] (**2**) contains a molecule that, as expected, adopts a tetrahedral arrangement around the aluminium centre. The structural features of the adduct are consistent with similar reported structures. The Al—F distances of 1.690(3) Å and 1.681(3) Å are slightly shorter than the Al—F distance of the related [(CAAC)AlMe$_2$F] (**1**) (1.751(2) Å), but agree well with the previously reported Al—F distance of 1.679(1) Å [42], and 1.703(1) Å [39] of reported organoaluminium fluoride compounds. Moreover, the Al—C$_{CAAC}$ distance of 2.086(3) Å and the Al—C$_{Me}$ distance of 1.898(4) Å are comparable to the Al—C$_{CAAC}$ distance of 2.124(1) Å and the average Al—C$_{Me}$ distances of 1.994 Å reported for the parent compound [(CAAC)AlMe$_3$] [203]. The Al—C$_{Me}$ distances are also consistent with the Al—C$_{Me}$ distance of 1.944(2) Å of the structurally related β-diketiminato complex [42].

4.1.1.3 Synthesis of [(CAAC)AlF$_3$] (3) and instability of the adducts

The reaction of [(CAAC)AlMe$_3$] with 3 equivalents of Me$_3$SnF usually resulted in a mixture of various neutral compounds and salts. Some of the products were isolated and structurally characterised, but unfortunately the [(CAAC)AlF$_3$] (**3**) adduct was not. To understand the course of the reaction, both reactants were mixed in an NMR tube in C_6D_6. The NMR tube was then sealed and the reaction was run at 55 °C for 5 days. The ^{1}H, ^{19}F and ^{27}Al NMR spectra were measured at approximately the same time each day to monitor the progress of the reaction. The results of the ^{19}F and ^{27}Al NMR measurements are shown in Figure 4.4.

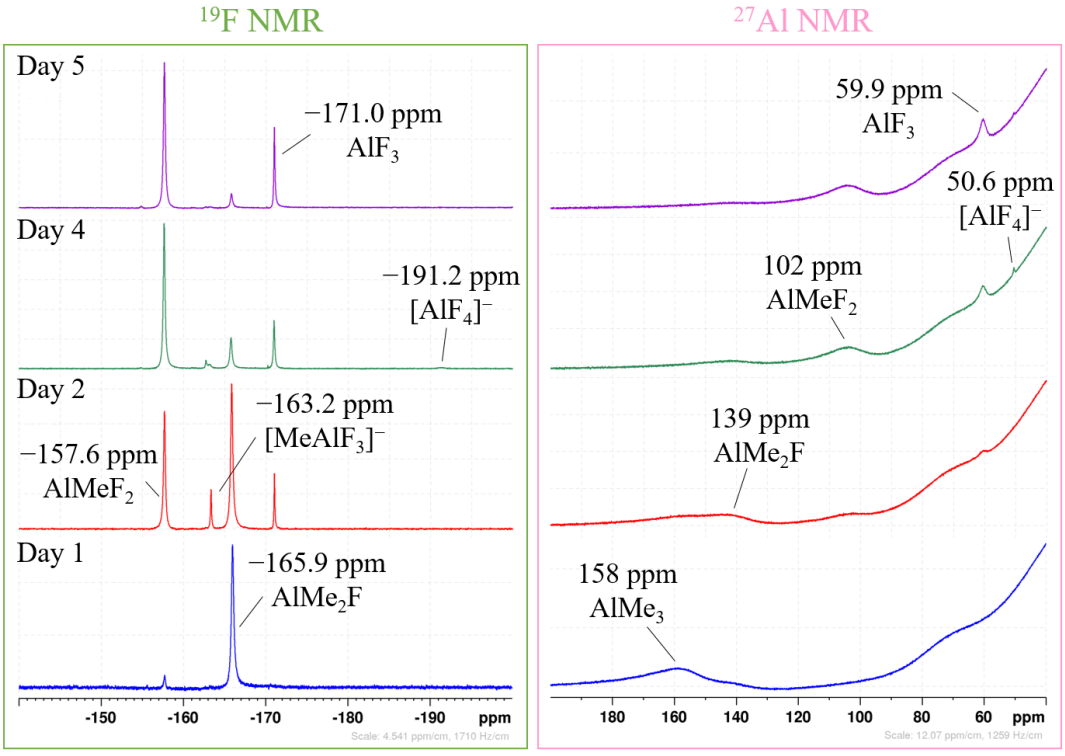

Figure 4.4: ^{19}F and ^{27}Al NMR spectra measuring the course of the reaction of [(CAAC)AlMe$_3$] with 3 equivalents of Me$_3$SnF in C_6D_6. The reaction was carried out at 55 °C in an NMR tube. The spectra were measured daily.

It can be seen that the fluorination proceeded stepwise. First, the [(CAAC)$AlMe_2F$] (**1**) adduct was formed, which was fluorinated to [(CAAC)$AlMeF_2$] (**2**) and [(CAAC)AlF_3] (**3**). Further fluorination also led to the formation of the salts [CAACH][$MeAlF_3$] (**4**) and [CAACH][AlF_4] (**5**), which are only partially soluble in nonpolar solvents. Over time, they precipitated out of the solution and formed a white solid at the bottom of the NMR tube. After five days, a mixture of [(CAAC)$AlMeF_2$] (**2**) and [(CAAC)AlF_3] (**3**) remained in solution.

We concluded that [(CAAC)AlF_3] (**3**) is definitely formed in solution but cannot be isolated due to competing reactions. It is known that AlF_3, formed *in situ*, reacts with AlR_3 to form R_2AlF [224]. A similar tendency was also observed by us. We believe that the organoaluminium fluorides are in equilibrium with each other. For example, in the synthesis of [(CAAC)$AlMe_2F$] (**1**), part of [(CAAC)$AlMe_3$] remained unreacted while part of [(CAAC)$AlMeF_2$] (**2**) formed. Crystals of [(CAAC)$AlMe_2F$] (**1**) could also not be purified as they decomposed in solution to [(CAAC)$AlMe_3$] and [(CAAC)$AlMeF_2$] (**2**). However, the reaction proved to be reversible, as [(CAAC)$AlMe_2F$] (**1**) was also formed in a mixture of the other two.

Curiously, when the reaction was carried out in toluene on a 1.4 mmol scale in a Schlenk flask, relatively pure [(CAAC)$AlMeF_2$] (**2**) and [CAACH][AlF_4] (**5**) were obtained. [CAACH][AlF_4] (**5**) formed as a white precipitate and was separated from the other products by filtration, while [(CAAC)$AlMeF_2$] (**2**) remained dissolved in toluene and was purified by washing with hexane after removal of the volatiles. Initially, we assumed that the formation of the salts was due to the presence of a small amount of water in the reaction mixture. Bour's group reported a similar observation when adventitious water caused the formation of [IPrH][GaF_4] during the reaction of IPr and GaF_3 [15]. However, after repeatedly obtaining the same results, we realised that this was probably due to competing reactions. One such possibility would be the autoionization of the metal fluoride [225], another the deprotonation of the organoaluminium moiety by the carbene [226]. In 2006, it was reported that an NHC-stabilised $AlMe_3$ adduct [(ItBu)$AlMe_3$] tends to react with an excess of $AlMe_3$ to form a salt with a trinuclear aluminate anion [ItBuH][$Me_3Al(\mu^3\text{-}CH_2)(AlMe_2)_2(\mu_2\text{-}CH_3)$] [226]. In our opinion, such a mechanism would also be plausible in our case, since CAACs are anything but innocent ligands. They have been found to be susceptible to intramolecular C−H activation, as well as to the activation of other sp-, sp^2-, and sp^3-hybridised C−H bonds [84].

At this point, we would like to point out that the formation of all organoaluminium fluorides was not straightforward. As we observed in the NMR analysis, each reaction was accompanied by others that led to side products. One side product observed in all reactions of the CAAC-stabilised organoaluminium fluorides was CAAC(H)Me (**6**). The mechanism of its formation remains unknown for now, but we were able to isolate and characterise it from the reaction mixtures. CAAC(H)Me (**6**) was washed off with hexane during product purification and crystallised upon slow evaporation of hexane under static vacuum. CAAC(H)Me (**6**) crystallises in the monoclinic space group $P2_1/n$ and its crystal structure is shown in Figure 4.5.

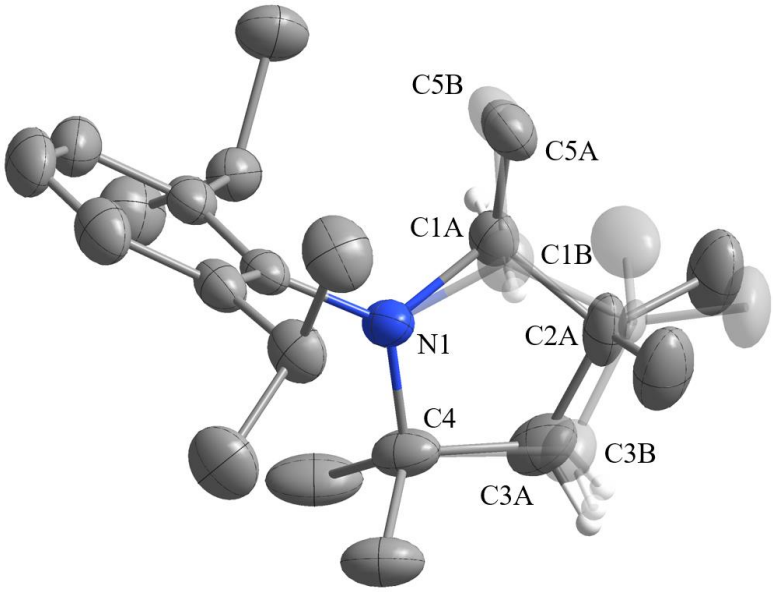

Figure 4.5: Crystal structure of CAAC(H)Me (**6**). The ellipsoids are drawn at 50 % probability. For clarity, all hydrogen atoms are omitted, except those on the heterocyclic ring. The positions of the disordered atoms are shown in domain A and B (shaded).

4.1.1.4 Synthesis of [CAACH][MeAlF$_3$] (4)

The formation of [CAACH][MeAlF$_3$] (**4**) was observed in the reaction of [(CAAC)AlMe$_3$] with 3 equivalents of Me$_3$SnF. However, this salt was only a minor component in the mixture with [CAACH][AlF$_4$] (**5**) and could not be selectively separated. In order to properly characterise this compound, a different synthetic approach was used, which is described in detail in the following chapters of this thesis. The synthesis of pure [CAACH][MeAlF$_3$] (**4**) is described in Chapter 4.4.3.

Single crystals of [CAACH][MeAlF$_3$] (**4**) formed in a saturated acetonitrile solution stored at −20 °C. It crystallises in the monoclinic space group $P2_1/c$ and its crystal structure is shown in Figure 4.6. The asymmetric unit of [CAACH][MeAlF$_3$] (**4**) contains a [CAACH]$^+$ cation and a discrete, tetrahedrally coordinated [MeAlF$_3$]$^-$ anion. The fluorine atoms on the fluoroaluminate anion are disordered. Their positions were modelled and refined in two preferred orientations, with occupancies of domain A being 58 % and domain B 42 %. The anion interacts with the cation and forms a hydrogen bond. Since F(1) is disordered in two preferred orientations, the hydrogen bonds are as follows: C(2)−H(2)···F(1A) with an H···F distance of 2.041(4) Å (C···F distance of 2.973(5) Å) and C(2)−H(2)···F(1B) with an H···F distance of 2.048(8) Å (C···F distance of 2.996(8) Å). The Al−C distances of 1.937(3) Å and the average Al−F distance of 1.660 Å are consistent with the Al−C distances of 2.006(6) Å and the Al−F distances of 1.666(3) Å reported for the structurally characterised [(C$_2$F$_5$)AlF$_3$]$^-$ anion [25].

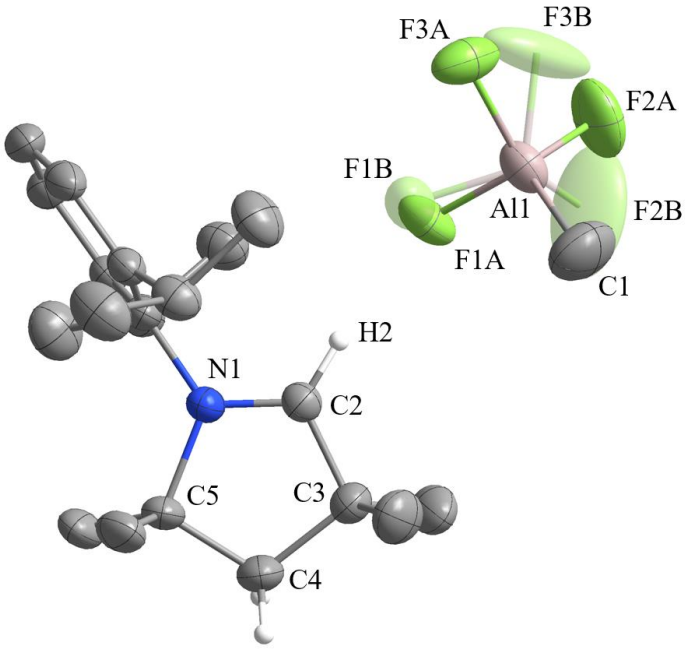

Figure 4.6: Crystal structure of [CAACH][MeAlF$_3$] (**4**). The ellipsoids are drawn at 50 % probability. For clarity, all hydrogen atoms are omitted, except those on the heterocyclic ring. The positions of the disordered atoms are shown in domain A and B (shaded).

4.1.1.5 Synthesis of [CAACH][AlF$_4$] (5)

The formation of [CAACH][AlF$_4$] (**5**) was observed in the reaction of [(CAAC)AlMe$_3$] with Me$_3$SnF in practically all stoichiometric ratios in different quantities. The use of a higher ratio of Me$_3$SnF resulted in the formation of a higher quantity of [CAACH][AlF$_4$] (**5**). Since it is sparingly soluble in toluene, it precipitated out of the reaction mixture as a white solid. After filtration, the solid was purified by washing with hexane and characterised. Pure [CAACH][AlF$_4$] (**5**) can also be prepared by another approach, which is described in detail in the following chapters. The alternative synthetic approach is presented in Chapter 4.4.3.

Single crystals of [CAACH][AlF$_4$] (**5**) were obtained by slow evaporation of acetonitrile under static vacuum. It crystallizes in the monoclinic space group $P2_1/c$ and its crystal structure is presented in Figure 4.7. The asymmetric unit of [CAACH][AlF$_4$] (**5**) contains a [CAACH]$^+$ cation and a discrete, tetrahedrally coordinated [AlF$_4$]$^-$ anion. The fluorine atoms F(3) and F(4) on the fluoroaluminate anion are disordered. Their positions were modelled and refined in two preferred orientations, with occupancies of domain A being 45 % and domain B 55 %. The anion interacts with the cation and forms a hydrogen bond C(2)–H(2)$\cdots$F(1) with an H$\cdots$F distance of 2.106(1) Å (C$\cdots$F distance of 3.030(2) Å). The average Al–F distance of 1.652 Å is consistent with the average Al–F distances reported for discrete [AlF$_4$]$^-$ anions (1.636 Å [60], 1.618 Å [19], and 1.712 [25]).

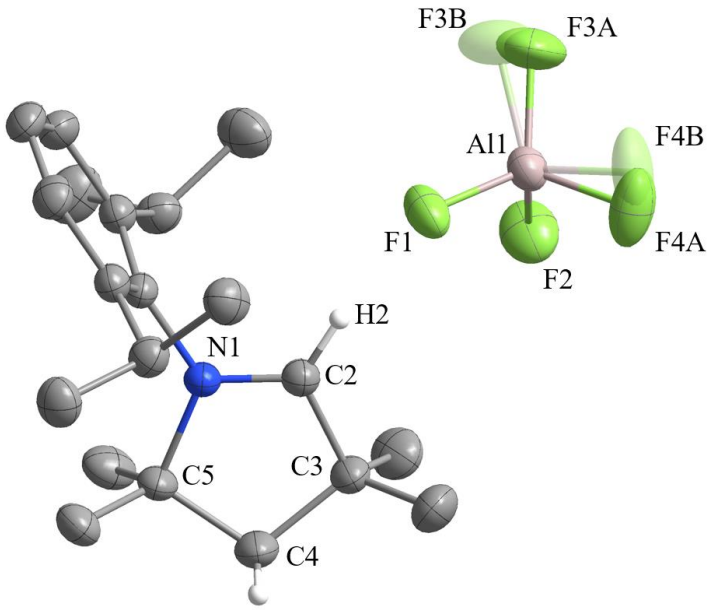

Figure 4.7: Crystal structure of [CAACH][AlF_4] (**5**). The ellipsoids are drawn at 50 % probability. For clarity, all hydrogen atoms are omitted, except those on the heterocyclic ring. The positions of the disordered atoms are shown in domain A and B (shaded).

4.1.2 NMR spectroscopy

All compounds obtained were characterised by NMR spectroscopy. The spectra agree with the crystal structures of the compounds. Selected NMR peaks of the prepared organoaluminium fluorides and fluoroaluminate salts are listed in Table 4.1. The ^{1}H NMR peaks of the organoaluminium fluorides are shifted upfield with increasing number of fluorine atoms. The ^{1}H NMR chemical shifts of [(CAAC)$AlMe_2F$] (**1**) are observed as a doublet at −0.55 ppm and agree well with the Al−CH_3 peak observed as a doublet at −0.40 ppm in the structurally related [((t-Bu)NH_2)$AlMe_2F$] [39].

Table 4.1: Selected NMR peaks of [(CAAC)$AlR_{3-n}F_n$] (n = 1–3) and [CAACH][$R_{4-n}AlF_n$] (n = 3–4) in C_6D_6 (**1**, **2**, **3**) and acetonitrile (**4**, **5**).

Compound	δ(^{1}H) Al−CH_3	δ(^{19}F) Al−F	δ(^{27}Al)
[(CAAC)$AlMe_2F$] (**1**)	−0.55 (d)	−165.86	139 (br)
[(CAAC)$AlMeF_2$] (**2**)	−0.80 (s)	−157.79	102 (br)
[(CAAC)AlF_3] (**3**)	/	−171.04	59.88
[CAACH][$MeAlF_3$] (**4**)	−1.22 (s)	−167.14	84.95
[CAACH][AlF_4] (**5**)	/	−194.56	49.41

The ^{19}F NMR peaks of the organoaluminium fluorides cannot be compared with other discrete neutral compounds because the chemical shifts are strongly influenced by the nature of the ligand. Nevertheless, the chemical shifts of our compounds are in the same region as those for other discrete tetrahedrally coordinated R_2AlF compounds at −169.9 ppm [11], −155.5 ppm [39], and −161.3 ppm [223], $RAlF_2$ compounds at −159.2 ppm [35], and AlF_3 compounds at −164.5 ppm [11]. In the literature, the chemical shifts for discrete octahedrally coordinated AlF_3 complexes are reported at −176.1 ppm and −169.9 ppm [10], or −162.0 ppm and −177.3 ppm [9], and also agree well with our

observations. The ^{19}F NMR peaks of organofluoroaluminate anions are in agreement with other reported values [3]. For more information on organofluoroaluminate anions, see Chapter 4.2.

The ^{27}Al NMR peaks of all compounds prepared are broad, which is due to the quadrupolar nature of ^{27}Al ($I = 5/2$). The ^{27}Al NMR signals are shifted more upfield with each additional fluorine atom on the Al centre. For example, the chemical shifts of organoaluminium fluorides arrange themselves in this order: [(CAAC)$AlMe_3$] at 154 ppm, [(CAAC)$AlMe_2F$] (**1**) at 139 ppm, [(CAAC)$AlMeF_2$] (**2**) at 102 ppm, and [(CAAC)AlF_3] (**3**) at 59.88 ppm. The same trend was observed for organofluoroaluminate anions by Roesky and Finze [3], [25].

4.1.3 Computational results

The crystal structures of the prepared organoaluminium fluorides and organofluoroaluminate salts were used as a starting point for calculating the optimised structures using DFT calculations. The optimised structures were then examined in comparison with experimentally obtained crystal data. The optimised structures of all compounds are shown in Figure 4.8, while the experimental and calculated bond distances of CAAC-stabilised organoaluminium fluorides and the corresponding organofluoroaluminate salts are summarised in Table 4.2.

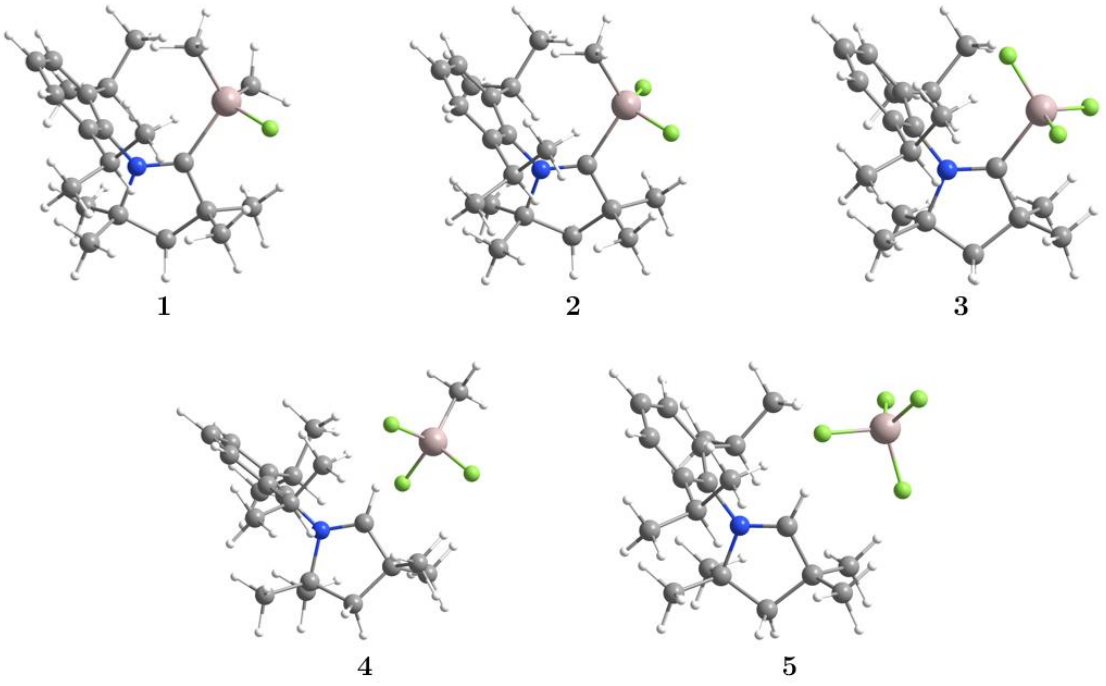

Figure 4.8: Optimized structures of CAAC-stabilised organoaluminium fluorides and the corresponding organofluoroaluminate salts.

Table 4.2 shows that the calculated Al−C and Al−F distances are generally longer, but still agree with the experimental values. The only exception is the calculated Al−F distance of [(CAAC)$AlMe_2F$] (**1**), which is slightly shorter. The difference between the calculated and experimental values can be explained by the fact that the effect of crystal structure packing was not taken into account in the gas phase calculations. In some cases, the difference may also be caused by the disorder of the fluorine and carbon atoms in the crystal structure.

Table 4.2: Experimental and calculated bond distances of CAAC-stabilised organoaluminium fluorides and the corresponding organofluoroaluminate salts.

Compound	d(Al−CH_3) (Å)		d(Al−F) (Å)	
	Experimental	Calculated	Experimental	Calculated
[(CAAC)$AlMe_3$][a]	1.990(2) 1.998(2) 1.996(2)	2.03 2.01 2.01	–	–
[(CAAC)$AlMe_2F$] (**1**)	1.890(4) 1.964(4)	2.01 1.99	1.751(2)	1.72
[(CAAC)$AlMeF_2$] (**2**)	1.898(4)	1.97	1.681(3) 1.690(3)	1.71 1.71
[(CAAC)AlF_3] (**3**)	–	–	n.a.	1.69 1.69 1.69
[CAACH][$MeAlF_3$] (**4**)	1.937(33)	1.96	1.692(5)[b], [c] 1.649(4)[c] 1.755(4)[c]	1.74[b] 1.74 1.72
[CAACH][AlF_4] (**5**)	–	–	1.668(1)[b] 1.659(2) 1.58(2)[c] 1.66(2)[c]	1.74[b] 1.72 1.69 1.68

[a] Reported in reference [203].
[b] These Al−F distances refer to the strongest hydrogen bonds formed between the cation and the nearest fluorine atom of the anion.
[c] Where fluorine atoms are disordered, Al−F distances are reported for domain A.

In Table 4.2, it can be seen that within the organoaluminium fluoride series [(CAAC)$AlMe_{3-n}F_n$] (n = 0–3) both the calculated and experimental Al−C and Al−F bonds become shorter with each additional fluorine atom in the structure. For example, the calculated Al−C distances change from 2.03 ($n = 0$) to 2.01 ($n = 1$) and 1.97 ($n = 2$), while the calculated Al−F distances change from 1.72 ($n = 1$) to 1.71 ($n = 2$) and 1.69 ($n = 3$). The same trend was also observed for the anionic species. Further details on the organofluoroaluminate anions can be found in Chapter 4.2.

Using the DFT calculations, we also estimated the amount of energy released during the formation of neutral adducts. The energy of the reactions was generally calculated according to the following reaction:

$$[(CAAC)AlMe_3] + nMe_3\mathrm{SnF} \rightarrow [(CAAC)AlMe_{3-n}F_n] + nMe_4Sn$$

The calculated electronic energies and the calculated energies of the reactions are given in Appendix A.4. The calculations show that the formation of more fluorinated products is favoured. Within the [(CAAC)$AlMe_{3-n}F_n$] (n = 0–3) series, the calculated reaction energies become more exothermic as the number of fluorine atoms increases. Although the formation of the adducts is thermodynamically favourable, their synthesis remains challenging due to competing reactions.

4.1.4 Summary

In this chapter we have presented the reactivity of the CAAC-stabilised organoaluminium compound [(CAAC)$AlMe_3$] with Me_3SnF. The use of 1 or 2 equivalents of Me_3SnF led to the formation of [(CAAC)$AlMe_2F$] (**1**) and [(CAAC)$AlMeF_2$] (**2**). Me_4Sn formed as a by-product and was easily removed from the reaction mixture *in vacuo*. The single crystals of the desired products were collected and analysed. Both are rare examples of structurally characterised discrete organoaluminium fluorides. However, further purification of the compounds was not possible due to their instability. In solution, they tend to be in equilibrium with other CAAC-stabilised organoaluminium fluorides and the parent $AlMe_3$ adduct. The use of higher amounts of Me_3SnF led to mixtures of various neutral compounds, including [(CAAC)AlF_3] (**3**), and salts, such as [CAACH][$MeAlF_3$] (**4**) and [CAACH][AlF_4] (**5**). The formation of [(CAAC)AlF_3] (**3**) was observed by NMR, but the compound could not be isolated or characterised separately due to other competing reactions. In our opinion, the formation of the salts could be a consequence of autoionisation of the metal fluoride or deprotonation of the organoaluminium moiety by the carbene.

All the reactions described were accompanied by a side reaction leading to CAAC(H)Me (**6**). The compound is very soluble in nonpolar solvents and can be easily washed out of the reaction mixtures with hexane. However, the mechanism of its formation remains unknown to us for the time being.

According to DFT calculations, the stability of the discrete organoaluminium fluorides increases with the number of fluorine atoms at the aluminium centre. However, although the adducts are thermodynamically favourable, their synthesis remains a challenge.

To summarise, in our study we have prepared some rare examples of discrete organoaluminium fluorides and structurally characterise them. We have shown that CAACs are suitable ligands for the stabilisation of discrete AlF_3. Such reactive compounds usually tend to form dimers, trimers or higher polymeric species and are rarely characterised in their discrete form.

4.2 Discrete Organofluoroaluminates

This chapter is based on the article "Discrete Organofluoroaluminate Anions: Synthetic, Structural and Spectroscopic Aspects" by E. Gruden, M. Tramšek and G. Tavčar, published in Organometallics in 2022 [26].

In our work, the reactivity of alkyl- and arylaluminium compounds with the series of imidazolium-based fluorinating reagents $[IPrH][(HF)_nF]$ (n = 0–2) was investigated. The use of fluorinating reagents with an appropriate amount of HF resulted in the formation of discrete triorganofluoroaluminate $[R_3AlF]^-$, diorganodifluoroaluminate $[R_2AlF_2]^-$, or organotrifluoroaluminate $[RAlF_3]^-$ anions and was accompanied by the release of RH. All products obtained were characterised by NMR and Raman spectroscopy. Where single crystals could be obtained, the structural features of the compounds were determined and compared with DTF calculations of structurally optimised salts.

4.2.1 Synthesis and crystal structure determination

The detailed synthesis procedures of all compounds are presented in Appendix A.2 together with all data obtained by their characterisation.

The reactivity of the two alkylaluminium compounds used, $AlMe_3$ and $Al(n\text{-}Bu)_3$, was very similar, while the reactivity of the arylaluminium compound, $AlPh_3$, was somewhat different. Therefore, the reactivity of $AlMe_3$ and $Al(n\text{-}Bu)_3$ is presented in parallel in the next sections, while the reactivity of $AlPh_3$ is discussed separately.

4.2.1.1 Synthesis of trialkylfluoroaluminate salts

The two alkylaluminium compounds AlR_3 (R = Me, n-Bu) reacted with the imidazolium-based fluorinating reagent [IPrH][F] to form salts with $[R_3AlF]^-$ anions. $AlMe_3$ reacted to form $[IPrH][Me_3AlF]$ (**7**) in quantitative yield, and similarly $Al(n\text{-}Bu)_3$ formed the salt $[IPrH][(n\text{-}Bu)_3AlF]$ (**8**). Both reactions were carried out in acetonitrile at room temperature and proceeded according to Scheme 4.3. In the past, similar procedures have been used to prepare $M[R_3AlF]$ compounds with metal fluoride reagents [63], [227]. However, discrete $[R_3AlF]^-$ anions could only be isolated later by using sterically demanding cations [65], [66].

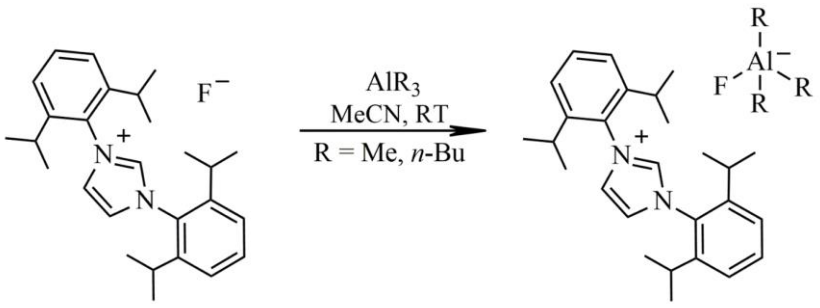

7 (R = Me)
8 (R = n-Bu)

Scheme 4.3: Reactivity of AlR_3 with [IPrH][F] (R = Me, n-Bu).

We observed that $[IPrH][Me_3AlF]$ (**7**) and $[IPrH][(n\text{-}Bu)_3AlF]$ (**8**) are stable at low temperatures but tend to decompose at room temperature to form the salt $[IPrH][R_2AlF_2]$ and the adduct $[(IPr)AlR_3]$. Decomposition was also observed when the salts were washed with toluene or when the salts were stirred in solution for 24 hours, as shown in Scheme 4.4.

For this reason, compounds **7** and **8** were stored at −20 °C under an inert atmosphere and used as are for characterisation and analysis. They were not further purified, although they contained small quantities of [IPrH][R_2AlF_2].

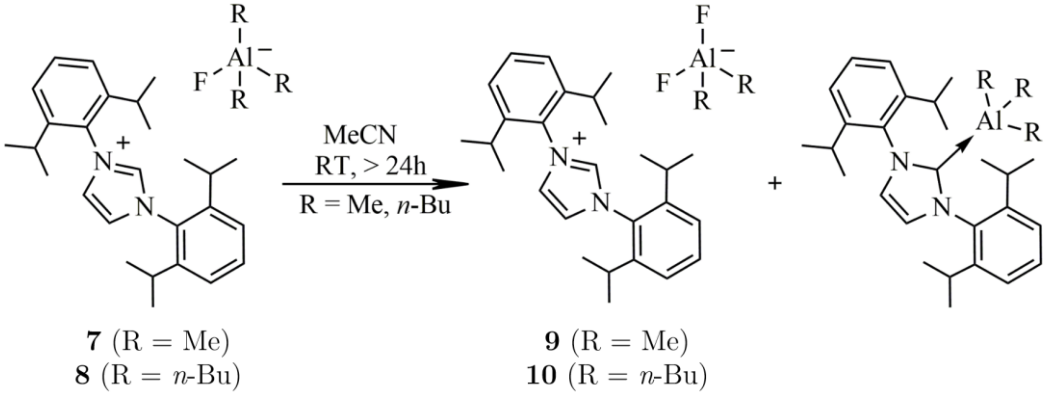

Scheme 4.4: Decomposition of [IPrH][R_3AlF] in acetonitrile (R = Me, *n*-Bu).

The decomposition process of [IPrH][Me_3AlF] (**7**) and [IPrH][(*n*-Bu)$_3$AlF] (**8**) was investigated by NMR spectroscopy. The results are shown in Figure 4.9.

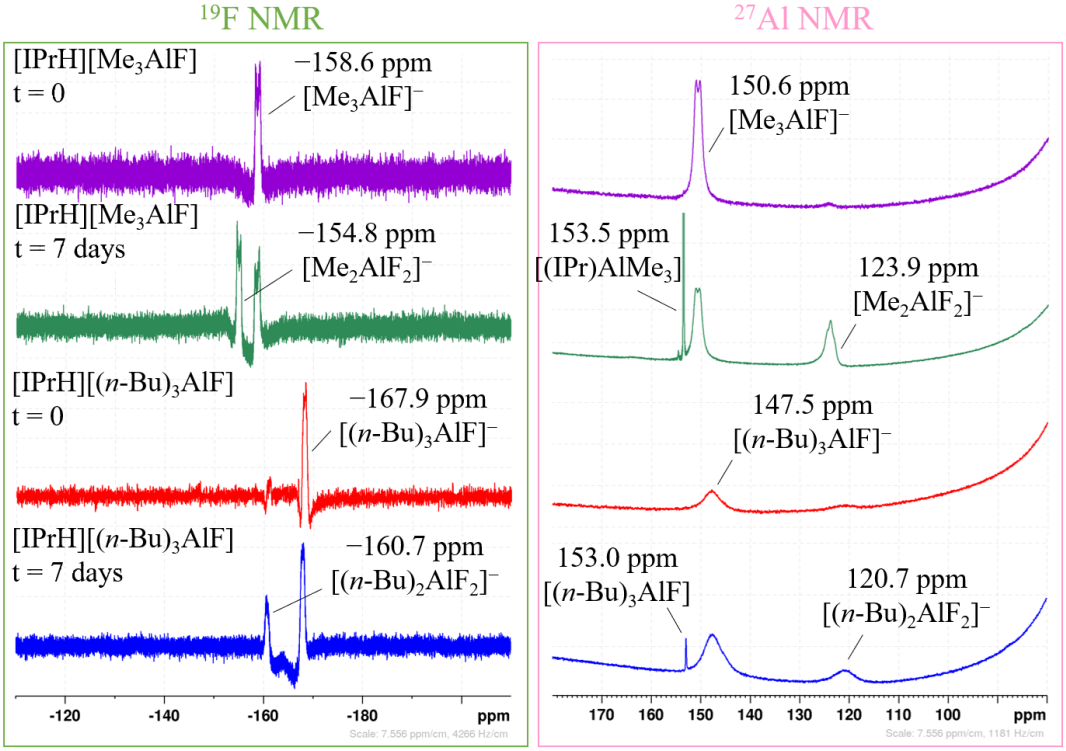

Figure 4.9: ^{19}F and ^{27}Al NMR spectra measuring the decomposition of [IPrH][R_3AlF] (R = Me, *n*-Bu) salts in acetonitrile. The acetonitrile solution of [IPrH][Me_3AlF] (**7**) and [IPrH][(*n*-Bu)$_3$AlF] (**8**) was measured first immediately after dissolution and then after one week. All measurements were carried out at room temperature.

The samples were dissolved in acetonitrile. The ^{19}F and ^{27}Al NMR spectra were first measured immediately after the dissolution and then after one week. In the meantime, the samples were kept at room temperature under inert conditions. The results show that the

[IPrH][R_3AlF] salts partially decompose into more fluorinated [IPrH][R_2AlF_2] salts and [(IPr)AlR_3] adducts within one week.

Crystallisation is a relatively slow process during which decomposition of the samples was usually observed. Despite numerous attempts, no single crystals of [IPrH][Me_3AlF] (**7**) could be obtained from different solvents. Crystallisation in DCM even led to the formation of single crystals of the solvate [IPrH][Me_2AlF_2]·0.95DCM (**9b**).

Fortunately, we were able to obtain single crystals of [IPrH][(n-Bu)$_3$AlF] (**8**) by slow evaporation of acetonitrile during product isolation. It crystallises in the monoclinic space group $P2_1/c$ and is a rare example of a structurally characterised salt with discrete $[R_3AlF]^-$ anions. It is also the first known anion with aliphatic substituents. The crystal structure of [IPrH][(n-Bu)$_3$AlF] (**8**) is shown in Figure 4.10. The asymmetric unit contains an $[IPrH]^+$ cation and a tetrahedrally coordinated $[(n\text{-Bu})_3AlF]^-$ anion. The n-butyl substituents of the anion are disordered. The cation and anion interact to form a hydrogen bond C(22)—H(22)···F(1) with an H···F distance of 1.889(1) Å (C···F distance of 2.819(2) Å). The average Al—C distance of 1.997 Å and Al—F distance of 1.733(1) Å are comparable to the average Al—C distance and Al—F distances of previously reported $[R_3AlF]^-$ anions (2.018 Å, 1.682(5) Å, respectively) [65]. The crystal data were collected at 189 K, as the crystals break and lose their crystallinity at lower temperatures.

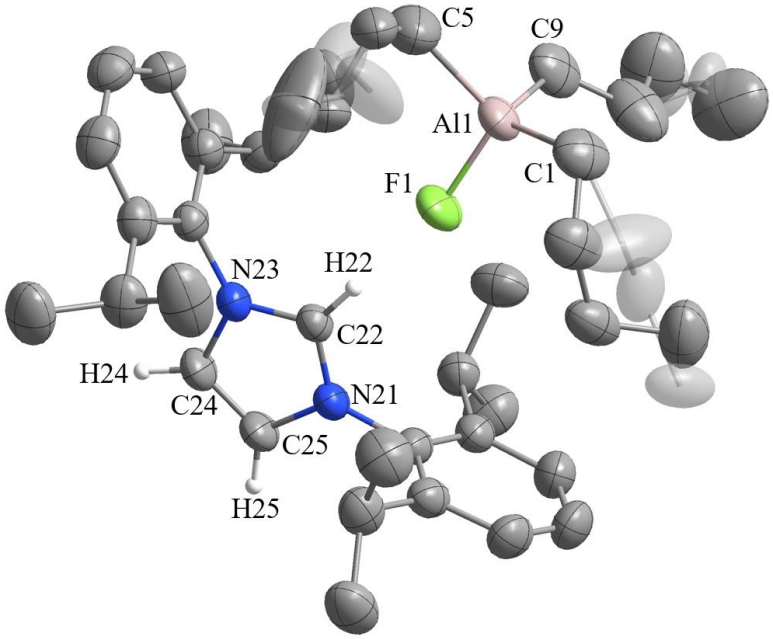

Figure 4.10: Crystal structure of [IPrH][(n-Bu)$_3$AlF] (**8**). The ellipsoids are drawn at 50 % probability. For clarity, all hydrogen atoms are omitted, except those on the imidazolium ring. The positions of the disordered atoms are shown in domain A and B (shaded).

4.2.1.2 Synthesis of dialkyldifluoroaluminate salts

The two alkylaluminium compounds AlR_3 (R = Me, n-Bu) reacted readily with the bifluoride reagent [IPrH][(HF)F] to form salts with $[R_2AlF_2]^-$ anions and an alkane RH. The latter was removed from the reaction mixtures *in vacuo*. The reactions were carried out in acetonitrile at room temperature and the salts were isolated as white solids in quantitative yield. $AlMe_3$ reacted to form [IPrH][Me_2AlF_2] (**9**) and methane, while Al(n-Bu)$_3$ formed [IPrH][(n-Bu)$_2$$AlF_2$] (**10**) and n-butane. The reaction proceeded

according to Scheme 4.5. During the reaction, a RH was eliminated from the metal-bonded alkyl groups and 2 fluoride anions were added to the aluminium centre. Both salts proved to be stable at room temperature under an inert atmosphere. They were stored in a glovebox for long periods without decomposing. The synthesis of $[R_2AlF_2]^-$ anions has already been described by Roesky's group, and our results agree well with their findings [60], [61].

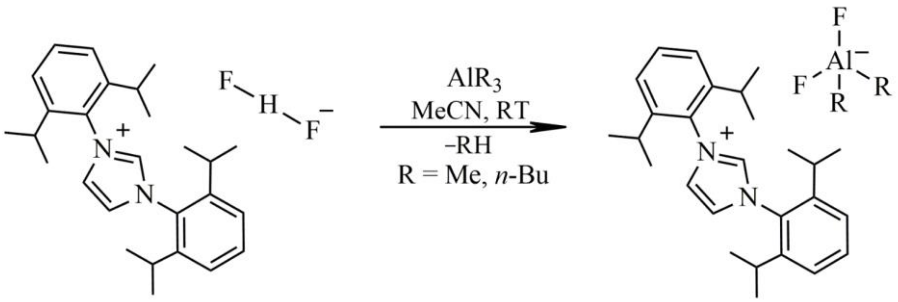

9 (R = Me)
10 (R = *n*-Bu)

Scheme 4.5: Reactivity of AlR_3 with [IPrH][(HF)F] (R = Me, *n*-Bu).

The crystal structure was determined for both compounds. $[IPrH][Me_2AlF_2]$ (**9**) crystalised as the solvate $[IPrH][Me_2AlF_2]\cdot C_6D_6$ (**9a**) during the slow evaporation of C_6D_6, and in DCM as $[IPrH][Me_2AlF_2]\cdot 0.95DCM$ (**9b**) during the decomposition of $[IPrH][Me_3AlF]$. The crystal structure of $[IPrH][Me_2AlF_2]$ (**9**) in the structure of $[IPrH][Me_2AlF_2]\cdot C_6D_6$ (**9a**) is shown in Figure 4.11.

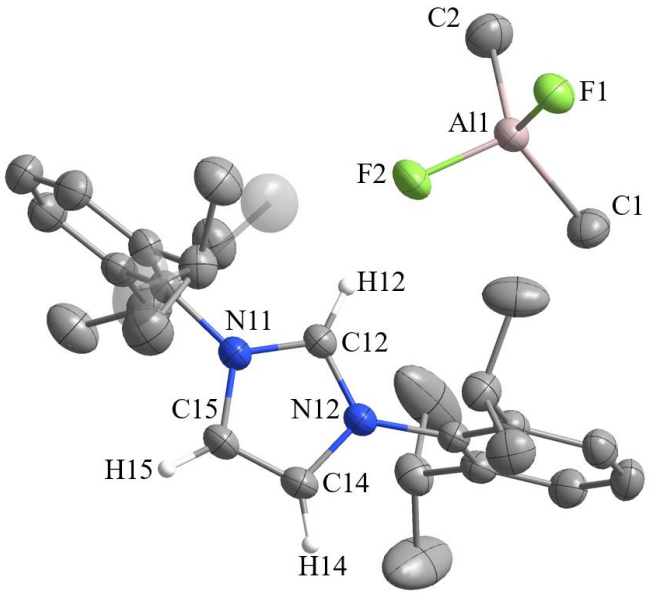

Figure 4.11: Crystal structure of $[IPrH][Me_2AlF_2]$ (**9**) in $[IPrH][Me_2AlF_2]\cdot C_6D_6$ (**9a**). The ellipsoids are drawn at 50 % probability. For clarity, all hydrogen atoms are omitted, except those on the imidazolium ring. The positions of the disordered atoms are shown in domain A and B (shaded).

The data collected for $[IPrH][Me_2AlF_2]\cdot C_6D_6$ (**9a**) are of better quality than the data for $[IPrH][Me_2AlF_2]\cdot 0.95DCM$ (**9b**). Therefore, the bond lengths and crystal properties of the latter are not discussed further.

$[IPrH][Me_2AlF_2]\cdot C_6D_6$ (**9a**) crystallises in the triclinic space group $P\bar{1}$. Its asymmetric unit contains a $[IPrH]^+$ cation and a discrete, tetrahedrally coordinated $[Me_2AlF_2]^-$ anion. In addition, it contains two halves of C_6D_6 located in channels along a axis and aligned to allow C−H π-interaction between the C_6D_6 molecules in the channels. The unit cell packing in the crystal structure of $[IPrH][Me_2AlF_2]\cdot C_6D_6$ (**9a**) is shown in Figure 4.12. The cation and the anion interact with each other and form two hydrogen bonds. The shortest is formed between the proton on C2 position and the nearest fluorine atom C(12)−H(12)···F(2) with H···F distances of 1.985(1) Å (C···F distances of 2.931(2) Å), while the second hydrogen bond is formed between the second fluorine atom and a hydrogen atom from the imidazolium backbone of a symmetrically generated unit C(15)−H(15)···F(1) with a H···F distance of 2.299(1) Å (C···F distance of 2.996(2) Å). The average Al−C distances of 1.958 Å and the average Al−F distances of 1.714 Å agree well with the average Al−C distances (1.986 Å, 1.969 Å, and 1.978 Å) and the average Al−F distances (1.711 Å, 1.712 Å, and 1.691 Å) reported by other groups for discrete $[R_2AlF_2]^-$ anions [60], [61].

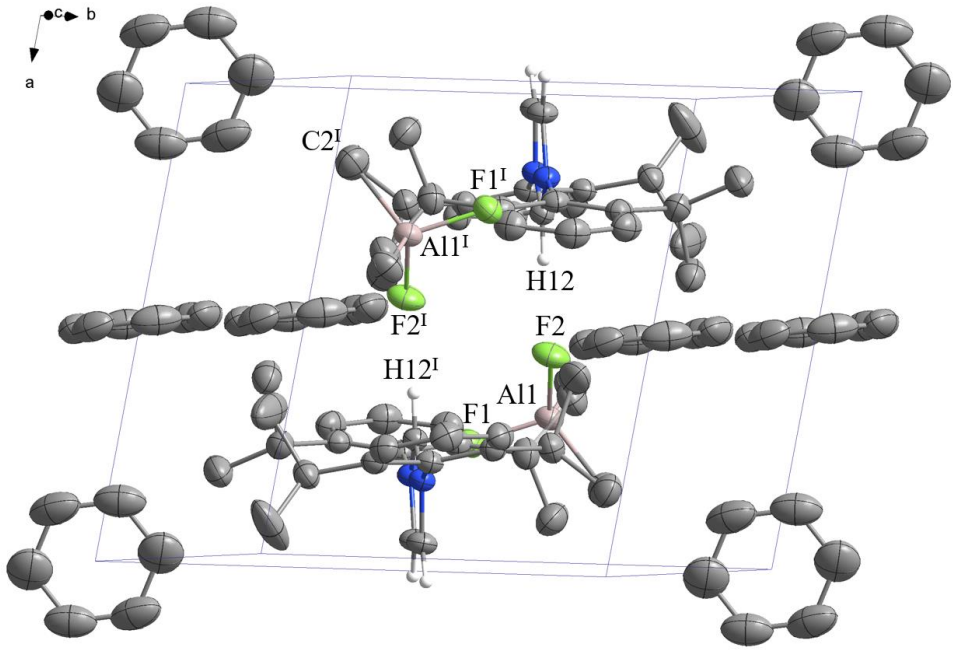

Figure 4.12: Unit cell packing in the crystal structure of $[IPrH][Me_2AlF_2]\cdot C_6D_6$ (**9a**). The ellipsoids are drawn at 50 % probability. For clarity, only atoms in domain A are shown and all hydrogen atoms are omitted, except those on the imidazolium ring.

Single crystals of $[IPrH][(n\text{-}Bu)_2AlF_2]$ (**10**) were formed by slow evaporation of acetonitrile. Its crystal structure is shown in Figure 4.13. It crystallises in the monoclinic space group $P2_1/n$. The asymmetric unit contains an $[IPrH]^+$ cation and a discrete, tetrahedrally coordinated $[(n\text{-}Bu)_2AlF_2]^-$ anion. The two n-butyl substituents in the $[(n\text{-}Bu)_2AlF_2]^-$ anion are disordered. Two preferred orientations of the substituents were modelled and refined, with occupancies of domain A being 53 % and domain B 47 %. Both domains are shown in Figure 4.13, with domain B shaded for clarity. The cation and the anion interact with each other and form two hydrogen bonds. The shortest is formed between the proton on C2 position and the nearest fluorine atom C(12)−H(12)···F(2)

with H···F distances of 1.999(1) Å (C···F distances of 2.900(1) Å), while the second hydrogen bond is formed between the second fluorine atom and a hydrogen atom from the imidazolium backbone of a symmetrically generated unit C(14)–H(14)···F(1) with a H···F distance of 2.043(1) Å (C···F distance of 2.988(2) Å). The average Al–C distances of 2.026 Å (domain A), and 1.926 Å (domain B) and the average Al–F distance of 1.708 Å are consistent with the average Al–C distances (1.986 Å, 1.969 Å, and 1.978 Å) and the average Al–F distances (1.711 Å, 1.712 Å, and 1.691 Å), respectively.

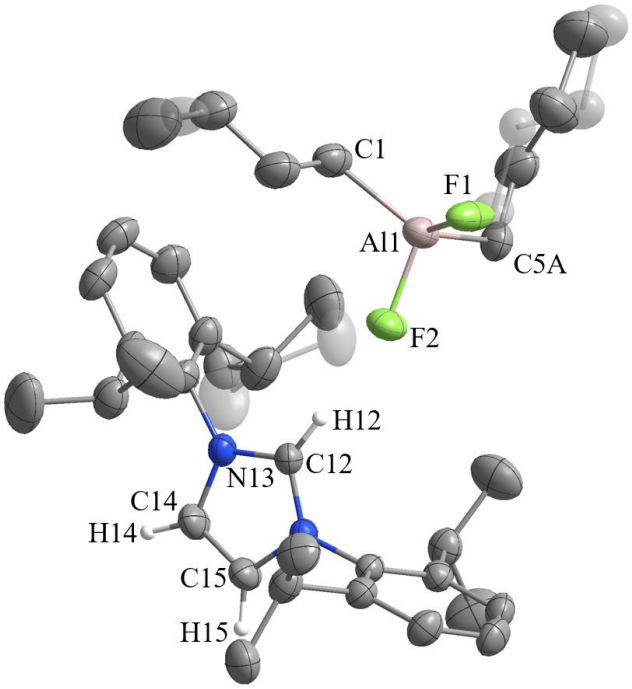

Figure 4.13: Crystal structure of [IPrH][(n-Bu)$_2$AlF$_2$] (**10**). The ellipsoids are drawn at 50 % probability. For clarity, all hydrogen atoms are omitted, except those on the imidazolium ring. The positions of the disordered atoms are shown in domain A and B (shaded).

4.2.1.3 Synthesis of alkyltrifluoroaluminate salts

The two alkylaluminium compounds AlR$_3$ (R = Me, n-Bu) reacted readily with the trifluoride reagent [IPrH][(HF)$_2$F] to form salts with [RAlF$_3$]$^-$ anions and 2 equivalents of alkane RH. The latter was removed from the reaction mixtures *in vacuo*. The reactions were carried out in acetonitrile at room temperature and the salts were isolated as white solids in high yield. AlMe$_3$ reacted to form [IPrH][MeAlF$_3$] (**11**) and 2 equivalents of methane, while Al(n-Bu)$_3$ formed [IPrH][(n-Bu)AlF$_3$] (**12**) and 2 equivalents of n-butane. The reactions proceeded according to Scheme 4.6. During the reactions, 2 RH were eliminated from the metal-bonded alkyl groups and 3 fluoride anions were added to the aluminium centre. Both salts proved to be stable at room temperature under an inert atmosphere. They were stored in a glovebox for long periods without decomposing.

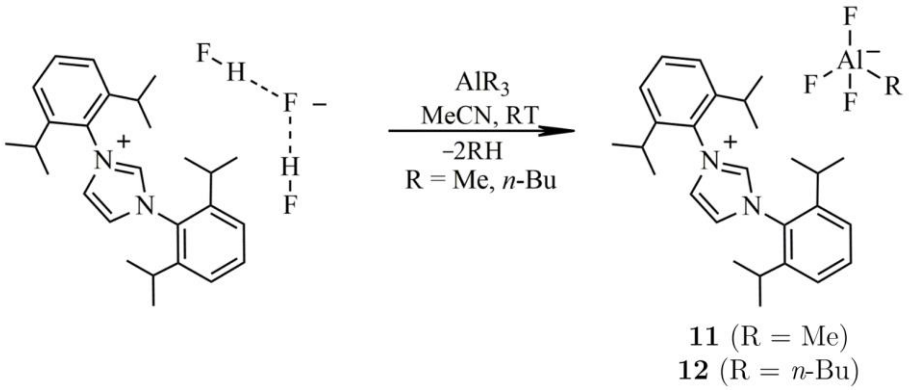

Scheme 4.6: Reactivity of AlR_3 with $[IPrH][(HF)_2F]$ (R = Me, *n*-Bu).

Prior to the publication of our article [26], no simple synthetic procedure had been proposed for the preparation of salts containing discrete $[RAlF_3]^-$ anions. Previously, the only structurally characterised $[(C_2F_5)AlF_3]^-$ anion was obtained upon decomposition of $[(C_2F_5)_4Al]^-$ anions [25]. In our work, we used a trifluoride-containing reagent $[IPrH][(HF)_2F]$ bearing a sterically demanding cation. The reaction was very similar to the one described in the previous chapter, which led to $[R_2AlF_2]^-$ anions. It proved to be a useful, simple and straightforward method for the synthesis of salts with discrete $[RAlF_3]^-$ anions from the corresponding alkylaluminium compounds.

The crystal structure was determined for both compounds. Single crystals of $[IPrH][MeAlF_3]$ (**11**) were obtained by slow evaporation of acetonitrile. It crystallises in the orthorhombic space group *Pnma* and its crystal structure is shown in Figure 4.14.

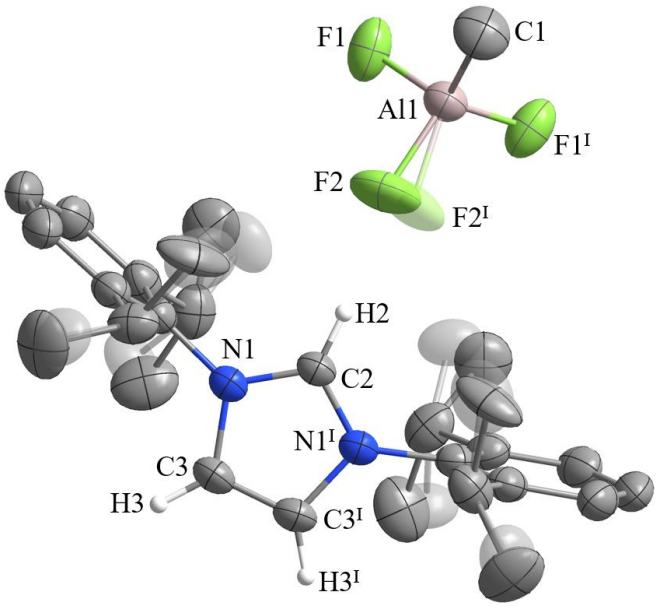

Figure 4.14: Crystal structure of $[IPrH][MeAlF_3]$ (**11**). The ellipsoids are drawn at 50 % probability. For clarity, all hydrogen atoms are omitted, except those on the imidazolium ring. The positions of the disordered atoms are shown in domain A and B (shaded). Symmetry code: (i) x, 1/2−y, z.

The structure has a mirror plane passing through C(1), Al(1), H(2) and C(2) atoms. It contains an $[IPrH]^+$ cation and a discrete, tetrahedrally coordinated $[MeAlF_3]^-$ anion, which interact with each other and form 3 hydrogen bonds. The shortest one forms between the hydrogen atom at C2 position and the nearest fluorine atom C(2)—H(2)···F(2) with a H···F distance of 2.003(3) Å (C···F distance of 2.889(3) Å), while the other hydrogen bonds C(3)—H(3)···F(1) with a H···F distance of 2.303(1) Å (C···F distance of 3.082(2) Å) are formed between the other fluorine atoms and the hydrogen atoms of the imidazolium backbone of a symmetrically generated unit. The Al—C distances of 1.945(3) Å and the average Al—F distances of 1.687 Å are consistent with the Al—C distances of 2.006(6) Å and the Al—F distances of 1.666(3) Å reported for the structurally characterised $[(C_2F_5)AlF_3]^-$ anion [25].

Single crystals of [IPrH][(*n*-Bu)AlF_3] (**12**) formed by slow evaporation of acetonitrile. It crystallises in the monoclinic space group $P2_1/m$ and its crystal structure is shown in Figure 4.15. Crystal data for this compound were collected at 240 K. Measurements at lower temperatures were not possible because the crystals repeatedly broke and lost their crystallinity. As can be seen from Figure 4.15, the structure contains an $[IPrH]^+$ cation and a discrete, tetrahedrally coordinated $[(n\text{-Bu})AlF_3]^-$ anion that is highly disordered. It suffers from orientational disorder. The *n*-butyl group and the fluorine atoms tend to adopt different orientations around the Al centre. The positions of the substituents were modelled and refined as disordered in two preferred orientations, with occupancies of domain A being 63.5 % and domain B 36.5 %. Similar to the structure of its methyl compound, the structure of [IPrH][(*n*-Bu)AlF_3] (**12**) features a mirror plane passing through C(4), C(3), C(2), F(2B), Al(1), F(1A), H(12) and C(12) atoms. However, other structural details and bond lengths are not discussed due to poor data quality.

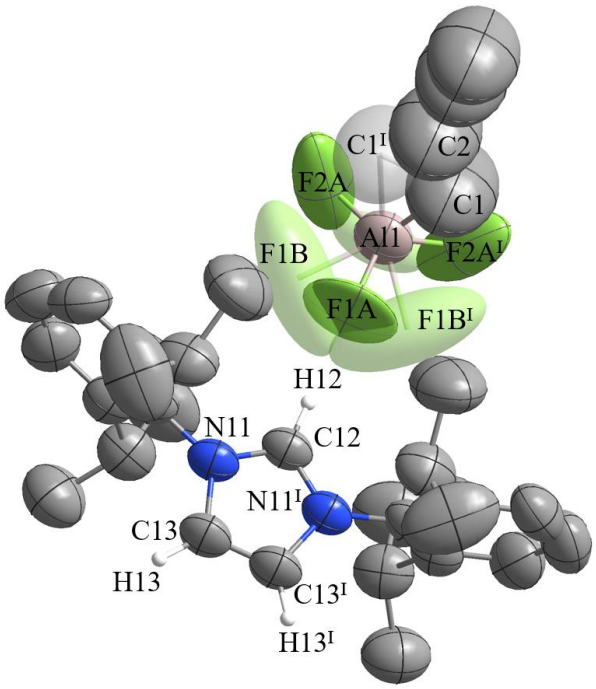

Figure 4.15: Crystal structure of [IPrH][(*n*-Bu)AlF_3] (**12**). The ellipsoids are drawn at 50 % probability. For clarity, all hydrogen atoms are omitted, except those on the imidazolium ring. The positions of the disordered atoms are shown in domain A and B (shaded). Symmetry code: (i) x, 1/2−y, z.

4.2.1.4 Synthesis of tetrafluoroaluminate salts

The reactivity of organoaluminium compounds with imidazolium-based reagents depends strongly on the stoichiometric ratio. We observed that the desired products were formed only when the reactants were used strictly in a 1:1 ratio. A slight excess of the fluorinating reagent led to the formation of more stable aluminate anions containing more fluorine atoms. Therefore, the synthesis of [IPrH][$RAlF_3$] also gave the tetrafluoroaluminate salt [IPrH][AlF_4] (**13**). Its amount was proportional to the excess of the fluorinating reagent used. Pure [IPrH][AlF_4] (**13**) was prepared and characterised separately. It was formed by adding anhydrous HF to the [(IPr)$AlMe_3$] adduct. After all volatiles were removed, it was purified by recrystallisation in acetonitrile. Single crystals formed in a saturated acetonitrile solution stored at −20 °C. [IPrH][AlF_4] (**13**) crystallises in the orthorhombic space group *Pccn* and its crystal structure is shown in Figure 4.16. The structure has a mirror plane passing through Al(1), H(2), and C(2) atoms. It contains an $[IPrH]^+$ cation and a discrete, tetrahedrally coordinated $[AlF_4]^-$ anion, which interact with each other to form four weak hydrogen bonds. Two of them are formed between two fluorine atoms and the hydrogen atoms of the imidazolium backbone C(3)−H(3)···F(2) with an H···F distance of 2.214(1) Å (C···F distance of 3.025(2) Å), while the other two bonds are formed between the remaining fluorine atoms and the hydrogen atom at C2 position of a symmetrically generated unit C(2)−H(2)···F(1) with an H···F distance of 2.403(1) Å (C···F distance of 3.238(2) Å). The average Al−F distance of 1.665 Å is consistent with the average Al−F distances reported for discrete $[AlF_4]^-$ anions (1.636 Å [60], 1.618 Å [19], and 1.712 [25]).

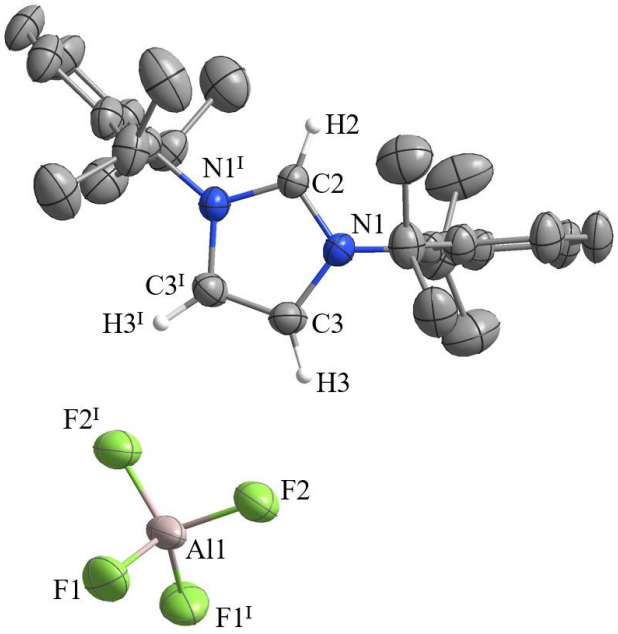

Figure 4.16: Crystal structure of [IPrH][AlF_4] (**13**). The ellipsoids are drawn at 50 % probability. For clarity, all hydrogen atoms are omitted, except those on the imidazolium ring. Symmetry code: (i) 3/2−x, 3/2−y, z.

4.2.1.5 Synthesis of phenylfluoroaluminate salts

$AlPh_3$ was chosen as a representative of the arylaluminium compounds. Its reactivity with the 3 imidazolium-based fluorinating reagents [IPrH][F], [IPrH][(HF)F] and [IPrH][$(HF)_2F$] was investigated. The reactions in 1:1 stoichiometry led to the formation of different

mixtures of [IPrH][Ph_3AlF] (**14**), [IPrH][Ph_2AlF_2] (**15**), [IPrH][$PhAlF_3$] (**16**) and [IPrH][AlF_4] (**13**). Despite all our attempts, we did not succeed in producing the pure products. However, we were able to prepare a relatively pure mixture of [IPrH][Ph_3AlF] (**14**) and [IPrH][$PhAlF_3$] (**16**) by mixing $AlPh_3$ and 1.1 equivalents of [IPrH][(HF)F] in C_6D_6 for 2 days. The mixture proved stable under inert conditions but tended to decompose on air. Single crystals of [IPrH][AlF_4]$\cdot C_6D_6$ (**13a**) were formed when the mixture was crystallised by slow evaporation of the solvent on air. We also obtained a mixture of [IPrH][$PhAlF_3$] (**16**) and [IPrH][AlF_4] (**13**) when a small excess of [IPrH][$(HF)_2F$] reacted with $AlPh_3$. Fortunately, we were able to structurally characterise [IPrH][Ph_3AlF] (**14**) and [IPrH][$PhAlF_3$] (**16**). Single crystals suitable for single crystal X-ray analysis of both compounds were obtained from the crystallisation of mixtures. As far as we know there was only one structurally characterised discrete $[R_3AlF]^-$ anion with perfluoroaryl substituents before the publication of our paper [25], [65]. On this basis, we assumed that phenyl substituents would also be stable and that discrete anions could be isolated. As it turned out, the aromatic substituents influence the reactivity of AlR_3 compounds and the stability of the products differently than the alkyl substituents.

Single crystals of [IPrH][Ph_3AlF] (**14**) were formed from the reaction of $AlPh_3$ with 1 equivalent of [IPrH][F] in C_6D_6, followed by slow evaporation of the solvent. [IPrH][Ph_3AlF] (**14**) crystallises in the monoclinic space group $P2_1/n$ and its asymmetric unit is shown in Figure 4.17. The asymmetric unit contains an $[IPrH]^+$ cation and a discrete, tetrahedrally coordinated $[Ph_3AlF]^-$ anion that interact to form a hydrogen bond C(22)—H(22)$\cdots$F(1) with an H$\cdots$F distance of 2.078(1) Å (C$\cdots$F distance of 2.910(1) Å). The average Al—C distances of 2.003 Å and the Al—F distance of 1.730(1) Å are consistent with the average Al—C distances of 2.018 Å and the Al—F distances of 1.682(5) Å of the previously reported $[(C_{12}F_9)_3AlF]^-$ anion [65].

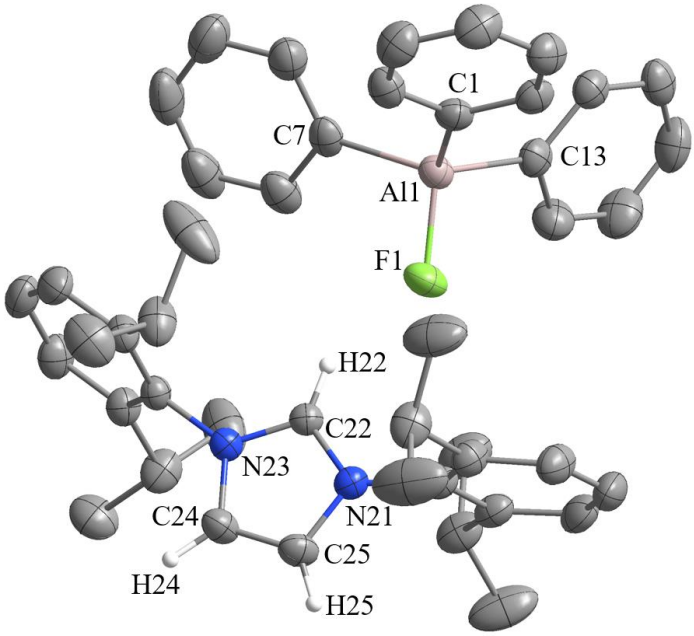

Figure 4.17: Crystal structure of [IPrH][Ph_3AlF] (**14**). The ellipsoids are drawn at 50 % probability. For clarity, all hydrogen atoms are omitted, except those on the imidazolium ring.

Single crystals of [IPrH][PhAlF$_3$] (**16**) were formed from the reaction of AlPh$_3$ with 1 equivalent of [IPrH][(HF)$_2$F] in acetonitrile, followed by slow evaporation of the solvent. [IPrH][PhAlF$_3$] (**16**) crystallises in the triclinic space group *P−1* and its asymmetric unit is shown in Figure 4.18. The asymmetric unit contains an [IPrH]$^+$ cation and a discrete, tetrahedrally coordinated [PhAlF$_3$]$^-$ anion. The fluorine atoms F(2) and F(3) on the fluoroaluminate anion are disordered. Their positions were modelled and refined in two preferred orientations, with occupancies of domain A being 64 % and domain B 36 %. The anion interacts with neighbouring cations and forms 2 hydrogen bonds. The shortest one forms between a fluorine atom and the hydrogen atom on C2 position from a symmetrically generated unit C(12)−H(12)···F(2B) with an H···F distance of 2.23(1) Å (C···F distance of 3.09(1) Å), while the other hydrogen bond connects another fluorine atom and the hydrogen atom on the imidazolium backbone C(15)−H(15)···F(1) with a H···F distance of 2.403(2) Å (C···F distance of 3.001(3) Å). The Al−C distance of 1.960(3) Å is consistent with the Al−C distance of 2.006(6) Å reported for the known [(C$_2$F$_5$)AlF$_3$]$^-$ anion [25]. Since two fluorine atoms are disordered in this structure, the average Al−F distance cannot be compared with other reported distances. The average Al−F distance is slightly longer than expected, but the Al−F distance of the non-disordered fluorine atom of 1.683(2) Å is in agreement with the Al−F distance of 1.666(3) Å reported for the known [(C$_2$F$_5$)AlF$_3$]$^-$ anion [25].

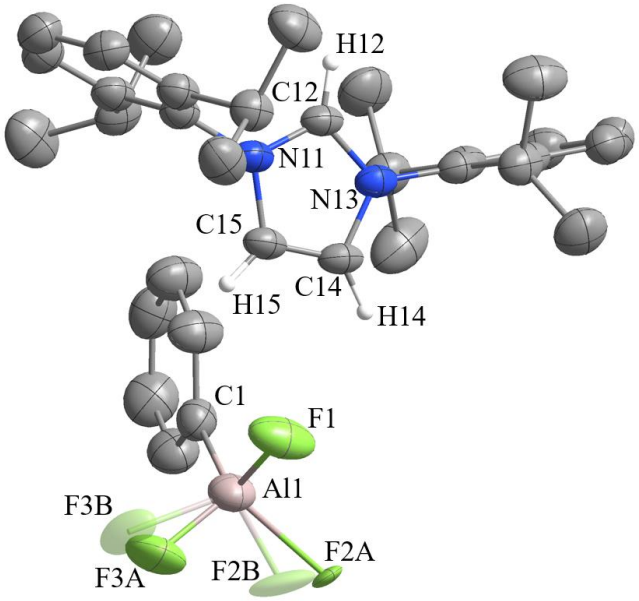

Figure 4.18: Crystal structure of [IPrH][PhAlF$_3$] (**16**). The ellipsoids are drawn at 50 % probability. For clarity, all hydrogen atoms are omitted, except those on the imidazolium ring. The positions of the disordered atoms are shown in domain A and B (shaded).

4.2.2 NMR spectroscopy

All synthesised compounds were characterised by NMR spectroscopy. The spectra are consistent with the crystal structures of the compounds. Selected NMR peaks of the prepared fluoroaluminate salts are listed in Table 4.3. The ^{13}C NMR values listed in the table were determined by ^{1}H–^{13}C HSQC experiments, since the signals of the carbon atoms bonded directly to aluminium could not be observed by ^{13}C NMR experiments. Due to the coupling with protons, ^{1}H–^{13}C HSQC experiments are much more sensitive. However, the

signals of carbon atoms bound to aluminium in phenyl groups could not be observed. Table 4.3 shows that in the [IPrH][$R_{4-n}AlF_n$] (n = 1–4 and R = Me, n-Bu, Ph) series, the chemical shifts of the ^{13}C, ^{19}F and ^{27}Al NMR peaks are affected by the number of fluorine atoms and the nature of the substituents. The effects are described in the following sections.

The ^{13}C NMR peaks in each [IPrH][$R_{4-n}AlF_n$] (n = 1–4) series are shifted upfield with increasing number of fluorine atoms. The peaks are also shifted upfield much more when the substituents are methyl groups compared to n-butyl groups.

Table 4.3: Selected ^{13}C, ^{19}F and ^{27}Al NMR peaks of [IPrH][$R_{4-n}AlF_n$] (n = 1–4 and R = Me, n-Bu, Ph) in acetonitrile.

Compound	δ(^{13}C)[a] Al–C	δ(^{19}F) Al–F	δ(^{27}Al)
[IPrH][Me_3AlF] (**7**)	−5.4	−158.64	150.64
[IPrH][Me_2AlF_2] (**9**)	−11.1	−154.78	123.90
[IPrH][$MeAlF_3$] (**11**)	−13.7	−167.07	84.96
[IPrH][AlF_4] (**13**)	/	−194.62	49.37
[IPrH][(n-Bu)$_3$AlF] (**8**)	11.7	−167.90	147.51
[IPrH][(n-Bu)$_2$$AlF_2$] (**10**)	10.1	−160.74	120.71
[IPrH][(n-Bu)AlF_3] (**12**)	6.6	−169.61	82.71
[IPrH][Ph_3AlF] (**14**)	n.o.	−169.90	97.52
[IPrH][Ph_2AlF_2] (**15**)	n.o.	−166.39	86.17
[IPrH][$PhAlF_3$] (**16**)	n.o.	−175.48	71.38

[a] Determined with ^{1}H–^{13}C HSQC experiments.

The ^{19}F NMR peaks of the organofluoroaluminate anions are broad, which is due to the coupling with ^{27}Al, a quadrupolar nucleus ($I = 5/2$). The highly symmetrical $[AlF_4]^-$ anion is the only exception among the fluoroaluminates. Its peak at −194.62 ppm is split into six lines due to scalar coupling with ^{27}Al and agrees well with previous reports (δ −195.9 ppm, −194.2 ppm [19], [25]). The ^{19}F NMR signals of the organofluoroaluminate anions with 2 fluorine atoms are the most downfield in each [IPrH][$R_{4-n}AlF_n$] (n = 1–3) series, while the anions with 3 fluorine atoms are the most upfield. For example, the chemical shifts of the anions with methyl substituents arrange in the order $[Me_2AlF_2]^-$ at −154.78 ppm, $[Me_3AlF]^-$ at −158.64 ppm and $[MeAlF_3]^-$ at −167.07 ppm. Furthermore, anions with methyl substituents have the more downfield signals than anions with n-butyl substituents, while anions with phenyl substituents are the most upfield. For example, the signals for $[R_3AlF]^-$ anions line up in the order $[Me_3AlF]^-$ at −158.64 ppm, $[(n\text{-Bu})_3AlF]^-$ at −167.90 ppm and $[Ph_3AlF]^-$ at −169.90 ppm. The same trend is observed for the anions described by other groups. ^{19}F NMR chemical shifts for $[Me_3AlF]^-$ and $[Me_2AlF_2]^-$ were reported to be −148.2 ppm and −154.82 ppm [61], [64], while the chemical shift for $[(C_{12}F_9)_3AlF]^-$ was reported to be −176.81 ppm [65].

The ^{27}Al NMR peaks of the organofluoroaluminate anions are broad, which is due to the coupling with ^{19}F and the quadrupolar nature of ^{27}Al. The highly symmetric $[AlF_4]^-$ anion is the only exception among the fluoroaluminates. Its peak at −49.37 ppm has the shape of a quintet, which is due to the coupling with ^{19}F ($I = 1/2$). In each [IPrH][$R_{4-n}AlF_n$] (n = 1–4) series, the ^{27}Al NMR signals are shifted more upfield with each additional fluorine atom in the anions. For example, the chemical shifts of the anions with methyl substituents arrange in the order $[Me_3AlF]^-$ at 150.64 ppm, $[Me_2AlF_2]^-$ at 123.90 ppm, $[MeAlF_3]^-$ at 84.96 ppm and $[AlF_4]^-$ at 49.37 ppm. The same trend was also observed by Roesky and Finze [3], [25]. Furthermore, the nature of the substituents has a similar influence on the

^{27}Al NMR peaks as on the ^{19}F NMR signals. Anions with methyl substituent have more downfield signals than anions with *n*-butyl substituents, while those with phenyl substituents are most upfield. For example, the signals for $[R_3AlF]^-$ anions are in the order $[Me_3AlF]^-$ at 150.64 ppm, $[(n\text{-Bu})_3AlF]^-$ at 147.51 ppm and $[Ph_3AlF]^-$ at 97.52 ppm.

4.2.3 Raman spectroscopy

All synthesised compounds were characterised by Raman spectroscopy. Table 4.4 lists the relevant vibrational bands for the organofluoroaluminate salts. The bands of the $[IPrH]^+$ cation usually obscured the vibrations of the Al—F and Al—C bonds, making them difficult to assign. For the organofluoroaluminate anions, the Al—F vibrations could not be assigned. The Al—F vibrations were assigned only for $[IPrH][AlF_4]$ (**13**) at 321 and 634 cm^{-1} and agree with the Al—F vibrations of $[AlF_4]^-$ anions measured by other groups (635, 322, and 622 cm^{-1} [19], [228]).

Table 4.4: Selected Al—C and Al—F Raman bands of $[IPrH][R_{4-n}AlF_n]$ (n = 1–4 and R = Me, *n*-Bu, Ph).

Compound	Raman Shift / cm^{-1}
$[IPrH][Me_3AlF]$ (**7**)	505 (Al—C)
$[IPrH][Me_2AlF_2]$ (**9**)	533 (Al—C)
$[IPrH][MeAlF_3]$ (**11**)	567 (Al—C)
$[IPrH][AlF_4]$ (**13**)	321 and 634 (Al—F)
$[IPrH][(n\text{-Bu})_3AlF]$ (**8**)	493 (Al—C)
$[IPrH][(n\text{-Bu})_2AlF_2]$ (**10**)	494 (Al—C)
$[IPrH][(n\text{-Bu})AlF_3]$ (**12**)	495 (Al—C)
$[IPrH][Ph_3AlF]$ (**14**) and $[IPrH][PhAlF_3]$ (**16**)	999 and 1030 (Al—Ph)

For $[Me_{4-n}AlF_n]^-$ (n = 1–3) anions, the Al—C vibrations were assigned according to the literature data (Al—CH_3 at 530 cm^{-1} [229]). The full Raman spectra with the assigned Al—F and Al—C vibrations of the $[IPrH][Me_{4-n}AlF_n]$ (n = 1—4) series are shown in Figure 4.19. Within the $[Me_{4-n}AlF_n]^-$ (n = 1–3) series of anions the Al—C vibrations are shifted to higher frequencies with each additional fluorine atom. This effect could be explained by the fact that the presence of fluorine, a rather electronegative element, strengthens the Al—C bond. This increases the energy of the Al—C bond energy and the Raman vibration shifts to higher frequencies.

For $[(n\text{-Bu})_{4-n}AlF_n]$ (n = 1–3) anions, the Al—C vibrations were difficult to assign. They are broad and tend to be obscured by other vibrations. We assigned lower frequencies to them than to the methyl counterparts, which is consistent with published data (Al—C_2H_5 at 489 cm^{-1} [229]). The full Raman spectra with the assigned Al—F and Al—C vibrations of the $[IPrH][(n\text{-Bu})_{4-n}AlF_n]$ (n = 1—4) series are shown in Figure 4.20.

For the mixture of $[IPrH][Ph_3AlF]$ (**14**) and $[IPrH][PhAlF_3]$ (**16**), the Al—C vibrations were assigned according to the published data (Al—C_6H_5 1085 cm^{-1} [229]). The complete Raman spectra with the assigned Al—F and Al—C vibrations of the $[IPrH][(Ph_{4-n}AlF_n]$ (n = 1, 3, 4) series are shown in Figure 4.21.

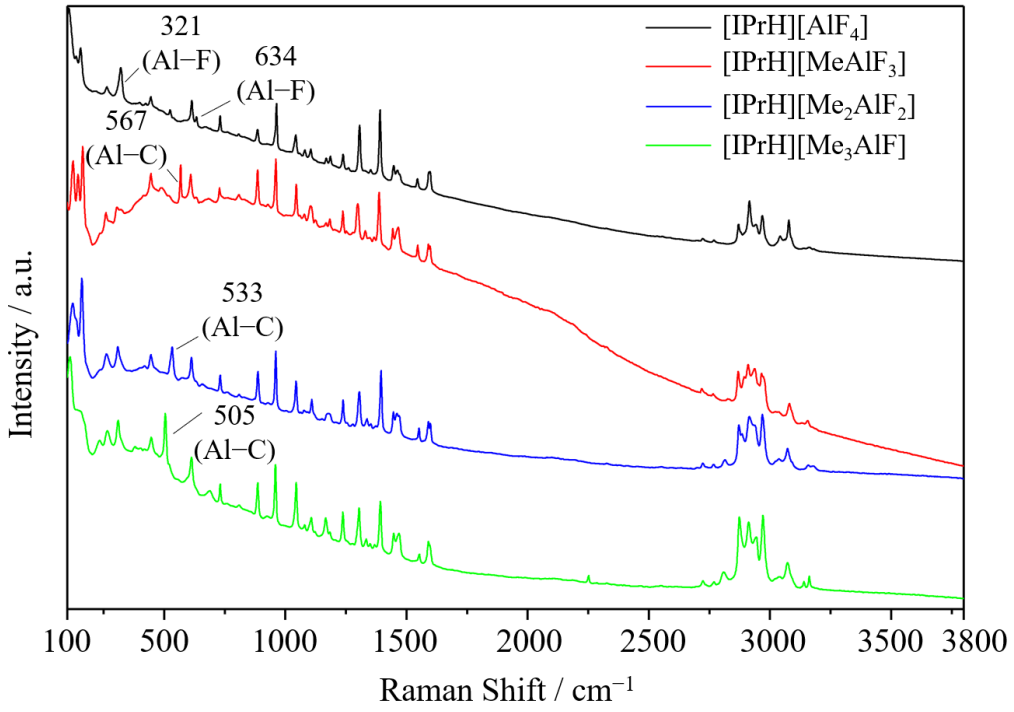

Figure 4.19: Raman spectra of $[IPrH][Me_{4-n}AlF_n]$ ($n = 1$–4). Where possible, Al–F and Al–C vibrations are assigned.

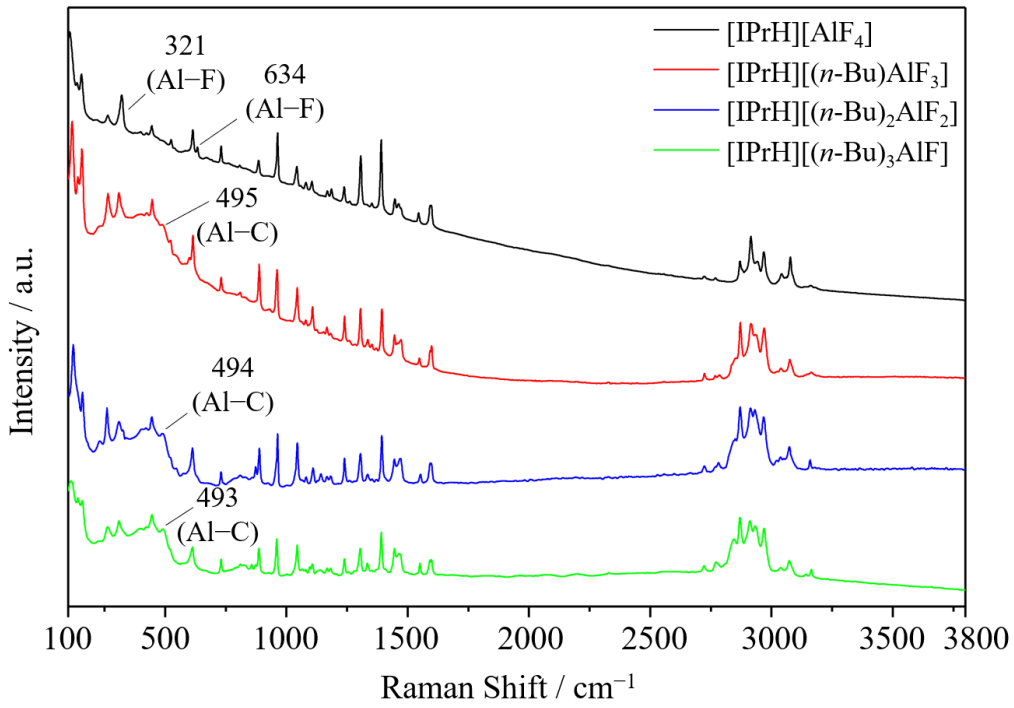

Figure 4.20: Raman spectra of $[IPrH][(n\text{-}Bu)_{4-n}AlF_n]$ ($n = 1$–4). Where possible, Al–F and Al–C vibrations are assigned.

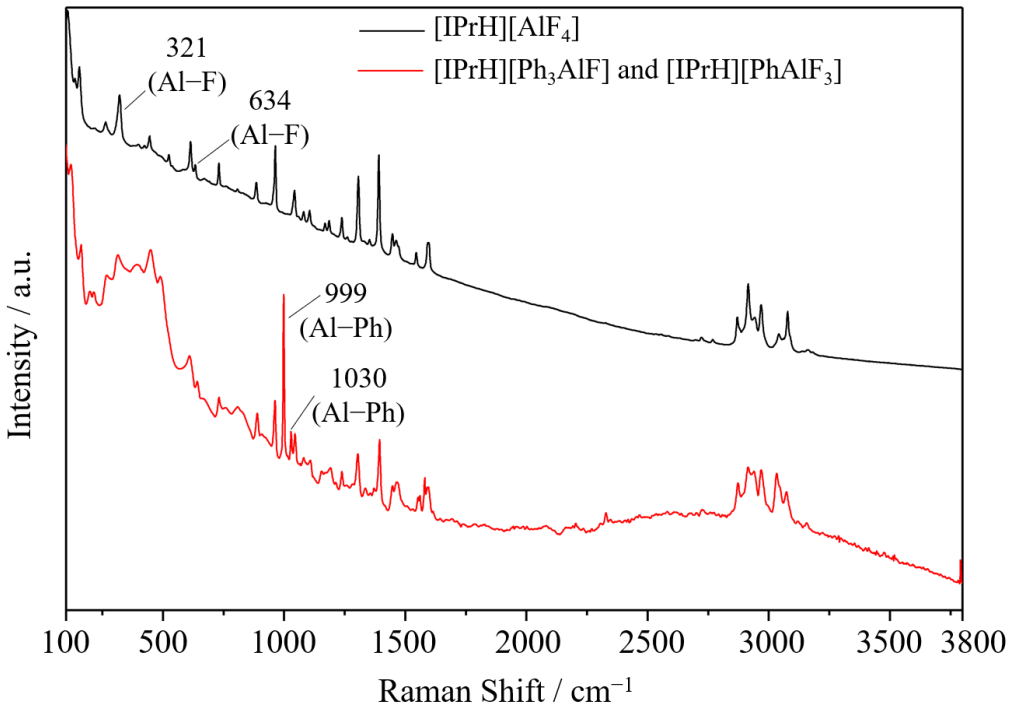

Figure 4.21: Raman spectra of [IPrH][$Ph_{4-n}AlF_n$] (n = 1, 3, 4). Where possible, Al—F and Al—C vibrations are assigned.

4.2.4 Computational results

The crystal structures of [IPrH][$R_{4-n}AlF_n$] (n = 1–4, R = Me, n-Bu, Ph) were used as a starting point for calculating optimised structures using DFT calculations. The optimised structures were then examined in comparison with experimentally obtained crystal structures. The optimised structures of the [IPrH][$R_{4-n}AlF_n$] (n = 1–4, R = Me, n-Bu, Ph) salts are shown in Figure 4.22, while the experimental and calculated bond distances of [IPrH][$R_{4-n}AlF_n$] (n = 1–4, R = Me, n-Bu, Ph) are summarised in Table 4.5.

From Table 4.5 it can be seen that the calculated Al—C distances are slightly longer but still in agreement with the experimental values, while the calculated Al—F distances are significantly longer compared to the experimental values. For example, the calculated and experimental Al—C bonds of [IPrH][$MeAlF_3$] (**11**) are 1.97 Å and 1.945(3) Å, respectively, while the calculated and experimental Al—F bonds are 1.75 Å and 1.696(3) Å, respectively. The difference can be explained by the fact that the calculations in the gas phase did not take into account the effect of crystal structure packing. In some cases, the difference may also be caused by the disorder of the fluorine and carbon atoms in the crystal structure.

In Table 4.5, it can be seen that within each [IPrH][$R_{4-n}AlF_n$] (n = 1–3) series, both the calculated and experimental Al—C bonds become shorter with each additional fluorine atom in the structure. For example, in the [IPrH][(n-Bu)$_{4-n}AlF_n$] (n = 1–3) series, the calculated Al—C distances change from 2.03 (n = 1) to 2.01 (n = 2) and 1.98 (n = 3). This observation agrees well with the Raman results. Shorter Al—C bonds lead to higher energies and Raman signals at higher frequencies.

Table 4.5: Experimental and calculated Al−C and Al−F bond distances of [IPrH][$R_{4-n}AlF_n$] (n = 1–4, R = Me, n-Bu, Ph).

Compound	d(Al−C) (Å)		d(Al−F) (Å)	
	Experimental	Calculated	Experimental	Calculated
[IPrH][Me_3AlF] (**7**)	n.a.	2.01 2.00 2.01	n.a.	1.82[a]
[IPrH][Me_2AlF_2] (**9**)[b]	1.951(2) 1.965(2)	1.98 1.99	1.717(1)[a] 1.711(1)	1.77[a] 1.76
[IPrH][$MeAlF_3$] (**11**)	1.945(3)	1.97	1.696(3)[a],[c] 1.683(1)[c]	1.75[a] 1.74 1.70
[IPrH][AlF_4] (**13**)	–	–	1.669(1) 1.660(1)	1.73 1.73 1.68 1.68
[IPrH][(n-Bu)$_3$AlF] (**8**)	2.013(3) 1.994(3) 1.984(3)	2.03 2.02 2.02	1.733(1)[a]	1.81[a]
[IPrH][(n-Bu)$_2AlF_2$] (**10**)	2.073(4) 1.980(2)	2.01 2.00	1.7096(9)[a] 1.7072(9)	1.78[a] 1.71
[IPrH][(n-Bu)AlF_3] (**12**)	1.923(18)	1.98	1.539(4)[c] 1.592(5)[c]	1.75[a] 1.74 1.71
[IPrH][Ph_3AlF] (**14**)	2.004(2) 2.004(2) 2.000(2)	2.03 2.00 2.00	1.730(1)[a]	1.77[a]
[IPrH][Ph_2AlF_2] (**15**)	n.a.	1.98 1.99	n.a.	1.76[a] 1.75
[IPrH][$PhAlF_3$] (**16**)	1.960(3)	1.97	1.683(2) 2.155(4)[c] 1.703(6)[c]	1.74[a] 1.74 1.69

[a] These Al−F distances refer to the strongest hydrogen bonds formed between the hydrogen atoms on C2 position and the nearest fluorine atoms.
[b] Reported for [IPrH][Me_2AlF_2]·C_6D_6 (**9a**).
[c] Where fluorine atoms are disordered, Al−F distances are reported for domain A.

By using DFT calculations, we also estimated the amount of energy released during the formation of organofluoroaluminate salts. The energies of the reactions were generally calculated according to the following reaction:

$$[IPrH][F] + nHF + AlR_3 \rightarrow [IPrH][R_{4-n}AlF_n] + nRH$$

The calculated electronic energies and the calculated energies of the reactions are given in Appendix A.4. The calculations show that the formation of more fluorinated products is favoured. Within each [IPrH][$R_{4-n}AlF_n$] (n = 1–4) series, the calculated reaction energies

become more exothermic as the number of fluorine atoms increases. This also contributes to the stability of the organofluoroaluminate anions. This observation is in agreement with the experimental results. We reported that [IPrH][R_3AlF] (R = Me, *n*-Bu) salts tend to decompose into [IPrH][R_2AlF_2] and [(IPr)AlR_3] adducts. The instability of the [IPrH][R_3AlF] salts was confirmed by calculated reaction energies, which show that decomposition is an energetically more favourable process than the formation of two [IPrH][R_3AlF] salts. The energies of the decomposition reactions were calculated to be −486 kJ/mol (R = Me) and −494 kJ/mol (R = *n*-Bu), while the reaction energies for the formation of two [IPrH][R_3AlF] salts were calculated to be −346 kJ/mol (R = Me) and −400 kJ/mol (R = *n*-Bu).

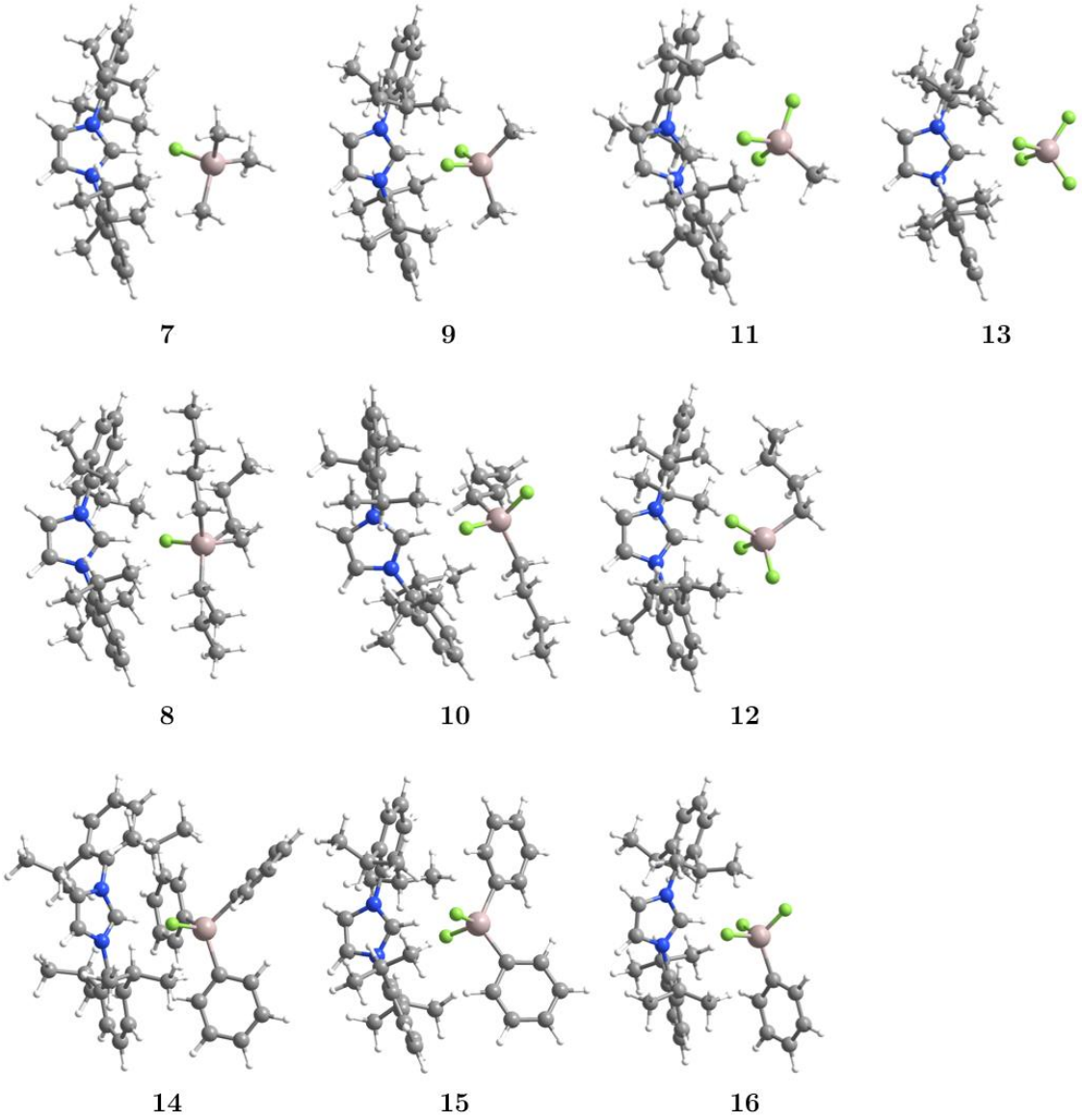

Figure 4.22: Optimised structures of [IPrH][$R_{4-n}AlF_n$] (n = 1–4, R = Me, *n*-Bu, Ph).

4.2.5 Summary

In this chapter, we have presented the reactivity of alkyl- and arylaluminium compounds ($AlMe_3$, $Al(n\text{-}Bu)_3$ and $AlPh_3$) with the series of imidazolium-based fluorinating reagents $[IPrH][(HF)_nF]$ ($n = 0$–2). The alkylaluminium compounds reacted with imidazolium-based fluorinating reagents with the appropriate amount of HF to form salts with discrete triorganofluoroaluminate $[R_3AlF]^-$ anions (**7** and **8**), diorganodifluoroaluminate $[R_2AlF_2]^-$ anions (**9** and **10**) or organotrifluoroaluminate $[RAlF_3]^-$ anions (**11** and **12**). The reaction of poly(hydrogen fluoride) reagents was accompanied by the release of an alkane RH, which was easily removed *in vacuo*. All reactions with alkylaluminium compounds were selective, quantitative and straightforward. In addition, the reactions were strongly dependent on the stoichiometric ratio, as any excess led to the formation of anions with more fluorine atoms. Ultimately, the excess of any fluorinating reagent led to the formation of the tetrafluoroaluminate $[AlF_4]^-$ salt (**13**). The use of imidazolium-based fluorinating reagents with the right amount of HF proved to be very convenient. Even the sterically demanding cation helped stabilise the discrete anions, as its bulkiness prevented possible oligomerisation reactions of the organofluoroaluminate species.

On the other hand, the arylaluminium compound reacted with imidazolium-based reagents to form mixtures of various salts with discrete $[Ph_3AlF]^-$ (**14**), $[Ph_2AlF_2]^-$ (**15**) and $[PhAlF_3]^-$ (**16**) anions. Pure salts could not be prepared or separated.

The experimentally obtained results agree with the DFT calculations. The stability of the organofluoroaluminate salts increases with the increasing number of fluorine atoms in the anions within each $[IPrH][R_{4-n}AlF_n]$ (n = 1–4) series. DFT calculations also proved that the decomposition of $[IPrH][R_3AlF]$ (R = Me, n-Bu) to more stable $[IPrH][R_2AlF_2]$ and $[(IPr)AlR_3]$ is a thermodynamically favourable process.

To summarise, this comprehensive study demonstrates that [IPrH][F], $[IPrH][(HF)F]$ and $[IPrH][(HF)_2F]$ are useful reagents for the synthesis of salts containing discrete alkylfluoroaluminate anions from organoaluminium compounds. We have also proposed the first general procedure for the preparation of salts with $[RAlF_3]^-$ anions. The fluorination ability of the anion and the stabilising properties of the bulky cation give imidazolium-based fluorinating reagents the potential to be used in the search for new discrete fluorinated anions in the future.

4.3 Functionalisation of NHC-Stabilised Aluminium Hydride

This chapter is based on the article "Synthesis and characterization of partially substituted NHC supported alane adducts using triflate or chloride salts" by E. Gruden and G. Tavčar, published in Polyhedron in 2021 [153].

In this work, the reactivity of the NHC adduct [(IPr)AlH_3] with aldiminium-based triflate and chloride salt was investigated. Aldiminium-based salts were found to be suitable group transfer reagents in aluminium hydride chemistry. Substitution of the hydrides with triflate or chloride substituents led to the formation of partially substituted adducts, which were characterised by X-ray structural analysis, NMR and Raman spectroscopy.

4.3.1 Synthesis and crystal structure determination

Detailed synthetic procedures for all compounds are presented in Appendix A.2 together with all data obtained by their characterisation.

4.3.1.1 Synthesis of [(IPr)AlH_2OTf] (17)

The [(IPr)AlH_3] reacted with [CAACH][OTf] to form [(IPr)AlH_2OTf] (**17**) a neutral adduct and $CAACH_2$ (**18**). The reaction was carried out in toluene and proceeded according to Scheme 4.7. $CAACH_2$ (**18**) was easily removed from the reaction mixture by washing with hexane. The [(IPr)AlH_2OTf] adduct (**17**) was isolated in high yield as a white solid. The reaction proceeds rapidly and its progress can be monitored by dissolving of the aldiminium salt. During the reaction, one hydride atom at the aluminium centre is exchanged by a triflate substituent. The exchange of two hydride atoms did not take place. Despite several attempts, the reaction of [(IPr)AlH_3] with [CAACH][OTf] in the molar ratio 1:2 gave only the [(IPr)AlH_2OTf] (**17**), while part of the salt remained undissolved. These results are consistent with previously reported data. Inoue's group obtained the monosubstituted triflate hydride product using excess Me_3SiOTf. The group did not obtain a disubstituted product even at elevated temperature [111]. Other known monosubstituted aluminium hydride triflate compounds were stabilised by imidazolin-2-iminato, β-diketiminato and phosphinimine ligands [111], [132], [149]. As far as we know, no NHC-stabilised (trifluoromethanesulfonyl)oxyalane adduct was known before the publication of our paper. [(IPr)AlH_2OTf] (**17**) was also the first aluminium dihydride triflate compound to be structurally characterised.

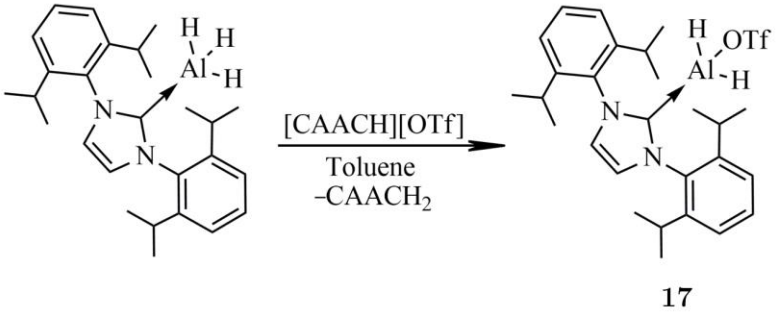

17

Scheme 4.7: Reactivity of [(IPr)AlH_3] with [CAACH][OTf].

Single crystals of [(IPr)AlH_2OTf] (**17**) were formed by slow evaporation of toluene under static vacuum. It crystallised in the orthorhombic space groups $P2_12_12_1$ and its crystal structure is shown in Figure 4.23. The asymmetric unit contained a molecule of [(IPr)AlH_2OTf] (**1**) which, as expected, adopts a tetrahedral arrangement at the aluminium centre. The structural features of the adduct are consistent with similar reported structures. The Al—C_{NHC} distance of 2.048(2) Å agrees well with previously reported Al—C_{NHC} distances of 2.059(2) Å and 2.041(2) Å for NHC-supported AlH_3 adducts [77], [139]. Moreover, the Al—O distance of 1.845(2) Å, and the Al—H distances of 1.49(5) and 1.46(4) Å, are similar to the values of 1.804(2) Å and 1.54(2) Å reported by Roesky, respectively [149].

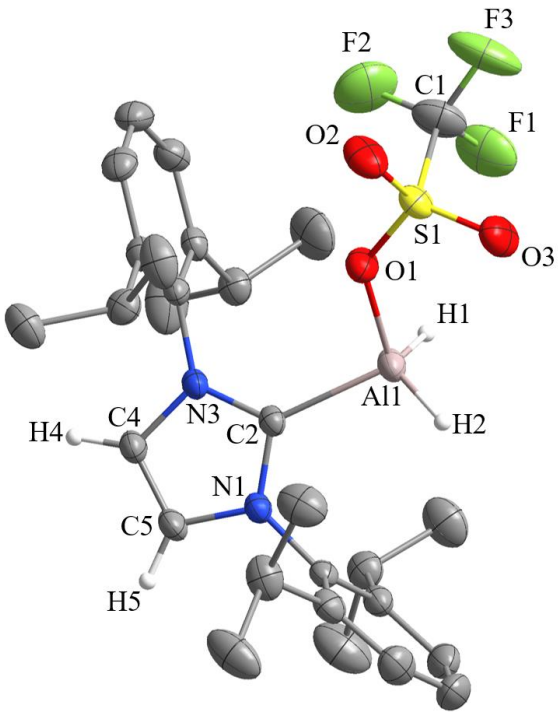

Figure 4.23: Crystal structure of [(IPr)AlH_2OTf] (**17**). The ellipsoids are drawn at 50 % probability. For clarity, all hydrogen atoms are omitted, except those on aluminium and the imidazolium ring.

$CAACH_2$ (**18**) formed as a by-product and was washed out of the reaction mixture with hexane. It crystallised during the slow evaporation of hexane and formed single crystals suitable for X-ray structural analysis. $CAACH_2$ (**18**) crystallises in the orthorhombic space groups *Pbcn* and its crystal structure is shown in Figure 4.24.

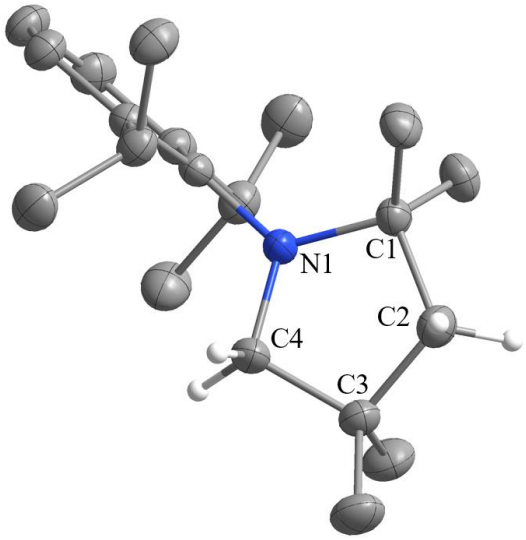

Figure 4.24: Crystal structure of $CAACH_2$ (**18**). The ellipsoids are drawn at 50 % probability. For clarity, all hydrogen atoms are omitted, except those on the heterocyclic ring.

4.3.1.2 Synthesis of $[(IPr)AlH_{3-x}Cl_x]$ ($x = 1, 2$) (19)

The $[(IPr)AlH_3]$ reacted with aldiminium-based chloride salt to give a mixture of $[(IPr)AlH_2Cl]$ and $[(IPr)AlHCl_2]$, two aluminium hydride chloride adducts and $CAACH_2$ (**18**). The reaction was carried out in toluene and proceeded according to Scheme 4.8. $CAACH_2$ (**18**) was easily removed from the reaction mixture by washing with hexane. The mixture of $[(IPr)AlH_2Cl]$ and $[(IPr)AlHCl_2]$ was isolated as a white solid in high yield and is described in this work with the formula $[(IPr)AlH_{3-x}Cl_x]$ ($x = 1, 2$) (**19**). The reaction is also rapid and as described for the triflate counterpart, the progress of the reaction can be monitored by dissolving of aldiminium salt. During the reaction, the hydride atoms on aluminium centre are exchanged by chloride substituents. The two aluminium hydride chloride adducts could not be separated from each other. Selective syntheses of one or the other ware also unsuccessful. Despite several attempts, all reactions led to the formation of mixtures. Even the crystallisation of $[(IPr)AlH_{3-x}Cl_x]$ ($x = 1, 2$) (**19**) ended in a disordered co-crystal of $[(IPr)AlH_2Cl]$ and $[(IPr)AlHCl_2]$. The reaction of $[(IPr)AlH_3]$ with aldiminium-based chloride salt in a molar ration of 1:2 gave a mixture of different aluminium compounds in which 1, 2, or 3 hydride atoms were replaced by chlorides.

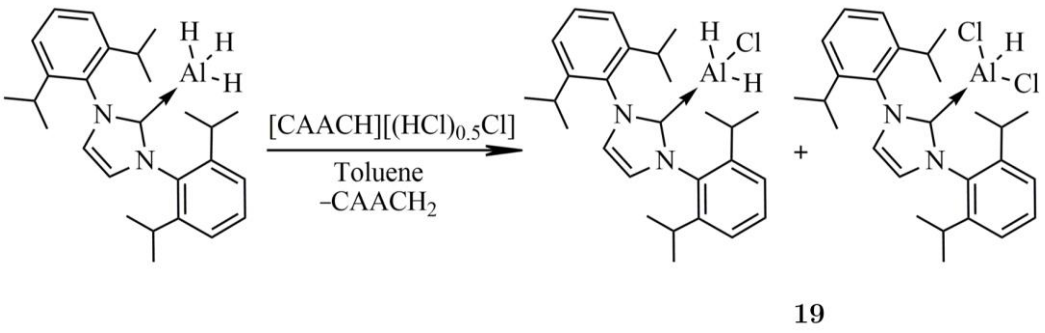

Scheme 4.8: Reactivity of $[(IPr)AlH_3]$ with $[CAACH][(HCl)_{0.5}Cl]$.

At first we assumed that the formation of the [(IPr)$AlH_{3-x}Cl_x$] ($x = 1, 2$) (**19**) was the result of a kinetically controlled reaction. However, it turned out that this was not the case. Elemental analysis of the aldiminium-based chloride salt showed that it was in fact a mixture of salts containing chloride and hydrogen dichloride anions. The two anions are in a molar ratio of about 1:1, which means that the aldiminium salt contains about 1.5 equivalents of Cl and can be written as [CAACH][$(HCl)_{0.5}$Cl]. The formation of aldiminium-based chloride salts containing more than one equivalent of chloride has been observed by other research groups [230], and is in agreement with our results. Consequently, mixing [(IPr)AlH_3] with [CAACH][$(HCl)_{0.5}$Cl] formed a mixture of [(IPr)AlH_2Cl] and [(IPr)$AlHCl_2$] in a ratio of about 1:1, which can be attributed to 1.5 equivalents of Cl in the mixture.

The exchange of hydrides with chlorides and the formation of aluminium hydride chloride adducts were found to be strongly dependent on the stoichiometric ratio. We believed that the selective synthesis of pure [(IPr)AlH_2Cl] and [(IPr)$AlHCl_2$] required the use of pure [CAACH][Cl] and [CAACH][(HCl)Cl] salts. By modifying the original synthesis for aldiminium-based chloride salts [208], we attempted to prepare salts containing only chloride or hydrogen dichloride anions. However, pure [CAACH][Cl] and [CAACH][(HCl)Cl] could not be obtained. Mixtures of both salts were always obtained, but in different stoichiometric ratios. Further reactions with [(IPr)AlH_3] also led to the formation of mixtures with different numbers of substituted atoms. The synthesis of [CAACH][$(HCl)_{0.5}$Cl] was reliable and reproducible and we used this salt for further research. We have also described and published the modified synthesis procedure in our article in Polyhedron [153].

Many different synthetic procedures have been proposed in the literature for the synthesis of aluminium hydride chlorides [148]. Some of them involve the use of salts as HCl sources. For example, ammonium-based chloride salts have been used in many studies [150], [154], [231]. However, all the proposed synthesis methods required very stringent reaction conditions, as they usually lead to the formation of mixtures with different amounts of chlorine [(L)AlH_nCl_{3-n}] ($n = 1$–3) [154]. So far, two pure aluminium hydride chloride adducts stabilised by IMes carbenes were synthesised by Cole's group in 2009. The preparation of [(IMes)AlH_2Cl] and [(IMes)$AlHCl_2$] required the use of very pure reagents. Single-phase aluminium hydride chlorides were purified by sublimation before being used in ligand exchange reactions [150].

Single crystals of [(IPr)$AlH_{3-x}Cl_x$] ($x = 1, 2$) (**19**) were obtained by slow evaporation of toluene under static vacuum. It crystallises in the monoclinic space group $P2_1/c$ and its crystal structure is shown in Figure 4.25. The asymmetric unit contains two tetrahedrally coordinated aluminium hydride chloride adducts in which the positions of the hydrides and chlorides are disordered. The positions of the substituents were modelled and refined in two preferred orientations (domain A and B). Both domains are shown in Figure 4.25, with domain B shaded for clarity. The partial occupancies of the disordered atoms are as follows, indicating that the [(IPr)$AlHCl_2$] and [(IPr)AlH_2Cl] co-crystallise in the crystal structure: Cl2A 0.579(3), H2B 0.421(3), Cl4A 0.500, H4B 0.500, H5A 0.801(2) and Cl5B 0.199(2). We have calculated that molecule 1 contains 1.58 equivalents of chloride and 1.42 equivalents of hydride, while molecule 2 carries 1.70 equivalents of chloride and 1.30 equivalents of hydride substituents.

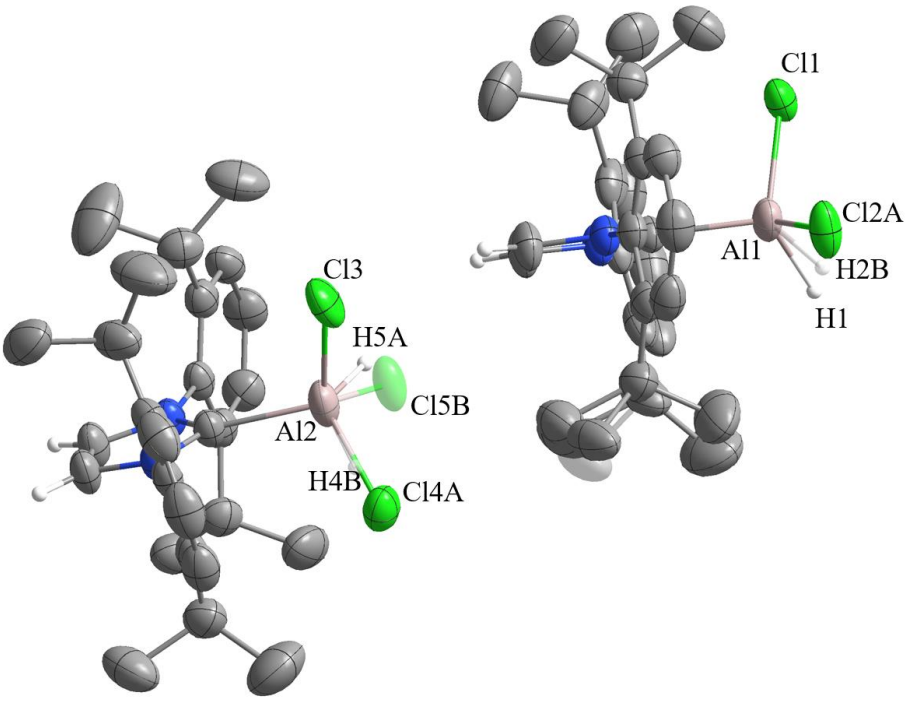

Figure 4.25: Crystal structure of $[(IPr)AlH_{3-x}Cl_x]$ ($x = 1$, 2) (**19**). The ellipsoids are drawn at 50 % probability. For clarity, all hydrogen atoms are omitted, except those on aluminium and the imidazolium ring. The positions of the disordered atoms are shown in domain A and B (shaded).

The structural features of the $[(IPr)AlH_{3-x}Cl_x]$ ($x = 1$, 2) (**19**) adduct are consistent with other similar structures reported by other groups. The Al—C_{NHC} distance of 2.038(2) Å agrees well with the previously reported Al—C_{NHC} distances of 2.059(2) Å and 2.041(2) Å for NHC-supported aluminium hydride adducts [77], [139]. Although the positions of the chloride and hydride substituents in this structure are disordered, the average Al—Cl distance of 2.11 Å and the average Al—H distance of 1.68 Å are in agreement with the reported Al—Cl distance of 2.164(1) Å and the average Al—H distance of 1.72 Å of the $[(IMes)AlH_2Cl]$ adduct [150].

4.3.1.3 Synthesis of $[(IPr)AlCl_3]$ (20)

The $AlCl_3$ adduct $[(IPr)AlCl_3]$ (**20**) was prepared separately to complete the $[(IPr)AlH_{3-n}Cl_n]$ ($n = 0$–3) series and to compare their properties easily. The reaction of the IPr carbene with $AlCl_3$ was carried out in toluene and proceeded according to Scheme 4.9. After removal of the volatiles, $[(IPr)AlCl_3]$ (**20**) was isolated in high yield as a white solid. Single crystals of $[(IPr)AlCl_3]$ (**20**) were obtained by slow evaporation of toluene under static vacuum. It crystallises in the monoclinic space group $P2_1/c$ and its crystal structure is shown in Figure 4.26.

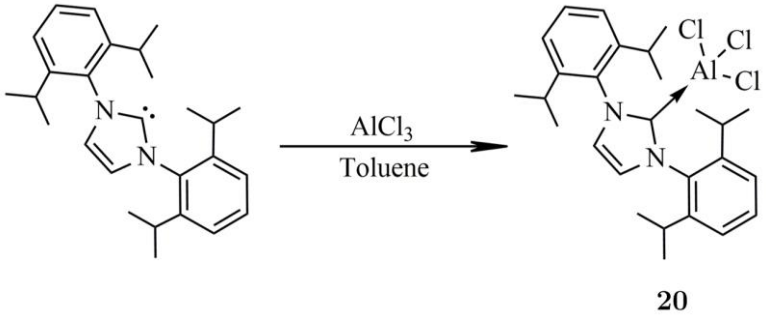

20

Scheme 4.9: Synthesis of [(IPr)$AlCl_3$] (**20**).

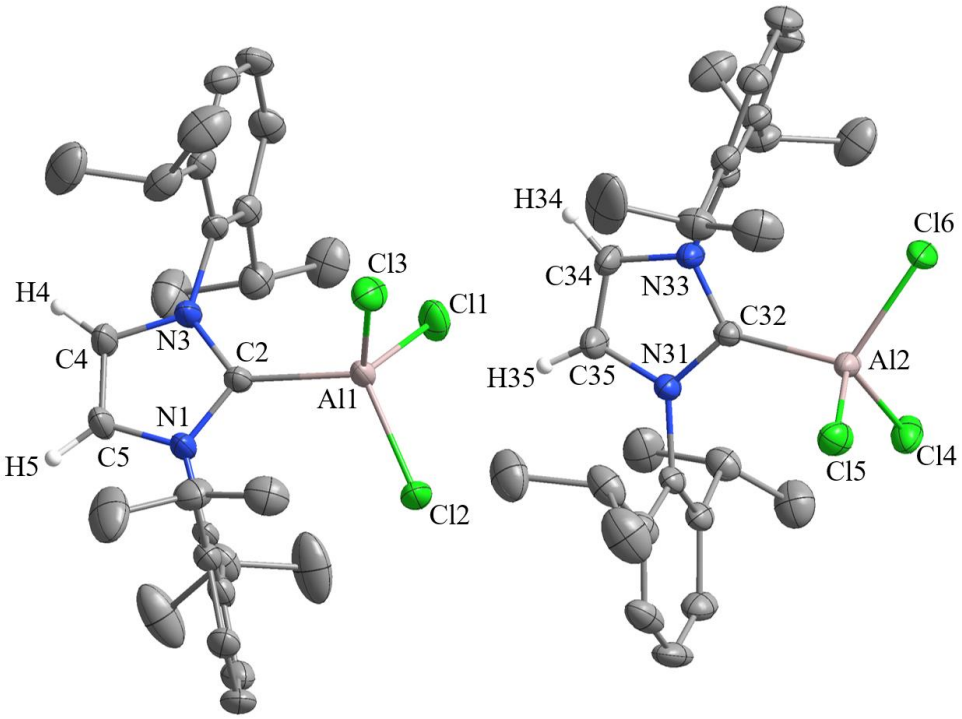

Figure 4.26: Crystal structure of [(IPr)$AlCl_3$] (**20**). The ellipsoids are drawn at 50 % probability. For clarity, all hydrogen atoms are omitted, except those on the heterocyclic ring.

The asymmetric unit contains two tetrahedrally coordinated $AlCl_3$ adducts. The structural features are consistent with similar reported structures. The Al—C_{NHC} distance of 2.019(2) Å is consistent with previously reported Al—C_{NHC} distances of 2.009(5) Å [232] and 2.017(2) Å [233] for [(NHC)$AlCl_3$] adducts. Furthermore, the average Al—Cl distance of 2.13 Å is similar to the average Al—Cl distances of 2.10 Å [232] and 2.12 Å [233] reported for other [(NHC)$AlCl_3$] adducts.

The adduct was prepared by a procedure similar to that described in the literature for [(NHC)$AlCl_3$] adducts with various NHC ligands [232]–[234]. Shortly after the publication of our article, a different approach for the synthesis of the [(IPr)$AlCl_3$] (**20**) adduct was described. It was prepared using the copper(I)-NHC transfer reagent [235].

4.3.2 NMR spectroscopy

All synthesised compounds were characterised by NMR spectroscopy. The spectra agree with the crystal structures of the compounds. In the ^{1}H NMR spectra of all products, the distinct peaks of the IPr carbene ligands can be seen. The two doublets belonging to the methyl groups on the *iso*propyl group are split in a way typical for coordinated NHCs [138]. The NMR spectra of [(IPr)$AlH_{3-x}Cl_x$] (x = 1, 2) (**19**) show the presence of two compounds that are structurally related. The spectrum contains two groups of peaks that are slightly shifted against each other.

NMR spectroscopy was used to compare the properties of [(IPr)AlH_3] [77] and the substituted counterparts. Selected ^{1}H and ^{27}Al NMR peaks of [(IPr)$AlH_{3-n}Cl_n$] (n = 0–3) are listed in Table 4.6. The Al−H peaks in the ^{1}H and ^{27}Al NMR spectra are broad and were not easy to find. In part, the broadening of the Al−H peaks is caused by the quadrupolar nature of the aluminium centre ($I = 5/2$); in part, broad signals may also be caused by the reduced symmetry of the substituted adducts compared with AlH_3 counterpart [77].

Table 4.6: Selected ^{1}H and ^{27}Al NMR peaks of [(IPr)AlH_2OTf] (**17**) and [(IPr)$AlH_{3-n}Cl_n$] (n = 0–3) series in C_6D_6.

Compound	δ(^{1}H) Al−H	δ(^{1}H) CH=CH	δ(^{27}Al)
[(IPr)AlH_3][a]	3.67	6.44	107.9
[(IPr)AlH_2OTf] (**17**)	3.94	6.37	118 (broad)
[(IPr)$AlH_{3-x}Cl_x$] (x = 1, 2) (**19**)	3.7–4.1	6.41, 6.40	113 (broad)
[(IPr)$AlCl_3$] (**20**)	/	6.41	103.8

[a] Values reported in reference [77].

The Al−H peaks in the ^{1}H NMR are hidden in the baseline as broad singlets. The peaks belonging to the substituted adducts [(IPr)AlH_2OTf] (**17**) at 3.94 ppm and [(IPr)$AlH_{3-x}Cl_x$] (x = 1, 2) (**19**) at 3.7–4.1 ppm are shifted downfield compared to the parent [(IPr)AlH_3] at 3.67 ppm. The shift can be explained as a consequence of the more electronegative substituents at the aluminium centre.

The ^{1}H NMR shifts of the proton at the CH=CH carbene backbone provide us with useful information about the Lewis acidity of the adduct. The Lewis acidity of the metal centre influences the Lewis acidity of the adduct and the delocalisation of the electrons of the NHC heterocycle. Consequently, the signals of the CH=CH protons shift [150], [236]. In our case, the CH=CH ^{1}H signals of the substituted adducts [(IPr)AlH_2OTf] (**17**) at 6.37 ppm and [(IPr)$AlH_{3-x}Cl_x$] (x = 1, 2) (**19**) at 6.41 and 6.40 ppm are shifted upfield compared to the parent compound [(IPr)AlH_3] at 6.45 ppm. This effect can be explained by the increase in Lewis acidity of the metal centres [148]. The CH=CH ^{1}H NMR peaks within the [(IPr)$AlH_{3-n}Cl_n$] (n = 0–3) series show that the peaks of [(IPr)AlH_3] at 6.44 ppm are more downfield compared to the peaks of [(IPr)$AlH_{3-x}Cl_x$] (x = 1, 2) (**19**) at 6.41 and 6.40 ppm, and [(IPr)$AlCl_3$] (**20**) at 6.41 ppm. The latter two adducts have very similar CH=CH shifts, implying that the aluminium hydride chlorides and the $AlCl_3$ adducts have similar Lewis acidities. This observation is consistent with the results of Cole, who reported that the Lewis acidity of substituted aluminium hydride halide adducts increases with each additional halide in the structure [150].

The Al−H peaks in the ^{27}Al NMR are broad for aluminium hydride adducts and were difficult to find due to the high background signal from the probe. The peaks belonging to the substituted adducts [(IPr)AlH_2OTf] (**17**) at 118 ppm and [(IPr)$AlH_{3-x}Cl_x$] (x = 1, 2)

(**19**) at 113 ppm were observed in the range typical for NHC-supported aluminium hydride adducts (between 100 and 140 ppm) [77]. The ^{27}Al NMR peak of [(IPr)AlCl$_3$] (**20**) is much sharper compared to aluminium hydride counterparts and is observed at 103.8 ppm. This is consistent with previous reports for [(NHC)AlCl$_3$] adducts [232].

4.3.3 Raman spectroscopy

All synthesised compounds were characterised by Raman spectroscopy. The complete Raman spectra with the assigned Al–H, Al–Cl, S–O, C–S and C–F vibrations are shown in Figure 4.27.

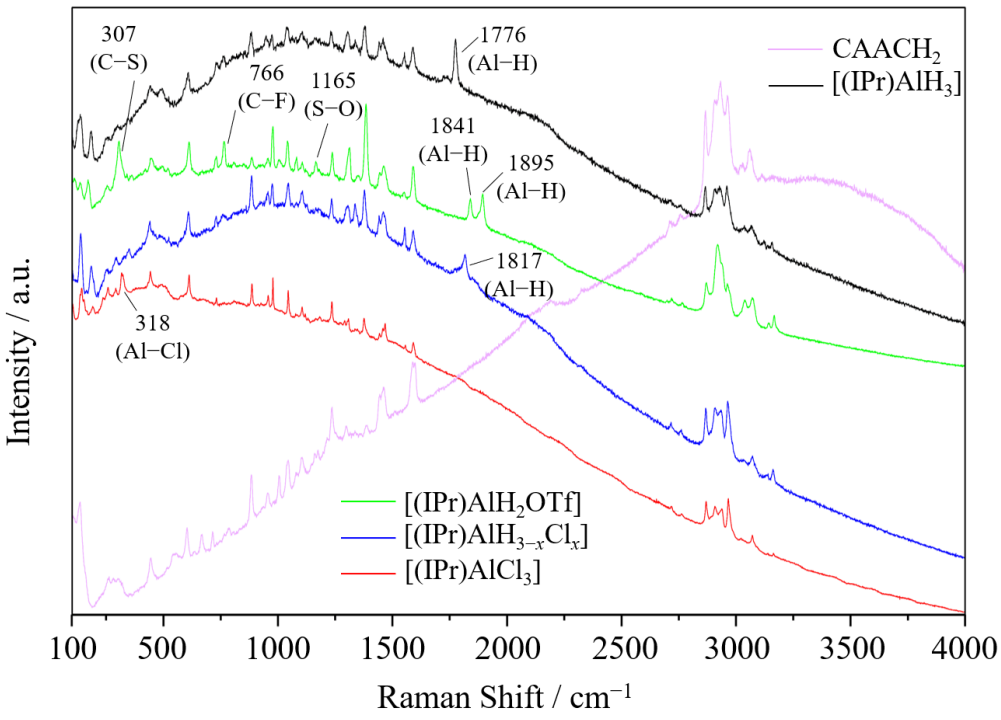

Figure 4.27: Raman spectra of NHC-stabilised AlH$_3$, functionalised aluminium hydrides and related compounds. Spectra of [(IPr)AlH$_3$], [(IPr)AlH$_2$OTf] (**17**), CAACH$_2$ (**18**), [(IPr)AlH$_{3-x}$Cl$_x$] (x = 1, 2) (**19**) and [(IPr)AlCl$_3$] (**20**) have assigned bands for Al–H, Al–Cl, S–O, C–S, and C–F vibrations where possible.

Relevant vibrational bands for [(IPr)AlH$_3$] and the substituted counterparts are listed in Table 4.7. The bands of the IPr carbene ligand generally obscured the relevant vibrations, making them difficult to assign. For [(IPr)AlH$_{3-x}$Cl$_x$] (x = 1, 2) (**19**) the Al–Cl vibrations could not be assigned.

Table 4.7: Selected Raman bands of Al–H and Al–Cl stretching of [(IPr)AlH$_2$OTf] (**17**) and [(IPr)AlH$_{3-n}$Cl$_n$] (n = 0–3) series.

Compound	ν / cm^{-1} Al–H	ν / cm^{-1} Al–Cl
[(IPr)AlH$_3$]	1775	/
[(IPr)AlH$_2$OTf] (**17**)	1841, 1893	/
[(IPr)AlH$_{3-x}$Cl$_x$] (x = 1, 2) (**19**)	1777, 1818	n.o.
[(IPr)AlCl$_3$] (**20**)	/	318

The determined vibrational bands of [(IPr)AlH_3] were compared with the vibrations of the substituted counterparts and the effect of the substituents was evaluated. The Al−H Raman bands of the substituted aluminium hydride adducts are shifted to higher frequencies. The shift may be a consequence of the Al−H bond elongation in the presence of more electronegative substituents. The same effect was also observed in 1H NMR spectra for Al−H peaks. The negative inductive effect of an electronegative element strengthens the Al−H bond and increases its energy. Consequently, the Raman shifts are observed at higher frequencies [150]. This is in agreement with other reports in which the Al−H bonds of aluminium hydride chloride adducts were studied with IR spectroscopy [150], [237].

4.3.4 Summary

In this chapter, we have presented the use of aldiminium-based salts in the functionalisation of aluminium hydride adducts. The reaction of [(IPr)AlH_3] and [CAACH][OTf] gave [(IPr)AlH_2OTf] (**17**), the first structurally characterised (trifluoromethanesulfonyl)-oxyalane NHC adduct and the first aluminium dihydride triflate compound. Meanwhile, the use of [CAACH][$(HCl)_{0.5}$Cl] gave the mixture of [(IPr)AlH_2Cl] and [(IPr)$AlHCl_2$] in a ratio of about 1:1, written as [(IPr)$AlH_{3-x}Cl_x$] (x = 1, 2) (**19**). In both reactions, the protonated $CAACH_2$ (**18**) was formed as a by-product, which was easily removed from the products with hexane. The mixture [(IPr)$AlH_{3-x}Cl_x$] (x = 1, 2) contains about 1.6 equivalents of chlorine and is formed because the aldiminium-based chloride salt is a mixture of [CAACH][Cl] and [CAACH][(HCl)Cl] containing about 1.5 equivalents of chlorine. Although the [CAACH][$(HCl)_{0.5}$Cl] was prepared by a modified method in our research, we believe that similar mixtures can also be obtained by using published methods. Since the aldiminium-based chloride salts are mostly used as precursors for CAACs, the formation of salts with more than 1 equivalent of chlorine probably goes unnoticed.

The analysis of the obtained products showed that the substitution of a hydride by a more electronegative element affects the Lewis acidity of the adducts by strengthening the Al−H bonds. The Lewis acidity of [(IPr)$AlH_{3-x}Cl_x$] (x = 1, 2) was found to be more similar to that of [(IPr)$AlCl_3$] (**20**) than that of the starting compound [(IPr)AlH_3]. [(IPr)$AlCl_3$] (**20**) was prepared separately from IPr carbene and $AlCl_3$.

To summarise, we have shown that even unconventional reagents such as aldiminium-based salts can be used as group transfer reagents in the chemistry of aluminium hydrides. So far, the reactivity of aldiminium-based salts has not been well explored. The field of aldiminium-based salts and their use as group transfer reagents therefore has the potential to be further explored.

4.4 Aldiminium-Based Fluorinating Reagents

This chapter is based on as of yet unpublished results. Most of the data presented here are gathered in an unpublished manuscript currently entitled "From Cyclic (Alkyl)(Amino)Carbene (CAAC) Precursors to Fluorinating Reagents". This chapter also includes some results that are not part of the manuscript, but an ongoing study on the reactivity of aldiminium-based fluorinating reagents.

As shown in the previous chapter, aldiminium-based salts can be used as group transfer reagents. To extend the knowledge and explore the reactivity of this class of compounds, we prepared a group of aldiminium-based poly(hydrogen fluoride) salts. Starting from the aldiminium-based chloride salt [CAACH][$(HCl)_{0.5}$Cl] prepared by our modified synthetic procedure, we have obtained aldiminium-based salts with a high content of HF by the addition of anhydrous HF. By removing HF step by step, we selectively prepared a series of poly(hydrogen fluoride) salts [CAACH][$(HF)_n$F] (n = 1–3) and a fluorinated compound with remarkable properties.

All the obtained products were characterised by X-ray structural analysis, NMR and Raman spectroscopy.

The compounds that were found to be stable enough were tested for their fluorination ability on alkylaluminium compounds.

4.4.1 Synthesis and crystal structure determination

The detailed synthesis procedures of all compounds are given in Appendix A.2, together with all the data obtained by their characterisation.

The syntheses of the aldiminium-based fluorinating reagents required the use of anhydrous HF. *Caution! Anhydrous HF should be handled with care by an experienced experimenter.* Since HF etches glass, all reactions were carried out in FEP vessels with PTFE valves. The products obtained were stored in plastic containers, as most of them also tend to react with glass.

4.4.1.1 Synthesis of [CAACH][$(HF)_3$F] (21)

The [CAACH][$(HCl)_{0.5}$Cl] was dissolved in anhydrous HF, which served as both solvent and reactant. The reaction proceeded rapidly and according to Scheme 4.10. The excess HF was then removed overnight under reduced pressure, yielding [CAACH][$(HF)_3$F] (**21**) in quantitative yield. According to the literature, similar procedures involving the addition of anhydrous HF have been used to synthesise imidazolium-based poly(hydrogen fluoride) salts [186], [199].

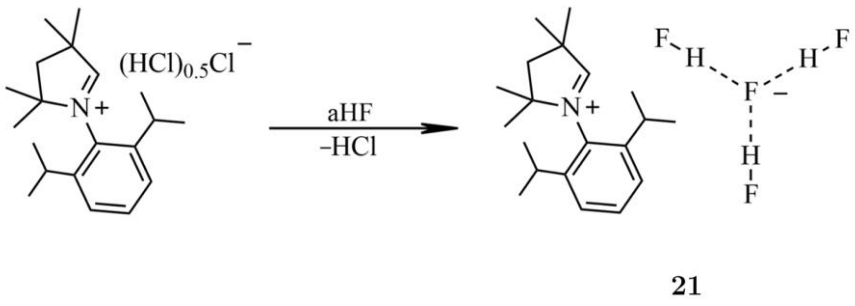

21

Scheme 4.10: Synthesis of [CAACH][$(HF)_3$F] (**21**).

[CAACH][$(HF)_3F$] (**21**) is a solid product that can be easily transferred and handled. However, over time it tends to slowly release HF and form a more stable salt. To minimise its decomposition, we stored [CAACH][$(HF)_3F$] (**21**) under an inert atmosphere at −20 °C.

Single crystals of [CAACH][$(HF)_3F$] (**21**) were obtained during product isolation by slow evaporation of HF. It crystallises in the monoclinic space group $P2_1/c$ and its crystal structure is shown in Figure 4.28. The asymmetric unit contains a $[CAACH]^+$ cation and a $[(HF)_3F]^-$ anion in the form of a branched chain. The structure of the anion is virtually planar and is consistent with similar reported structures [238]. The cation and the anion interact with each other and form a hydrogen bond C(2)—H(2)···F(1) with H···F distances of 2.111(1) Å (C···F distances of 3.037(2) Å). The average F···F distance between the central and terminal F atoms of 2.357 Å is comparable to the average F···F distances of previously reported $[(HF)_3F]^-$ anions (2.377 Å, 2.379 Å) [238]. The angles between fluorine atoms at the central F(2) (average F-F(2)-F angle of 119.7°) are also comparable to reported data (average angles of 119.8° and 116.5°) [238]. There are many examples in the literature of similar star-shaped $[(HF)_3F]^-$ anions, which generally have a trigonal pyramidal shape [239]. Our anion also falls into this category. On the other hand, the chain-like structures of $[(HF)_3F]^-$ anions are rare [239].

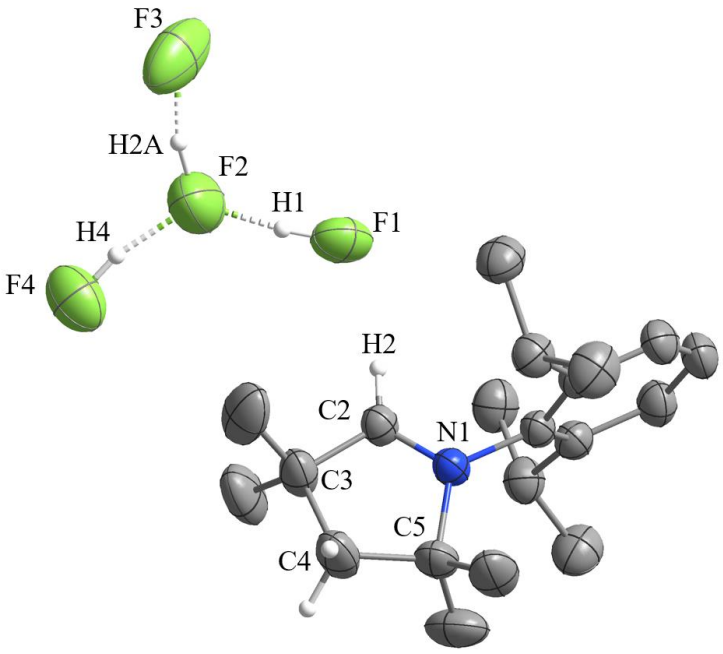

Figure 4.28: Crystal structure of [CAACH][$(HF)_3F$] (**21**). The ellipsoids are drawn at 50 % probability. For clarity, all hydrogen atoms are omitted, except of the $[(HF)_3F]^-$ anion and those on the heterocyclic ring.

4.4.1.2 Synthesis of [CAACH][$(HF)_2F$] (22)

The compound [CAACH][$(HF)_2F$] (**22**) was obtained by removing 1 equivalent HF from [CAACH][$(HF)_3F$] (**21**), as shown in Scheme 4.11. Although [CAACH][$(HF)_3F$] (**21**) slowly releases HF by itself, the complete transition to [CAACH][$(HF)_2F$] (**22**) takes a long time. We kept [CAACH][$(HF)_3F$] (**21**) under high vacuum for 2 days to ensure complete conversion to [CAACH][$(HF)_2F$] (**22**). This compound proved to be the most stable among the aldiminium-based compounds described in this chapter. It can be stored on air in plastic containers without decomposing, and in the absence of moisture it does not react with glass.

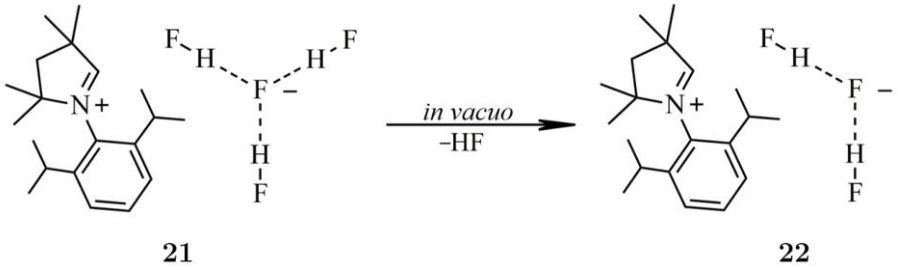

Scheme 4.11: Synthesis of [CAACH][$(HF)_2F$] (**22**).

Single crystals of [CAACH][$(HF)_2F$] (**22**) were obtained from a saturated acetonitrile solution stored at −20 °C. It crystallises in the monoclinic space group $P2_1/n$ and its crystal structure is shown in Figure 4.29. The asymmetric unit contains a $[CAACH]^+$ cation and a non-linear $[(HF)_2F]^-$ anion. The cation and the anion interact with each other and form two hydrogen bonds, as F(1) and F(2) are almost equidistant from H(2). F(1) forms the hydrogen bond C(2)−H(2)···F(1) with H···F distances of 2.343(2) Å (C···F distances of 3.173(2) Å), while F(2) forms the bond C(2)−H(2)···F(1) with H···F distances of 2.542(2) Å (C···F distances of 3.398(2) Å). The F···F distances of 2.263(2) Å and 2.320(2) Å are consistent with those reported for other $[(HF)_2F]^-$ anions [192], [199]. The anion is bent, with the angle between the fluorine atoms F(1)-F(2)-F(3) being 108.54(8)°.

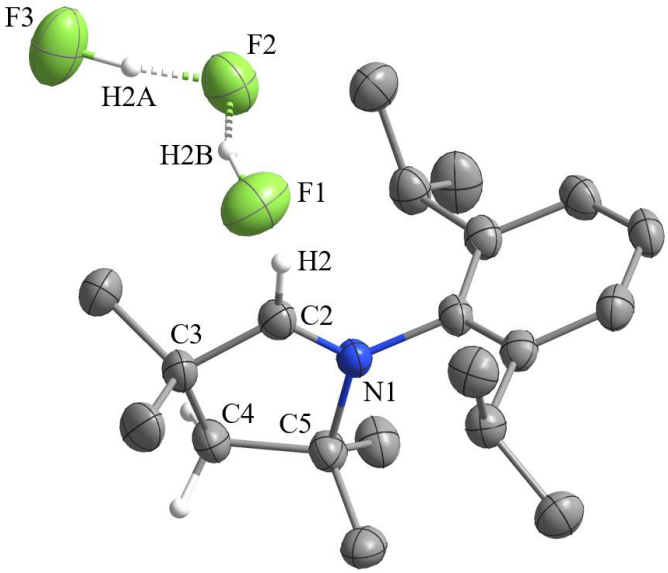

Figure 4.29: Crystal structure of [CAACH][$(HF)_2F$] (**22**). The ellipsoids are drawn at 50 % probability. For clarity, all hydrogen atoms are omitted, except those on the heterocyclic ring.

4.4.1.3 Synthesis of higher poly(hydrogen fluorides)

The reaction of [CAACH][$(HCl)_{0.5}Cl$] with excess HF resulted in the formation of a liquid mixture containing higher poly(hydrogen fluoride) salts. By removing the excess HF, different fractions could be obtained. In an attempt to prepare or characterise higher poly(hydrogen fluoride) salts, a mixture was prepared and the excess HF was removed stepwise by evacuation to constant weight at −20 °C, 0 °C, 25 °C and under high vacuum. The four samples prepared under different conditions were characterised by NMR analysis.

A comparison of the four ^{19}F NMR spectra measured in acetonitrile is shown in Figure 4.30. It can be seen that the ^{19}F NMR peaks of the sample prepared under high vacuum and the sample evacuated at 25 °C correspond to [CAACH][$(HF)_2F$] (**22**) and [CAACH][$(HF)_3F$] (**21**), respectively. The chemical shifts of the peaks also shift upfield with an increasing amount of HF. As expected, the samples prepared by evacuation at 0 °C and −20 °C have an even higher amount of HF than [CAACH][$(HF)_3F$] (**21**). Both samples prepared at low temperatures were liquid and readily released HF even when stored at −20 °C. Due to their constantly changing HF contents, further characterisation was not possible.

Fortunately, when the sample isolated at 0 °C was stored at −20 °C, single crystals were obtained. We characterised them as [CAACH][$(HF)_{3.5}F$] (**23**), which is indeed a co-crystal of [CAACH][$(HF)_3F$] and [CAACH][$(HF)_4F$] in a 1:1 ratio. The formation of a co-crystal proves that higher poly(hydrogen fluorides) actually exist in this system.

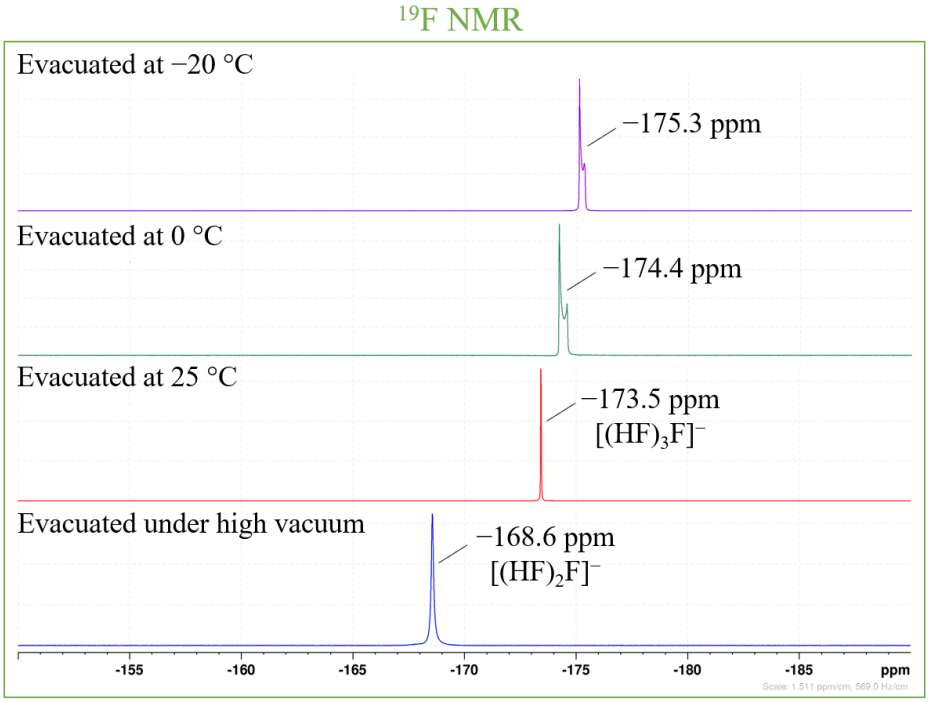

Figure 4.30: ^{19}F NMR spectra of aldiminium-based poly(hydrogen fluoride) salts. Samples were prepared by evacuation to constant weight at −20 °C, 0 °C, 25 °C and under high vacuum. Spectra were measured in acetonitrile solutions.

[CAACH][$(HF)_{3.5}F$] (**23**) crystalises in the monoclinic space group $P2_1/n$ and its crystal structure is shown in Figure 4.31. The asymmetric unit contains two $[CAACH]^+$ cations and two poly(hydrogen fluoride) anions. The $[(HF)_3F]^-$ anion is disordered. The positions of the fluorine atoms were modelled and refined in two preferred orientations, with occupancies of domain A being 70 % and domain B 30 %. The shape of the $[(HF)_3F]^-$ anion is the same as in [CAACH][$(HF)_3F$] (**21**) and therefore its structure is not described further.

On the other hand, the $[(HF)_4F]^-$ anion has the form of a branched chain and is a rare example of such isomers. For $[(HF)_4F]^-$ anions, there are three possible isomers. The most commonly observed is the tetrahedral type [239], the branched isomer has so far only been found in $Me_3N \cdot 5HF$ [238], while to our knowledge, the chain type has yet to be discovered [240]. The $[(HF)_4F]^-$ anion in [CAACH][$(HF)_{3.5}F$] (**23**) is virtually centred. It has one notably short inner hydrogen bond F(22)—H(22A)$\cdots$F(23) with an F$\cdots$F distance of 2.274(3) Å, which is typical for $[FHF]^-$ anions. This means that the $[(HF)_4F]^-$ anion has a $[FHF]^-$ core surrounded by 3 HF molecules. The chemical formula of the anion could also

be written as $[(FH)(FHF)(HF)_2]^-$. The structural features of the $[(HF)_4F]^-$ anion are consistent with the previously reported branched isomers [238]. The $[(HF)_4F]^-$ anion interacts with the cation and forms a hydrogen bond C(22)−H(22)···F(21) with H···F distances of 2.304(2) Å (C···F distances of 3.146(3) Å).

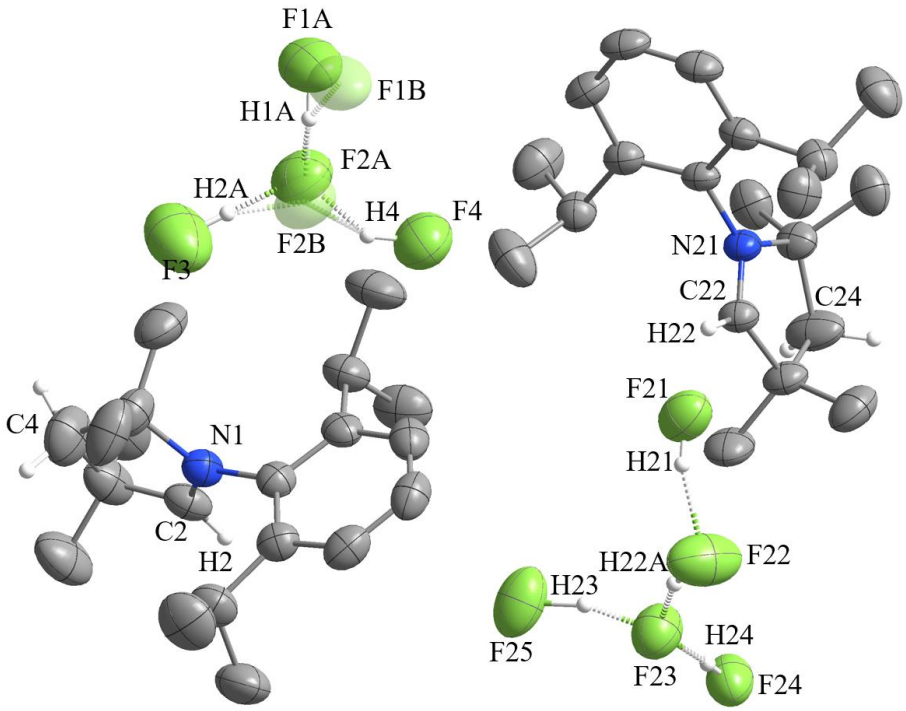

Figure 4.31: Crystal structure of $[CAACH][(HF)_{3.5}F]$ (**23**). The ellipsoids are drawn at 50 % probability. For clarity, all hydrogen atoms are omitted, except those on the heterocyclic ring. The positions of the disordered atoms are shown in domain A and B (shaded).

4.4.1.4 Synthesis of CAAC(H)F (24)

$[CAACH][(HF)_2F]$ (**22**) was mixed with excess CsF or KF and suspended in toluene. The reaction was stirred for 3 days and resulted in the quantitative formation of CAAC(H)F (**24**). $CsHF_2$ or KHF_2 formed as by-products and were easily separated from the reaction mixture by filtration. The reaction proceeded according to Scheme 4.12.

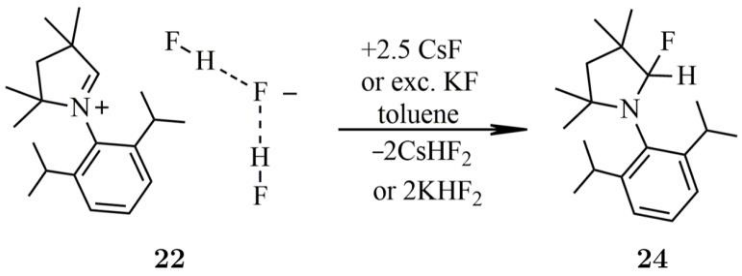

22 **24**

Scheme 4.12: Synthesis of CAAC(H)F (**24**).

[CAACH][$(HF)_2F$] (**22**) is the most stable of the aldiminium-based poly(hydrogen fluoride) salts. Compounds with a lower amount of HF could not be prepared simply by evacuation, but required a different approach. The use of reagents that form very stable bifluorides proved to be a very effective method for the synthesis of CAAC(H)F (**24**).

Single crystals of CAAC(H)F (**24**) were obtained from a saturated acetonitrile solution at −20 °C. It crystallises in the monoclinic space group $P2_1/c$ and its crystal structure is shown in Figure 4.32.

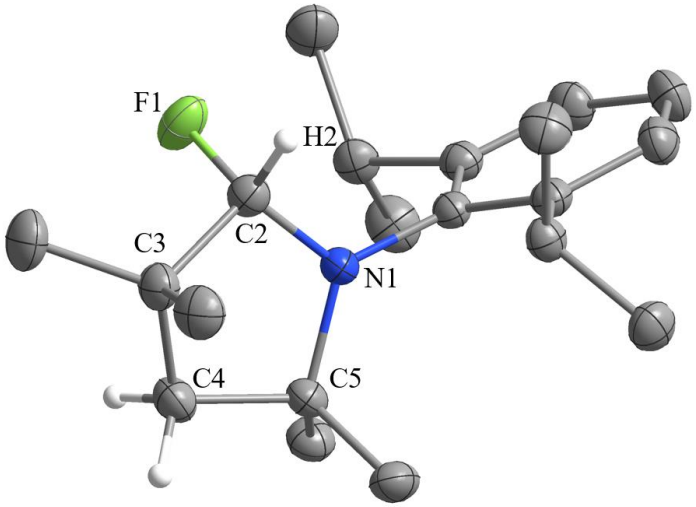

(a)

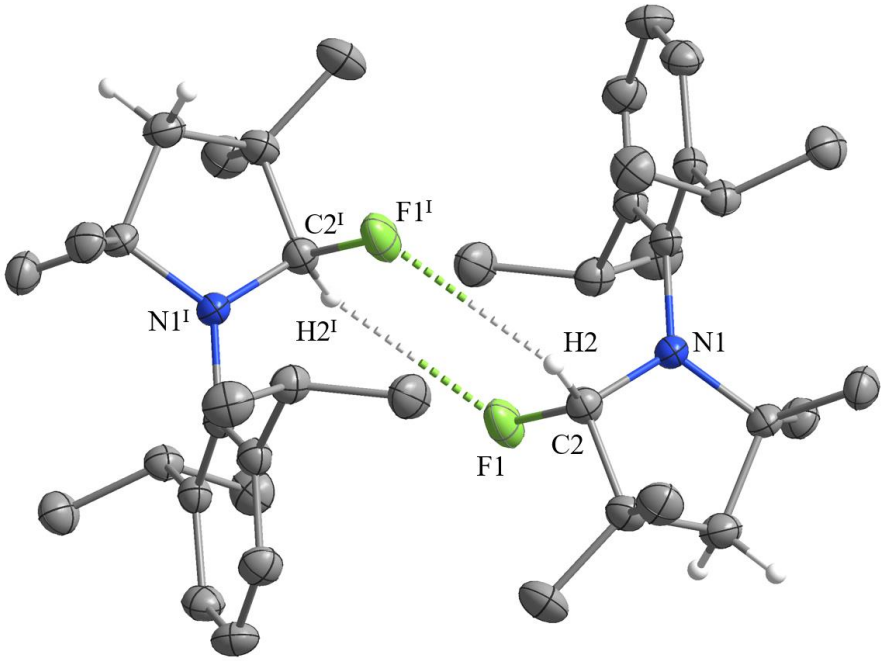

(b)

Figure 4.32: Crystal structure of CAAC(H)F (**24**). (a) Structure of the monomeric unit, and (b) packing of two monomeric units. The ellipsoids are drawn at 50 % probability. For clarity, all hydrogen atoms are omitted, except those on the heterocyclic ring. Symmetry code: (i) 1−x, 1−y, 1−z.

The asymmetric unit contains a chiral fluorinated organic compound with hydrogen and fluorine bonded at C2 position. We had expected CAAC(H)F (**24**) to have an ionic form, just as the imidazolium-based fluoride [IPrH][F] consists of an ion pair. But unlike [IPrH][F], where the $[IPrH]^+$ cation has a delocalised aromatic ring, the saturated CAAC(H)F (**24**) prefers sp^3 hybridisation at C2 in the solid state [161]. Fluorine is the most electronegative element in the periodic table, which makes the C−F bond strongly polarised [161]. In the crystal structure, the length of the C−F bond is 1.450(3) Å, which is significantly longer compared to bonds of other structurally related compounds (1.378(8) Å [241], 1.402(5) Å [242]). It is interesting that two CAAC(H)F units interact with each other in the crystal structure and form dimers through hydrogen bonding. The two units orient themselves in such a way that the hydrogen and fluorine atom at C2 position of the first molecule interact with the same fluorine and hydrogen atoms of the second molecule. Consequently, the two fluorine bonds C(2)−H(2)···F(2) with H···F distance of 2.800(1) Å (C···F distance of 3.646(3) Å) allow the formation of a six-membered ring. Within the molecule, another hydrogen bond forms as the fluorine atom interacts with a proton on a methyl group of *i*-Pr wingtips C(21)−H(21A)···F(1) with the H···F distance of 2.509(2) Å (C···F distance of 3.472(3) Å).

4.4.1.5 Synthesis of [CAACH][(HF)F] (25)

[CAACH][(HF)F] (**25**) was prepared by mixing CAAC(H)F (**24**) and $[CAACH][(HF)_2F]$ (**22**) in a 1:1 ratio in acetonitrile. After 24 hours, all volatiles were removed and [CAACH][(HF)F] (**25**) was isolated. The reaction proceeded according to Scheme 4.13. Unfortunately, the reaction is reversible and the bifluoride salt tends to decompose readily back into the reactants.

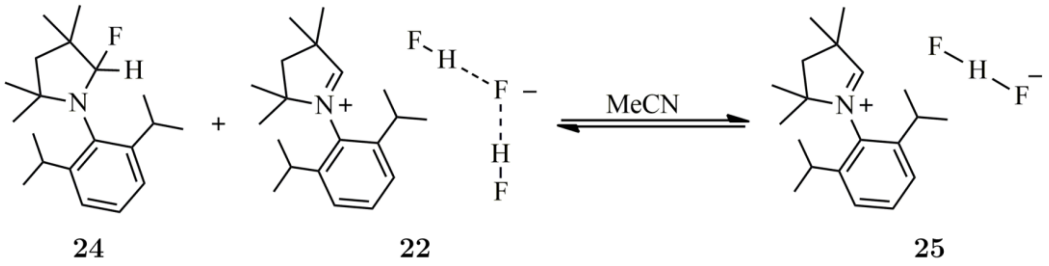

24 **22** **25**

Scheme 4.13: Synthesis of [CAACH][(HF)F] (**25**).

Crystallisation of [CAACH][(HF)F] (**25**) usually ended with the formation of either single crystals of $[CAACH][(HF)_2F]$ or CAAC(H)F, depending on the conditions. Fortunately, we were able to structurally characterise [CAACH][(HF)F] (**25**) as it crystallised in a co-crystal with 2 CAAC(H)F molecules. Its crystal structure is shown in Figure 4.33. Single crystals of [CAACH][(HF)F]·2CAAC(H)F (**25a**) were obtained by slowly evaporating the solvent from the solution of [CAACH][(HF)F] (**25**) in *t*-BuOH and acetonitrile. At the same time, the formation of $[CAACH][(HF)_2F]$ (**22**) single crystals occurred during crystallisation. This result shows us that [CAACH][(HF)F] (**25**) exists in equilibrium with other fluorinated species. A polar environment, such as the mixture of *t*-BuOH and acetonitrile, promoted the formation of ionic species and enabled the crystallisation of [CAACH][(HF)F]. On the other hand, [CAACH][(HF)F] (**25**) is thermodynamically less favourable in less polar solvents and tends to decompose to CAAC(H)F (**24**) and $[CAACH][(HF)_2F]$ (**22**). It is worth noting that single crystals of [CAACH][(HF)F]·2CAAC(H)F (**25a**) were formed even when CAAC(H)F (**24**) was crystallised under the same conditions as [CAACH][(HF)F] (**25**). This indicates that the

fluoride species are in equilibrium with each other depending on the environment they are in.

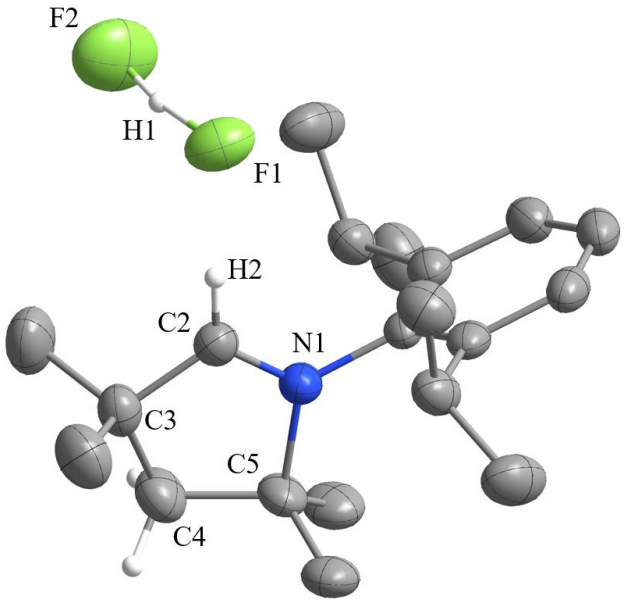

Figure 4.33: Crystal structure of [CAACH][(HF)F] (**25**) in the co-crystal [CAACH][(HF)F]·2CAAC(H)F (**25a**). The ellipsoids are drawn at 50 % probability. For clarity, all hydrogen atoms are omitted, except those on the imidazolium ring.

[CAACH][(HF)F]·2CAAC(H)F (**25a**) crystallises in the triclinic space group *P*−*1*. Its asymmetric unit contains a central [CAACH][(HF)F] unit surrounded by two CAAC(H)F molecules, each on one side of the $[FHF]^-$ anion. The two CAAC(H)F molecules are aligned so that the hydrogen and fluorine atoms at the C2 position are opposite one of the fluorine atoms of the $[FHF]^-$ anion. The structures of the CAAC(H)F molecules are disordered. Their structural features are as described in the previous section and will not be discussed further here. The crystal structure of [CAACH][(HF)F] (**25**) contains a $[CAACH]^+$ cation and a $[FHF]^-$ anion that interact to form a hydrogen bond C(2)−H(2)···F(1) with H···F distances of 2.043(2) Å (C···F distances of 2.988(3) Å). The F···F distance between fluorine atoms in the $[FHF]^-$ anion of 2.234(2) Å is shorter than for other bifluoride salts (typically 2.26−2.28 Å), but according to the literature, shorter distances have also been reported for $[FHF]^-$ anions (2.213(4) Å) [243].

4.4.2 NMR spectroscopy

All synthesised compounds were characterised by NMR spectroscopy. The spectra agree with the crystal structures of the compounds. Selected ^{1}H and ^{19}F NMR peaks of the aldiminium-based fluoride and poly(hydrogen fluoride) salts are listed in Table 4.8. The measurements were carried out in acetonitrile solutions at room temperature and at −30 °C, since the species exist in equilibrium and could not otherwise be properly characterised. In ^{1}H NMR spectra of $[CAACH][(HF)_2F]$ (**22**) and $[CAACH][(HF)_3F]$ (**21**) distinct peaks of the $[CAACH]^+$ cation can be seen. Their ^{19}F NMR peaks at −168.57 ppm and −173.45 ppm are also in good agreement with the chemical shifts to the $[(HF)_2F]^-$ and $[(HF)_3F]^-$ anions [244]. These two compounds are completely ionic and their structure does not change with temperature. For this reason, the NMR measurements for them were not carried out at low temperatures.

Table 4.8: Selected ^{1}H and ^{19}F NMR peaks of aldiminium-based fluoride and poli(hydrogen fluoride) compounds in acetonitrile at room temperature and at −30 °C.

Compound	Room temperature (25 °C)		Low temperature (−30 °C)	
	δ(^{1}H) C−H	δ(^{19}F)	δ(^{1}H) C−H	δ(^{19}F)
CAAC(H)F (**24**)	5.25 (s)	−106.85	5.13 (d, J = 82.9 Hz)	−105.30 (d, J = 82.9 Hz)
[CAACH][(HF)F] (**25**)	7.90 (br)	n.o.	9.34 (br)	−105.18 (s) −144.51 (br) −166.42 (br)
[CAACH][$(HF)_2F$] (**22**)	8.84 (s)	−168.57 (br)	–	–
[CAACH][$(HF)_3F$] (**21**)	8.78 (s)	−173.45 (br)	–	–

On the other hand, the compound CAAC(H)F (**24**) does not behave like a salt in solution. In its solid state, CAAC(H)F (**24**) adopts the form of a neutral chiral compound with hydrogen and fluorine bonded at C2 position. The NMR spectra measured at low temperature confirm this observation. In the ^{1}H NMR spectra of CAAC(H)F (**24**) at low temperature, the peaks are split in a manner typical for two pyrrolidine conformers. Moreover, the proton-fluorine coupling can be observed in both the ^{1}H and ^{19}F NMR spectra as a doublet at 5.13 ppm (J = 82.9 Hz) and −105.30 ppm (J = 82.9 Hz), respectively. With increasing temperature, the signals for the two conformers disappear together with the proton-fluorine coupling. We assume that at elevated temperature the compound CAAC(H)F (**24**) exists in equilibrium with the [CAACH][F] ion pair.

The compound [CAACH][(HF)F] (**25**) does not behave like a salt in solution, but neither does it behave like a neutral compound. As described earlier, [CAACH][(HF)F] (**25**) is not stable and tends to decompose into [CAACH][$(HF)_2F$] and CAAC(H)F. We believe that in solution there is an equilibrium between the two forms. No peaks could be observed in ^{19}F NMR because fluorides are constantly changing from one form to the other. Therefore, measurements at low temperature were necessary to slow down the transition between the species. Three distinct peaks were observed in the ^{19}F NMR measurement at low temperature. They were assigned to CAAC(H)F (**24**) at −105.18 ppm, [CAACH][(HF)F] (**25**) at −144.51 ppm and [CAACH][$(HF)_2F$] (**22**) at −166.42 ppm.

4.4.3 Reactivity with $AlMe_3$ compounds

The compounds [CAACH][$(HF)_3F$] (**21**), [CAACH][$(HF)_2F$] (**22**) and CAAC(H)F (**24**), which were found to be stable enough, were tested for their fluorination ability on $AlMe_3$ compounds. The two salts were reacted with $AlMe_3$ to test their efficiency in the synthesis of discrete anionic compounds. On the other hand, the CAAC(H)F (**24**) was tested for its reactivity as a neutral group transfer reagent in the chemistry of CAAC-supported organoaluminium fluorides.

4.4.3.1 Reactivity of $AlMe_3$ with [CAACH][$(HF)_3F$] (21)

The $AlMe_3$ reacted with [CAACH][$(HF)_3F$] (**21**) to form [CAACH][AlF_4] (**5**), a salt with discrete $[AlF_4]^-$ anions, and 3 equivalents of methane. The reaction was carried out in acetonitrile at 0 °C and proceeded according to Scheme 4.14. During the reaction, methane was eliminated from the metal-bonded methyl groups and 4 fluoride anions were added to the aluminium centre. The salt proved stable at room temperature under an inert atmosphere. It was stored in a glovebox for long periods without decomposition. The

synthesis of [CAACH][AlF_4] (**5**) is very similar to the reactions described in Chapter 4.2 for the formation of discrete organofluoroaluminate salts and represents an alternative approach to the synthesis of [CAACH][AlF_4] (**5**) described in Chapter 4.1. The structural characterisation of [CAACH][AlF_4] (**5**) is described in Chapter 4.1.

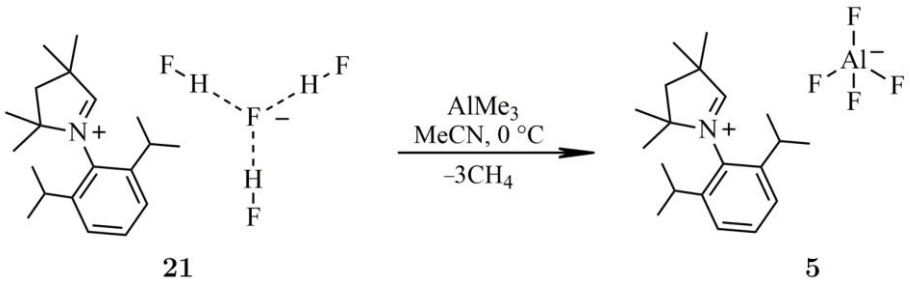

21 **5**

Scheme 4.14: Reactivity of $AlMe_3$ with [CAACH][$(HF)_3F$] (**21**).

Discrete $[AlF_4]^-$ anions are generally formed when AlR_3 compounds react with excess HF, leading to the complete removal of the substituents [19], [60]. In our case, the use of the aldiminium-based reagent with the corresponding amount of HF led to the same result.

4.4.3.2 Reactivity of $AlMe_3$ with [CAACH][$(HF)_2F$] (22)

The $AlMe_3$ reacted with [CAACH][$(HF)_2F$] (**22**) to form [CAACH][$MeAlF_3$] (**4**), a salt with discrete $[MeAlF_3]^-$ anions, and 2 equivalents of methane. The reaction was carried out in acetonitrile at room temperature and proceeded according to Scheme 4.15. During the reaction, methane was eliminated from the metal-bonded methyl groups and 3 fluoride anions were added to the aluminium centre. The salt proved to be unstable at room temperature even under an inert atmosphere. It slowly decomposed to the more fluorinated [CAACH][AlF_4] (**5**). To avoid rapid decomposition, it was stored in a glovebox at −20 °C.

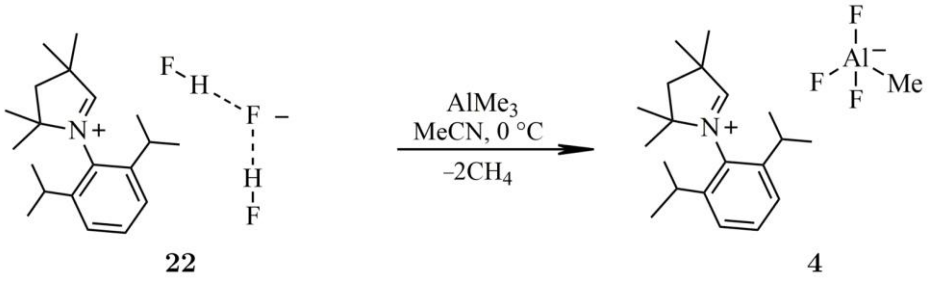

22 **4**

Scheme 4.15: Reactivity of $AlMe_3$ with [CAACH][$(HF)_2F$] (**22**).

The synthesis proceeds according to the reactions described in Chapter 4.2 for the synthesis of discrete organotrifluoroaluminate salts. This procedure allowed us to characterise [CAACH][$MeAlF_3$] (**4**), the formation of which was only observed in the reaction of [(CAAC)$AlMe_3$] with 3 equivalents of Me_3SnF in Chapter 4.1. The structural characterisation of [CAACH][$MeAlF_3$] (**4**) is described in Chapter 4.1.

4.4.3.3 Reactivity of [(CAAC)$AlMe_3$] with CAAC(H)F (24)

The reactivity of [(CAAC)$AlMe_3$] with CAAC(H)F (**24**) was tested on a small scale in NMR tubes. The reaction of [(CAAC)$AlMe_3$] with 1 equivalent of CAAC(H)F (**24**) was carried out in C_6D_6 at room temperature overnight. During the reaction, a methyl

substituent at the aluminium centre was exchanged for a fluoride atom, as shown in Scheme 4.16. NMR analysis of the reaction mixture showed the formation of [(CAAC)AlMe$_2$F] (**1**) and CAAC(H)Me (**6**), while some [(CAAC)AlMe$_3$] remained unreacted.

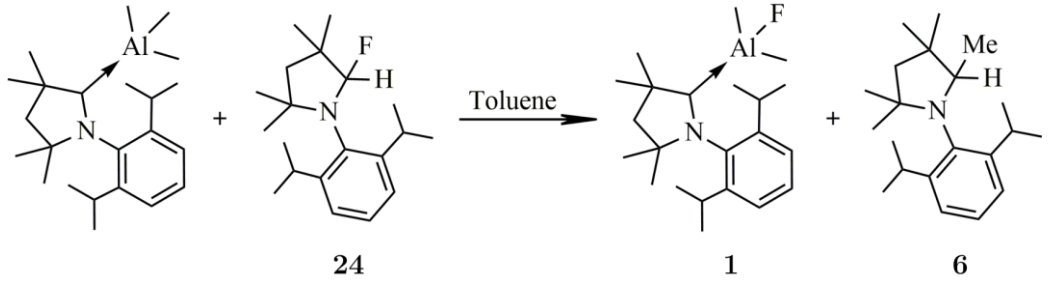

24 **1** **6**

Scheme 4.16: Reactivity of [(CAAC)AlMe$_3$] with CAAC(H)F (**24**).

The synthesis represents an alternative approach to the discrete organoaluminium fluorides described in Chapter 4.1. In Chapter 4.3, we presented the use of aldiminium-based chloride and triflate salts as group transfer reagents in the chemistry of aluminium hydrides. CAAC(H)F (**24**) does not have a salt structure like its chloride and triflate counterpart, but it reacted in a similar way. It formed neutral aluminium fluoride compounds from organoaluminium compounds by a fluoride/alkyl exchange reaction.

Little research has been done on the reactivity of CAAC(H)F (**24**). However, it proved to be a potentially useful reagent in the fluorination of organoaluminium compounds. Further studies are needed to evaluate its use as a group transfer reagent.

4.4.4 Summary

In this chapter we describe the synthesis of aldiminium-based fluoride and poly(hydrogen fluoride) compounds and their application in the fluorination of organoaluminium compounds. Addition of anhydrous HF to [CAACH][(HCl)$_{0.5}$Cl] resulted in the formation of an aldiminium-based poly(hydrogen fluoride) salt with a high HF content. By removing the excess HF *in vacuo* under various conditions, we selectively obtained [CAACH][(HF)$_3$F] (**21**) and [CAACH][(HF)$_2$F] (**22**). The latter proved to be the most stable aldiminium-based poly(hydrogen fluoride) salt and, unlike its heavy counterpart, did not tend to release HF by itself.

Compound CAAC(H)F (**24**) was accessible by using KF or CsF. It was prepared by the reaction of [CAACH][(HF)$_2$F] (**22**) with an excess of CsF or KF in toluene, while [CAACH][(HF)F] (**25**) was obtained by the combination of [CAACH][(HF)$_2$F] (**22**) and CAAC(H)F (**24**) in acetonitrile. CAAC(H)F (**24**) adopts the form of a neutral compound in the solid state and in solution, while [CAACH][(HF)F] (**25**) is rather unstable and tends to decompose back into the reactants. In solution, [CAACH][(HF)F] (**25**) is in equilibrium with the other two aldiminium-based compounds (**22** and **24**).

The compounds described have the potential to be used as fluorinating reagents. The reactivity of [CAACH][(HF)$_3$F] (**21**) and [CAACH][(HF)$_2$F] (**22**) was tested on AlMe$_3$. Their use led to the formation of salts (**5** and **4**) with discrete $[AlF_4]^-$ and $[MeAlF_3]^-$ anions, respectively. The reactivity of CAAC(H)F (**24**) was tested on [(CAAC)AlMe$_3$] and led to the formation of [(CAAC)AlMe$_2$F] (**1**) and CAAC(H)Me (**6**) by fluoride/alkyl exchange reaction.

The aldiminium-based fluoride and poly(hydrogen fluoride) compounds are useful fluorinated reagents in organoaluminium chemistry. Further research is needed to properly assess their utility not only for aluminium but also for other areas of chemistry.

Chapter 5

Conclusions

The first part of our study focused on the search for stable discrete AlF_3 and organoaluminium fluoride compounds by testing the reactivity of [(CAAC)$AlMe_3$] with Me_3SnF. The reactions in 1:1 and 1:2 stoichiometry resulted in the formation of [(CAAC)$AlMe_2F$] (**1**) and [(CAAC)$AlMeF_2$] (**2**). During the reactions, Me_4Sn was formed as a by-product. The reactions with higher amounts of Me_3SnF resulted in the formation of mixtures of various neutral adducts and salts. The formation of the adducts [(CAAC)$AlMe_2F$] (**1**), [(CAAC)$AlMeF_2$] (**2**) and [(CAAC)AlF_3] (**3**) was observed by NMR together with the formation of salts [CAACH][$MeAlF_3$] (**4**) and [CAACH][AlF_4] (**5**). The neutral adducts proved to be rather unstable. In solution, they were in equilibrium with the [(CAAC)$AlMe_3$] and other organoaluminium fluorides. Therefore, further purification of the compounds was not possible. All compounds were characterised by NMR analysis, while compounds **1**, **2**, **4**, and **5** were also structurally characterised. The reactions of [(CAAC)$AlMe_3$] with Me_3SnF were accompanied by the formation of the side product CAAC(H)Me (**6**), whose formation mechanism is still unknown. DFT calculations proved that CAAC-stabilised discrete organoaluminium fluorides are thermodynamically favourable products, with their stability increasing with the number of fluorine atoms. However, their synthesis remains a challenge.

In the end, CAACs turned out to be suitable ligands for the stabilisation of discrete AlF_3 and organoaluminium fluoride adducts and that the formation of discrete species is possible by the fluorination of [(CAAC)$AlMe_3$] with Me_3SnF. Some rare examples of discrete organoaluminium fluorides have been prepared and structurally characterised.

The second part of our study focused on testing the reactivity of different organoaluminium compounds ($AlMe_3$, Al(*n*-Bu)$_3$ and $AlPh_3$) with nucleophilic fluorinating reagents based on imidazolium salts [IPrH][$(HF)_nF$] (n = 0–2). Salts with discrete triorganofluoroaluminate $[R_3AlF]^-$, diorganodifluoroaluminate $[R_2AlF_2]^-$ and organotrifluoroaluminate $[RAlF_3]^-$ anions have been prepared. Alkylaluminium compounds reacted with [IPrH][F] to form [IPrH][Me_3AlF] (**7**) and [IPrH][(*n*-Bu)$_3$AlF] (**8**), with [IPrH][(HF)F] to form [IPrH][Me_2AlF_2] (**9**) and [IPrH][(*n*-Bu)$_2AlF_2$] (**10**), and with [IPrH][$(HF)_2F$] to form [IPrH][$MeAlF_3$] (**11**) and [IPrH][(*n*-Bu)AlF_3] (**12**). The reactions with [IPrH][(HF)F] and [IPrH][$(HF)_2F$] were accompanied by the evolution of an alkane (methane or *n*-butane). The reactions were selective, quantitative and straightforward, but depended strongly on the stoichiometric ratio. The excess of any fluorinating reagent led to more fluorinated species, which eventually led to the formation of [IPrH][AlF_4] (**13**). On the other hand, arylaluminium compounds reacted with [IPrH][$(HF)_nF$] (n = 0–2) to form salt mixtures, including [IPrH][Ph_3AlF] (**14**), [IPrH][Ph_2AlF_2] (**15**) and [IPrH][$PhAlF_3$] (**16**), which could not be separated or prepared separately. All compounds were characterised by NMR and Raman spectroscopy, while compounds **8**, **9**, **10**, **11**, **12**, **13**,

14, and **16** were also structurally characterised. DFT calculations proved that the stability of the anions increases with a higher number of fluorine atoms in the anions. They also demonstrated that the decomposition of [IPrH][R_3AlF] (R = Me, *n*-Bu) to [IPrH][R_2AlF_2] and [(IPr)AlR_3] is thermodynamically favourable, which is consistent with our experimental observation.

The second part of the study showed that fluorinating reagents based on imidazolium salts [IPrH][$(HF)_nF$] (n = 0–2) can be used as fluorinating reagents in organoaluminium chemistry. By using them, compounds with discrete [R_3AlF]$^-$, [R_2AlF_2]$^-$ and [$RAlF_3$]$^-$ anions were selectively prepared. The fluorinating reagents with the right amount of HF and a sterically demanding cation proved to be very convenient. The right amount of HF enabled selective fluorination, as the reactions require strict stoichiometric conditions, while the bulky cation helped stabilise the anion by preventing possible oligomerisation reactions.

The third part of our research was directed towards the synthesis of partially substituted NHC-stabilised aluminium hydride compounds using nucleophilic reagents based on aldiminium salts. The [(IPr)AlH_3] reacted with [CAACH][OTf] to form [(IPr)AlH_2OTf] (**17**), while the reaction with [CAACH][$(HCl)_{0.5}$Cl] gave [(IPr)$AlH_{3-x}Cl_x$] (x = 1, 2) (**19**), a mixture of [(IPr)AlH_2Cl] and [(IPr)$AlHCl_2$] in approximately equimolar ratio. Both reactions were accompanied by the formation of $CAACH_2$ (**18**), which was easily removed by washing with hexane. Despite our efforts, we were not able to selectively synthesise [(IPr)AlH_2Cl] or [(IPr)$AlHCl_2$] or to separate them from the mixture. The formation of a mixture was due to the presence of about 1.5 equivalents of chlorine in the aldiminium salt. In addition, the compound [(IPr)$AlCl_3$] (**20**) was prepared from IPr carbene and $AlCl_3$ to compare the effect of substituents within the [(IPr)$AlH_{3-x}Cl_x$] (x = 1, 2) series. It turned out that the substitution of a hydride atom by a more electronegative element strengthens the Al—H bonds, which affects the Lewis acidity of the neutral adducts. It was found that the Lewis acidity of [(IPr)$AlH_{3-x}Cl_x$] (x = 1, 2) is more similar to that of [(IPr)$AlCl_3$] (**20**) than that of the parent compound [(IPr)AlH_3]. Compounds **17**, **18**, **19**, and **20** were characterised by NMR and Raman spectroscopy as well as with X-ray structural analysis.

Aldiminium-based triflate and chloride salts proved to be useful group transfer reagents in the chemistry of aluminium hydrides. The first aluminium dihydride triflate compound stabilised by NHC and a mixture of NHC-supported aluminium hydride chloride adducts were successfully prepared by hydride/triflate and hydride/chloride exchange reactions.

The last part of our study focused on the development of a series of nucleophilic fluorinating reagents based on aldiminium salts. In the third part of our study, the aldiminium-based salts were found to be good group transfer reagents. Therefore, the utility of the new fluorinating reagents was tested on aluminium compounds. The [CAACH][$(HCl)_{0.5}$Cl] reacted with the anhydrous HF to form a poly(hydrogen fluoride) salt with a high HF content. By stepwise removal of HF under vacuum, [CAACH][$(HF)_3F$] (**21**) and [CAACH][$(HF)_2F$] (**22**) were selectively prepared. Next, a neutral molecule CAAC(H)F (**24**) was prepared by the reaction of [CAACH][$(HF)_2F$] (**22**) with an excess of CsF or KF in toluene. To complete the series, [CAACH][(HF)F] (**25**) was obtained by the reaction of [CAACH][$(HF)_2F$] (**22**) and CAAC(H)F (**24**) in acetonitrile. However, [CAACH][(HF)F] (**25**) is rather unstable and readily decomposes back into the reactants. All compounds **21**, **22**, **24**, and **25** were characterised by NMR and Raman spectroscopy as well as X-ray structural analysis.

In this part of the study we proved that poly(hydrogen fluoride) salts can be prepared from the corresponding chloride salts by using anhydrous HF, while CAAC(H)F (**24**) can be obtained by abstraction of HF from the salt [CAACH][$(HF)_2F$] (**22**).

In addition, the reactivity of [CAACH][$(HF)_3F$] (**21**) and [CAACH][$(HF)_2F$] (**22**) was tested on $AlMe_3$, while the reactivity of CAAC(H)F (**24**) was tested on [(CAAC)$AlMe_3$]. The reaction of $AlMe_3$ with **21** and **22** led to the formation of [CAACH][AlF_4] (**5**) and [CAACH][$MeAlF_3$] (**4**), respectively. The formation of both salts was also observed in the first part of our study during the reaction of [(CAAC)$AlMe_3$] with excess Me_3SnF. This time the reactions were selective and quantitative. The reaction of [CAACH][$(HF)_2F$] (**22**) is consistent with the procedures described in the second part of our study for the organofluoroaluminate anions, while the reaction of [CAACH][$(HF)_3F$] (**21**) is an extension of the same work. The CAAC(H)F (**24**) reacted with [(CAAC)$AlMe_3$] to form [(CAAC)$AlMe_2F$] (**1**) and CAAC(H)Me (**6**) by a fluoride/alkyl exchange reaction. The reaction is an alternative process to [(CAAC)$AlMe_2F$] (**1**), which was first prepared with [(CAAC)$AlMe_3$] and Me_3SnF in the first part of our study.

To summarize, we have shown that discrete AlF_3 and organoaluminium fluoride compounds can be prepared by using suitable fluorinating reagents. We have demonstrated that aldiminium-based reagents can act as group transfer reagents and have prepared a series of aldiminium-based fluoride salts. They have the potential to be used as nucleophilic fluorinating reagents, however, little research has been done on the reactivity of such compounds. Further research is needed to evaluate their utility in discrete aluminium fluoride chemistry, main group element chemistry or other research areas.

Appendix A

Experimental Results

A.1 Modified Synthetic Procedures of Starting Materials

A.1.1 Al(*n*-Bu)$_3$

The synthesis is based on a previously reported procedure with a slight modification [206].

$AlCl_3$ (2 g, 15 mmol) and 80 mL of hexane were placed in a 100 mL Schlenk flask and cooled to −78 °C. 3 equivalents of *n*-BuLi in hexane (18 mL, 2.5 M, 45 mmol) were added slowly and the mixture was allowed to warm to room temperature overnight while stirring. The solution was filtered and dried under dynamic vacuum at 0 °C, yielding Al(*n*-Bu)$_3$ as a light pale-yellow liquid. Yield: 1.6 g (54 %). Calculated for $C_{12}H_{27}Al$ (M_w = 198.32 g/mol).

^{1}H NMR (C_6D_6, 25 °C, 400.14 MHz) δ 1.54 (m, 2H, *n*-Bu-C2H$_2$), 1.42 (m, 2H, J = 7.3 Hz, *n*-Bu-C3H$_2$), 0.98 (t, 3H, J = 7.2 Hz, *n*-Bu-C4H$_3$), 0.45 (m, 2H, Al−*n*-Bu-C1H$_2$) ppm.

^{13}C NMR (C_6D_6, 25 °C, 100.62 MHz) δ 28.5 (CH_2), 27.6 (CH_2), 13.6 (*n*-Bu-C4H$_3$), 10.2 (Al−*n*-Bu-C1H$_2$) ppm.

A.1.2 AlPh$_3$

The synthesis is based on a previously reported procedure with a slight modification [207].

$AlCl_3$ (1.6 g, 12 mmol) and 80 mL of hexane were placed in a 100 mL Schlenk flask and cooled to −78 °C. 3 equivalents of PhLi in dibutyl ether (19 mL, 1.9 M, 36 mmol) were added slowly and the mixture was allowed to warm to room temperature overnight while stirring. The solution was filtered and dried under dynamic vacuum at 0 °C, yielding [(*n*-Bu$_2$O)$_{1.25}$AlPh$_3$] as a pale-yellow liquid. Yield: 1.4 g (28 %). Calculated for $C_{28}H_{37,5}O_{1,25}Al$ (M_w = 421,12 g/mol).

^{1}H NMR (C_6D_6, 25 °C, 400.14 MHz): δ 8.10–8.02 (m, 6H, *m*-PhH), 7.43–7.26 (m, 9H, *o*-PhH and *p*-PhH), 3.55 (t, 5H, J = 7.7 Hz, *n*-Bu-C1H$_2$), 1.24 (quint, 5H, J = 7.6 Hz, *n*-Bu-C2H$_2$), 0.76 (m, 5H, J = 7.4 Hz, *n*-Bu-C3H$_2$), 0.53 (t, 7.5H, J = 7.3 Hz, *n*-Bu-C4H$_3$) ppm.

^{13}C NMR (C_6D_6, 25 °C, 100.62 MHz): δ 138.5 (PhH), 137.8 (PhH), 72.1 (*n*-Bu-C1H$_2$), 29.5 (*n*-Bu-C2H$_2$), 18.0 (*n*-Bu-C3H$_2$), 13.1 (*n*-Bu-C4H$_3$).

A.1.3 [CAACH][(HCl)$_{0.5}$Cl]

The synthesis is based on a previously reported procedure with a slight modification [208].

The corresponding alkenyl aldimine (2.00 g, 7.0 mmol) and approximately 30 mL of hexane were added into a 100 mL Schlenk flask and cooled to −78 °C. 2 equivalents of HCl

in diethyl ether solution (7 mL, 3.5 mmol) were added. After 15 minutes, the mixture was left to warm to room temperature and the stirring was continued for 30 minutes. All volatiles were removed under dynamic vacuum. The product was dissolved in approximately 50 mL of acetonitrile and heated at 50 °C for 24 h, affording the aldiminium-based chloride salt. All volatiles were removed under dynamic vacuum. The remaining solid was purified by washing with toluene.

^{1}H NMR (CD_3CN, 25 °C, 600.18 Hz): δ 9.75 (s, 1H, C2−H), 7.60 (t, 1H, J = 7.8 Hz, *p*-ArH), 7.47 (d, 2H, J = 7.8 Hz, *m*-ArH), 2.73 (sept, 2H, J = 6.7 Hz, *i*-Pr-CH), 2.43 (s, 2H, CH_2), 1.61 (s, 6H, C5-CH_3), 1.51 (s, 6H, C3-CH_3), 1.34 (d, 6H, J = 6.7 Hz, *i*-Pr-CH_3), 1.13 (d, 6H, J = 6.8 Hz, *i*-Pr-CH_3) ppm. The ^{1}H NMR data was in accordance with the aldiminium-based chloride salt prepared in the literature [208].

Elemental analysis: calculated for $C_{20}H_{32.5}NCl_{1.5}$ (M_w = 340.14 g/mol): C 70.62, H 9.63, N 4.12 %; found: C 70.12, H 10.27, N 4.13 %.

A.2 Synthesis and Characterization of Products

A.2.1 [(CAAC)AlMe$_2$F] (1)

[(CAAC)$AlMe_3$] (500 mg, 1.40 mmol) and Me_3SnF (257 mg, 1.40 mmol) were weighed into a Schlenk flask. 50 mL of toluene was added and the reaction mixture was stirred for 7 days at 55 °C. Small amounts of white precipitate remained. The solution was filtered through a PTFE filter and the solvent was removed under vacuum. [(CAAC)$AlMe_2F$] (**1**) was obtained in a mixture with equivalent amounts of [(CAAC)$AlMe_3$], and [(CAAC)$AlMeF_2$] (**2**). The solid was purified by washing with dry hexane. Single crystals of [(^{Me}CAAC)$AlMe_2F$] (**1**) suitable for X-ray analysis were obtained by slow evaporation of toluene under static vacuum.

^{1}H NMR (C_6D_6, 25 °C, 600.18 MHz): δ 7.14–7.09 (m, 1H, *p*-ArH), 7.04–6.98 (m, 2H, *m*-ArH), 2.66 (sept, 2H, J = 6.5 Hz, *i*-Pr-CH), 1.44 (s, 6H, C5-CH_3), 1.38–1.36 (m, 8H, CH_2 and *i*-Pr-CH_3), 1.07 (m, 6H, *i*-Pr-CH_3), 0.86 (s, 6H, C3-CH_3), −0.55 (d, 6H, J = 2.6 Hz, Al−CH_3) ppm.

^{19}F NMR (C_6D_6, 25 °C, 564.73 MHz): δ −165.86 ppm.

^{27}Al NMR (C_6D_6, 25 °C, 104.26 MHz): δ 139 (br) ppm.

A.2.2 [(CAAC)AlMeF$_2$] (2)

[(CAAC)$AlMe_3$] (500 mg, 1.40 mmol) and Me_3SnF (514 mg, 2.80 mmol) were weighed into a Schlenk flask. 50 mL of toluene was added and the reaction mixture was stirred for 7 days at 55 °C. Small amounts of white precipitate remained. The solution was filtered through a PTFE filter and the solvent was removed under vacuum. [(CAAC)$AlMeF_2$] (**2**) was obtained in a mixture with other adducts and salts such as [(CAAC)$AlMe_2F$] (**1**), [(CAAC)AlF_3] (**3**), [CAACH][$MeAlF_3$] (**4**), and [CAACH][AlF_4] (**5**). The solid was purified by washing with dry hexane. Single crystals of [(^{Me}CAAC)$AlMeF_2$] (**2**) suitable for X-ray analysis were obtained by slow evaporation of toluene under static vacuum.

^{1}H NMR (C_6D_6, 25 °C, 600.18 MHz): δ 7.11 (t, 1H, J = 7.7 Hz, *p*-ArH), 6.99 (d, 2H, J = 7.8 Hz, *m*-ArH), 2.65 (sept, 2H, J = 6.7 Hz, *i*-Pr-CH), 1.51 (s, 6H, C5-CH_3), 1.38 (d, 6H, J = 6.7 Hz, *i*-Pr-CH_3), 1.34 (s, 2H, CH_2), 1.06 (d, 6H, J = 6.7 Hz, *i*-Pr-CH_3), 0.81 (s, 6H, C3-CH_3), −0.80 (s, 3H, Al−CH_3) ppm.

^{19}F NMR (C_6D_6, 25 °C, 564.73 MHz): δ −157.79 ppm.

^{27}Al NMR (C_6D_6, 25 °C, 104.26 MHz): δ 102 (br) ppm.

A.2.3 [(CAAC)AlF_3] (3)

Formation of [(CAAC)AlF_3] (**3**) was observed with NMR spectroscopy when following the reaction process. [(CAAC)$AlMe_3$] (30 mg, 0.08 mmol) and 3 equivalents of Me_3SnF (45 mg, 0.25 mmol) were weighed into an NMR tube and dissolved in C_6D_6. The tube was heated in an oil bath at 50 °C for 5 days. [(CAAC)AlF_3] (**3**) formed in the mixture of [(CAAC)$AlMe_2F$] (**1**), [(CAAC)$AlMeF_2$] (**2**), [CAACH][$MeAlF_3$] (**4**), [CAACH][AlF_4] (**5**) and other side products.

^{1}H NMR spectra could not be assigned.

^{19}F NMR (CD_3CN, 25 °C, 376.51 MHz): δ −171.04 ppm.

^{27}Al NMR (C_6D_6, 25 °C, 104.26 MHz): δ 59.88 ppm.

A.2.4 [CAACH][$MeAlF_3$] (4)

[CAACH][$(HF)_2F$] (**22**) (197 mg, 0.6 mmol) was weighed into a Schlenk flask and dissolved with 15 mL of acetonitrile. 1 equivalent of $AlMe_3$ (0.3 mL, 2 M, 0.6 mmol) was slowly added to the solution, which was stirred overnight at room temperature. All volatiles were removed under dynamic vacuum, yielding a white solid. Concentration and storage of the reaction mixture at −20 °C gave colourless crystals of [CAACH][$MeAlF_3$] (**4**) suitable for X-ray analysis.

^{1}H NMR (CD_3CN, 25 °C, 600.06 MHz): δ 8.78 (s, 1H, C2−H), 7.61 (t, 1H, J = 7.8 Hz, *p*-ArH), 7.48 (d, 2H, J = 7.9 Hz, *m*-ArH), 2.72 (sept, 2H, J = 6.7 Hz, *i*-Pr-CH), 2.45 (s, 2H, CH_2), 1.60 (s, 6H, C5-CH_3), 1.53 (s, 6H, C3-CH_3), 1.35 (d, 6H, J = 6.7 Hz, *i*-Pr-CH_3), 1.10 (d, 6H, J = 6.8 Hz, *i*-Pr-CH_3) ppm, −1.22 (s, 3H, Al−CH_3).

^{19}F NMR (CD_3CN, 25 °C, 564.62 MHz): δ −167.14 (br, Al−F) ppm.

^{27}Al NMR (CD_3CN, 25 °C, 156.36 MHz): δ 84.95 (q, J = 66.9 Hz, Al−F) ppm.

A.2.5 [CAACH][AlF_4] (5)

[(CAAC)$AlMe_3$] (500 mg, 1.40 mmol) and Me_3SnF (514 mg, 2.80 mmol) were weighed into a Schlenk flask. 50 mL of toluene was added and the reaction mixture was stirred for 7 days at 55 °C. Substantial amounts of white precipitate formed. The solid was separated by filtration, dried under vacuum and purified by washing with dry hexane. Single crystals of [CAACH][AlF_4] (**5**) suitable for X-ray analysis were obtained by slow evaporation of acetonitrile under static vacuum.

^{1}H NMR (CD_3CN, 25 °C, 600.18 MHz): δ 8.72 (s, 1H, C2−H), 7.61 (t, 1H, J = 7.8 Hz, *p*-ArH), 7.48 (d, 2H, J = 7.8 Hz, *m*-ArH), 2.72 (sept, 2H, J = 6.7 Hz, *i*-Pr-CH), 2.46 (s, 2H, CH_2), 1.59 (s, 6H, C5-CH_3), 1.53 (s, 6H, C3-CH_3), 1.35 (d, 6H, J = 6.7 Hz, *i*-Pr-CH_3), 1.10 (d, 6H, J = 6.8 Hz, *i*-Pr-CH_3) ppm.

^{19}F NMR (CD_3CN, 25 °C, 564.73 MHz): δ −194.56 (m, Al−F) ppm.

^{27}Al NMR (CD_3CN, 25 °C, 156.36 MHz): δ 49.41 (q, J = 37.8 Hz, Al−F) ppm.

Alternative synthetic procedure:

[CAACH][$(HF)_3F$] (**21**) (219 mg, 0.6 mmol) was weighed into a Schlenk flask and dissolved with 15 mL of acetonitrile. The solution was cooled to 0 °C and 1 equivalent of $AlMe_3$ (0.3 mL, 2 M, 0.6 mmol) was slowly added. The solution was stirred for 4 hours at room temperature. All volatiles were removed under dynamic vacuum, yielding a white solid [CAACH][AlF_4] (**5**).

A.2.6 CAAC(H)Me (6)

CAAC(H)Me ($C_{22}H_{35}N$, M_w = 313.52 g/mol) was obtained as a side product in the reaction of [(CAAC)$AlMe_3$] with Me_3SnF. CAAC(H)Me (**6**) was washed away with hexane, dried under vacuum and characterised. Single crystals suitable for X-ray analysis were obtained by slow evaporation of hexane under static vacuum.

^{1}H NMR (C_6D_6, 25 °C, 600.18 MHz): δ 7.21–7.17 (m, 2H, *p*-Ar-H), 7.12–7.10 (m, 1H, *m*-ArH), 4.06 (sept, 1H, J = 6.7 Hz, *i*-Pr-CH_3), 1.82–1.71 (m, 2H, CH_2), 1.32 (d, 3H, J = 6.9 Hz, *i*-Pr-CH_3), 1.26 (d, 3H, J = 6.8 Hz, *i*-Pr-CH_3), 1.21 (s, 3H, CH_3), 1.19–1.15 (m, 6H, *i*-Pr-CH_3), 1.12 (s, 3H, CH_3), 1.06 (s, 3H, CH_3), 0.98 (s, 3H, CH_3), 0.78 (d, 3H, J = 6.4 Hz, C2-CH_3) ppm.

A.2.7 [IPrH][Me_3AlF] (7)

[IPrH][F] (326 mg, 0.8 mmol) was weighed into a Schlenk flask and dissolved with 15 mL of acetonitrile. 1 equivalent of $AlMe_3$ (0.4 mL, 2 M, 0.8 mmol) was slowly added to the solution, which was stirred for 2 hours at room temperature. All volatiles were removed under dynamic vacuum, yielding [IPrH][Me_3AlF] (**7**) as a pale-yellow solid. Due to its instability, this product was not further purified and stored in a freezer at −20 °C in a glovebox. Yield: 376 mg (98 %).

^{1}H NMR (CD_3CN, 25 °C, 600.06 MHz): δ 9.05–8.99 (m, 1H, C2−H), 7.87 (s, 2H, CH=CH), 7.65 (t, 2H, J = 7.8 Hz, *p*-ArH), 7.48 (d, 4H, J = 7.8 Hz, *m*-ArH), 2.42 (sept, 4H, J = 6.8 Hz, *i*-Pr-CH), 1.27 (d, 12H, J = 6.8 Hz, *i*-Pr-CH_3), 1.20 (d, 12H, J = 6.9 Hz, *i*-Pr-CH_3), −1.29 (s, 9H, Al−CH_3) ppm.

^{13}C{^{1}H} NMR (CD_3CN, 25 °C, 150.88 MHz): δ 138.7 (C2−H), 133.1 (*p*-ArC), 127.0 (CH=CH), 125.7 (*m*-ArC), 29.8 (*i*-Pr-CH), 24.5 (*i*-Pr-CH_3), 23.7 (*i*-Pr-CH_3), −5.4 (Al−CH_3) ppm.

^{19}F NMR (CD_3CN, 25 °C, 564.62 MHz): δ −158.64 (br, Al−F) ppm.

^{27}Al NMR (CD_3CN, 25 °C, 156.36 MHz): δ 150.64 (d, J = 119.8 Hz) ppm.

Raman [ν(Al−C) range]: 505 cm^{-1}.

Elemental analysis calculated for $C_{30}H_{46}N_2AlF$ (M_w = 480.68 g/mol): C 74.96, H 9.65, N 5.83 %; found: C 74.52, H 9.39, N 6.42 %. Although these results are outside the range viewed as establishing analytical purity, they are provided to illustrate the best values obtained to date for this sample.

A.2.8 [IPrH][(*n*-Bu)$_3$AlF] (8)

[IPrH][F] (412 mg, 1 mmol) was weighed into a Schlenk flask and dissolved with 20 mL of acetonitrile. 1 equivalent of Al(*n*-Bu)$_3$ (200 mg, 1 mmol) was slowly added to the solution, which was stirred for 2 hours at room temperature. All volatiles were removed under dynamic vacuum, yielding a pale-yellow oily product. Due to its instability, [IPrH][(*n*-Bu)$_3$AlF] (**8**) was not further purified and was stored in a freezer at −20 °C in a glovebox. Storage of the product at −20 °C yields colourless crystals suitable for X-ray analysis. Crystal data were collected at 189 K. Yield: 530 mg (87 %).

^{1}H NMR (CD_3CN, 25 °C, 600.06 MHz): δ 9.05 (s, 1H, C2−H), 7.88 (s, 2H, CH=CH), 7.65 (t, 2H, J = 7.8 Hz, *p*-ArH), 7.48 (d, 4H, J = 7.8 Hz, *m*-ArH), 2.42 (sept, 4H, J = 6.8 Hz, *i*-Pr-CH), 1.31–1.18 (m, 36H, *i*-Pr-CH_3, *n*-Bu-C2H_2, *n*-Bu-C3H_2), 0.82 (m, 9H, *n*-Bu-C4H_3), −0.50 (m, 6H, Al−*n*-Bu-C1H_2) ppm.

^{13}C{^{1}H} NMR (CD_3CN, 25 °C, 150.89 MHz): δ 138.0 (C2−H), 132.2 (*p*-ArC), 126.1 (CH=CH), 124.8 (*m*-ArC), 29.7 (*n*-Bu-C2H_2, *n*-Bu-C3H_2), 28.9 (*i*-Pr-CH), 23.6 (*i*-Pr-CH_3), 22.8 (*i*-Pr-CH_3), 13.6 (*n*-Bu-C4H_3), 11.7 (Al−*n*-Bu-C1H_2) ppm.

^{19}F NMR (CD_3CN, 25 °C, 564.62 MHz): δ −167.90 (br, Al−F) ppm.

^{27}Al NMR (CD_3CN, 25 °C, 156.36 MHz): δ 147.51 ppm.

Raman [ν(Al−C) range]: 493 cm^{-1}.

This compound is unstable, therefore acceptable elemental analysis results could not be obtained.

A.2.9 [IPrH][Me_2AlF_2] (9)

[IPrH][(HF)F] (340 mg, 0.8 mmol) was weighed into a Schlenk flask and dissolved with 15 mL of acetonitrile. 1 equivalent of $AlMe_3$ (0.4 mL, 2 M, 0.8 mmol) was slowly added to the solution, which was stirred overnight at room temperature. All volatiles were removed under dynamic vacuum, yielding [IPrH][Me_2AlF_2] (**9**) as a white solid. Single crystals suitable for X-ray analysis were obtained by slow evaporation of C_6D_6 (**9a**) and dichloromethane (**9b**). Yield: 264 mg (95 %).

^{1}H NMR (CD_3CN, 25 °C, 600.06 MHz): δ 9.01 (m, 1H, C2−H), 7.87 (s, 2H, CH=CH), 7.65 (t, 2H, J = 7.8 Hz, *p*-ArH), 7.47 (d, 4H, J = 7.8 Hz, *m*-ArH), 2.43 (sept, 4H, J = 6.2 Hz, *i*-Pr-CH), 1.27 (d, 12H, J = 6.8 Hz, *i*-Pr-CH_3), 1.19 (d, 12H, J = 6.9 Hz, *i*-Pr-CH_3), −1.30 (s, 6H, Al−CH_3) ppm.

^{13}C{^{1}H} NMR (CD_3CN, 25 °C, 150.88 MHz): δ 138.7 (C2−H), 133.1 (*p*-ArC), 127.0 (CH=CH), 125.7 (*m*-ArC), 29.8 (*i*-Pr-CH), 24.5 (*i*-Pr-CH_3), 23.7 (*i*-Pr-CH_3), −11.1 (Al−CH_3) ppm.

^{19}F NMR (CD_3CN, 25 °C, 376.51 MHz): δ −154.78 (br, Al−F) ppm.

^{27}Al NMR (CD_3CN, 25 °C, 104.26 MHz): δ 123.90 (t, J = 122.8 Hz) ppm.

Raman [ν(Al−C) range]: 533 cm^{-1}.

Elemental analysis calculated for $C_{29}H_{43}N_2AlF_2$ (M_w = 484.64 g/mol): C 71.87, H 8.94, N 5.78 %; found: C 72.04, H 8.93, N 5.86 %.

A.2.10 [IPrH][(*n*-Bu)$_2$$AlF_2$] (10)

[IPrH][(HF)F] (216 mg, 0.5 mmol) was weighed into a Schlenk flask and dissolved with 10 mL of acetonitrile. 1 equivalent of Al(*n*-Bu)$_3$ (100 mg, 0.5 mmol) was slowly added to the solution, which was stirred overnight at room temperature. Concentrating and storing of the reaction mixture at −20 °C gives colourless crystals of [IPrH][(*n*-Bu)$_2$$AlF_2$] (**10**) suitable for X-ray analysis. Yield: 253 mg (89 %).

^{1}H NMR (CD_3CN, 25 °C, 600.06 MHz): δ 8.98 (s, 1H, C2−H), 7.88 (s, 2H, CH=CH), 7.65 (t, 2H, J = 7.8 Hz, *p*-ArH), 7.48 (d, 4H, J = 7.8 Hz, *m*-ArH), 2.42 (sept, 4H, J = 6.8 Hz, *i*-Pr-CH), 1.41–1.07 (m, 32H, *i*-Pr-CH_3, *n*-Bu-C2H_2, *n*-Bu-C3H_2), 0.83 (m, 6H, *n*-Bu-C4H_3), −0.50 (m, 4H, Al−*n*-Bu-C1H_2) ppm.

^{13}C{^{1}H} NMR (CD_3CN, 25 °C, 150.89 MHz): δ 138.8 (C2−H), 133.1 (*p*-ArC), 127.1 (CH=CH), 125.7 (*m*-ArC), 29.9 (*n*-Bu-C2H_2, *n*-Bu-C3H_2), 29.8 (*i*-Pr-CH), 24.5 (*i*-Pr-CH_3), 23.8 (*i*-Pr-CH_3), 14.6 (*n*-Bu-C4H_3), 10.1 (Al−*n*-Bu-C1H_2) ppm.

^{19}F NMR (CD_3CN, 25 °C, 564.62 MHz): δ −160.74 (br, Al−F) ppm.

^{27}Al NMR (CD_3CN, 25 °C, 156.36 MHz): δ 120.71 ppm.

Raman [ν(Al−C) range]: 494 cm^{-1}.

Elemental analysis calculated for $C_{35}H_{55}N_2AlF_2$ (M_w = 568.80 g/mol): C 73.91, H 9.75, N 4.92 %; found: C 73.55, H 9.89, N 5.22 %.

A.2.11 [IPrH][MeAlF$_3$] (11)

[IPrH][(HF)$_2$F] (357 mg, 0.8 mmol) was weighed into a Schlenk flask and dissolved with 15 mL of acetonitrile. 1 equivalent of AlMe$_3$ (0.4 mL, 2 M, 0.8 mmol) was slowly added to the solution, which was stirred overnight at room temperature. All volatiles were removed under dynamic vacuum, yielding [IPrH][MeAlF$_3$] (**11**) as a white solid. Concentration and storage of the reaction mixture at −20 °C gave colourless crystals suitable for X-ray analysis. Yield: 334 mg (85 %).

^{1}H NMR (CD$_3$CN, 25 °C, 400.14 MHz): δ 8.98 (t, 1H, J = 1.6 Hz, C2−H), 7.88 (d, 2H, J = 1.6 Hz, CH=CH), 7.65 (t, 2H, J = 7.8 Hz, *p*-ArH), 7.49 (d, 4H, J = 7.8 Hz, *m*-ArH), 2.42 (sept, 4H, J = 6.8 Hz, *i*-Pr-CH), 1.27 (d, 12H, J = 6.8 Hz, *i*-Pr-CH$_3$), 1.20 (d, 12H, J = 6.9 Hz, *i*-Pr-CH$_3$), −1.24 (s, Al−CH$_3$) ppm.

^{13}C{^{1}H} NMR (CD$_3$CN, 25 °C, 150.89 MHz): δ 138.8 (C2−H), 133.1 (*p*-ArC), 127.1 (CH=CH), 125.7 (*m*-ArC), 29.8 (*i*-Pr-CH), 24.5 (*i*-Pr-CH$_3$), 23.8 (*i*-Pr-CH$_3$), −13.7 (Al−CH$_3$) ppm.

^{19}F NMR (CD$_3$CN, 25 °C, 376.51 MHz): δ −167.07 (m, Al−F) ppm.

^{27}Al NMR (CD$_3$CN, 25 °C, 104.26 MHz): δ 84.96 (q, J = 69.67 Hz) ppm.

Raman [ν(Al−C) range]: 567 cm^{-1}.

Elemental analysis calculated for $C_{28}H_{40}N_2AlF_3$ (M_w = 488.61 g/mol): C 68.83, H 8.25, N 5.73 %; found: C 68.61, H 8.19, N 5.67 %.

A.2.12 [IPrH][(*n*-Bu)AlF$_3$] (12)

[IPrH][(HF)$_2$F] (226 mg, 0.5 mmol) was weighed into a Schlenk flask and dissolved with 10 mL of acetonitrile. 1 equivalent of Al(*n*-Bu)$_3$ (100 mg, 0.5 mmol) was slowly added to the solution, which was stirred overnight at room temperature. All volatiles were removed under dynamic vacuum, yielding [IPrH][(*n*-Bu)AlF$_3$] (**12**) as a white solid. Concentration and storage of the reaction mixture at −20 °C gave colourless crystals suitable for X-ray analysis. Crystal data were collected at 240 K. Yield: 220 mg (83 %).

^{1}H NMR (CD$_3$CN, 25 °C, 600.06 MHz): δ 9.00 (t, 1H, J = 1.6 Hz, C2−H), 7.88 (d, 2H, J = 1.6 Hz, CH=CH), 7.66 (t, 2H, J = 7.8 Hz, *p*-ArH), 7.48 (d, 4H, J = 7.8 Hz, *m*-ArH), 2.42 (sept, 4H, J = 6.9 Hz, *i*-Pr-CH), 1.38–1.10 (m, 28H, *i*-Pr-CH$_3$, *n*-Bu-C2H$_2$, *n*-Bu-C3H$_2$), 0.84 (t, 3H, J = 7.2 Hz, *n*-Bu-C4H$_3$), −0.39 (m, 2H, Al−*n*-Bu-C1H$_2$) ppm.

^{13}C{^{1}H} NMR (CD$_3$CN, 25 °C, 150.89 MHz): δ 137.9 (C2−H), 132.2 (*p*-ArC), 126.1 (CH=CH), 124.8 (*m*-ArC), 28.9 (*i*-Pr-CH), 28.5 (*n*-Bu-C2H$_2$, *n*-Bu-C3H$_2$), 23.6 (*i*-Pr-CH$_3$), 22.8 (*i*-Pr-CH$_3$), 13.4 (*n*-Bu-C4H$_3$), 6.6 (Al−*n*-Bu-C1H$_2$) ppm.

^{19}F NMR (CD$_3$CN, 25 °C, 564.62 MHz): δ −169.61 (br, Al−F) ppm.

^{27}Al NMR (CD$_3$CN, 25 °C, 156.36 MHz): δ 82.71 ppm.

Raman [ν(Al−C) range]: 495 cm^{-1}.

Elemental analysis calculated for $C_{31}H_{46}N_2AlF_3$ (M_w = 530.69 g/mol): C 70.16, H 8.74, N 5.28 %; found: C 69.82, H 8.91, N 5.55 %.

A.2.13 [IPrH][AlF$_4$] (13)

[(IPr)AlMe$_3$] (212 mg, 0.46 mmol) was dissolved in 3 mL acetonitrile and transferred to a FEP reaction vessel. The solution was frozen in liquid nitrogen and 1 mL of aHF was condensed over the solution. The solution was allowed to warm to room temperature while stirring. After 2 hours, all volatiles were removed under dynamic vacuum, yielding a white solid product. Single crystals of [IPrH][AlF$_4$] (**13**) were obtained from a saturated acetonitrile solution stored in the freezer at −20 °C (**13**) and by slow evaporation of C$_6$D$_6$ (**13a**). Yield: 221 mg (97 %).

^{1}H NMR (CD_3CN, 25 °C, 600.06 MHz): δ 8.92 (s, 1H, C2−H), 7.86 (d, 2H, J = 1.5 Hz, CH=CH), 7.65 (t, 2H, J = 7.8 Hz, *p*-ArH), 7.48 (d, 4H, J = 7.8 Hz, *m*-ArH), 2.41 (sept, 4H, J = 6.9 Hz, *i*-Pr-CH), 1.27 (d, 12H, J = 6.8 Hz, *i*-Pr-CH_3), 1.19 (d, 12H, J = 6.9 Hz, *i*-Pr-CH_3) ppm.

^{13}C{^{1}H} NMR (CD_3CN, 25 °C, 150.88 MHz): δ 146.71, 139.09, 133.58, 131.15, 127.47, 126.12, 30.27, 24.86, 24.20 ppm.

^{19}F NMR (CD_3CN, 25 °C, 564.62 MHz): δ −194.62 (m, J = 37.55 Hz, Al−F) ppm.

^{27}Al NMR (CD_3CN, 25 °C, 156.36 MHz): δ 49.37 (q, J = 37.85 Hz, Al−F) ppm.

Raman [ν(Al−F) range]: 321 cm^{-1}, 634 cm^{-1}.

Elemental analysis calculated for $C_{27}H_{37}N_2AlF_4$ (M_w = 492.57 g/mol): C 65.84, H 7.57, N 5.69 %; found: C 65.90, H 7.64, N 5.92 %.

A.2.14 [IPrH][Ph$_3$AlF] (14) and [IPrH][PhAlF$_3$] (16)

The reaction between [(*n*-Bu_2O)$_{1.25}$$AlPh_3$] and imidazolium-based fluorinating reagents [IPrH][F], [IPrH][(HF)F] and [IPrH][$(HF)_2$F] usually leads to the formation of mixtures containing [IPrH][Ph_3AlF] (**14**), [IPrH][Ph_2AlF_2] (**15**) and [IPrH][$PhAlF_3$] (**16**). By using [IPrH][(HF)F] and [(*n*-Bu_2O)$_{1.25}$$AlPh_3$] in the ration 1:1, a mixture of relatively pure [IPrH][Ph_3AlF] (**14**) and [IPrH][$PhAlF_3$] (**16**) was obtained. The reaction was carried out on a small scale in a glovebox. [IPrH][(HF)F] (55 mg, 0.13 mmol) was weighed into a PP plastic container and suspended in 0.5 mL of C_6D_6. [(*n*-Bu_2O)$_{2.5}$$AlPh_3$] (50 mg, 0.12 mmol) was added slowly and the reactants were mixed together until a clear solution was obtained. After two days, all volatiles were removed and a white solid powder was obtained. It was characterised as a mixture of [IPrH][Ph_3AlF] (**14**) and [IPrH][$PhAlF_3$] (**16**). Due to C_6D_6 residues in the solid sample, yield determination and CHN analysis were not possible. Single crystals of [IPrH][Ph_3AlF] (**14**) were prepared by the reaction of [IPrH][F] and [(*n*-Bu_2O)$_{1.25}$$AlPh_3$] in 1:1 ratio in C_6D_6 and slow evaporation of the solvent, while single crystals of [IPrH][$PhAlF_3$] (**16**) were obtained by the reaction of [IPrH][$(HF)_2$F] and [(*n*-Bu_2O)$_{1.25}$$AlPh_3$] in 1:1 ratio in acetonitrile and slow evaporation of the solvent.

^{1}H NMR (CD_3CN, 25 °C, 400.14 MHz): δ 8.97 (s, 1H, C2−H), 7.85 (d, 2H, J = 1.4 Hz, CH=CH), 7.65 (t, 2H, J = 7.8 Hz, *p*-ArH), 7.67–7.53 (m, 3H, *m*-PhH), 7.47 (d, 4H, J = 7.9 Hz, *m*-ArH), 7.18–7.06(m, 4.4H, *o*-PhH and *p*-PhH), 2.41 (sept, 4H, J = 6.8 Hz, *i*-Pr-CH), 1.27 (d, 12H, J = 6.8 Hz, *i*-Pr-CH_3), 1.19 (d, 12H, J = 6.9 Hz, *i*-Pr-CH_3) ppm.

^{13}C{^{1}H} NMR (CD_3CN, 25 °C, 100.62 MHz): δ 137.8 (C2−H), 137.4 (*o*-PhC and *p*-PhC), 132.2 (*p*-ArC), 126.2 (*m*-PhC), 126.1 (CH=CH), 124.7 (*m*-ArC), 28.9 (*i*-Pr-CH), 23.5 (*i*-Pr-CH_3), 22.9 (*i*-Pr-CH_3) ppm.

^{19}F NMR (CD_3CN, 25 °C, 564.62 MHz): δ −170.10 (br, Ph_3Al−F), −175.57 (br, PhAl−$(F)_3$) ppm.

^{27}Al NMR (CD_3CN, 25 °C, 156.36 MHz): δ 97.53 (Ph_3Al−F), 71.23 (PhAl−$(F)_3$) ppm.

Raman [ν(Al−C) range]: 999 cm^{-1}, 1030 cm^{-1}.

A.2.15 [(IPr)AlH$_2$OTf] (17)

[(IPr)AlH_3] (500 mg, 1.20 mmol) and [CAACH][OTf] (506 mg, 1.19 mmol) were weighed into a 100 mL Schlenk flask. Approximately 30 mL of toluene was added and the reaction mixture was stirred overnight at ambient temperature. Solvent was removed under dynamic vacuum. The product was purified by washing with hexane. The remaining white solid was dried under vacuum, yielding [(IPr)AlH_2OTf] (**17**). Single crystals suitable for X-ray analysis were obtained by slow evaporation of toluene under static vacuum. Yield: 626 mg (94 %). Calculated for $C_{28}H_{38}N_2AlO_3SF_3$ (M_w = 556.57 g/mol).

^{1}H NMR (C_6D_6, 25 °C, 600.06 MHz): δ 7.25 (t, 2H, J = 7.8 Hz, *p*-ArH), 7.09 (d, 4H, J = 7.8 Hz, *m*-ArH), 6.36 (s, 2H, CH=CH), 3.95 (Al−H), 2.51 (sept, 4H, J = 6.9 Hz, *i*-Pr-CH), 1.35 (d, 12H, J = 6.9 Hz, *i*-Pr-CH_3), 0.96 (d, 12H, J = 6.9 Hz, *i*-Pr-CH_3) ppm.

^{13}C NMR (C_6D_6, 25 °C, 150.89 MHz): δ 145.59 (CH=CH), 133.31 (ArC), 131.96 (ArC), 125.17 (ArC), 125.01 (ArC), 29.49 (*i*-Pr-CH), 25.59 (*i*-Pr-CH_3), 23.21 (*i*-Pr-CH_3) ppm.

^{19}F NMR (C_6D_6, 25 °C, 564.62 MHz): δ −77.47 (CF_3) ppm.

^{27}Al NMR (C_6D_6, 25 °C, 156.36 MHz): δ 120 (Al−H) ppm.

Raman [ν(Al−H) range]: 1841 cm^{-1}, 1893 cm^{-1}.

A.2.16 $CAACH_2$ (18)

$CAACH_2$ (**18**) ($C_{20}H_{33}N$, M_w = 287.47 g/mol) was obtained as a side product in the reaction of [(IPr)AlH_3] with aldiminium-based salts (see above). $CAACH_2$ (**18**) was washed away with hexane, dried under vacuum and characterized. Single crystals suitable for X-ray analysis were obtained by slow evaporation of hexane under static vacuum.

^{1}H NMR (C_6D_6, 25 °C, 600.18 MHz): δ 7.22–7.19 (m, 1H, *p*-ArH), 7.14 (d, 1H, J = 7.1 Hz, *m*-ArH), 3.76 (sept, 2H, J = 6.9 Hz, *i*-Pr-CH), 3.32 (s, 2H, C2-CH_2), 1.76 (s, 2H, C4-CH_2), 1.30 (d, 6H, J = 6.9 Hz, *i*-Pr-CH_3), 1.21 (s, 6H, $C(CH_3)_2$), 1.17 (d, 6H, J = 6.9 Hz, *i*-Pr-CH_3), 1.15 (s, 6H, $C(CH_3)_2$) ppm.

A.2.17 [(IPr)$AlH_{3-x}Cl_x$] (x = 1, 2) (19)

[(IPr)AlH_3] (500 mg, 1.20 mmol) and [CAACH][$(HCl)_{0.5}$Cl] (390 mg, 1.14 mmol) were weighed into a 100 mL Schlenk flask. Approximately 30 mL of toluene was added and the reaction mixture was stirred overnight at ambient temperature. Solvent was removed under dynamic vacuum. The product was purified by washing with hexane. The remaining white solid was dried under vacuum, yielding [(IPr)$AlH_{3-x}Cl_x$] (x = 1, 2) (**19**). Single crystals suitable for X-ray analysis were obtained by slow evaporation of toluene under static vacuum. Yield: 500 mg (88 %). Calculated from the structure obtained with crystal structure determination, $C_{27}H_{37.36}AlCl_{1.64}N_2$ (M_w = 475,06 g/mol).

^{1}H NMR (C_6D_6, 25 °C, 600.06 MHz): δ 7.24–7.20 (m, 4H, *p*-ArH), 7.10–7.06 (m, 8H, *m*-ArH), 6.41 (s, 2H, CH=CH), 6.40 (s, 2H, CH=CH), 3.7–4.1 (Al−H), 2.72–2.64 (m, 8H, *i*-Pr-CH), 1.46–1.39 (m, 24H, *i*-Pr-CH_3), 1.01 (d, 12H, J = 6.8 Hz, *i*-Pr-CH_3), 0.97 (d, 12H, J = 6.9 Hz, *i*-Pr-CH_3) ppm.

^{13}C NMR (C_6D_6, 25 °C, 150.89 MHz): δ 146.06 (CH=CH), 146.01 (CH=CH), 134.37 (ArC), 133.96 (ArC), 131.70 (ArC), 131.43 (ArC), 125.18 (ArC), 124.73 (ArC), 124.67 (ArC), 124.64 (ArC), 29.55 (*i*-Pr-CH), 29.49 (*i*-Pr-CH), 26.10 (*i*-Pr-CH_3), 25.77 (*i*-Pr-CH_3), 23.42 (*i*-Pr-CH_3), 23.21 (*i*-Pr-CH_3) ppm.

^{27}Al NMR (C_6D_6, 25 °C, 156.36 MHz): δ 115 (Al−H) ppm.

Raman [ν(Al−H) range]: 1777 cm^{-1}, 1818 cm^{-1}.

A.2.18 [(IPr)$AlCl_3$] (20)

IPr (500 mg, 1.29 mmol) and $AlCl_3$ (172 mg, 1.29 mmol) were weighed into a 100 mL Schlenk flask. Approximately 30 mL of toluene was added to the reaction mixture, which was stirred overnight at ambient temperature. Solvent was removed under dynamic vacuum. The product was washed with hexane and dried in vacuum. Colourless single crystals of [(IPr)$AlCl_3$] (**20**) were obtained by slow evaporation of toluene under static vacuum. Yield: 624 mg (93 %) Calculated for $C_{27}H_{36}N_2AlCl_3$ (M_w = 521.93 g/mol).

^{1}H NMR (C_6D_6, 25 °C, 600.06 MHz): δ 7.23 (t, 2H, J = 7.8 Hz, *p*-ArH), 7.09 (d, 4H, J = 7.8 Hz, *m*-ArH), 6.43 (s, 2H, CH=CH), 2.67 (sept, 4H, J = 6.8 Hz, *i*-Pr-CH), 1.43 (d, 12H, J = 6.8 Hz, *i*-Pr-CH_3), 0.96 (d, 12H, J = 6.9 Hz, *i*-Pr-CH_3) ppm.

^{13}C NMR (C_6D_6, 25 °C, 150.89 MHz): δ 146.15 (CH=CH), 134.14 (ArC), 131.93 (ArC), 125.83 (ArC), 124.85 (ArC), 29.59 (*i*-Pr-CH), 26.28 (*i*-Pr-CH_3), 23.14 (*i*-Pr-CH_3) ppm.

^{27}Al NMR (C_6D_6, 25 °C, 156.36 MHz): δ 105.34 ppm.

Raman [ν(Al−Cl) range]: 318.1 cm^{-1}.

A.2.19 [CAACH][$(HF)_3F$] (21)

[CAACH][$(HCl)_{0.5}Cl$] (1.10 g, 3.23 mmol) was loaded into a FEP tube. Approximately 5 mL of anhydrous HF was condensed at −196 °C. The reaction mixture was warmed to room temperature and left stirring for 2 h. After that the excess of HF was removed in vacuum overnight, under reduced pressure of 10^{-2}–10^{-3} bar, to yield a white solid. Single crystals of [CAACH][$(HF)_3F$] (**21**) suitable for X-ray analysis were formed during slow evaporation of HF. Yield: 1.16 g (98 %).

^{1}H NMR (CD_3CN, 25 °C, 400.14 MHz): δ 8.78 (s, 1H, C2−H), 7.61 (t, 1H, J = 7.8 Hz, *p*-ArH), 7.47 (d, 2H, J = 7.8 Hz, *m*-ArH), 2.72 (sept, 2H, J = 6.7 Hz, *i*-Pr-CH), 2.46 (s, 2H, CH_2), 1.60 (s, 6H, C5-CH_3), 1.53 (s, 6H, C3-CH_3), 1.35 (d, 6H, J = 6.7 Hz, *i*-Pr-CH_3), 1.10 (d, 6H, J = 6.8 Hz, *i*-Pr-CH_3) ppm.

^{13}C NMR (CD_3CN, 25 °C, 100.62 MHz): δ 191.9 (C2−H), 145.6 (*ipso*-ArC), 133.1 (*p*-ArC), 130.1 (*o*-ArC), 126.6 (*m*-ArC), 85.9 (C5), 48.8 (C3), 48.8 (CH_2), 30.4 (*i*-Pr-CH), 28.5 (C3-CH_3), 26.3 (*i*-Pr-CH_3), 26.2 (C5-CH_3), 22.2 (*i*-Pr-CH_3) ppm.

^{19}F NMR (CD_3CN, 25 °C, 376.51 MHz): δ −173.45 (br, H_3F_4) ppm.

Elemental analysis calculated for $C_{20}H_{35}NF_4$ (M_w = 365.49 g/mol): C 65.72, H 9.65, N 3.83 %; found: C 65.16, H 9.74, N 4.51 %. Although these results are outside the range viewed as establishing analytical purity, they are provided to illustrate the best values obtained to date for this sample.

A.2.20 [CAACH][$(HF)_2F$] (22)

[CAACH][$(HF)_3F$] (**21**) (2.70 g, 7.39 mmol) was loaded into a FEP tube. The removal of HF was conducted for 2 days in high vacuum, under reduced pressure of 10^{-5}–10^{-7} mbar. Single crystals of [CAACH][$(HF)_2F$] (**22**) suitable for X-ray analysis were obtained from a saturated acetonitrile solution stored in the freezer at −20 °C. Yield: 2.37 g (93 %).

^{1}H NMR (CD_3CN, 25 °C, 400.14 MHz): δ 8.84 (s, 1H, C2−H), 7.62 (t, 1H, J = 7.8 Hz, *p*-ArH), 7.47 (d, 2H, J = 7.8 Hz, *m*-ArH), 2.73 (sept, 2H, J = 6.7 Hz, *i*-Pr-CH), 2.46 (s, 2H, CH_2), 1.60 (s, 6H, C5-CH_3), 1.53 (s, 6H, C3-CH_3), 1.35 (d, 6H, J = 6.7 Hz, *i*-Pr-CH_3), 1.10 (d, 6H, J = 6.8 Hz, *i*-Pr-CH_3) ppm.

^{13}C NMR (CD_3CN, 25 °C, 100.62 MHz): δ 192.1 (C2−H), 145.6 (*ipso*-ArC), 133.1 (*p*-ArC), 130.1 (*o*-ArC), 126.6 (*m*-ArC), 85.8 (C5), 48.8 (C3), 48.8 (CH_2), 30.4 (*i*-Pr-CH), 28.5 (C3-CH_3), 26.3 (*i*-Pr-CH_3), 26.2 (C5-CH_3), 22.2 (*i*-Pr-CH_3) ppm.

^{19}F NMR (CD_3CN, 25 °C, 376.51 MHz): δ −168.57 (br, H_2F_3).

Elemental analysis calculated for $C_{20}H_{34}NF_3$ (M_w = 345.48 g/mol): C 69.53, H 9.92, N 4.05 %; found: C 69.87, H 9.80, N 4.20 %.

A.2.21 CAAC(H)F (24)

[CAACH][$(HF)_2F$] (**22**) (1.20 g, 3.47 mmol) and 2.5 equivalent portion of CsF (1.31 g, 8.62 mmol) were loaded in a FEP tube and suspended in 10 mL of toluene. The mixture was left stirring for 3 days at room temperature. The solution was filtered through a PTFE

filter and collected in another FEP tube. After that all volatiles were removed under dynamic vacuum yielding a white solid. Single crystals of CAAC(H)F (**24**) were obtained from a saturated acetonitrile solution stored in the freezer at −20 °C. Yield: 0.94 g (91 %).

^{1}H NMR (C_6D_6, 25 °C, 400.14 MHz): δ 7.25–7.17 (m, 3H, ArH), 5.27 (s, 1H, C2−H), 3.74 (m, 2H, J = 6.9 Hz, *i*-Pr-CH), 1.81 (s, 2H, CH_2), 1.25 (d, 6H, J = 7.0 Hz, *i*-Pr-CH_3), 1.23 (s, 6H, C5-CH_3), 1.19 (d, 6H, J = 6.4 Hz, *i*-Pr-CH_3), 1.12 (s, 6H, C3-CH_3) ppm.

^{13}C NMR (C_6D_6, 25 °C, 100.62 MHz): δ 151.9 (*ipso*-ArC), 136.1 (*o*-ArC), 125.1 (*m*-ArC), 114.3 (C2−H), 65.3 (C5), 53.7 (CH_2), 43.2 (C3), 30.5 (C3-CH_3), 28.8 (*i*-Pr-CH), 27.9 (C5-CH_3), 27.0 (*i*-Pr-CH_3), 24.0 (*i*-Pr-CH_3) ppm.

^{19}F NMR (C_6D_6, 25 °C, 376.51 MHz): δ −106.80 (s, C2−F) ppm.

Elemental analysis calculated for $C_{20}H_{32}NF$ (M_w = 305.47 g/mol): C 78.64, H 10.56, N 4.59 %; found: C 78.98, H 10.53, N 4.60 %.

A.2.22 [CAACH][(HF)F] (25)

[CAACH][$(HF)_2$F] (**22**) (113 mg, 0.33 mmol) and CAAC(H)F (**24**) (100 mg, 0.33 mmol) were loaded in a FEP tube and dissolved in 3 mL acetonitrile. The solution was left stirring overnight at room temperature. All volatiles were removed under dynamic vacuum yielding a white solid. Single crystals of [CAACH][(HF)F]·2CAAC(H)F (**25a**) were obtained by slow evaporation of solvent from the solution in *t*-BuOH and acetonitrile Yield: 209 mg (98 %).

^{1}H NMR (CD_3CN, 25 °C, 400.14 MHz): δ 13.89 (br, 1H, HF_2), 8.20–7.70 (br, 1H, C2−H), 7.50 (t, 1H, J = 7.7 Hz, *p*-ArH), 7.39 (d, 2H, J = 7.8 Hz, *m*-ArH), 3.00 (m, 2H, *i*-Pr-CH), 2.31 (s, 2H, CH_2), 1.50 (s, 6H, C5-CH_3), 1.41 (s, 6H, C3-CH_3), 1.31 (d, 6H, J = 6.7 Hz, *i*-Pr-CH_3), 1.09 (d, 6H, J = 6.7 Hz, *i*-Pr-CH_3) ppm.

^{13}C NMR (CD_3CN, 25 °C, 100.62 MHz): δ 147.7 (*ipso*-ArC), 132.1 (*o*-ArC), 131.8 (*p*-ArC), 130.5 (C2−H), 126.2 (*m*-ArC), 50.4 (C5), 47.2 (C3), 29.9 (*i*-Pr-CH), 29.2 (C3-CH_3), 26.7 (C5-CH_3), 26.4 (*i*-Pr-CH_3), 22.7 (*i*-Pr-CH_3).

Elemental analysis calculated for $C_{20}H_{33}NF_2$ (M_w = 325.48 g/mol): C 73.80, H 10.22, N 4.30 %; found: C 73.59, H 9.96, N 4.24 %.

A.3 Crystal Structure Data

Table A1: Selected crystal data for [(CAAC)AlMe$_2$F] (**1**), [(CAAC)AlMe$_2$F]·LiOTf·THF (**1a**) and [(CAAC)AlMeF$_2$] (**2**).

	[(CAAC)AlMe$_2$F] (**1**)	[(CAAC)AlMe$_2$F]· LiOTf·THF (**1a**)	[(CAAC)AlMeF$_2$] (**2**)
CCDC No.			
Chemical formula	$C_{20}H_{31}N \cdot AlFC_2H_6$	$2(C_{20}H_{31}N \cdot AlFC_2H_6 \cdot LiSO_3CF_3 \cdot OC_4H_8)$	$C_{20}H_{31}N \cdot AlF_2CH_3$
F_W (g/mol)	361.50	1179.23	365.47
T (K)	150	150	150
λ (Å)	1.54184	1.54184	1.54184
Crystal size (mm)	0.43 × 0.34 × 0.17	0.40 × 0.33 × 0.11	0.24 × 0.13 × 0.09
Crystal system	Monoclinic	Monoclinic	Orthorhombic
Space group	$I2/a$	$P2_1/c$	$P2_12_12_1$
a (Å)	17.4714(6)	30.1662(6)	9.3865(4)
b (Å)	9.6151(3)	9.8040(2)	9.7460(4)
c (Å)	27.2397(1)	21.7753(4)	22.8532(8)
α (°)	90	90	90
β (°)	102.895(4)	91.467(2)	90
γ (°)	90	90	90
V (Å^3)	4460.6(3)	6437.9(2)	2090.6(1)
Z	8	4	4
ρ_{calc} (g/cm^3)	1.077	1.217	1.161
μ (mm^{-1})	0.878	1.620	1.014
$F(000)$	1584	2512	792
Θ range (°)	2.8–71.6	3.5–72.5	5.1–69.4
Index ranges	$-21 \leq h \leq 18$ $-11 \leq k \leq 11$ $-23 \leq l \leq 32$	$-36 \leq h \leq 37$ $-7 \leq k \leq 11$ $-26 \leq l \leq 25$	$-11 \leq h \leq 11$ $-12 \leq k \leq 12$ $-23 \leq l \leq 28$
Reflections collected	11422	25735	9684
Independent reflections	4283	12391	4042
Reflections with ($I > 2\sigma(I)$)	3462	9671	3477
R_{int}	0.0176	0.0247	0.0377
Data / restraints / parameters	4283 / 0 / 236	12391 / 0 / 771	4042 / 0 / 265
S[a]	1.031	1.040	1.039
R_1[b], wR_2[c] ($I > 2\sigma(I)$)	0.0655, 0.1756	0.0475, 0.1258	0.0471, 0.1165
R_1[b], wR_2[c] (all data)	0.0788, 0.1877	0.0631, 0.1358	0.0581, 0.1250
$\Delta\rho_{min}$, $\Delta\rho_{max}$ (eÅ^{-3})	−0.375, 0.426	−0.282, 0.383	−0.199, 0.043

[a] $S = [\Sigma(w(F_o^2 - F_c^2)^2)/(N_o - N_p)]^{1/2}$.

[b] $R_1 = ||F_o| - |F_c||/\Sigma|F_o|$.

[c] $wR_2 = [\Sigma(w(F_o^2 - F_c^2)^2)/\Sigma(w(F_o^2)^2)]^{1/2}$.

Table A2: Selected crystal data for [CAACH][$MeAlF_3$] (**4**), [CAACH][AlF_4] (**5**) and CAAC(H)Me (**6**).

	[CAACH][$MeAlF_3$] (**4**)	[CAACH][AlF_4] (**5**)	CAAC(H)Me (**6**)
CCDC No.			
Chemical formula	$C_{20}H_{32}N \cdot AlF_3CH_3$	$C_{20}H_{32}N \cdot AlF_4$	$C_{22}H_{35}N$
F_W (g/mol)	385.48	389.44	301.50
T (K)	150	150	150
λ (Å)	1.54184	1.54184	1.54184
Crystal size (mm)	0.50 × 0.22 × 0.10	0.21 × 0.14 × 0.10	0.37 × 0.23 × 0.18
Crystal system	Monoclinic	Monoclinic	Monoclinic
Space group	$P2_1/c$	$P2_1/n$	$P2_1/n$
a (Å)	10.1941(2)	10.5971(2)	7.8538(2)
b (Å)	10.8048(2)	19.7206(4)	14.7104(4)
c (Å)	21.3743(5)	10.6073(2)	16.8606(5)
α (°)	90	90	90
β (°)	102.556(2)	91.757(2)	93.504(3)
γ (°)	90	90	90
V (Å^3)	2297.97(8)	2215.68(7)	1944.31(9)
Z	4	4	4
ρ_{calc} (g/cm^3)	1.114	1.167	1.030
μ (mm^{-1})	1.009	1.120	0.429
$F(000)$	832	832	672
Θ range (°)	4.1–71.5	4.2–72.1	2.6–72.3
Index ranges	$-12 \leq h \leq 11$ $-12 \leq k \leq 10$ $-25 \leq l \leq 26$	$-13 \leq h \leq 9$ $-23 \leq k \leq 22$ $-13 \leq l \leq 12$	$-6 \leq h \leq 9$ $-11 \leq k \leq 17$ $-20 \leq l \leq 17$
Reflections collected	20963	9932	7320
Independent reflections	4479	4232	3748
Reflections with ($I > 2\sigma(I)$)	3379	3746	3008
R_{int}	0.0409	0.0197	0.0177
Data / restraints / parameters	4479 / 0 / 272	4232 / 0 / 262	3748 / 0 / 260
S[a]	1.030	1.080	1.024
R_1[b], wR_2[c] ($I > 2\sigma(I)$)	0.0478, 0.1208	0.0446, 0.1153	0.0468, 0.1177
R_1[b], wR_2[c] (all data)	0.0664, 0.1340	0.0502, 0.1195	0.0600, 0.1281
$\Delta\rho_{min}$, $\Delta\rho_{max}$ (eÅ^{-3})	−0.496, 0.553	−0.261, 0.249	−0.164, 0.224

[a] $S = [\Sigma(w(F_o^2 - F_c^2)^2)/(N_o - N_p)]^{1/2}$.

[b] $R_1 = ||F_o| - |F_c||/\Sigma|F_o|$.

[c] $wR_2 = [\Sigma(w(F_o^2 - F_c^2)^2)/\Sigma(w(F_o^2)^2)]^{1/2}$.

Table A3: Selected crystal data for [IPrH][(*n*-Bu)$_3$AlF] (**8**), [IPrH][Me_2AlF_2]·C_6D_6 (**9a**) and [IPrH][Me_2AlF_2]·0.95DCM (**9b**).

	[IPrH][(*n*-Bu)$_3$AlF] (**8**)	[IPrH][Me_2AlF_2]·C_6D_6 (**9a**)	[IPrH][Me_2AlF_2]·0.95DCM (**9b**)
CCDC No.	2116487	2116482	2116483
Chemical formula	$C_{27}H_{37}N_2 \cdot AlFC_{12}H_{27}$	$C_{27}H_{37}N_2 \cdot AlF_2C_2H_6 \cdot C_6H_6$	$C_{27}H_{37}N_2 \cdot AlF_2C_2H_6 \cdot C_{0.95}H_{1.9}Cl_{1.9}$
F_W (g/mol)	606.90	562.74	565.31
T (K)	189	150	150
λ (Å)	1.54184	1.54184	1.54184
Crystal size (mm)	0.62 × 0.28 × 0.21	0.88 × 0.18 × 0.10	0.46 × 0.28 × 0.18
Crystal system	Monoclinic	Triclinic	Triclinic
Space group	$P2_1/c$	$P\bar{1}$	$P\bar{1}$
a (Å)	18.4658(4)	10.0113(4)	9.7859(5)
b (Å)	10.4398(2)	13.2295(5)	10.7423(5)
c (Å)	20.1175(5)	14.3963(6)	16.7898(9)
α (°)	90	113.971(4)	81.600(4)
β (°)	95.789(2)	97.920(3)	85.736(4)
γ (°)	90	94.020(3)	70.600(5)
V (Å^3)	3858.5(2)	1708.8(1)	1646.3(2)
Z	4	2	2
ρ_{calc} (g/cm^3)	1.045	1.094	1.140
μ (mm^{-1})	0.685	0.789	2.204
F(000)	1336	608	604
Θ range (°)	3.4–72.3	3.8–73.2	2.6–72.0
Index ranges	$-22 \le h \le 22$ $-12 \le k \le 12$ $-17 \le l \le 23$	$-11 \le h \le 10$ $-15 \le k \le 15$ $-17 \le l \le 17$	$-12 \le h \le 12$ $-13 \le k \le 13$ $-20 \le l \le 20$
Reflections collected	27379	18218	28031
Independent reflections	7400	6054	6352
Reflections with ($I > 2\sigma(I)$)	5692	5111	4773
R_{int}	0.0297	0.024	0.0412
Data / restraints / parameters	7400 / 0 / 477	6054 / 0 / 392	6352 / 0 / 381
S[a]	1.049	1.035	1.030
R_1[b], wR_2[c] ($I > 2\sigma(I)$)	0.0574, 0.1571	0.0422, 0.1121	0.0600, 0.1632
R_1[b], wR_2[c] (all data)	0.0743, 0.1759	0.0513, 0.1201	0.0790, 0.1819
$\Delta\rho_{min}$, $\Delta\rho_{max}$ (eÅ^{-3})	−0.238, 0.530	−0.329, 0.369	−0.387, 0.690

[a] $S = [\Sigma(w(F_o^2 - F_c^2)^2)/(N_o - N_p)]^{1/2}$.

[b] $R_1 = ||F_o| - |F_c||/\Sigma|F_o|$.

[c] $wR_2 = [\Sigma(w(F_o^2 - F_c^2)^2)/\Sigma(w(F_o^2)^2)]^{1/2}$.

Table A4: Selected crystal data for [IPrH][(n-Bu)$_2$AlF$_2$] (**10**), [IPrH][MeAlF$_3$] (**11**) and [IPrH][(n-Bu)AlF$_3$] (**12**).

	[IPrH][(n-Bu)$_2$AlF$_2$] (**10**)	[IPrH][MeAlF$_3$] (**11**)	[IPrH][(n-Bu)AlF$_3$] (**12**)
CCDC No.	2116488	2116484	2116489
Chemical formula	$C_{27}H_{37}N_2 \cdot AlF_2C_8H_{18}$	$C_{27}H_{37}N_2 \cdot AlF_3CH_3$	$C_{27}H_{37}N_2 \cdot AlF_3C_4H_7$
F_W (g/mol)	568.79	488.60	528.66
T (K)	150	150	240
λ (Å)	1.54184	1.54184	1.54184
Crystal size (mm)	0.49 × 0.42 × 0.20	0.38 × 0.23 × 0.12	0.47 × 0.31 × 0.16
Crystal system	Monoclinic	Orthorhombic	Monoclinic
Space group	$P2_1/n$	$Pnma$	$P2_1/m$
a (Å)	10.8908(2)	16.7958(3)	10.0812(6)
b (Å)	19.6662(2)	17.7836(4)	15.543(1)
c (Å)	17.7021(3)	9.5102(2)	10.9707(9)
α (°)	90	90	90
β (°)	107.246(2)	90	103.460(8)
γ (°)	90	90	90
V (Å^3)	3621.0(1)	2840.6(1)	1671.8(2)
Z	4	4	2
ρ_{calc} (g/cm^3)	1.043	1.142	1.050
μ (mm^{-1})	0.745	0.930	0.823
F(000)	1240	1048	568
Θ range (°)	3.4–72.3	3.6–72.2	4.1–72.2
Index ranges	$-13 \leq h \leq 13$ $-16 \leq k \leq 26$ $-21 \leq l \leq 20$	$-19 \leq h \leq 20$ $-21 \leq k \leq 21$ $-11 \leq l \leq 7$	$-10 \leq h \leq 12$ $-18 \leq k \leq 18$ $-11 \leq l \leq 13$
Reflections collected	25803	19912	7359
Independent reflections	7080	2891	3346
Reflections with ($I > 2\sigma(I)$)	6308	2406	2054
R_{int}	0.0183	0.0318	0.0257
Data / restraints / parameters	7080 / 0 / 441	2891 / 0 / 209	3346 / 0 / 188
S[a]	1.017	1.044	1.060
R_1[b], wR_2[c] ($I > 2\sigma(I)$)	0.0462, 0.1287	0.0465, 0.1234	0.0828, 0.2484
R_1[b], wR_2[c] (all data)	0.0512, 0.1344	0.0563, 0.1333	0.1153, 0.2905
$\Delta\rho_{min}$, $\Delta\rho_{max}$ (eÅ^{-3})	−0.341, 0.353	−0.297, 0.423	−0.332, 0.465

[a] $S = [\Sigma(w(F_o^2 - F_c^2)^2)/(N_o - N_p)]^{1/2}$.

[b] $R_1 = ||F_o| - |F_c||/\Sigma|F_o|$.

[c] $wR_2 = [\Sigma(w(F_o^2 - F_c^2)^2)/\Sigma(w(F_o^2)^2)]^{1/2}$.

Table A5: Selected crystal data for [IPr][AlF_4] (**13**), [IPr][AlF_4]·C_6D_6 (**13a**) and [IPrH][Ph_3AlF] (**14**).

	[IPr][AlF_4] (**13**)	[IPr][AlF_4]·C_6D_6 (**13a**)	[IPrH][Ph_3AlF] (**14**)
CCDC No.	2116485	2116486	2116491
Chemical formula	$C_{27}H_{37}N_2 \cdot AlF_4$	$C_{27}H_{37}N_2 \cdot AlF_4 \cdot C_6D_6$	$C_{27}H_{37}N_2 \cdot AlFC_{18}H_{15}$
F_W (g/mol)	492.56	570.67	666.86
T (K)	150	150	150
λ (Å)	1.54184	1.54184	1.54184
Crystal size (mm)	0.35 × 0.31 × 0.22	0.64 × 0.05 × 0.04	0.32 × 0.23 × 0.14
Crystal system	Orthorhombic	Monoclinic	Monoclinic
Space group	$Pccn$	$I2/a$	$P2_1/n$
a (Å)	11.1930(2)	17.202(2)	17.0471(4)
b (Å)	12.6491(2)	9.8532(6)	12.1991(2)
c (Å)	19.9010(3)	21.322(2)	20.7609(4)
α (°)	90	90	90
β (°)	90	112.44(1)	112.540(2)
γ (°)	90	90	90
V (Å^3)	2817.60(8)	3340.1(5)	3987.6(1)
Z	4	4	4
ρ_{calc} (g/cm^3)	1.161	1.135	1.111
μ (mm^{-1})	0.995	0.905	0.717
F(000)	1048	1216.0	1432
Θ range (°)	4.5–72.3	4.4–71.2	4.2–72.3
Index ranges	$-8 \le h \le 13$ $-15 \le k \le 15$ $-23 \le l \le 24$	$-21 \le h \le 19$ $-11 \le k \le 9$ $-24 \le l \le 26$	$-21 \le h \le 20$ $-10 \le k \le 14$ $-23 \le l \le 25$
Reflections collected	20987	7268	40111
Independent reflections	2783	3215	7826
Reflections with ($I > 2\sigma(I)$)	2498	2140	6596
R_{int}	0.0232	0.0447	0.0305
Data / restraints / parameters	2783 / 0 / 159	3215 / 4 / 207	7826 / 0 / 450
S[a]	1.063	1.020	1.033
R_1[b], wR_2[c] ($I > 2\sigma(I)$)	0.0431, 0.1255	0.0649, 0.1713	0.0454, 0.1255
R_1[b], wR_2[c] (all data)	0.0466, 0.1300	0.0982, 0.1949	0.0538, 0.1338
$\Delta\rho_{min}$, $\Delta\rho_{max}$ (eÅ^{-3})	−0.240, 0.237	−0.284, 0.292	−0.291, 0.377

[a] $S = [\Sigma(w(F_o^2 - F_c^2)^2)/(N_o - N_p)]^{1/2}$.

[b] $R_1 = ||F_o| - |F_c||/\Sigma|F_o|$.

[c] $wR_2 = [\Sigma(w(F_o^2 - F_c^2)^2)/\Sigma(w(F_o^2)^2)]^{1/2}$.

Table A6: Selected crystal data for [IPrH][PhAlF$_3$] (**16**), [(IPr)AlH$_2$OTf] (**17**) and CAACH$_2$ (**18**).

	[IPrH][PhAlF$_3$] (**16**)	[(IPr)AlH$_2$OTf] (**17**)	CAACH$_2$ (**18**)
CCDC No.	2116490	2036577	2036584
Chemical formula	$C_{27}H_{37}N_2 \cdot AlF_3C_6H_5$	$C_{28}H_{38}AlF_3N_2O_3S$	$C_{20}H_{33}N$
F_W (g/mol)	550.66	566.64	287.47
T (K)	150	150	150
λ (Å)	1.54184	1.54184	1.54184
Crystal size (mm)	0.34 × 0.27 × 0.18	0.67 × 0.25 × 0.17	0.39 × 0.31 × 0.18
Crystal system	Triclinic	Orthorhombic	Orthorhombic
Space group	$P\bar{1}$	$P2_12_12_1$	$Pbcn$
a (Å)	10.2609(3)	10.6930(2)	12.4174(2)
b (Å)	10.9869(3)	15.1726(3)	12.3716(2)
c (Å)	14.6809(4)	19.3385(4)	23.6662(3)
α (°)	90.406(3)	90.0000	90
β (°)	92.012(2)	90.0000	90
γ (°)	105.708(3)	90.0000	90
V (Å^3)	1592.03(8)	3137.5(1)	3635.68(9)
Z	2	4	8
ρ_{calc} (g/cm^3)	1.149	1.200	1.050
μ (mm^{-1})	0.886	1.592	0.438
$F(000)$	588	1200	1280
Θ range (°)	3.0–72.2	3.7–72.4	3.7–72.2
Index ranges	$-12 \leq h \leq 12$ $-13 \leq k \leq 13$ $-17 \leq l \leq 17$	$-12 \leq h \leq 9$ $-18 \leq k \leq 18$ $-23 \leq l \leq 22$	$-15 \leq h \leq 14$ $-14 \leq k \leq 15$ $-29 \leq l \leq 26$
Reflections collected	48472	14915	27068
Independent reflections	5687	6052	3589
Reflections with ($I > 2\sigma(I)$)	4327	5740	3168
R_{int}	0.0575	0.0269	0.0270
Data / restraints / parameters	5687 / 0 / 379	6052 / 0 / 359	3589 / 0 / 198
S[a]	1.037	1.054	1.053
R_1[b], wR_2[c] ($I > 2\sigma(I)$)	0.0694, 0.1980	0.0390, 0.1015	0.0429, 0.1188
R_1[b], wR_2[c] (all data)	0.0876, 0.2148	0.0415, 0.1044	0.0479, 0.1240
$\Delta\rho_{min}$, $\Delta\rho_{max}$ (eÅ^{-3})	−0.316, 0.595	−0.187, 0.328	−0.191, 0.289

[a] $S = [\Sigma(w(F_o^2 - F_c^2)^2)/(N_o - N_p)]^{1/2}$.

[b] $R_1 = ||F_o| - |F_c||/\Sigma|F_o|$.

[c] $wR_2 = [\Sigma(w(F_o^2 - F_c^2)^2)/\Sigma(w(F_o^2)^2)]^{1/2}$.

Table A7: Selected crystal data for [(IPr)$AlH_{3-x}Cl_x$] (x = 1, 2) (**19**), [(IPr)$AlCl_3$] (**20**) and [CAACH][$(HF)_3F$] (**21**).

	[(IPr)$AlH_{3-x}Cl_x$] (x = 1, 2) (**19**)	[(IPr)$AlCl_3$] (**20**)	[CAACH][$(HF)_3F$] (**21**)
CCDC No.	2036581	2036582	
Chemical formula	$C_{27}H_{37.42}AlCl_{1.58}N_2 \cdot C_{27}H_{37.30}AlCl_{1.70}N_2$	$C_{27}H_{36}AlCl_3N_2$	$C_{20}H_{32}N \cdot H_3F_4$
F_W (g/mol)	950.04	521.91	365.49
T (K)	150	150	150
λ (Å)	1.54184	1.54184	1.54184
Crystal size (mm)	0.55 × 0.29 × 0.22	0.63 × 0.18 × 0.15	0.61 × 0.42 × 0.27
Crystal system	Monoclinic	Monoclinic	Monoclinic
Space group	$P2_1/c$	$P2_1/c$	$P2_1/c$
a (Å)	16.5486(2)	16.5398(2)	10.4339(3)
b (Å)	18.9163(3)	19.4383(2)	14.8964(5)
c (Å)	19.4559(4)	19.3569(2)	14.3883(5)
α (°)	90	90	90
β (°)	111.847(2)	111.998(1)	100.056(3)
γ (°)	90	90	90
V (Å^3)	5653.0(2)	5770.3(1)	2202.0(1)
Z	4	8	4
ρ_{calc} (g/cm^3)	1.116	1.202	1.102
μ (mm^{-1})	2.157	3.291	0.724
F(000)	2033.8	2208	792
Θ range (°)	2.8–72.2	3.6–73.2	2.9–71.9
Index ranges	$-17 \leq h \leq 19$ $-22 \leq k \leq 23$ $-23 \leq l \leq 21$	$-19 \leq h \leq 19$ $-23 \leq k \leq 22$ $-22 \leq l \leq 23$	$-11 \leq h \leq 12$ $-18 \leq k \leq 17$ $-15 \leq l \leq 17$
Reflections collected	61408	31591	16124
Independent reflections	10949	10276	4295
Reflections with ($I > 2\sigma(I)$)	9168	9090	3212
R_{int}	0.0293	0.0244	0.0356
Data / restraints / parameters	10949 / 1 / 626	10276 / 0 / 611	4295 / 0 / 243
S[a]	1.026	1.031	1.044
R_1[b], wR_2[c] ($I > 2\sigma(I)$)	0.0484, 0.1354	0.0375, 0.0998	0.0502, 0.1323
R_1[b], wR_2[c] (all data)	0.0581, 0.1458	0.0429, 0.1043	0.0671, 0.1475
$\Delta\rho_{min}$, $\Delta\rho_{max}$ (eÅ^{-3})	−0.323, 0.708	−0.434, 0.628	−0.149, 0.313

[a] $S = [\Sigma(w(F_o^2 - F_c^2)^2)/(N_o - N_p)]^{1/2}$.

[b] $R_1 = ||F_o| - |F_c||/\Sigma|F_o|$.

[c] $wR_2 = [\Sigma(w(F_o^2 - F_c^2)^2)/\Sigma(w(F_o^2)^2)]^{1/2}$.

Table A8: Selected crystal data for [CAACH][$(HF)_2F$] (**22**), [CAACH][$(HF)_{3.5}F$] (**23**) and CAAC(H)F (**24**).

	[CAACH][$(HF)_2F$] (**22**)	[CAACH][$(HF)_{3.5}F$] (**23**)	CAAC(H)F (**24**)
CCDC No.			
Chemical formula	$C_{20}H_{32}N \cdot H_2F_3$	$2(C_{20}H_{32}N) \cdot H_3F_4 \cdot H_4F_5$	$C_{20}H_{32}NF$
F_W (g/mol)	345.48	750.98	305.46
T (K)	150	150	150
λ (Å)	1.54184	1.54184	1.54184
Crystal size (mm)	0.46 × 0.22 × 0.20	0.34 × 0.23 × 0.21	0.38 × 0.37 × 0.27
Crystal system	Monoclinic	Monoclinic	Monoclinic
Space group	$P2_1/n$	$P2_1/n$	$P2_1/c$
a (Å)	10.8109(4)	10.9151(2)	12.3387(2)
b (Å)	9.4778(3)	31.7156(5)	12.4225(2)
c (Å)	20.4419(7)	12.9575(2)	12.3727(2)
α (°)	90	90	90
β (°)	103.161(4)	90.408(1)	106.491(2)
γ (°)	90	90	90
V (Å^3)	2039.5(1)	4485.5(1)	1818.44(5)
Z	4	4	4
ρ_{calc} (g/cm^3)	1.125	1.112	1.116
μ (mm^{-1})	0.684	0.755	0.548
$F(000)$	752	1624	672
Θ range (°)	4.2–71.8	2.8–72.1	3.6–76.4
Index ranges	$-13 \leq h \leq 13$ $-9 \leq k \leq 11$ $-25 \leq l \leq 25$	$-13 \leq h \leq 12$ $-39 \leq k \leq 38$ $-14 \leq l \leq 15$	$-15 \leq h \leq 15$ $-15 \leq k \leq 15$ $-15 \leq l \leq 14$
Reflections collected	16584	38516	36245
Independent reflections	3973	8748	3793
Reflections with ($I > 2\sigma(I)$)	3211	7037	3560
R_{int}	0.0388	0.0340	0.0287
Data / restraints / parameters	3973 / 0 / 232	8748 / 0 / 496	3793 / 0 / 208
S[a]	1.056	1.067	1.165
R_1[b], wR_2[c] ($I > 2\sigma(I)$)	0.0498, 0.1293	0.0659, 0.1845	0.0633, 0.1904
R_1[b], wR_2[c] (all data)	0.0619, 0.1395	0.0783, 0.1995	0.0657, 0.1919
$\Delta\rho_{min}$, $\Delta\rho_{max}$ (eÅ^{-3})	−0.163, 0.469	−0.372, 0.435	−0.258, 0.434

[a] $S = [\Sigma(w(F_o^2 - F_c^2)^2)/(N_o - N_p)]^{1/2}$.

[b] $R_1 = ||F_o| - |F_c||/\Sigma|F_o|$.

[c] $wR_2 = [\Sigma(w(F_o^2 - F_c^2)^2)/\Sigma(w(F_o^2)^2)]^{1/2}$.

Table A9: Selected crystal data for [CAACH][(HF)F]·2CAAC(H)F (**25a**).

	[CAACH][(HF)F]· 2CAAC(H)F (**25a**)
CCDC No.	
Chemical formula	$C_{20}H_{32}N \cdot HF_2 \cdot 2(C_{20}H_{32}NF)$
F_W (g/mol)	936.40
T (K)	150
λ (Å)	1.54184
Crystal size (mm)	0.35 × 0.27 × 0.12
Crystal system	Triclinic
Space group	$P\bar{1}$
a (Å)	9.3894(3)
b (Å)	17.6755(7)
c (Å)	17.8951(7)
α (°)	96.869(3)
β (°)	96.961(3)
γ (°)	93.453(3)
V (Å^3)	2918.4(2)
Z	2
ρ_{calc} (g/cm^3)	1.066
μ (mm^{-1})	0.546
$F(000)$	1028
Θ range (°)	3.3–72.1
Index ranges	$-11 \leq h \leq 11$ $-21 \leq k \leq 21$ $-22 \leq l \leq 22$
Reflections collected	11761
Independent reflections	11761
Reflections with ($I > 2\sigma(I)$)	8607
R_{int}	/
Data / restraints / parameters	11761 / 0 / 703
S[a]	1.035
R_1[b], wR_2[c] ($I > 2\sigma(I)$)	0.0564, 0.1488
R_1[b], wR_2[c] (all data)	0.0760, 0.1597
$\Delta\rho_{min}$, $\Delta\rho_{max}$ (eÅ^{-3})	−0.192, 0.352

[a] $S = [\Sigma(w(F_o^2 - F_c^2)^2)/(N_o - N_p)]^{1/2}$.

[b] $R_1 = ||F_o| - |F_c||/\Sigma|F_o|$.

[c] $wR_2 = [\Sigma(w(F_o^2 - F_c^2)^2)/\Sigma(w(F_o^2)^2)]^{1/2}$.

A.4 Molecular Calculations

Table A10: Calculated electronic energies (E) for the [(CAAC)AlMe$_{3-n}$F$_n$] ($n = 0$–3) and [CAACH][Me$_n$AlF$_{4-n}$] ($n = 0$–1) series, and calculated energies of reactions ΔE. Calculations were performed at the PBE/def2TZVP level of theory. ΔE are given in a.u. and kJ/mol.

Compound	E / a.u.	Reaction	ΔE / a.u.	ΔE / kJ/mol
[(CAAC)AlMe$_3$]	−1196.70062242	–	–	–
Me$_3$SnF	−433.747153331	–	–	–
Me$_4$Sn	−373.77735715	–	–	–
[(CAAC)AlMe$_2$F] (**1**)	−1256.71081484	[(CAAC)AlMe$_3$] + Me$_3$SnF → [(CAAC)AlMe$_2$F] + Me$_4$Sn	−0.040396139	−106
[(CAAC)AlMeF$_2$] (**2**)	−1316.72109225	[(CAAC)AlMe$_3$] + 2Me$_3$SnF → [(CAAC)AlMeF$_2$] + 2Me$_4$Sn	−0.080877468	−212
[(CAAC)AlF$_3$] (**3**)	−1376.72769343	[(CAAC)AlMe$_3$] + 3Me$_3$SnF → [(CAAC)AlF$_3$] + 3Me$_4$Sn	−0.117682357	−309
[CAACH][MeAlF$_3$] (**4**)	−1417.17402594	–	–	–
[CAACH][AlF$_4$] (**5**)	−1477.17505806	–	–	–
CAAC(H)Me (**6**)	−875.244423975	–	–	–

Table A11: Calculated electronic energies (E) for the [IPrH][$R_{4-n}AlF_n$] ($n = 1-4$, R = Me, n-Bu, Ph) series and calculated energies of reactions ΔE. Calculations were performed at the PBE/def2TZVP level of theory. ΔE are given in a.u. and kJ/mol.

Compound	E / a.u.	Reaction	ΔE / a.u.	ΔE / kJ/mol
[IPrH][F]	−1259.411123	–	–	–
HF	−100.3913792	–	–	–
$AlMe_3$	−361.9220025	–	–	–
$AlBu_3$	−715.3628002	–	–	–
$AlPh_3$	−936.6345615	–	–	–
CH_4	−40.46417895	–	–	–
BuH	−158.2801283	–	–	–
PhH	−232.0300314	–	–	–
[IPrH][Me_3AlF] (**1**)	−1621.399002	[IPrH][F] + $AlMe_3$ → [IPrH][Me_3AlF]	−0.0658759	−173
[IPrH][Me_2AlF_2] (**2**)	−1681.422418	[IPrH][F] + HF + $AlMe_3$ → [IPrH][Me_2AlF_2] + CH_4	−0.1620916	−426
[IPrH][$MeAlF_3$] (**3**)	−1741.432198	[IPrH][F] + 2HF + $AlMe_3$ → [IPrH][$MeAlF_3$] + $2CH_4$	−0.2446717	−642
[IPrH][AlF_4] (**4**)	−1801.432451	[IPrH][F] + 3HF + $AlMe_3$ → [IPrH][AlF_4] + $3CH_4$	−0.3177247	−834
[(IPr)$AlMe_3$]	−1520.964628	2[IPrH][F] + 2$AlMe_3$ → [IPrH][Me_2AlF_2] + [(IPr)$AlMe_3$] + CH_4	−0.1849731	−486
2[IPrH][Me_3AlF] (**1**)	−3242.798003	2[IPrH][F] + 2$AlMe_3$ → 2[IPrH][Me_3AlF]	−0.13175173	−346
[IPrH][(n-Bu)$_3$AlF] (**5**)	−1974.850042	[IPrH][F] + Al(n-Bu)$_3$ → [IPrH][(n-Bu)$_3$AlF]	−0.0761185	−200
[IPrH][(n-Bu)$_2$$AlF_2$] (**6**)	−1917.046026	[IPrH][F] + HF + Al(n-Bu)$_3$ → [IPrH][(n-Bu)$_2$$AlF_2$] + n-BuH	−0.1608517	−422
[IPrH][(n-Bu)AlF_3] (**7**)	−1859.249810	[IPrH][F] + 2HF + Al(n-Bu)$_3$ → [IPrH][(n-Bu)AlF_3] + 2n-BuH	−0.2533845	−665
[IPrH][AlF_4] (**4**)	−1801.432451	[IPrH][F] + 3HF + Al(n-Bu)$_3$ → [IPrH][AlF_4] + 3n-BuH	−0.3247751	−853
[(IPr)$AlBu_3$]	−1874.409759	2[IPrH][F] + 2Al(n-Bu)$_3$ → [IPrH][(n-Bu)$_2$$AlF_2$] + [(IPr)Al($n$-Bu)$_3$] + n-BuH	−0.1880667	−494
2[IPrH][(n-Bu)$_3$ AlF] (**5**)	−3949.700084	2[IPrH][F] + 2Al(n-Bu)$_3$ → 2[IPrH][(n-Bu)$_3$AlF]	−0.15223709	−400
[IPrH][Ph_3AlF] (**8**)	−2196.136413	[IPrH][F] + $AlPh_3$ → [IPrH][Ph_3AlF]	−0.0907278	−238
[IPrH][Ph_2AlF_2] (**9**)	−2064.572196	[IPrH][F] + HF + $AlPh_3$ → [IPrH][Ph_2AlF_2] + C_6H_6	−0.1651634	−434
[IPrH][$PhAlF_3$] (**10**)	−1933.006025	[IPrH][F] + 2HF + $AlPh_3$ → [IPrH][$PhAlF_3$] + $2C_6H_6$	−0.2376442	−624
[IPrH][AlF_4] (**4**)	−1801.432451	[IPrH][F] + 3HF + $AlPh_3$ → [IPrH][AlF_4] + $3C_6H_6$	−0.3027230	−795
[(IPr)$AlPh_3$]	−2095.692660	2[IPrH][F] + 2$AlPh_3$ → [IPrH][Ph_2AlF_2] + [(IPr)$AlPh_3$] + C_6D_6	−0.2035181	−534
2[IPrH][Ph_3AlF] (**8**)	−4392,272825	2[IPrH][F] + 2$AlPh_3$ → 2[IPrH][Ph_3AlF]	−0,18145565	−476

References

[1] S. J. Lindsay, "Aluminum Fluoride - A Users Guide," in *Essential Readings in Light Metals*, vol. 2, G. Bearne, M. Dupuis, and G. Tarcy, Eds. Hoboken, NJ, USA: John Wiley & Sons, Inc., pp. 608–612, 2013. DOI: 10.1002/9781118647851.ch90

[2] T. Krahl and E. Kemnitz, "Aluminium fluoride – the strongest solid Lewis acid: structure and reactivity," *Catalysis Science & Technology*, vol. 7, no. 4, pp. 773–796, 2017. DOI: 10.1039/C6CY02369J

[3] J. Pinkas and H. W. Roesky, "Organoaluminum fluorides," *Journal of Fluorine Chemistry*, vol. 122, no. 2, pp. 125–150, 2003. DOI: 10.1016/S0022-1139(03)00093-9

[4] S. L. Benjamin, W. Levason, and G. Reid, "Medium and high oxidation state metal/non-metal fluoride and oxide–fluoride complexes with neutral donor ligands," *Chemical Society Reviews*, vol. 42, no. 4, pp. 1460–1499, 2013. DOI: 10.1039/C2CS35263J

[5] K. Adil, A. Cadiau, A. Hémon-Ribaud, M. Leblanc, and V. Maisonneuve, "Polyanion Condensation in Inorganic and Hybrid Fluoroaluminates," in *Functionalized Inorganic Fluorides*, A. Tressaud, Ed. Chichester, UK: John Wiley & Sons, Ltd, pp. 347–381, 2010. DOI: 10.1002/9780470660768.ch12

[6] J. K. Murthy *et al.*, "Aluminum Chloride as a Solid Is Not a Strong Lewis Acid," *The Journal of Physical Chemistry B*, vol. 110, no. 16, pp. 8314–8319, 2006. DOI: 10.1021/jp0601419

[7] H. W. Roesky, "Playing the Keyboard of Fluorine Chemistry," *Inorganic Chemistry*, vol. 38, no. 26, pp. 5934–5943, 1999. DOI: 10.1021/ic990624+

[8] W. Levason, F. M. Monzittu, and G. Reid, "Coordination chemistry and applications of medium/high oxidation state metal and non-metal fluoride and oxide-fluoride complexes with neutral donor ligands," *Coordination Chemistry Reviews*, vol. 391, pp. 90–130, 2019. DOI: 10.1016/j.ccr.2019.04.005

[9] R. Bhalla *et al.*, "Hydrothermal synthesis of Group 13 metal trifluoride complexes with neutral N-donor ligands," *Dalton Transactions*, vol. 44, no. 20, pp. 9569–9580, 2015. DOI: 10.1039/C5DT01120E

[10] R. Bhalla *et al.*, "Triaza-macrocyclic complexes of aluminium, gallium and indium halides: fast ^{18}F and ^{19}F incorporation *via* halide exchange under mild conditions in aqueous solution," *Chemical Science*, vol. 5, no. 1, pp. 381–391, 2014. DOI: 10.1039/C3SC52104D

[11] P. Tomar, T. Braun, and E. Kemnitz, "Preparation of NHC Stabilized Al(III)fluorides: Fluorination of [(SIMes)$AlMe_3$] with SF_4 or Me_3SnF," *European Journal of Inorganic Chemistry*, vol. 2019, no. 44, pp. 4735–4739, 2019. DOI: 10.1002/ejic.201900921

[12] W. Levason, S. K. Luthra, G. McRobbie, F. M. Monzittu, and G. Reid, "[$AlCl_3$($BnMe_2$-tacn)] – a new metal chelate scaffold for radiofluorination by Cl/F exchange," *Dalton Transactions*, vol. 46, no. 42, pp. 14519–14522, 2017. DOI: 10.1039/C7DT02122D

[13] A. Dimitrov, D. Heidemann, and E. Kemnitz, "F/Cl-Exchange on $AlCl_3$-Pyridine Adducts: Synthesis and Characterization of *trans*-Difluoro-tetrakis-pyridine-aluminum-chloride, $[AlF_2(Py)_4]^+Cl^-$," *Inorganic Chemistry*, vol. 45, no. 26, pp. 10807–10814, 2006. DOI: 10.1021/ic061493x

[14] R. Bhalla *et al.*, "Complexes of aluminium, gallium and indium trifluorides with neutral oxygen donor ligands: Synthesis, properties and reactions," *Polyhedron*, vol. 106, pp. 65–74, 2016. DOI: 10.1016/j.poly.2015.12.032

[15] C. Bour, J. Monot, S. Tang, R. Guillot, J. Farjon, and V. Gandon, "Structure, Stability, and Catalytic Activity of Fluorine-Bridged Complexes $IPr \cdot GaCl_2(\mu\text{-}F)EF_{n-1}$ (EF_n^- = SbF_6^-, PF_6^-, or BF_4^-)," *Organometallics*, vol. 33, no. 2, pp. 594–599, 2014. DOI: 10.1021/om4012054

[16] F. Xu, K. Matsumoto, and R. Hagiwara, "The first crystallographic example of a face-sharing fluoroaluminate anion $Al_2F_9^{3-}$," *Dalton Transactions*, vol. 42, no. 6, pp. 1965–1968, 2013. DOI: 10.1039/C2DT32624H

[17] P. Bukovec, "Untersuchungen von Fluorometallaten (III), 11. Mitt.: Synthese und Kristallstruktur von Guanidinium Hexalfuoroaluminat, -gallat und -indat," *Monatshefte für Chemie Chemical Monthly*, vol. 114, no. 3, pp. 277–279, 1983. DOI: 10.1007/BF00798950

[18] G. Veryasov, K. Matsumoto, and R. Hagiwara, "The Discrete AlF_5^{2-} Fluoroaluminate Anion in the Structure of [Tetraethylammonium]$_2$[AlF_5](H_2O)$_2$," *European Journal of Inorganic Chemistry*, vol. 2015, no. 32, pp. 5306–5310, 2015. DOI: 10.1002/ejic.201501036

[19] N. Herron, D. L. Thorn, R. L. Harlow, and F. Davidson, "Organic cation salts of the tetrafluoroaluminate anion. Yes, it does exist, and yes, it is tetrahedral," *Journal of the American Chemical Society*, vol. 115, no. 7, pp. 3028–3029, 1993. DOI: 10.1021/ja00060a082

[20] B. Gilbert and T. Materne, "Reinvestigation of Molten Fluoroaluminate Raman Spectra: The Question of the Existence of AlF_5^{2-} Ions," *Applied Spectroscopy*, vol. 44, no. 2, pp. 299–305, 1990. DOI: 10.1366/0003702904085525

[21] F. Bouyer, G. Picard, and J. Legendre, "Geometrical and spectroscopical characterizations of some complex entities of aluminum(III) with fluoride ions by LDF-based calculations," *International Journal of Quantum Chemistry*, vol. 52, no. 4, pp. 927–934, 1994. DOI: 10.1002/qua.560520418

[22] B. Gilbert, E. Robert, E. Tixhon, J. E. Olsen, and T. Østvold, "Structure and Thermodynamics of $NaF-AlF_3$ Melts with Addition of CaF_2 and MgF_2," *Inorganic Chemistry*, vol. 35, no. 14, pp. 4198–4210, 1996. DOI: 10.1021/ic951660l

[23] U. Groß, D. Müller, and E. Kemnitz, "Coordination Geometry of the Discrete Pentafluoroaluminate Dianion $[AlF_5]^{2-}$," *Angewandte Chemie International Edition*, vol. 42, no. 23, pp. 2626–2629, 2003. DOI: 10.1002/anie.200350885

[24] S. Dilsky and W. A. Schenk, "Diastereomeric Halfsandwich Rhenium Complexes Containing Hemilabile Phosphane Ligands," *European Journal of Inorganic Chemistry*, vol. 2004, no. 24, pp. 4859–4870, 2004. DOI: 10.1002/ejic.200400552

[25] L. A. Bischoff *et al.*, "Pentafluoroethylaluminates: A Combined Synthetic, Spectroscopic, and Structural Study," *Chemistry – A European Journal*, vol. 26, no. 60, pp. 13615–13620, 2020. DOI: 10.1002/chem.202000667

[26] E. Gruden, M. Tramšek, and G. Tavčar, "Discrete Organofluoroaluminate Anions: Synthetic, Structural, and Spectroscopic Aspects," *Organometallics*, vol. 41, no. 1, pp. 41–51, 2022. DOI: 10.1021/acs.organomet.1c00601

[27] S. Singh and H. W. Roesky, "Fluorine functionalized compounds of group 13 elements," *Journal of Fluorine Chemistry*, vol. 128, no. 4, pp. 369–377, 2007. DOI: 10.1016/j.jfluchem.2006.07.018

[28] M. Witt and H. W. Roesky, "Organoaluminum Chemistry at the Forefront of Research and Development," *Current Science*, vol. 78, no. 4, pp. 410–430, 2000.

[29] L. L. Böhm, "The Ethylene Polymerization with Ziegler Catalysts: Fifty Years after the Discovery," *Angewandte Chemie International Edition*, vol. 42, no. 41, pp. 5010–5030, 2003. DOI: 10.1002/anie.200300580

[30] C. E. Housecroft and A. G. Sharpe, *Inorganic Chemistry, 4th Edition*. Pearson, 2012.

[31] P. Yu, M. L. Montero, C. E. Barnes, H. W. Roesky, and I. Usón, "Formation of $[Cp_2Ti(\mu_2\text{-}F)_2AlEt_2]_2$ and $[Cp(C_5H_4)Ti(\mu_2\text{-}H)AlEt_2]_2$ in the Reaction of Cp_2TiF_2 with $AlEt_3$. Structure of $[Cp_2Ti(\mu_2\text{-}F)_2AlEt_2]_2$," *Inorganic Chemistry*, vol. 37, no. 10, pp. 2595–2597, 1998. DOI: 10.1021/ic971160n

[32] H. Wessel, C. Rennekamp, H. W. Roesky, M. L. Montero, P. Müller, and I. Usón, "Reactions of Group 4 Metal Cyclopentadienyl Trifluorides with a Trimeric Iminoalane," *Organometallics*, vol. 17, no. 10, pp. 1919–1921, 1998. DOI: 10.1021/om9800748

[33] A. Herzog, H. W. Roesky, F. Jäger, A. Steiner, and M. Noltemeyer, "Reactions of $(\eta^5\text{-}C_5Me_5)ZrF_3$, $(\eta^5\text{-}C_5Me_4Et)ZrF_3$, $(\eta^5\text{-}C_5Me_5)_2ZrF_2$, $(\eta^5\text{-}C_5Me_5)HfF_3$, and $(\eta^5\text{-}C_5Me_5)TaF_4$ with $AlMe_3$. Structure of the First Hafnium−Aluminum−Carbon Cluster," *Organometallics*, vol. 15, no. 3, pp. 909–917, 1996. DOI: 10.1021/om950590n

[34] B. Neumüller, "Organometal fluorides of aluminium, gallium, indium and thallium," *Coordination Chemistry Reviews*, vol. 158, pp. 69–101, 1997. DOI: 10.1016/S0010-8545(97)90053-9

[35] C. Schnitter *et al.*, "Synthesis and Characterization of Tris(trimethylsilyl)methyl Halide Derivatives of Aluminum: Potential Precursors for Low-Valent Aluminum Compounds. Crystal Structures of $[\{(Me_3Si)_3CAlF_2\}_3]$, $[(Me_3Si)_3CAlX_2\cdot THF]$ (X = Cl, Br, I), and $[\{(THF)_2K(Me_3Si)_3CAlF_2(\mu\text{-}F)F_2AlC(SiMe_3)_3\}_2]$," *Organometallics*, vol. 17, no. 11, pp. 2249–2257, 1998. DOI: 10.1021/om980036o

[36] H. Wessel, H.-S. Park, P. Müller, H. W. Roesky, and I. Usón, "[{MeAl(μ_2-F)}$_2$N(2,6-*i*Pr$_2$C$_6$H$_3$)]$_4$ – A Molecular Al-F-N Cage Compound," *Angewandte Chemie International Edition*, vol. 38, no. 6, pp. 813–815, 1999. DOI: 10.1002/(SICI)1521-3773(19990315)38:6<813::AID-ANIE813>3.0.CO;2-6

[37] A. Herzog *et al.*, "Trimethyltin Fluoride: A New Fluorinating Reagent for the Preparation of Organometallic Fluorides," *Organometallics*, vol. 13, no. 4, pp. 1251–1256, 1994. DOI: 10.1021/om00016a030

[38] S. D. Waezsada *et al.*, "Aminodimethylalanes (R^{1}R^{2}NAlMe$_2$) as Useful Synthetic Precursors of Aminoalane Difluorides Using Trimethyltin Fluoride: Crystal Structures of (2,6-*i*-Pr$_2$C$_6$H$_3$)N(SiMe$_3$)AlMe$_2$ and (2,6-*i*-Pr$_2$C$_6$H$_3$)N(SiMe$_3$)AlF$_2$," *Organometallics*, vol. 16, no. 6, pp. 1260–1264, 1997. DOI: 10.1021/om960810c

[39] C. Rennekamp *et al.*, "Reaction of dimethylaluminumfluoride with primary amines RNH$_2$ (R = *t*-Bu, 2,6-*i*-Pr$_2$C$_6$H$_3$)," *Journal of Fluorine Chemistry*, vol. 102, no. 1–2, pp. 17–20, 2000. DOI: 10.1016/S0022-1139(99)00236-5

[40] K. M. Waggoner, H. Hope, and P. P. Power, "Synthesis and Structure of [MeAlN(2,6-*i*Pr$_2$C$_6$H$_3$)]$_3$: An Aluminum-Nitrogen Analogue of Borazine," *Angewandte Chemie International Edition*, vol. 27, no. 12, pp. 1699–1700, 1988. DOI: 10.1002/anie.198816991

[41] Y. Liu, J. Li, X. Ma, Z. Yang, and H. W. Roesky, "The chemistry of aluminum(I) with β-diketiminate ligands and pentamethylcyclopentadienyl-substituents: Synthesis, reactivity and applications," *Coordination Chemistry Reviews*, vol. 374, pp. 387–415, 2018. DOI: 10.1016/j.ccr.2018.07.004

[42] S. Singh *et al.*, "Syntheses, Characterization, and X-ray Crystal Structures of β-Diketiminate Group 13 Hydrides, Chlorides, and Fluorides," *Inorganic Chemistry*, vol. 45, no. 4, pp. 1853–1860, 2006. DOI: 10.1021/ic0517826

[43] M. R. Crimmin, M. J. Butler, and A. J. P. White, "Oxidative addition of carbon–fluorine and carbon–oxygen bonds to Al(I)," *Chemical Communications*, vol. 51, no. 88, pp. 15994–15996, 2015. DOI: 10.1039/C5CC07140B

[44] T. Chu, Y. Boyko, I. Korobkov, and G. I. Nikonov, "Transition Metal-like Oxidative Addition of C–F and C–O Bonds to an Aluminum(I) Center," *Organometallics*, vol. 34, no. 22, pp. 5363–5365, 2015. DOI: 10.1021/acs.organomet.5b00793

[45] C. Bakewell, A. J. P. White, and M. R. Crimmin, "Reactions of Fluoroalkenes with an Aluminium(I) Complex," *Angewandte Chemie International Edition*, vol. 57, no. 22, pp. 6638–6642, 2018. DOI: 10.1002/anie.201802321

[46] W. Chen, T. N. Hooper, J. Ng, A. J. P. White, and M. R. Crimmin, "Palladium-Catalyzed Carbon–Fluorine and Carbon–Hydrogen Bond Alumination of Fluoroarenes and Heteroarenes," *Angewandte Chemie International Edition*, vol. 56, no. 41, pp. 12687–12691, 2017. DOI: 10.1002/anie.201706378

[47] S. Yow, S. J. Gates, A. J. P. White, and M. R. Crimmin, "Zirconocene Dichloride Catalyzed Hydrodefluorination of C_{sp^2}–F bonds," *Angewandte Chemie International Edition*, vol. 51, no. 50, pp. 12559–12563, 2012. DOI: 10.1002/anie.201207036

[48] O. Ekkert, S. D. A. Strudley, A. Rozenfeld, A. J. P. White, and M. R. Crimmin, "Rhodium Catalyzed, Carbon–Hydrogen Bond Directed Hydrodefluorination of Fluoroarenes," *Organometallics*, vol. 33, no. 24, pp. 7027–7030, 2014. DOI: 10.1021/om501113j

[49] W. Uhl, C. Appelt, and M. Lange, "Surprising Stability of an Al/P-Based Frustrated Lewis-Pair Towards Protolysis: HX Adducts (X = F, Cl) with Intramolecular H···X Hydrogen Bonds," *Zeitschrift für anorganische und allgemeine Chemie*, vol. 641, no. 2, pp. 311–315, 2015. DOI: 10.1002/zaac.201400527

[50] W. Uhl, M. Lange, A. Hepp, and M. Layh, "Supramolecular Chemistry Based on Frustrated Lewis Pairs - Reactions of an Al/P FLP with Potassium Formate and Cesium Fluoride," *Zeitschrift für anorganische und allgemeine Chemie*, vol. 644, no. 22, pp. 1469–1479, 2018. DOI: 10.1002/zaac.201800256

[51] W. Uhl, C. Appelt, A. Wollschläger, A. Hepp, and E.-U. Würthwein, "An Al/P-Based Frustrated Lewis Pair as an Efficient Ambiphilic Ligand: Coordination of Boron Trihalides, Rearrangement, and Formation of HBX_2 Complexes (X = Br, I)," *Inorganic Chemistry*, vol. 53, no. 17, pp. 8991–8999, 2014. DOI: 10.1021/ic5009126

[52] G. Allegra and G. Perego, "The crystal structure of the $KF.2Al(C_2H_5)_3$ complex," *Acta Crystallographica*, vol. 16, no. 3, pp. 185–190, 1963. DOI: 10.1107/S0365110X63000463

[53] M.-C. Chen, J. A. S. Roberts, and T. J. Marks, "New Mononuclear and Polynuclear Perfluoroarylmetalate Cocatalysts for Stereospecific Olefin Polymerization," *Organometallics*, vol. 23, no. 5, pp. 932–935, 2004. DOI: 10.1021/om0341698

[54] M.-C. Chen *et al.*, "Diversity in Weakly Coordinating Anions. Mono- and Polynuclear Halo(perfluoroaryl)metalates as Cocatalysts for Stereospecific Olefin Polymerization: Synthesis, Structure, and Reactivity," *Organometallics*, vol. 25, no. 11, pp. 2833–2850, 2006. DOI: 10.1021/om0508334

[55] J. L. Atwood and W. R. Newberry, "The interaction of aromatic hydrocarbons with organometallic compounds of the main group elements, III. The crystal structure of $K[Al_2(CH_3)_6F]\cdot C_6D_6$," *Journal of Organometallic Chemistry*, vol. 66, no. 1, pp. 15–21, 1974. DOI: 10.1016/S0022-328X(00)93882-8

[56] C. B. Caputo, L. J. Hounjet, R. Dobrovetsky, and D. W. Stephan, "Lewis Acidity of Organofluorophosphonium Salts: Hydrodefluorination by a Saturated Acceptor," *Science (1979)*, vol. 341, no. 6152, pp. 1374–1377, 2013. DOI: 10.1126/science.1241764

[57] H. Hatop, M. Schiefer, H. W. Roesky, R. Herbst-Irmer, and T. Labahn, "Synthesis and Structures of $[((Me_3Si)_3CAlF_2)_2(\mu\text{-}O)Li_2(THF)_4]$ and $[\{Li(Me_3Si)_3CAlF_3(THF)\}_3LiF(THF)]$," *Organometallics*, vol. 20, no. 12, pp. 2643–2646, 2001. DOI: 10.1021/om0100941

[58] H. Hatop, H. W. Roesky, T. Labahn, A. Fischer, H.-G. Schmidt, and M. Noltemeyer, "Syntheses and Structures of New Organoaluminum Fluorides," *Organometallics*, vol. 19, no. 5, pp. 937–940, 2000. DOI: 10.1021/om990731b

[59] H. Hatop, M. Schiefer, H. W. Roesky, H.-G. Schmidt, and M. Noltemeyer, "Synthesis and crystal structure of a novel aluminum–fluorine–potassium compound $[((Me_3Si)_3C)_2Al_2(\mu\text{-}F)F_4K]_x$ with a supramolecular chain," *Journal of Fluorine Chemistry*, vol. 112, no. 2, pp. 219–223, 2001. DOI: 10.1016/S0022-1139(01)00525-5

[60] M. Ferbinteanu, H. W. Roesky, F. Cimpoesu, M. Atanasov, S. Köpke, and R. Herbst-Irmer, "New Synthetic and Structural Aspects in the Chemistry of Alkylaluminum Fluorides. The Mutual Influence of Hard and Soft Ligands and the Hybridization as Rigorous Structural Criterion," *Inorganic Chemistry*, vol. 40, no. 19, pp. 4947–4955, 2001. DOI: 10.1021/ic010131g

[61] H. W. Roesky *et al.*, "A Facile Route to Group 13 Difluorodiorganometalates: $[n\text{Bu}_4\text{N}][R_2MF_2]$ (M=Al, Ga, In)," *Angewandte Chemie International Edition*, vol. 39, no. 1, pp. 171–173, 2000. DOI: 10.1002/(SICI)1521-3773(20000103)39:1<171::AID-ANIE171>3.0.CO;2-N

[62] K. Ziegler, R. Köster, H. Lehmkuhl, and K. Reinert, "Metallorganische Verbindungen, XXX Neue Komplexverbindungen der Aluminiumalkyle," *Justus Liebigs Annalen der Chemie*, vol. 629, no. 1, pp. 33–49, 1960. DOI: 10.1002/jlac.19606290106

[63] K. Mach, "Infrared spectra of aluminium trialkyl complexes with alkali metal fluorides. II. 1:1 − Complex of trimethyl- and triethylaluminium with NaF and KF," *Collection of Czechoslovak Chemical Communications*, vol. 32, no. 10, pp. 3777–3779, 1967. DOI: 10.1135/cccc19673777

[64] B. Werner and B. Neumüller, "Cäsium-Fluor-Vierringe als Strukturmotiv in Cäsium-Triorganofluorometallaten der Gruppe 13," *Chemische Berichte*, vol. 129, no. 3, pp. 355–359, 1996. DOI: 10.1002/cber.19961290317

[65] Y.-X. (Eugene) Chen, M. v. Metz, L. Li, C. L. Stern, and T. J. Marks, "Sterically Encumbered (Perfluoroaryl) Borane and Aluminate Cocatalysts for Tuning Cation−Anion Ion Pair Structure and Reactivity in Metallocene Polymerization Processes. A Synthetic, Structural, and Polymerization Study," *Journal of the American Chemical Society*, vol. 120, no. 25, pp. 6287–6305, 1998. DOI: 10.1021/ja973769t

[66] Y.-X. Chen, C. L. Stern, and T. J. Marks, "Very Large Counteranion Modulation of Cationic Metallocene Polymerization Activity and Stereoregulation by a Sterically Congested (Perfluoroaryl)fluoroaluminate," *Journal of the American Chemical Society*, vol. 119, no. 10, pp. 2582–2583, 1997. DOI: 10.1021/ja963834j

[67] M. N. Hopkinson, C. Richter, M. Schedler, and F. Glorius, "An overview of N-heterocyclic carbenes," *Nature*, vol. 510, no. 7506, pp. 485–496, 2014. DOI: 10.1038/nature13384

[68] A. Igau, H. Grutzmacher, A. Baceiredo, and G. Bertrand, "Analogous α,α'-Bis-Carbenoid Triply Bonded Species: Synthesis of a Stable λ^3-Phosphinocarbene-λ^5-Phosphaacetylene," *Journal of the American Chemical Society*, vol. 110, no. 19, pp. 6463–6466, 1988. DOI: 10.1021/ja00227a028

[69] A. J. Arduengo, R. L. Harlow, and M. Kline, "A stable crystalline carbene," *Journal of the American Chemical Society*, vol. 113, no. 1, pp. 361–363, 1991. DOI: 10.1021/ja00001a054

[70] A. Doddi, M. Peters, and M. Tamm, "N-Heterocyclic Carbene Adducts of Main Group Elements and Their Use as Ligands in Transition Metal Chemistry," *Chemical Reviews*, vol. 119, no. 12, pp. 6994–7112, 2019. DOI: 10.1021/acs.chemrev.8b00791

[71] V. Nesterov *et al.*, "NHCs in Main Group Chemistry," *Chemical Reviews*, vol. 118, no. 19, pp. 9678–9842, 2018. DOI: 10.1021/acs.chemrev.8b00079

[72] M. C. Jahnke and F. Ekkehardt Hahn, "CHAPTER 1: Introduction to N-Heterocyclic Carbenes: Synthesis and Stereoelectronic Parameters," in *N-Heterocyclic Carbenes: From Laboratory Curiosities to Efficient Synthetic Tools*, 2nd ed., vol. 2017-January, no. 27, Royal Society of Chemistry, pp. 1–45, 2016. DOI: 10.1039/9781782626817-00001

[73] W. A. Herrmann and C. Köcher, "N-Heterocyclic Carbenes," *Angewandte Chemie International Edition*, vol. 36, no. 20, pp. 2162–2187, 1997. DOI: 10.1002/anie.199721621

[74] D. J. Nelson and S. P. Nolan, "Quantifying and understanding the electronic properties of *N*-heterocyclic carbenes," *Chemical Society Reviews*, vol. 42, no. 16, pp. 6723–6753, 2013. DOI: 10.1039/c3cs60146c

[75] H. V. Huynh, "Electronic Properties of N-Heterocyclic Carbenes and Their Experimental Determination," *Chemical Reviews*, vol. 118, no. 19, pp. 9457–9492, 2018. DOI: 10.1021/acs.chemrev.8b00067

[76] M. Soleilhavoup and G. Bertrand, "Cyclic (Alkyl)(Amino)Carbenes (CAACs): Stable Carbenes on the Rise," *Accounts of Chemical Research*, vol. 48, no. 2, pp. 256–266, 2015. DOI: 10.1021/ar5003494

[77] H. Schneider, A. Hock, R. Bertermann, and U. Radius, "Reactivity of NHC Alane Adducts towards N-Heterocyclic Carbenes and Cyclic (Alkyl)(amino)carbenes: Ring Expansion, Ring Opening, and Al−H Bond Activation," *Chemistry - A European Journal*, vol. 23, no. 50, pp. 12387–12398, 2017. DOI: 10.1002/chem.201702166

[78] H. Schneider, D. Schmidt, and U. Radius, "The reductive P–P coupling of primary and secondary phosphines mediated by N-heterocyclic carbenes," *Chemical Communications*, vol. 51, no. 50, pp. 10138–10141, 2015. DOI: 10.1039/C5CC02517F

[79] O. Hollóczki, P. Terleczky, D. Szieberth, G. Mourgas, D. Gudat, and L. Nyulászi, "Hydrolysis of Imidazole-2-ylidenes," *Journal of the American Chemical Society*, vol. 133, no. 4, pp. 780–789, 2011. DOI: 10.1021/ja103578y

[80] G. D. Frey, J. D. Masuda, B. Donnadieu, and G. Bertrand, "Activation of Si−H, B−H, and P−H Bonds at a Single Nonmetal Center," *Angewandte Chemie International Edition*, vol. 49, no. 49, pp. 9444–9447, 2010. DOI: 10.1002/anie.201005698

[81] M. Melaimi, R. Jazzar, M. Soleilhavoup, and G. Bertrand, "Cyclic (Alkyl)(amino)carbenes (CAACs): Recent Developments," *Angewandte Chemie International Edition*, vol. 56, no. 34, pp. 10046–10068, 2017. DOI: 10.1002/anie.201702148

[82] V. Lavallo, Y. Canac, B. Donnadieu, W. W. Schoeller, and G. Bertrand, "CO Fixation to Stable Acyclic and Cyclic Alkyl Amino Carbenes: Stable Amino Ketenes with a Small HOMO–LUMO Gap," *Angewandte Chemie International Edition*, vol. 45, no. 21, pp. 3488–3491, 2006. DOI: 10.1002/anie.200600987

[83] G. D. Frey, V. Lavallo, B. Donnadieu, W. W. Schoeller, and G. Bertrand, "Facile Splitting of Hydrogen and Ammonia by Nucleophilic Activation at a Single Carbon Center," *Science (1979)*, vol. 316, no. 5823, pp. 439–441, 2007. DOI: 10.1126/science.1141474

[84] Z. R. Turner, "Chemically Non-Innocent Cyclic (Alkyl)(Amino)Carbenes: Ligand Rearrangement, C−H and C−F Bond Activation," *Chemistry - A European Journal*, vol. 22, no. 32, pp. 11461–11468, 2016. DOI: 10.1002/chem.201602264

[85] O. Stecher and E. Wiberg, "Über einen nichtflüchtigen, polymeren Aluminiumwasserstoff $(AlH_3)_x$ und einige flüchtige Verbindungen des monomeren AlH_3," *Berichte der deutschen chemischen Gesellschaft (A and B Series)*, vol. 75, no. 12, pp. 2003–2012, 1942. DOI: 10.1002/cber.19420751280

[86] A. J. Downs and C. R. Pulham, "The hydrides of aluminium, gallium, indium, and thallium: a re-evaluation," *Chemical Society Reviews*, vol. 23, no. 3, p. 175, 1994. DOI: 10.1039/cs9942300175

[87] S. Aldridge and A. J. Downs, "Hydrides of the Main-Group Metals: New Variations on an Old Theme," *Chemical Reviews*, vol. 101, no. 11, pp. 3305–3366, 2001. DOI: 10.1021/cr960151d

[88] W. Jiang, H. Wang, and M. Zhu, "AlH_3 as a hydrogen storage material: recent advances, prospects and challenges," *Rare Metals*, vol. 40, no. 12, pp. 3337–3356, 2021. DOI: 10.1007/s12598-021-01769-2

[89] D. A. Doinikov *et al.*, "Thermal Decomposition of Aluminium Hydride Complexes with Trimethylamine and N-Heterocyclic Carbene," *Russian Journal of General Chemistry*, vol. 91, no. 10, pp. 1969–1976, 2021. DOI: 10.1134/S1070363221100078

[90] A. J. Downs, *Chemistry of aluminium, gallium, indium, and thallium*, Springer Netherlands, 1993.

[91] H. Liu *et al.*, "Aluminum hydride for solid-state hydrogen storage: Structure, synthesis, thermodynamics, kinetics, and regeneration," *Journal of Energy Chemistry*, vol. 52, pp. 428–440, 2021. DOI: 10.1016/j.jechem.2020.02.008

[92] A. E. Finholt, A. C. Bond, and H. I. Schlesinger, "Lithium Aluminum Hydride, Aluminum Hydride and Lithium Gallium Hydride, and Some of their Applications in Organic and Inorganic Chemistry," *Journal of the American Chemical Society*, vol. 69, no. 5, pp. 1199–1203, 1947. DOI: 10.1021/ja01197a061

[93] H. Elsen, C. Färber, G. Ballmann, and S. Harder, "$LiAlH_4$: From Stoichiometric Reduction to Imine Hydrogenation Catalysis," *Angewandte Chemie International Edition*, vol. 57, no. 24, pp. 7156–7160, 2018. DOI: 10.1002/anie.201803804

[94] J. A. Jegier and W. L. Gladfelter, "The use of aluminum and gallium hydrides in materials science," *Coordination Chemistry Reviews*, vol. 206–207, pp. 631–650, 2000. DOI: 10.1016/S0010-8545(00)00300-3

[95] W. Li, X. Ma, M. G. Walawalkar, Z. Yang, and H. W. Roesky, "Soluble aluminum hydrides function as catalysts in deprotonation, insertion, and activation reactions," *Coordination Chemistry Review*, vol. 350, pp. 14–29, 2017. DOI: 10.1016/j.ccr.2017.03.017

[96] G. I. Nikonov, "New Tricks for an Old Dog: Aluminum Compounds as Catalysts in Reduction Chemistry," *ACS Catalysis*, vol. 7, no. 10, pp. 7257–7266, 2017. DOI: 10.1021/acscatal.7b02460

[97] E. M. Marlett and W. S. Park, "Dimethylethylamine alane and *N*-methylpyrrolidine alane. A convenient synthesis of alane, a useful selective reducing agent in organic synthesis," *The Journal of Organic Chemistry*, vol. 55, no. 9, pp. 2968–2969, 1990. DOI: 10.1021/jo00296a078

[98] J. M. Davidson and T. Wartik, "A NEW TYPE OF ALUMINUM HYDRIDE ADDUCT," *Journal of the American Chemical Society*, vol. 82, no. 20, pp. 5506–5506, 1960. DOI: 10.1021/ja01505a051

[99] E. C. Ashby, "The Direct Synthesis of Amine Alanes," *Journal of the American Chemical Society*, vol. 86, no. 9, pp. 1882–1883, 1964. DOI: 10.1021/ja01063a066

[100] I. B. Gorrell, P. B. Hitchcock, and J. D. Smith, "Preparation and crystal structures of aluminium hydride adducts with tetrahydrofuran $[AlH_3 \cdot OC_4H_8]_2$ and $AlH_3 \cdot 2OC_4H_8$," *Journal of the Chemical Society, Chemical Communications*, no. 2, pp. 189–190, 1993. DOI: 10.1039/C39930000189

[101] C. Jones, G. A. Koutsantonis, and C. L. Raston, "Lewis base adducts of alane and gallane," *Polyhedron*, vol. 12, no. 15, pp. 1829–1848, 1993. DOI: 10.1016/S0277-5387(00)81421-7

[102] C. L. Raston, "Recent developments in the chemistry of alane (AlH_3) and gallane (GaH_3)," *Journal of Organometallic Chemistry*, vol. 475, no. 1–2, pp. 15–24, 1994. DOI: 10.1016/0022-328X(94)84003-2

[103] T. D. Humphries, K. T. Munroe, A. Decken, and G. S. McGrady, "Lewis base complexes of AlH_3: structural determination of monomeric and polymeric adducts by X-ray crystallography and DFT calculations," *Dalton Transactions*, vol. 42, no. 19, p. 6953, 2013. DOI: 10.1039/c3dt00046j

[104] N. N. Greenwood and B. S. Thomas, "Investigation of the properties and thermochemistry of some complexes of aluminium hydride with tertiary amines and diamines," *Journal of the Chemical Society A: Inorganic, Physical, Theoretical*, vol. 1, no. 0, p. 814, 1971. DOI: 10.1039/j19710000814

[105] J. L. Atwood, F. R. Bennett, F. M. Elms, C. Jones, C. L. Raston, and K. D. Robinson, "Tertiary amine stabilized dialane," *Journal of the American Chemical Society*, vol. 113, no. 21, pp. 8183–8185, 1991. DOI: 10.1021/ja00021a063

[106] C. Y. Tang, R. A. Coxall, A. J. Downs, T. M. Greene, and S. Parsons, "Oligomeric structures of the crystalline dimethylamine adducts $Me_2(H)N \cdot MH_3$ (M = Al or Ga) and the dimethylamido derivative $[Me_2NGaH_2]_3$," *Journal of the Chemical Society, Dalton Transactions*, no. 14, pp. 2141–2147, 2001. DOI: 10.1039/b102667b

[107] J. L. Atwood, F. R. Bennett, C. Jones, G. A. Koutsantonis, C. L. Raston, and K. D. Robinson, "Polydentate tertiary amine aluminium hydride adducts: monomeric *versus* polymeric species," *Journal of the Chemical Society, Chemical Communications*, no. 7, p. 541, 1992. DOI: 10.1039/c39920000541

[108] F. R. Bennett, F. M. Elms, M. G. Gardiner, G. A. Koutsantonis, C. L. Raston, and N. K. Roberts, "Stable tertiary phosphine adducts of alane," *Organometallics*, vol. 11, no. 4, pp. 1457–1459, 1992. DOI: 10.1021/om00040a013

[109] J. L. Atwood *et al.*, "Mixed-donor and monomeric N-donor adducts of alane," *Inorganic Chemistry*, vol. 32, no. 16, pp. 3482–3487, 1993. DOI: 10.1021/ic00068a017

[110] F. M. Elms, M. G. Gardiner, G. A. Koutsantonis, C. L. Raston, J. L. Atwood, and K. D. Robinson, "Tertiary phosphine adducts of alane and gallane," *Journal of Organometallic Chemistry*, vol. 449, no. 1–2, pp. 45–52, 1993. DOI: 10.1016/0022-328X(93)80105-K

[111] D. Franz, E. Irran, and S. Inoue, "Synthesis, characterization and reactivity of an imidazolin-2-iminato aluminium dihydride," *Dalton Transactions*, vol. 43, no. 11, pp. 4451–4461, 2014. DOI: 10.1039/C3DT52637B

[112] C.-Y. Lin *et al.*, "Insertion, Reduction, and Carbon–Carbon Coupling Induced by Monomeric Aluminum Hydride Compounds Bearing Substituted Pyrrolyl Ligands," *Chemistry - A European Journal*, vol. 12, no. 11, pp. 3067–3073, 2006. DOI: 10.1002/chem.200500989

[113] Y.-L. Lien *et al.*, "A New Type of Asymmetric Tridentate Pyrrolyl-Linked Pincer Ligand and Its Aluminum Dihydride Complexes," *Inorganic Chemistry*, vol. 49, no. 1, pp. 136–143, 2010. DOI: 10.1021/ic9016189

[114] A. R. Leverett, V. Diachenko, M. L. Cole, and A. I. McKay, "Kinetic stabilization of low-oxidation state and terminal hydrido main group metal complexes by a sterically demanding *N,N′*-bis(2,6-terphenyl)triazenide," *Dalton Transactions*, vol. 48, no. 35, pp. 13197–13204, 2019. DOI: 10.1039/C9DT02562F

[115] B. Prashanth and S. Singh, "A new bulky iminophosphonamide as an *N,N′*-chelating ligand: synthesis and structural characterization of heteroleptic group 13 element complexes," *Dalton Transactions*, vol. 43, no. 44, pp. 16880–16888, 2014. DOI: 10.1039/C4DT02637C

[116] U. Braun *et al.*, "Reactions of Group 13 and 14 Hydrides and Group 1, 2, 13 and 14 Organyl Compounds with (*tert*-Butylimino)(2,2,6,6-tetramethylpiperidino)borane," *European Journal of Inorganic Chemistry*, vol. 2004, no. 18, pp. 3612–3628, 2004. DOI: 10.1002/ejic.200300820

[117] B. Lyhs, D. Bläser, C. Wölper, and S. Schulz, "Syntheses and X-ray Crystal Structures of Organoantimony Diazides," *Chemistry – A European Journal*, vol. 17, no. 17, pp. 4914–4920, 2011. DOI: 10.1002/CHEM.201002730

[118] M. Dehmel, A. Köhler, H. Görls, and R. Kretschmer, "Synthesis, characterization, and reactivity of group 13 hydride complexes based on amido-amine ligands," *Dalton Transactions*, vol. 50, no. 24, pp. 8434–8445, 2021. DOI: 10.1039/D1DT01454D

[119] A. Rösch, C. M. Herzog, S. H. F. Schreiner, H. Görls, and R. Kretschmer, "Ditopic bis(*N*,*N*′,*N*′-substituted 1,2-ethanediamine) ligands: synthesis and coordination chemistry," *Dalton Transactions*, vol. 49, no. 39, pp. 13818–13828, 2020. DOI: 10.1039/D0DT03124K

[120] R. L. Falconer, G. S. Nichol, and M. J. Cowley, "Flexible Coordination of N,P-Donor Ligands in Aluminum Dimethyl and Dihydride Complexes," *Inorganic Chemistry*, vol. 58, no. 17, pp. 11439–11448, 2019. DOI: 10.1021/acs.inorgchem.9b01061

[121] Y. Wang, X. Ma, Y. Ding, J. Wang, and Z. Yang, "The study on the solubility of main group organometallics in selected solvents and the thermodynamic model of solubility correlation under inert atmosphere," *Journal of Molecular Liquids*, vol. 293, p. 111541, 2019. DOI: 10.1016/j.molliq.2019.111541

[122] C. Cui, H. W. Roesky, H. Hao, H.-G. Schmidt, and M. Noltemeyer, "The First Structurally Characterized Metal–SeH Compounds: [LAl(SeH)$_2$] and [L(HSe)AlSeAl(SeH)L]," *Angewandte Chemie International Edition*, vol. 39, no. 10, pp. 1815–1817, 2000. DOI: 10.1002/(SICI)1521-3773(20000515)39:10<1815::AID-ANIE1815>3.0.CO;2-W

[123] W. Uhl and B. Jana, "A Persistent Alkylaluminum Peroxide: Surprising Stability of a Molecule with Strong Reducing and Oxidizing Functions in Close Proximity," *Chemistry - A European Journal*, vol. 14, no. 10, pp. 3067–3071, 2008. DOI: 10.1002/chem.200701916

[124] N. Kuhn, S. Fuchs, and M. Steimann, "Vinamidin-stabilisierte Alane," *Zeitschrift für anorganische und allgemeine Chemie*, vol. 626, no. 6, pp. 1387–1392, 2000. DOI: 10.1002/(SICI)1521-3749(200006)626:6<1387::AID-ZAAC1387>3.0.CO;2-U

[125] W. Liu *et al.*, "Organic aluminum hydrides catalyze nitrile hydroboration," *Green Chemistry*, vol. 21, no. 14, pp. 3812–3815, 2019. DOI: 10.1039/C9GC01659G

[126] C. Sindlinger, S. Lawrence, D. Cordes, A. Slawin, and A. Stasch, "Methanediide Formation *via* Hydrogen Elimination in Magnesium versus Aluminium Hydride Complexes of a Sterically Demanding Bis(iminophosphoranyl)methanediide," *Inorganics*, vol. 5, no. 2, p. 29, 2017. DOI: 10.3390/inorganics5020029

[127] C.-C. Chia *et al.*, "Aluminum-Hydride-Catalyzed Hydroboration of Carbon Dioxide," *Inorganic Chemistry*, vol. 60, no. 7, pp. 4569–4577, 2021. DOI: 10.1021/acs.inorgchem.0c03507

[128] J. D. Masuda, D. M. Walsh, P. Wei, and D. W. Stephan, "Neutral and Cationic Group 13 Alkyl and Hydride Complexes of a Phosphinimine−Amide Ligand," *Organometallics*, vol. 23, no. 8, pp. 1819–1824, 2004. DOI: 10.1021/om0306776

[129] M. Dehmel, V. Vass, L. Prock, H. Görls, and R. Kretschmer, "Synthesis and Coordination Chemistry of 3,4-Ethylene-Bridged 1,1,2,5-Tetrasubstituted Biguanides," *Inorganic Chemistry*, vol. 59, no. 5, pp. 2733–2746, 2020. DOI: 10.1021/acs.inorgchem.9b03093

[130] N. Sarkar, S. Bera, and S. Nembenna, "Aluminum-Catalyzed Selective Hydroboration of Nitriles and Alkynes: A Multifunctional Catalyst," *The Journal of Organic Chemistry*, vol. 85, no. 7, pp. 4999–5009, 2020. DOI: 10.1021/acs.joc.0c00234

[131] T. Peddarao, N. Sarkar, and S. Nembenna, "Mono- and Bimetallic Aluminum Alkyl, Alkoxide, Halide and Hydride Complexes of a Bulky Conjugated Bis-Guanidinate(CBG) Ligand and Aluminum Alkyls as Precatalysts for Carbonyl Hydroboration," *Inorganic Chemistry*, vol. 59, no. 7, pp. 4693–4702, 2020. DOI: 10.1021/acs.inorgchem.9b03778

[132] S. Courtenay, D. Walsh, S. Hawkeswood, P. Wei, A. K. Das, and D. W. Stephan, "Boron and Aluminum Complexes of Sterically Demanding Phosphinimines and Phosphinimides," *Inorganic Chemistry*, vol. 46, no. 9, pp. 3623–3631, 2007. DOI: 10.1021/ic0700351

[133] M. C. Hodgson, M. A. Khan, and R. J. Wehmschulte, "Synthesis and Reactivity of Amidoaluminum Hydride Compounds as Potential Precursors to AlN," *Journal of Cluster Science*, vol. 13, no. 4, pp. 503–520, 2002. DOI: 10.1023/A:1021123628042

[134] M. Veith, A. Walgenbach, V. Huch, and H. Kohlmann, "Aluminum/Nitrogen Cycles and an Open Cage with Al—H and N—H Functions," *Zeitschrift für anorganische und allgemeine Chemie*, vol. 643, no. 20, pp. 1233–1239, 2017. DOI: 10.1002/zaac.201700278

[135] C. Y. Tang, A. J. Downs, T. M. Greene, and S. Parsons, "Dimeric piperidino-alane and -gallane: metal hydrides with a cyclic M(μ-N)$_2$M core (M = Al or Ga)," *Dalton Transactions*, vol. 3, no. 4, pp. 540–543, 2003. DOI: 10.1039/b209669m

[136] A. J. Arduengo, H. V. R. Dias, J. C. Calabrese, and F. Davidson, "A stable carbene-alane adduct," *Journal of the American Chemical Society*, vol. 114, no. 24, pp. 9724–9725, 1992. DOI: 10.1021/ja00050a098

[137] M. D. Francis, D. E. Hibbs, M. B. Hursthouse, C. Jones, and N. A. Smithies, "Carbene complexes of Group 13 trihydrides: synthesis and characterisation of [MH_3{$CN(Pr^i)C_2Me_2N(Pr^i)$}], M = Al, Ga or In," *Journal of the Chemical Society, Dalton Transactions*, no. 19, pp. 3249–3254, 1998. DOI: 10.1039/a805766d

[138] R. J. Baker, A. J. Davies, C. Jones, and M. Kloth, "Structural and spectroscopic studies of carbene and N-donor ligand complexes of Group 13 hydrides and halides," *Journal of Organometallic Chemistry*, vol. 656, no. 1–2, pp. 203–210, 2002. DOI: 10.1016/S0022-328X(02)01592-9

[139] L. L. Cao, E. Daley, T. C. Johnstone, and D. W. Stephan, "Cationic aluminum hydride complexes: reactions of carbene–alane adducts with trityl-borate," *Chemical Communications*, vol. 52, no. 30, pp. 5305–5307, 2016. DOI: 10.1039/C6CC01585A

[140] A. M. Chernysheva, M. Weinhart, M. Scheer, and A. Y. Timoshkin, "Normal to abnormal I^{t}Bu·AlH_3 isomerization in solution and in the solid state," *Dalton Transactions*, vol. 49, no. 15, pp. 4665–4668, 2020. DOI: 10.1039/C9DT04698D

[141] R. J. Baker, M. L. Cole, C. Jones, and M. F. Mahon, "Bidentate N-heterocyclic carbene complexes of Group 13 trihydrides and trihalides," *Journal of the Chemical Society, Dalton Transactions*, no. 9, pp. 1992–1996, 2002. DOI: 10.1039/b200500j

[142] M. Trose *et al.*, "*Normal* and *abnormal* NHC coordination in cationic hydride iodide complexes of aluminium," *Dalton Transactions*, vol. 47, no. 30, pp. 10281–10287, 2018. DOI: 10.1039/C8DT01798K

[143] S. J. Bonyhady, D. Collis, G. Frenking, N. Holzmann, C. Jones, and A. Stasch, "Synthesis of a stable adduct of dialane(4) (Al_2H_4) via hydrogenation of a magnesium(I) dimer," *Nature Chemistry*, vol. 2, no. 10, pp. 865–869, 2010. DOI: 10.1038/nchem.762

[144] L. L. Cao and D. W. Stephan, "Reversible 1,1-hydroaluminations and C–H activation in reactions of a cyclic (alkyl)(amino) carbene with alane," *Chemical Communications*, vol. 54, no. 60, pp. 8407–8410, 2018. DOI: 10.1039/C8CC05013A

[145] M. Zhong *et al.*, "$HAlCl_2$ and H_2AlCl as Precursors for the Preparation of Compounds with Four- and Five-Coordinate Aluminum," *Inorganic Chemistry*, vol. 58, no. 16, pp. 10625–10628, 2019. DOI: 10.1021/acs.inorgchem.9b02001

[146] D. Auerhammer, M. Arrowsmith, H. Braunschweig, R. D. Dewhurst, J. O. C. Jiménez-Halla, and T. Kupfer, "Nucleophilic addition and substitution at coordinatively saturated boron by facile 1,2-hydrogen shuttling onto a carbene donor," *Chemical Science*, vol. 8, no. 10, pp. 7066–7071, 2017. DOI: 10.1039/C7SC03193A

[147] S. K. Mellerup *et al.*, "Lewis-Base Stabilization of the Parent Al(I) Hydride under Ambient Conditions," *Journal of the American Chemical Society*, vol. 141, no. 42, pp. 16954–16960, 2019. DOI: 10.1021/jacs.9b09128

[148] S. G. Alexander and M. L. Cole, "Lewis Base Adducts of Heavier Group 13 Halohydrides – *Not Just Aspiring Trihydrides!*," *European Journal of Inorganic Chemistry*, vol. 2008, no. 29, pp. 4493–4506, 2008. DOI: 10.1002/ejic.200800686

[149] Z. Yang *et al.*, "An Aluminum Hydride That Functions like a Transition-Metal Catalyst," *Angewandte Chemie International Edition*, vol. 54, no. 35, pp. 10225–10229, 2015. DOI: 10.1002/anie.201503304

[150] S. G. Alexander, M. L. Cole, and C. M. Forsyth, "Tertiary Amine and *N*-Heterocyclic Carbene Coordinated Haloalanes — Synthesis, Structure, and Application," *Chemistry - A European Journal*, vol. 15, no. 36, pp. 9201–9214, 2009. DOI: 10.1002/chem.200900365

[151] A. Hock, H. Schneider, M. J. Krahfuß, and U. Radius, "Hydride Amide and Hydride Phenolate Complexes of NHC Coordinated Aluminum," *Zeitschrift für anorganische und allgemeine Chemie*, vol. 644, no. 21, pp. 1243–1251, 2018. DOI: 10.1002/zaac.201800251

[152] D. L. Schmidt and E. E. Flagg, "Bis(tetrahydrofuran)-haloalanes," *Inorganic Chemistry*, vol. 6, no. 6, pp. 1262–1265, 1967. DOI: 10.1021/ic50052a049

[153] E. Gruden and G. Tavčar, "Synthesis and characterization of partially substituted NHC supported alane adducts using triflate or chloride salts," *Polyhedron*, vol. 196, p. 115009, 2021. DOI: 10.1016/j.poly.2020.115009

[154] S. G. Alexander, M. L. Cole, M. Hilder, J. C. Morris, and J. B. Patrick, "The synthesis of a dichloroalane complex and its reaction with an α-diimine," *Dalton Transactions*, vol. 2, no. 45, p. 6361, 2008. DOI: 10.1039/b814839b

[155] S. G. Alexander, M. L. Cole, S. K. Furfari, and M. Kloth, "Hydride–bromide exchange at an NHC—a new route to brominated alanes and gallanes," *Dalton Transactions*, no. 16, p. 2909, 2009. DOI: 10.1039/b821367d

[156] A. Hock, L. Werner, M. Riethmann, and U. Radius, "Bis-NHC Aluminium and Gallium Dihydride Cations $[(NHC)_2EH_2]^+$ (E = Al, Ga)," *European Journal of Inorganic Chemistry*, vol. 2020, no. 42, pp. 4015–4023, 2020. DOI: 10.1002/ejic.202000720

[157] B. Ališ, M. Tramšek, A. Kokalj, and G. Tavčar, "Discrete GeF_5^- Anion Structurally Characterized with a Readily Synthesized Imidazolium Based Naked Fluoride Reagent," *Inorganic Chemistry*, vol. 56, no. 16, pp. 10070–10077, 2017. DOI: 10.1021/acs.inorgchem.7b01606

[158] T. E. Mallouk, B. Desbat, and N. Bartlett, "Structural studies of salts of cis and trans μ-fluoro-bridged polymers of GeF_5^- and of the GeF_5^- monomer," *Inorganic Chemistry*, vol. 23, no. 20, pp. 3160–3166, 1984. DOI: 10.1021/ic00188a027

[159] S. Caron, "Where Does the Fluorine Come From? A Review on the Challenges Associated with the Synthesis of Organofluorine Compounds," *Organic Process Research & Development*, vol. 24, no. 4, pp. 470–480, 2020. DOI: 10.1021/acs.oprd.0c00030

[160] D. E. Yerien, S. Bonesi, and A. Postigo, "Fluorination methods in drug discovery," *Organic & Biomolecular Chemistry*, vol. 14, no. 36, pp. 8398–8427, 2016. DOI: 10.1039/C6OB00764C

[161] D. O'Hagan, "Understanding organofluorine chemistry. An introduction to the C–F bond," *Chemical Society Reviews*, vol. 37, no. 2, pp. 308–319, 2008. DOI: 10.1039/B711844A

[162] P. A. Champagne, J. Desroches, J.-D. Hamel, M. Vandamme, and J.-F. Paquin, "Monofluorination of Organic Compounds: 10 Years of Innovation," *Chemical Reviews*, vol. 115, no. 17, pp. 9073–9174, 2015. DOI: 10.1021/cr500706a

[163] K. O. Christe and H. D. B. Jenkins, "Quantitative Measure for the "Nakedness" of Fluoride Ion Sources," *Journal of the American Chemical Society*, vol. 125, no. 31, pp. 9457–9461, 2003. DOI: 10.1021/ja035675r

[164] J.-W. Lee *et al.*, "Hydrogen-bond promoted nucleophilic fluorination: concept, mechanism and applications in positron emission tomography," *Chemical Society Reviews*, vol. 45, no. 17, pp. 4638–4650, 2016. DOI: 10.1039/C6CS00286B

[165] C. L. Liotta and H. P. Harris, "Chemistry of "naked" anions. I. Reactions of the 18-crown-6 complex of potassium fluoride with organic substrates in aprotic organic solvents," *Journal of the American Chemical Society*, vol. 96, no. 7, pp. 2250–2252, 1974. DOI: 10.1021/ja00814a044

[166] K. O. Christe, W. W. Wilson, R. D. Wilson, R. Bau, and J. A. Feng, "Syntheses, properties, and structures of anhydrous tetramethylammonium fluoride and its 1:1 adduct with *trans*-3-amino-2-butenenitrile," *Journal of the American Chemical Society*, vol. 112, no. 21, pp. 7619–7625, 1990. DOI: 10.1021/ja00177a025

[167] S. Liang, G. B. Hammond, and B. Xu, "Hydrogen Bonding: Regulator for Nucleophilic Fluorination," *Chemistry – A European Journal*, vol. 23, no. 71, pp. 17850–17861, 2017. DOI: 10.1002/chem.201702664

[168] D. W. Kim *et al.*, "A New Class of S_N2 Reactions Catalyzed by Protic Solvents: Facile Fluorination for Isotopic Labeling of Diagnostic Molecules," *Journal of the American Chemical Society*, vol. 128, no. 50, pp. 16394–16397, 2006. DOI: 10.1021/ja0646895

[169] D. W. Kim, H.-J. Jeong, S. T. Lim, and M.-H. Sohn, "Tetrabutylammonium Tetra(*tert*-Butyl Alcohol)-Coordinated Fluoride as a Facile Fluoride Source," *Angewandte Chemie International Edition*, vol. 120, no. 44, pp. 8532–8534, 2008. DOI: 10.1002/ANGE.200803150

[170] L. Pfeifer *et al.*, "Hydrogen-Bonded Homoleptic Fluoride–Diarylurea Complexes: Structure, Reactivity, and Coordinating Power," *Journal of the American Chemical Society,* vol. 138, no. 40, pp. 13314–13325, 2016. DOI: 10.1021/jacs.6b07501

[171] B. Baasner and E. Klauke, "Reactions in anhydrous hydrogen fluoride," *Journal of Fluorine Chemistry*, vol. 19, no. 3–6, pp. 553–564, 1982. DOI: 10.1016/S0022-1139(00)83153-X

[172] G. Haufe, "$Et_3N \cdot 3HF$ Complex Fluorination for Preparing Alkyl Fluorides," in *Fluorination*, Singapore: Springer Singapore, pp. 137–181, 2020. DOI: 10.1007/978-981-10-3896-9_26

[173] G. A. Olah *et al.*, "Ionic Liquid and Solid HF Equivalent Amine-Poly(Hydrogen Fluoride) Complexes Effecting Efficient Environmentally Friendly Isobutane−Isobutylene Alkylation," *Journal of the American Chemical Society*, vol. 127, no. 16, pp. 5964–5969, 2005. DOI: 10.1021/ja0424878

[174] G. A. Olah, J. T. Welch, Y. D. Vankar, M. Nojima, I. Kerekes, and J. A. Olah, "Synthetic methods and reactions. 63. Pyridinium poly(hydrogen fluoride) (30% pyridine-70% hydrogen fluoride): a convenient reagent for organic fluorination reactions," *The Journal of Organic Chemistry*, vol. 44, no. 22, pp. 3872–3881, 1979. DOI: 10.1021/jo01336a027

[175] K. M. Dawood, "Electrolytic fluorination of organic compounds," *Tetrahedron*, vol. 60, no. 7, pp. 1435–1451, 2004. DOI: 10.1016/j.tet.2003.11.017

[176] O. E. Okoromoba, J. Han, G. B. Hammond, and B. Xu, "Designer HF-Based Fluorination Reagent: Highly Regioselective Synthesis of Fluoroalkenes and *gem*-Difluoromethylene Compounds from Alkynes," *Journal of the American Chemical Society*, vol. 136, no. 41, pp. 14381–14384, 2014. DOI: 10.1021/ja508369z

[177] O. E. Okoromoba, G. B. Hammond, and B. Xu, "Preparation of Fluorinated Tetrahydropyrans and Piperidines using a New Nucleophilic Fluorination Reagent DMPU/HF," *Organic Letters*, vol. 17, no. 16, pp. 3975–3977, 2015. DOI: 10.1021/acs.orglett.5b01919

[178] S. Liang, F. J. Barrios, O. E. Okoromoba, Z. Hetman, B. Xu, and G. B. Hammond, "Bromofluorination of unsaturated compounds using DMPU/HF as a fluorinating reagent," *Journal of Fluorine Chemistry*, vol. 203, pp. 136–139, 2017. DOI: 10.1016/j.jfluchem.2017.07.016

[179] O. E. Okoromoba *et al.*, "Achieving regio- and stereo-control in the fluorination of aziridines under acidic conditions," *Chemical Communications*, vol. 52, no. 91, pp. 13353–13356, 2016. DOI: 10.1039/C6CC07855A

[180] Z. Lu, X. Zeng, G. B. Hammond, and B. Xu, "Widely Applicable Hydrofluorination of Alkenes via Bifunctional Activation of Hydrogen Fluoride," *Journal of the American Chemical Society*, vol. 139, no. 50, pp. 18202–18205, 2017. DOI: 10.1021/jacs.7b12704

[181] R. Hagiwara, T. Hirashige, T. Tsuda, and Y. Ito, "Acidic 1-ethyl-3-methylimidazolium fluoride: a new room temperature ionic liquid," *Journal of Fluorine Chemistry*, vol. 99, no. 1, pp. 1–3, 1999. DOI: 10.1016/S0022-1139(99)00111-6

[182] R. Hagiwara and Y. Ito, "Room temperature ionic liquids of alkylimidazolium cations and fluoroanions," *Journal of Fluorine Chemistry*, vol. 105, no. 2, pp. 221–227, 2000. DOI: 10.1016/S0022-1139(99)00267-5

[183] R. Hagiwara, T. Hirashige, T. Tsuda, and Y. Ito, "A Highly Conductive Room Temperature Molten Fluoride: EMIF·2.3HF," *Journal of The Electrochemical Society*, vol. 149, no. 1, pp. D1–D6, 2002. DOI: 10.1149/1.1421606

[184] R. Hagiwara *et al.*, "Physicochemical Properties of 1,3-Dialkylimidazolium Fluorohydrogenate Room-Temperature Molten Salts," *Journal of The Electrochemical Society*, vol. 150, no. 12, pp. D195–D199, 2003. DOI: 10.1149/1.1621414

[185] K. Matsumoto *et al.*, "Syntheses, structures and properties of 1-ethyl-3-methylimidazolium salts of fluorocomplex anions," *Dalton Transactions*, vol. 4, no. 1, pp. 144–149, 2004. DOI: 10.1039/B310162B

[186] K. Matsumoto, T. Tsuda, R. Hagiwara, Y. Ito, and O. Tamada, "Structural characteristics of 1-ethyl-3-methylimidazolium bifluoride: HF-deficient form of a highly conductive room temperature molten salt," *Solid State Sciences*, vol. 4, no. 1, pp. 23–26, 2002. DOI: 10.1016/S1293-2558(01)01223-7

[187] R. P. Singh and J. L. Martin, "Fluorination of α-bromomethyl aryl ketones with fluorohydrogenate-based ionic liquids," *Journal of Fluorine Chemistry*, vol. 181, pp. 7–10, 2016. DOI: 10.1016/j.jfluchem.2015.10.014

[188] H. Yoshino, K. Matsumoto, R. Hagiwara, Y. Ito, K. Oshima, and S. Matsubara, "Fluorination with ionic liquid $EMIMF(HF)_{2.3}$ as mild HF source," *Journal of Fluorine Chemistry*, vol. 127, no. 1, pp. 29–35, 2006. DOI: 10.1016/j.jfluchem.2005.09.016

[189] S. Bouvet, B. Pégot, J. Marrot, and E. Magnier, "Solvent free nucleophilic introduction of fluorine with [bmim][F]," *Tetrahedron Letters*, vol. 55, no. 4, pp. 826–829, 2014. DOI: 10.1016/j.tetlet.2013.12.020

[190] S. Bouvet, B. Pégot, P. Diter, J. Marrot, and E. Magnier, "Oxidative desulfurization–fluorination reaction promoted by [bdmim][F] for the synthesis of difluorinated methyl ethers," *Tetrahedron Letters*, vol. 56, no. 13, pp. 1682–1686, 2015. DOI: 10.1016/j.tetlet.2015.02.034

[191] Z. Chen *et al.*, "Partially Naked Fluoride in Solvate Ionic Liquids," *The Journal of Physical Chemistry Letters*, vol. 9, no. 22, pp. 6662–6667, 2018. DOI: 10.1021/acs.jpclett.8b03117

[192] T. Enomoto, Y. Nakamori, K. Matsumoto, and R. Hagiwara, "Ion−Ion Interactions and Conduction Mechanism of Highly Conductive Fluorohydrogenate Ionic Liquids," *The Journal of Physical Chemistry C*, vol. 115, no. 10, pp. 4324–4332, 2011. DOI: 10.1021/jp1101219

[193] N. W. Goldberg, X. Shen, J. Li, and T. Ritter, "AlkylFluor: Deoxyfluorination of Alcohols," *Organic Letters*, vol. 18, no. 23, pp. 6102–6104, 2016. DOI: 10.1021/acs.orglett.6b03086

[194] T. Fujimoto and T. Ritter, "PhenoFluorMix: Practical Chemoselective Deoxyfluorination of Phenols," *Organic Letters*, vol. 17, no. 3, pp. 544–547, 2015. DOI: 10.1021/ol5035518

[195] P. Tang, W. Wang, and T. Ritter, "Deoxyfluorination of Phenols," *Journal of the American Chemical Society*, vol. 133, no. 30, pp. 11482–11484, 2011. DOI: 10.1021/ja2048072

[196] H. Hayashi, H. Sonoda, K. Fukumura, and T. Nagata, "2,2-Difluoro-1,3-dimethylimidazolidine (DFI). A new fluorinating agent," *Chemical Communications*, vol. 2, no. 15, pp. 1618–1619, 2002. DOI: 10.1039/b204471d

[197] T. Böttcher *et al.*, "Carbene complexes of phosphorus(v) fluorides substituted with perfluoroalkyl-groups synthesized by oxidative addition. Cleavage of the complexes reveals a new synthetic protocol for ionic liquids," *Dalton Transactions*, vol. 43, no. 7, pp. 2979–2987, 2014. DOI: 10.1039/C3DT53043D

[198] A. Doddi, D. Bockfeld, T. Bannenberg, P. G. Jones, and M. Tamm, "N-Heterocyclic Carbene-Phosphinidyne Transition Metal Complexes," *Angewandte Chemie International Edition*, vol. 53, no. 49, pp. 13568–13572, 2014. DOI: 10.1002/anie.201408354

[199] B. Ališ and G. Tavčar, "Reaction of N-heterocyclic carbene (NHC) with different HF sources and ratios – A free fluoride reagent based on imidazolium fluoride," *Journal of Fluorine Chemistry*, vol. 192, pp. 141–146, 2016. DOI: 10.1016/j.jfluchem.2016.11.004

[200] Ž. Zupanek, M. Tramšek, A. Kokalj, and G. Tavčar, "The peculiar case of conformations in coordination compounds of group V pentahalides with N-heterocyclic carbene and synthesis of their imidazolium salts," *Journal of Fluorine Chemistry*, vol. 227, p. 109373, 2019. DOI: 10.1016/j.jfluchem.2019.109373

[201] Ž. Zupanek, M. Tramšek, A. Kokalj, and G. Tavčar, "Reactivity of VOF_3 with N-Heterocyclic Carbene and Imidazolium Fluoride: Analysis of Ligand–VOF_3 Bonding with Evidence of a Minute π Back-Donation of Fluoride," *Inorganic Chemistry*, vol. 57, no. 21, pp. 13866–13879, 2018. DOI: 10.1021/acs.inorgchem.8b02377

[202] B. Ališ, J. Petrovčič, J. Jelen, G. Tavčar, and J. Iskra, "Renewable Reagent for Nucleophilic Fluorination," *The Journal of Organic Chemistry*, vol. 87, no. 9, pp. 5987–5993, 2022. DOI: 10.1021/acs.joc.2c00247

[203] P. K. Vardhanapu, V. Bheemireddy, M. Bhunia, G. Vijaykumar, and S. K. Mandal, "Cyclic (Alkyl)amino Carbene Complex of Aluminum(III) in Catalytic Guanylation Reaction of Carbodiimides," *Organometallics*, vol. 37, no. 15, pp. 2602–2608, 2018. DOI: 10.1021/acs.organomet.8b00358

[204] J. Vela *et al.*, "Synthesis and Reactivity of Low-Coordinate Iron(II) Fluoride Complexes and Their Use in the Catalytic Hydrodefluorination of Fluorocarbons," *Journal of the American Chemical Society*, vol. 127, no. 21, pp. 7857–7870, 2005. DOI: 10.1021/ja042672l

[205] V. Lavallo, Y. Canac, C. Präsang, B. Donnadieu, and G. Bertrand, "Stable Cyclic (Alkyl)(Amino)Carbenes as Rigid or Flexible, Bulky, Electron-Rich Ligands for Transition-Metal Catalysts: A Quaternary Carbon Atom Makes the Difference," *Angewandte Chemie International Edition*, vol. 44, no. 35, pp. 5705–5709, 2005. DOI: 10.1002/anie.200501841

[206] H. Lehmkuhl, O. Olbrysch, and H. Nehl, "Metallorganische Verbindungen, LV, Donatorfreie tert.-Butyl- und sek.-Propylaluminium-Verbindungen," *Justus Liebigs Annalen der Chemie*, vol. 1973, no. 4, pp. 708–714, 1973. DOI: 10.1002/jlac.197319730418

[207] S. Krieck, H. Görls, and M. Westerhausen, "Synthesis and Properties of Calcium Tetraorganylalanates with $[Me_{4-n}AlPh_n]^-$ Anions," *Organometallics*, vol. 27, no. 19, pp. 5052–5057, 2008. DOI: 10.1021/om800509p

[208] R. Jazzar, R. D. Dewhurst, J.-B. Bourg, B. Donnadieu, Y. Canac, and G. Bertrand, "Intramolecular "Hydroiminiumation" of Alkenes: Application to the Synthesis of Conjugate Acids of Cyclic Alkyl Amino Carbenes (CAACs)," *Angewandte Chemie International Edition*, vol. 46, no. 16, pp. 2899–2902, 2007. DOI: 10.1002/anie.200605083

[209] R. K. Harris, E. D. Becker, S. M. C. de Menezes, P. Granger, R. E. Hoffman, and K. W. Zilm, "Further Conventions for NMR Shielding and Chemical Shifts (IUPAC Recommendations 2008)," *Magnetic Resonance in Chemistry*, vol. 46, no. 6, pp. 582–598, 2008. DOI: 10.1002/mrc.2225

[210] Agilent, "CrysAlisPro Data Collection and Processing Software for Agilent X-ray Diffractometers," *Technologies UK Ltd, Yarnton, Oxford, UK*, vol. 44, no. 0, pp. 1–53, 2014.

[211] R. C. Clark and J. S. Reid, "The analytical calculation of absorption in multifaceted crystals," *Acta Crystallographica Section A*, vol. 51, no. 6, pp. 887–897, 1995. DOI: 10.1107/S0108767395007367

[212] G. M. Sheldrick, "*SHELXT* – Integrated space-group and crystal-structure determination," *Acta Crystallographica Section A: Foundations and Advances*, vol. 71, no. 1, pp. 3–8, 2015. DOI: 10.1107/S2053273314026370

[213] G. M. Sheldrick, "Crystal structure refinement with *SHELXL*," *Acta Crystallographica Section C: Structural Chemistry*, vol. 71, no. 1, pp. 3–8, 2015. DOI: 10.1107/S2053229614024218

[214] O. v. Dolomanov, L. J. Bourhis, R. J. Gildea, J. A. K. Howard, and H. Puschmann, "*OLEX2*: a complete structure solution, refinement and analysis program," *Journal of Applied Crystallography*, vol. 42, no. 2, pp. 339–341, 2009. DOI: 10.1107/S0021889808042726

[215] K. Brandenburg and H. Putz, "Diamond - Crystal and Molecular Structure Visualization." Crystal Impact - Dr. H. Putz & Dr. K. Brandenburg GbR, Bonn, Germany. [Online]. Available: http://www.crystalimpact.com/diamond

[216] M. J. Frisch *et al.*, "Gaussian 16." Gaussian, Inc., Wallingford CT, 2016. Accessed: Aug. 31, 2021. [Online]. Available: https://gaussian.com/gaussian16/

[217] J. P. Perdew, K. Burke, and M. Ernzerhof, "Generalized Gradient Approximation Made Simple," *Physical Review Letters*, vol. 77, no. 18, pp. 3865–3868, 1996. DOI: 10.1103/PhysRevLett.77.3865

[218] S. Grimme, J. Antony, S. Ehrlich, and H. Krieg, "A consistent and accurate *ab initio* parametrization of density functional dispersion correction (DFT-D) for the 94 elements H-Pu," *Journal of Chemical Physics*, vol. 132, no. 15, p. 154104, 2010. DOI: 10.1063/1.3382344

[219] S. Grimme, S. Ehrlich, and L. Goerigk, "Effect of the damping function in dispersion corrected density functional theory," *Journal of Computational Chemistry*, vol. 32, no. 7, pp. 1456–1465, 2011. DOI: 10.1002/jcc.21759

[220] F. Weigend and R. Ahlrichs, "Balanced basis sets of split valence, triple zeta valence and quadruple zeta valence quality for H to Rn: Design and assessment of accuracy," *Physical Chemistry Chemical Physics*, vol. 7, no. 18, p. 3297, 2005. DOI: 10.1039/b508541a

[221] F. Weigend, "Accurate Coulomb-fitting basis sets for H to Rn," *Physical Chemistry Chemical Physics*, vol. 8, no. 9, p. 1057, 2006. DOI: 10.1039/b515623h

[222] A. D. Becke, "Density-functional thermochemistry. III. The role of exact exchange," *Journal of Chemical Physics*, vol. 98, no. 7, pp. 5648–5652, 1993. DOI: 10.1063/1.464913

[223] R. McLellan, M. Uzelac, A. R. Kennedy, E. Hevia, and R. E. Mulvey, "LiTMP Trans-Metal-Trapping of Fluorinated Aromatic Molecules: A Comparative Study of Aluminum and Gallium Carbanion Traps," *Angewandte Chemie International Edition*, vol. 56, no. 32, pp. 9566–9570, 2017. DOI: 10.1002/anie.201706064

[224] B. R. Jagirdar, E. F. Murphy, and H. W. Roesky, "Organometallic Fluorides of the Main Group Metals Containing the C-M-F Fragment," in *Progress in Inorganic Chemistry*, vol. 48, K. D. Karlin, Ed. John Wiley & Sons, INC, pp. 351–455, 2007. DOI: 10.1002/9780470166499.ch4

[225] B. Ališ, A. Štefančič, and G. Tavčar, "Small molecule activation: SbF_3 auto-ionization supported by transfer and mesoionic NHC rearrangement," *Dalton Transactions*, vol. 46, no. 10, pp. 3338–3346, 2017. DOI: 10.1039/C6DT04909E

[226] A.-L. Schmitt, G. Schnee, R. Welter, and S. Dagorne, "Unusual reactivity in organoaluminium and NHC chemistry: deprotonation of $AlMe_3$ by an NHC moiety involving the formation of a sterically bulky NHC–$AlMe_3$ Lewis adduct," *Chemical Communications*, vol. 46, no. 14, p. 2480, 2010. DOI: 10.1039/b922425d

[227] M. R. Kopp, T. Kräuter, B. Werner, and B. Neumüller, "CsF als Fluoridierungsmittel für Organometall-Verbindungen der Elemente der Gruppe 13," *Zeitschrift für anorganische und allgemeine Chemie*, vol. 624, no. 5, pp. 881–886, 1998. DOI: 10.1002/(SICI)1521-3749(199805)624:5<881::AID-ZAAC881>3.0.CO;2-J

[228] K. Nakamoto, *Infrared and Raman Spectra of Inorganic and Coordination Compounds*, Sixth Edit. Hoboken, NJ, USA: John Wiley & Sons, Inc., 2008. DOI: 10.1002/9780470405840

[229] K. Nakamoto, *Infrared and Raman Spectra of Inorganic and Coordination Compounds*, 6th Editio. Hoboken, NJ, USA: John Wiley & Sons, Inc., 2008. DOI: 10.1002/9780470405888

[230] P. Bissinger *et al.*, "Isolation of a Neutral Boron-Containing Radical Stabilized by a Cyclic (Alkyl)(Amino)Carbene," *Angewandte Chemie International Edition*, vol. 53, no. 28, pp. 7360–7363, 2014. DOI: 10.1002/anie.201403514

[231] C. Jones, P. C. Junk, and M. L. Cole, "THE MOLECULAR STRUCTURE OF [AlH_2Cl(Quinuclidine)$_2$]," *Main Group Metal Chemistry*, vol. 24, no. 4, pp. 249–250, 2001. DOI: 10.1515/MGMC.2001.24.4.249

[232] A. Stasch, S. Singh, H. W. Roesky, M. Noltemeyer, and H. Schmidt, "Adducts of Aluminum and Gallium Trichloride with a *N*-Heterocyclic Carbene and an Adduct of Aluminum Trichloride with a Thione," *European Journal of Inorganic Chemistry*, vol. 2004, no. 20, pp. 4052–4055, 2004. DOI: 10.1002/ejic.200400247

[233] B. Bantu, G. Manohar Pawar, K. Wurst, U. Decker, A. M. Schmidt, and M. R. Buchmeiser, "CO_2, Magnesium, Aluminum, and Zinc Adducts of N-Heterocyclic Carbenes as (Latent) Catalysts for Polyurethane Synthesis," *European Journal of Inorganic Chemistry*, vol. 2009, no. 13, pp. 1970–1976, 2009. DOI: 10.1002/ejic.200801161

[234] G. Schnee *et al.*, "Normal-to-Abnormal NHC Rearrangement of Al^{III}, Ga^{III}, and In^{III} Trialkyl Complexes: Scope, Mechanism, Reactivity Studies, and H_2 Activation," *Chemistry - A European Journal*, vol. 21, no. 49, pp. 17959–17972, 2015. DOI: 10.1002/chem.201503000

[235] V. N. Mikhaylov *et al.*, "The carbene transfer to strong Lewis acids: copper is better than silver," *Dalton Transactions*, vol. 50, no. 8, pp. 2872–2879, 2021. DOI: 10.1039/D1DT00235J

[236] F. Ekkehardt Hahn and M. C. Jahnke, "Heterocyclic Carbenes: Synthesis and Coordination Chemistry," *Angewandte Chemie International Edition*, vol. 47, no. 17, pp. 3122–3172, 2008. DOI: 10.1002/anie.200703883

[237] I. Krossing, H. Nöth, C. Tacke, M. Schmidt, and H. Schwenk, "Synthesis and Structures of Bis(tetramethylipiperidino)aluminum Halides — X-ray Crystal Structures of tmp_2AlX (X = Cl, Br, I) and [$tmp_2A1(\mu\text{-}F)]_2$," *Chemische Berichte*, vol. 130, no. 8, pp. 1047–1052, 1997. DOI: 10.1002/cber.19971300805

[238] D. Wiechert, D. Mootz, R. Franz, and G. Siegemund, "Amine-Poly(Hydrogen Fluoride) Solid Complexes: New Studies of Formation, Crystal Structures, and $H_{n-1}F_n^-$ Ion Diversity," *Chemistry - A European Journal*, vol. 4, no. 6, pp. 1043–1047, 1998. DOI: 10.1002/(SICI)1521-3765(19980615)4:6<1043::AID-CHEM1043>3.0.CO;2-N

[239] S. I. Ivlev, T. Soltner, A. J. Karttunen, M. J. Mühlbauer, A. J. Kornath, and F. Kraus, "Syntheses and Crystal Structures of Sodium Hydrogen Fluorides $NaF \cdot n$HF ($n = 2, 3, 4$)," *Zeitschrift für anorganische und allgemeine Chemie*, vol. 643, no. 21, pp. 1436–1443, 2017. DOI: 10.1002/zaac.201700228

[240] T. von Rosenvinge, M. Parrinello, and M. L. Klein, "*Ab initio* molecular dynamics study of polyfluoride anions," *Journal of Chemical Physics*, vol. 107, no. 19, pp. 8012–8019, 1997. DOI: 10.1063/1.475064

[241] M. Meanwell *et al.*, "A short de novo synthesis of nucleoside analogs," *Science (1979)*, vol. 369, no. 6504, pp. 725–730, 2020. DOI: 10.1126/science.abb3231

[242] F. Chen, X.-H. Xu, and F.-L. Qing, "Photoredox-Catalyzed Addition of Dibromofluoromethane to Alkenes: Direct Synthesis of 1-Bromo-1-fluoroalkanes," *Organic Letters*, vol. 23, no. 6, pp. 2364–2369, 2021. DOI: 10.1021/acs.orglett.1c00639

[243] W. W. Wilson, K. O. Christe, J. Feng, and R. Bau, "Tetramethylammonium bifluoride, crystal structure and vibrational spectra," *Canadian Journal of Chemistry*, vol. 67, no. 11, pp. 1898–1901, 1989. DOI: 10.1139/v89-295

[244] I. G. Shenderovich *et al.*, "Nuclear magnetic resonance of hydrogen bonded clusters between F^- and $(HF)_n$: Experiment and theory," *Berichte der Bunsengesellschaft für physikalische Chemie*, vol. 102, no. 3, pp. 422–428, 1998. DOI: 10.1002/bbpc.19981020322

Bibliography

Publications Related to the Thesis

Journal Articles

E. Gruden, M. Tramšek and G. Tavčar, "Discrete organofluoroaluminate anions : synthetic, structural, and spectroscopic aspects," *Organometallics,* vol. 41, no. 2, pp. 41-51, 2022. DOI: 10.1021/acs.organomet.1c00601

E. Gruden and G. Tavčar, "Synthesis and characterization of partially substituted NHC supported alane adducts using triflate or chloride salts," *Polyhedron,* vol. 196, pp. 115009-1-115009-8, 2021. DOI: 10.1016/j.poly.2020.115009

Conference Paper

G. G. Prinčič, J. Jelen, J. Hočevar, B. Omahen, G. Tavčar, E. Gruden and J. Iskra, "Renewable imidazolium-based reagents for nucleophilic fluorination," in *Proceedings of the 28th Annual Meeting of the Slovenian Chemical Society*, Septembre 21-23, 2022, pp. 126, Portorose, Slovenia, Ljubljana: Slovenian Chemical Society, 2022.

G. G. Prinčič, J. Jelen, E. Gruden, J. Hočevar, B. Omahen, G. Tavčar and J. Iskra, "Fluorination with renewable imidazolim based reagents," in *Book of abstracts of the Slovenian-Bavarian Summer School: for 2nd and 3rd Bologna level students: Materials for energy and environmental application*, Septembre 18-21, 2022, pp. 22-23, Ljubljana, Slovenia: University of Ljubljana, Faculty of Chemistry and Chemical Technology, 2022.

G. G. Prinčič, J. Jelen, E. Gruden, J. Hočevar, B. Omahen, G. Tavčar and J. Iskra, "Renewable reagents for nucleophilic fluorination," in *Proceedings of the 9th IUPAC International Conference on Green Chemistry*, Septembre 5-9, 2022, pp. 629, Athens, Greece: Association of Greek Chemists(AGC) in collaboration with the IUPAC Interdivisional Committee on Green Chemistry for Sustainable Development (ICGCSD), 2022.

G. Tavčar, E. Gruden, Ž. Zupanek, J. Jelen, M. Tramšek and A. Kokalj, "Influence of the imidazolium cation on the formation of fluoride anion," in *Proceedings of the 20th European Symposium on Fluorine Chemistry, ESFC 2022*, Avgust 14-19, 2022, pp. 114, Berlin, Germany: Humboldt-Universität, Institut für Chemie, 2022.

E. Gruden, M. Tramšek, G. Tavčar, "In search of a discrete and soluble aluminum trifluoride," in *Proceedings of the 20th European Symposium on Fluorine Chemistry, ESFC 2022*, Avgust 14-19, 2022, pp. 136, Berlin, Germany: Humboldt-Universität, Institut für Chemie, 2022.

E. Gruden, G. Tavčar, "Discrete Organofluoroaluminate Anions," in *Proceedings of the 27th Annual Meeting of the Slovenian Chemical Society*, Septembre 22-24, 2021, pp. 116, Portorose, Slovenia, Ljubljana: Slovenian Chemical Society, 2021.

E. Gruden, G. Tavčar, "Organoaluminium fluorides stabilized by cyclic (alkyl)(amino)carbenes," in *Proceedings of the 26th Annual Meeting of the Slovenian Chemical Society*, Septembre 16-18, 2020, pp. 87, Portorose, Slovenia, Ljubljana: Slovenian Chemical Society, 2020.

E. Gruden, G. Tavčar, "Aldiminium based poly(hydrogen fluorides) : potential nucleophilic fluorination reagents," in *Proceedings of the 12th Jožef Stefan International Postgraduate School Students' Conference and 14th Young Researchers' Day*, May 15, 2020, pp. 15, Ljubljana, Slovenia: Jožef Stefan International Postgraduate School, Jožef Stefan Institute, 2020.

G. Tavčar, B. Alič, Ž. Zupanek, E. Gruden, M. Tramšek, "Imidazolium based fluoride donor as a reagent for the preparation of discrete anionic species," in *Proceedings of the 19th International Symposium on Fluorine Chemistry*, Avgust 25-31, 2019, pp. 128, Warsaw, Poland: University of Warsaw, 2019.

G. Tavčar, B. Alič, Ž. Zupanek, E. Gruden, A. Kokalj, J. Petrovčič, J. Iskra, M. Tramšek, "Novel bulky imidazolium fluorine reagents in inorganic and organic chemistry," in *Proceedings of the International Conference on Flurine Chemistry 2019 Himeji*, May 22-24, 2019, pp. 19, Himeji, Hyogo, Japan: Society for the Promotion if Science, 2019.

E. Gruden, G. Tavčar, "Reactivity of imidazolium fluoride reagent with trimetylaluminium," in *Proceedings of the 11th Jožef Stefan International Postgraduate School Students' Conference and 13th Young Researchers' Day*, May 15-16, 2019, pp. 30, Planica, Slovenia: Jožef Stefan International Postgraduate School, Jožef Stefan Institute, 2019.

E. Gruden, G. Tavčar, "Discrete AlF_4 fluoroaluminate anion in the structure of [IPrH][AlF_4]," in *Proceedings of the 10th Jožef Stefan International Postgraduate School Students' Conference and 12th Young Researchers' Day*, May 10-11, 2018, pp. 16, Piran, Slovenia: Jožef Stefan International Postgraduate School, Jožef Stefan Institute, 2018.

Biography

The author of this thesis, Evelin Gruden, was born on 24th December 1992 in Šempeter pri Gorici, Slovenia. After finishing her primary education at the Primary School Šempas in 2007 and her secondary education at the high school Gimnazija Nova Gorica in 2011, she continued her education in Ljubljana, where she enrolled in the Chemistry study programme at the Faculty of Chemistry and Chemical Technology, University of Ljubljana, Slovenia. She obtained her Bachelor's Degree in 2014 for her work in inorganic chemistry. Her Bachelor's thesis with the title "Feasibility of biochar implementation as method for enrichment of degraded area" was done under the supervision of Asst. Prof. Dr. Marija Zupančič. She also obtained her Master's Degree under the supervision of Asst. Prof. Dr. Marija Zupančič in 2017. Her Master's thesis work in inorganic chemistry with the title "Effects of biochar amendments on metal mobility in tailings" was a year later awarded with the Environmental Award by Saubermacher Slovenia. In 2017 she received the funding from the Slovenian Research Agency and a position as a Young Researcher at the Department of Inorganic Chemistry and Technology at Jožef Stefan Institute, Ljubljana, Slovenia. At the same time, she also continued her academic education at a doctoral degree (PhD) under the supervision of Asst. Prof. Dr. Gašper Tavčar, by applying to the Ecotechnologies study programme at the Jožef Stefan International Postgraduated School, Ljubljana, Slovenia. Evelin Gruden reached the stage of a PhD candidate in her doctoral study in 2022.